STUDYING THE ROLE OF B-MYB DURING SOMATIC REPROGRAMMING AND IN IPSCS

by

CARL ROSS JAMES WARD

A thesis submitted to the University of Birmingham for the degree of
DOCTOR OF PHILOSOPHY

School of Infection and Immunity
College of Medical and Dental Sciences
University of Birmingham
September 2014

UNIVERSITY OF
BIRMINGHAM

University of Birmingham Research Archive

e-theses repository

This unpublished thesis/dissertation is copyright of the author and/or third parties. The intellectual property rights of the author or third parties in respect of this work are as defined by The Copyright Designs and Patents Act 1988 or as modified by any successor legislation.

Any use made of information contained in this thesis/dissertation must be in accordance with that legislation and must be properly acknowledged. Further distribution or reproduction in any format is prohibited without the permission of the copyright holder.

ABSTRACT

Somatic cell reprogramming towards a pluripotent stem cell-like state occurs in an organized way, with rapid changes in gene expression during the first days of induction. Little is known about the mechanisms that lead to DNA double strand breaks (DSB) and genome instability during reprogramming.

Amongst genes upregulated during reprogramming is that encoding the transcription factor B-Myb. *B-myb* RNA levels increase gradually from day 2 of reprogramming, earlier than those encoding pluripotency factors such as *Nanog*.

Despite its possible function as a regulator of the pluripotent state, B-Myb has a general role in the regulation of proliferation, and genome stability throughout the animal kingdom, raising the possibility that the activity of this protein is linked to the DSBs observed during reprogramming.

To explore this possibility, reprogramming studies were performed in which B-Myb expression was modified: B-*myb*$^{-/-}$ MEFs were incapable of reprogramming after transduction with OSKM lentivirus (Oct4/Sox2/Klf4/c-Myc). However, unexpectedly, co-expression of B-Myb together with OSK (OSKB lentivirus), severely impaired the efficiency of reprogramming.

Interestingly, the iPSC colonies appeared more ESC-like and had less DSBs.

My results show that both the level of the B-Myb expression is crucial during early stages of reprogramming, indicating that B-Myb is a gatekeeper for reprogramming.

ACKNOWLEDGEMENTS

Firstly I would like to thank my first supervisor Paloma García for helping make this thesis possible as I couldn't have done it without her. I am appreciative for all the guidance when things were not going well and for all the ideas of how to push the project forward. I am eternally grateful for all of the time and effort she put into mentoring me. I would also like to thank my second supervisor Jon Frampton for direction and critique of my work in lab meetings.

I am indebted to our collaborators that have also enabled this work to be done: George Murphy and Cesar Sommer for providing the reprogramming system and helping me redesign the system and Keisuke Kaji for hosting me in Edinburgh and teaching me his secondary reprogramming system.

I would also like to acknowledge the other members of the García group past and present for support and discussions: Laila Cancian, Maelle Lorvellec, and Michael Smith.

I must thank the members of the Frampton group for all their assistance and help over the years too: Mary Clarke Emilie Dasse, Stephanie Dumon, Lozan Sheriff, Giacomo Volpe, Dave Walton and Roger Watson.

Many thanks to all the administrative and technical staff in the IBR and BMSU who work hard to provide services that allow our research to proceed.

In addition, I am grateful to the Medical Research Council and the Wellcome Trust for the funding of this project.

I am also grateful to my mother Carol and my sister Michel for believing in me and for encouraging me to follow my dream of working in research.

Finally, I must thank my girlfriend Laura, for all of the emotional support and encouragement that she has given me whilst I was studying for this thesis. I am grateful to her for cheering me up whenever I was down because of my experiments failing for the tenth time and thank her for lending her car to come and feed my cells at the weekends!

TABLE OF CONTENTS

1 CHAPTER 1: GENERAL INTRODUCTION 1

1.1 MYB PROTEINS IN EVOLUTION 1

1.2 INVERTEBRATE MYB 1

1.3 VERTEBRATE MYB FAMILY 3

1.4 B-MYB 5

1.4.1 Regulation of B-Myb during the cell cycle 7

1.5 EMBRYONIC STEM CELLS 9

1.5.1 Ethical issues 10

1.5.2 Immune rejection 10

1.5.3 Tumour formation 11

1.6 SOMATIC REPROGRAMMING 11

1.6.1 Ethical issues 15

1.6.2 Immune rejection 15

1.6.3 Tumour formation 16

1.6.4 Limitations of somatic reprogramming 16

1.7 THE ORIGINAL YAMANAKA FACTORS 19

1.7.1.1 Oct4 19

1.7.1.2 Sox2 20

1.7.1.3 Klf4 21

1.7.1.4 c-Myc 22

1.8 THE EVOLUTION OF REPROGRAMMING 23

1.8.1 Transcription factor mediated reprogramming 23

1.8.2 Epigenetic regulators in reprogramming 25

1.8.3 P53 in reprogramming 25

1.8.4 microRNAs in reprogramming 26

1.8.5 Chemical reprogramming 27

1.9 THE MECHANISM OF REPROGRAMMING 28

1.9.1 Tracking reprogramming through surface antigens *28*

1.9.2 Epigenetic remodelling *29*

1.9.3 Models of reprogramming *30*

1.10 B-MYB TRANSCRIPTION FACTOR AND ITS POSSIBLE ROLE IN CELLULAR REPROGRAMMING 31

1.11 AIMS 33

2 CHAPTER 2: MATERIALS AND METHODS 34

2.1 CELL CULTURE AND GROWTH CONDITIONS 34

2.2 LENTIVIRAL PRODUCTION 35

2.3 LENTIVIRAL TITRATION 37

2.3.1 Flow cytometric titration *37*

2.3.2 qPCR Titration *38*

2.4 PRIMARY REPROGRAMMING 39

2.5 SECONDARY REPROGRAMMING 40

2.6 INDIVIDUAL IPSC COLONY ISOLATION 40

2.7 FLOW CYTOMETRIC ANALYSIS OF REPROGRAMMING PROCESS 41

2.8 MICE 41

2.9 MEF DERIVATION 42

2.10 FEEDER MEFS 42

2.11 GENOMIC DNA EXTRACTION FOR GENOTYPING 43

2.12 POLYMERASE CHAIN REACTION (PCR) FOR GENOTYPING 44

2.13 PCR FOR CLONING 44

2.14 AGAROSE GEL EXTRACTION 46

2.15 GIBSON ASSEMBLY 47

2.16 GATEWAY CLONING 47

2.17 SEQUENCING 48

2.18 COMPETENT BACTERIA TRANSFORMATION 49

2.19 BACTERIAL CULTURE 49

2.20 PLASMID DNA EXTRACTION 50

2.21 RESTRICTION ENDONUCLEASE DIGESTION 51
2.22 PROTEIN EXTRACTION 51
2.23 WESTERN BLOTTING 52
2.24 TRANSFECTION 54
2.25 NUCLEOFECTION 54
2.26 KARYOTYPING 55
2.27 FLUORESCENCE ACTIVATED CELL SORTING (FACS) 56
2.28 RNA EXTRACTION 56
2.29 CDNA SYNTHESIS 56
2.30 TAQMAN QPCR 57
2.31 CELL CYCLE ANALYSIS WITH PROPIDIUM IODIDE 59
2.32 Γ-H2AX AND RAD51 IMMUNOFLUORESCENCE 59
2.33 ALKALINE PHOSPHATASE STAINING 60
2.34 SENESCENCE STAINING 60
2.35 APOPTOSIS STAINING 61
2.36 CELL CYCLE ANALYSIS WITH AMINOACTINOMYCIN D (7AAD) 61
2.37 CELL VIABILITY ASSAY (CELL QUANTI-BLUE) 62

3 CHAPTER 3: GENERATION OF IPSCS WITH MODIFIED B-MYB ALLELES 63

3.1 INTRODUCTION 63
3.2 RESULTS 67
3.2.1 Generation and characterisation of B-myb$^{+/+}$, B-myb$^{+/\Delta}$ and B-myb$^{F/\Delta}$ iPSCs 67
3.2.1.1 Alkaline phosphatase staining of derived iPSC lines 67
Karyotyping derived iPSC lines 68
3.2.1.2 Cell cycle analysis of iPSC lines 69
3.2.1.3 Chimeric mouse generation with iPSC lines 72
3.2.2 Derivation of B-myb$^{\Delta/\Delta}$ iPSCs 74
3.2.3 Confirmation of B-Myb ablation and cassette removal 76
3.3 DISCUSSION 81

3.3.1 Chromosomal integrity 81

3.3.2 Cell cycle changes 81

3.3.3 Chimeric mice 82

3.3.4 Excision of OSKM and B-myb 83

4 CHAPTER 4: WHAT IS THE ROLE OF B-MYB IN IPSCS? 85

4.1 INTRODUCTION 85

4.2 RESULTS 86

4.2.1 Proliferation analysis of B-myb$^{\Delta/\Delta}$ iPSCs 86

4.2.2 Polyploid analysis of (OSKM) B-myb$^{\Delta/\Delta}$ iPSCs 87

4.2.3 Double strand break in (OSKM) B-myb$^{\Delta/\Delta}$ iPSCs 88

4.2.4 Which DNA damage repair pathway is B-Myb involved in? 91

4.3 DISCUSSION 98

4.3.1 iPSC growth in the absence of B-Myb 98

4.3.2 Lack of B-Myb leads to genomic instability 98

4.3.3 Double strand break analysis in iPSCs 99

4.3.4 DNA repair pathway analysis 100

5 CHAPTER 5: IS ENDOGENOUS B-MYB REQUIRED IN THE REPROGRAMMING PROCESS? 102

5.1 INTRODUCTION 102

5.2 RESULTS 104

5.2.1 Deletion of B-myb in MEFs by exogenous expression of Cre recombinase 104

5.2.2 Deletion of B-myb in MEFs through endogenous expression of Cre recombinase 106

5.2.3 Is the block in reprogramming caused by cell cycle arrest? 114

5.3 DISCUSSION 117

5.3.1 Removal of B-Myb in MEFs 117

5.3.2 Endogenous system 118

6 CHAPTER 6: COULD B-MYB INCREASE EFFICIENCY OF REPROGRAMMING? ..120

6.1 INTRODUCTION 120

6.2 RESULTS 122

6.2.1 Testing the B-myb lentivirus 122

6.2.2 The effect of additional B-Myb in reprogramming 124

6.2.3 Generation of the Oct4, Sox2, Klf4 and B-Myb (OSKB) lentivirus 128

6.2.4 Reprogramming with OSKB lentivirus 135

6.2.5 The reduced reprogramming efficiency is not caused by quiescence/ senescence in the MEFs. 139

6.2.6 The reduced reprogramming efficiency is not caused by apoptosis in the MEFs 143

6.2.7 Reprogramming kinetics are slower in OSKB reprogramming 148

6.2.8 RNA analysis of MEFs undergoing reprogramming 156

6.2.8.1 Early pluripotency gene expression at MOI 2 156

6.2.8.2 Early pluripotency gene expression at MOI 20 160

6.2.8.3 Late pluripotency gene expression at MOI 2 163

6.2.8.4 Late pluripotency gene expression at MOI 20 167

6.2.8.5 MET and proliferative gene expression at MOI 2 170

6.2.8.6 MET and proliferative gene expression at MOI 20 174

6.2.9 Do OSKB reprogrammed iPSCs have lower DNA damage? 177

6.3 DISCUSSION 179

6.3.1 Role of B-Myb in cell cycle arrest 180

6.3.2 The OSKB vector is not inducing additional apoptosis 180

6.3.3 OSKB vector is detrimental to kinetics of reprogramming 181

6.3.4 OSKB reprogrammed MEFs fail to activate pluripotency genes at low MOI 181

7 CHAPTER 7: DOES B-MYB OVEREXPRESSION AFFECT SECONDARY REPROGRAMMING? 183

7.1 INTRODUCTION 183

7.2 RESULTS 184

7.2.1 Generating a lentiviral backbone with a gateway destination cassette 184

7.2.2 Generating B-Myb-AmCyan lentiviral backbone 186

7.2.3 B-Myb overexpression lowers secondary reprogramming efficiency 191

7.2.4 Reduced efficiency of secondary reprogramming is not due to senescence in the MEFs 195

7.2.5 Reduced efficiency of secondary reprogramming is not due to apoptosis in the MEFs 199

7.3 DISCUSSION 202

7.3.1 Secondary reprogramming 202

7.3.2 Generating a B-myb-AmCyan expression vector 202

7.3.3 B-Myb over expression inhibits reprogramming 203

7.3.4 Reprogramming inhibition is not due to cell cycle arrest or apoptosis 203

8 CHAPTER 8: GENERAL DISCUSSION AND PERSPECTIVES 205

9 REFERENCES 209

LIST OF FIGURES

FIGURE 1.1: THE MYB FAMILY 4

FIGURE 1.2: B-MYB IN THE CELL CYCLE 8

FIGURE 1.3: THE REPROGRAMMING PROCESS 13

FIGURE 1.4: THE REPROGRAMMING FIELD TIMELINE 14

FIGURE 1.5: PROPOSED MODELS OF REPROGRAMMING 31

FIGURE 3.1: THE OSKM AND OSK LENTIVIRAL VECTORS 65

FIGURE 3.2: THE REPROGRAMMING PROCESS 66

FIGURE 3.3: ALKALINE PHOSPHATASE STAINING FOR B-*MYB*$^{+/+}$, B-*MYB*$^{+/\Delta}$ AND B-*MYB*$^{F/\Delta}$ IPSCS 68

FIGURE 3.4: KARYOTYPING OF THREE IPSC LINES 69

FIGURE 3.5: CELL CYCLE ANALYSIS BY PROPIDIUM IODIDE STAINING 71

FIGURE 3.6: CHIMERIC MICE 73

FIGURE 3.7: GENERATION OF (OSKM) B-*MYB*$^{\Delta/\Delta}$ IPSCS 75

FIGURE 3.8: GENOTYPING FOR *B-MYB*$^{+/\Delta}$ INDIVIDUAL COLONIES 76

FIGURE 3.9: GENOTYPING FOR B-*MYB*$^{\Delta/\Delta}$ INDIVIDUAL COLONIES 77

FIGURE 3.10: GENOTYPING TO DETECT OSKM CASSETTE 78

FIGURE 3.11: B-MYB MRNA EXPRESSION IN GENERATED (OSKM) B-*MYB*$^{\Delta/\Delta}$ IPSC LINE 79

FIGURE 3.12: B-MYB, NANOG AND OCT4 IN GENERATED IPSC LINES 80

FIGURE 4.1: GROWTH RATE OF (OSKM) B-*MYB*$^{+/+}$ OR (OSKM) B-*MYB*$^{\Delta/\Delta}$ IPSCS 87

FIGURE 4.2: POLYPLOID ANALYSIS OF (OSKM) B-*MYB*$^{+/+}$, (OSKM) B-*MYB*$^{+/\Delta}$ OR (OSKM) B-*MYB*$^{\Delta/\Delta}$ IPSCS 89

FIGURE 4.3: Γ-H2AX AND RAD51 IMMUNOFLUORESCENCE STAINING 90

FIGURE 4.4: SENSITIVITY OF IPSCS TO HYDROXYUREA 93

FIGURE 4.5: SENSITIVITY OF IPSCS TO PJ34 95

FIGURE 4.6: SENSITIVITY OF IPSCS TO CAMPTOTHECIN 97

FIGURE 5.1: DOES DELETION OF *B-MYB* BLOCK REPROGRAMMING? 105

FIGURE 5.2: TESTING CRE-ER^{T2} MEF DELETION OF B-*MYB* 107

FIGURE 5.3: REPROGRAMMING IN THE ABSENCE OF B-MYB 108

FIGURE 5.4: GENOTYPING FOR B-*MYB*$^{\Delta/\Delta}$ *OR* B-*MYB*$^{+/\Delta}$ INDIVIDUAL PICKED COLONIES GENERATED WITH MOI 2 OSKM .. 109

FIGURE 5.5: GENOTYPING FOR B-*MYB*$^{\Delta/\Delta}$ *OR* B-*MYB*$^{F/\Delta}$ INDIVIDUAL PICKED COLONIES 111

FIGURE 5.6: GENOTYPING FOR B-*MYB*$^{\Delta/\Delta}$ OR B-*MYB*$^{+/\Delta}$ INDIVIDUAL PICKED COLONIES GENERATED WITH MOI 20 OSKM 113

FIGURE 5.7: SENESCENCE RELATED GENE EXPRESSION DURING EARLY REPROGRAMMING AT MOI 2 115

FIGURE 5.8: SENESCENCE RELATED GENE EXPRESSION DURING EARLY REPROGRAMMING AT MOI 20 116

FIGURE 6.1: B-MYB OVEREXPRESSION ANALYSIS IN WILD TYPE MEFS 123

FIGURE 6.2: ALKALINE PHOSPHATASE STAINING FOR MEFS REPROGRAMMED WITH OSKM OR OSKM + B-*MYB* LENTIVIRUS 125

FIGURE 6.3: ALKALINE PHOSPHATASE STAINING OF REPROGRAMMED MEFS 127

FIGURE 6.4: GENERATION OF THE OSKB LENTIVIRAL BACKBONE 129

FIGURE 6.5: CLONING THE *SOX2-E2A*-B-*MYB* FUSION GENE 130

FIGURE 6.6: SANGER SEQUENCING FOR CLONED *SOX2-E2A*-B-*MYB* FUSION GENE 131

FIGURE 6.7: DIGESTION OF *SOX2-E2A*-B-*MYB* FRAGMENT AND CONFIRMATION OF OSKB PLASMID 132

FIGURE 6.8: PROTEIN EXPRESSION OF OSKB AND OSKM LENTIVIRAL BACKBONES IN TRANSFECTED 293T CELL LINE 134

FIGURE 6.9: REPROGRAMMING WITH OSKB LENTIVIRUS AT MOI 2 136

FIGURE 6.10: REPROGRAMMING WITH OSKB LENTIVIRUS AT MOI 20 138

FIGURE 6.11: B-GALACTOSIDASE STAINING IN MEFS TRANSDUCED WITH OSK OR OSKB 140

FIGURE 6.12: P21 MRNA EXPRESSION 141

FIGURE 6.13: P16 MRNA EXPRESSION 142

FIGURE 6.14: P53 MRNA EXPRESSION 143

FIGURE 6.15: TUNEL STAINING IN MEFS 145

FIGURE 6.16: REPROGRAMMING IN *P53*$^{-/-}$ MEFS 147

FIGURE 6.17: SCHEMATIC TO SHOW GATING STRATEGY USED IN FLOW CYTOMETRY 149

FIGURE 6.18: FULLY REPROGRAMED (CD54+,CD44-) IPSC QUANTIFICATION FOR OSKM, OSK OR OSKB AT MOI 2 151

FIGURE 6.19: FULLY REPROGRAMED (CD54+,CD44-) IPSC QUANTIFICATION FOR OSKM, OSK OR OSKB AT MOI 20 152

FIGURE 6.20: PARTIALLY REPROGRAMED (CD54-,CD44-) IPSC QUANTIFICATION FOR OSKM, OSK OR OSKB AT MOI 2 154

FIGURE 6.21: PARTIALLY REPROGRAMED (CD54-,CD44-) IPSC QUANTIFICATION FOR OSKM, OSK OR OSKB AT MOI 20 155

FIGURE 6.22: RNA EXPRESSION OF EARLY PLURIPOTENCY GENES DURING REPROGRAMMING WITH OSKB OR OSK AT MOI 2 159
FIGURE 6.23: RNA EXPRESSION OF EARLY PLURIPOTENCY GENES DURING REPROGRAMMING WITH OSKB OR OSK AT MOI 20 162
FIGURE 6.24: RNA EXPRESSION OF LATE PLURIPOTENCY GENES DURING REPROGRAMMING WITH MOI 2 OSKB OR OSK 166
FIGURE 6.25: RNA EXPRESSION OF LATE PLURIPOTENCY GENES DURING REPROGRAMMING WITH MOI 20 OSKB OR OSK 169
FIGURE 6.26: RNA EXPRESSION OF MET GENES AND C-MYC DURING REPROGRAMMING WITH MOI 2 OSKB OR OSK 173
FIGURE 6.27: RNA EXPRESSION OF MET GENES AND C-MYC DURING REPROGRAMMING WITH MOI 20 OSKB OR OSK... 176
FIGURE 6.28: Γ-H2AX IN EARLY PASSAGE IPSCS 178
FIGURE 7.1: GENERATION OF THE LENTIVIRAL BACKBONE WITH A GATEWAY® ACCEPTOR SITE 184
FIGURE 7.2: CLONING THE GATEWAY® ACCEPTOR SITE, REMOVING *ZSGREEN* GENE AND ASSEMBLING CONSTRUCT 186
FIGURE 7.3: GENERATION OF THE B-*MYB*-*P2A*-*AMCYAN* FUSION GENE 187
FIGURE 7.4: CONFIRMATION OF LIGATION INTO ENTRY PLASMIDS 189
FIGURE 7.5: CONFIRMATION OF RECOMBINATION INTO PHAGE-EF1A DESTINATION PLASMIDS 190
FIGURE 7.6: CONFIRMATION OF B-MYB EXPRESSION 191
FIGURE 7.7: GATING STRATEGY USED TO TRACK SECONDARY REPROGRAMMING 192
FIGURE 7.8: FULLY REPROGRAMED (CD54+,CD44-) IPSC QUANTIFICATION FOR MKOS MEFS TRANSDUCED WITH B-*MYB*-*AMCYAN* OR *AMCYAN* 194
FIGURE 7.9: PARTIALLY REPROGRAMED (CD54-, CD44-) IPSC QUANTIFICATION FOR MKOS MEFS TRANSDUCED WITH B-*MYB* OR *AMCYAN* 195
FIGURE 7.10: B-GALACTOSIDASE STAINING IN THE MKOS MEFS 196
FIGURE 7.11: P21 MRNA EXPRESSION IN MKOS 197
FIGURE 7.12: P16 MRNA EXPRESSION IN MKOS 198
FIGURE 7.13: P53 MRNA EXPRESSION IN MKOS 199
FIGURE 7.14: TUNEL ASSAY IN THE MKOS MEFS 201

LIST OF TABLES

TABLE 1: BACKBONE PLASMIDS 36

TABLE 2: PRIMERS USED IN GENOTYPING 44

TABLE 3: PRIMERS USED IN CLONING 45

TABLE 4: PRIMERS USED FOR SANGER SEQUENCING 48

TABLE 5: PRIMARY ANTIBODIES USED IN WESTERN BLOTTING 53

TABLE 6: SECONDARY ANTIBODIES USED IN WESTERN BLOTTING 53

TABLE 7: TAQMAN OLIGO AND PRIMER SETS USED TO ANALYSE RNA EXPRESSION 58

LIST OF ABBREVIATIONS

4-OHT – 4-Hydroxytamoxifen
AA – Amino Acid
AP – Alkaline Phosphatase
APC – Allophycocyanin
ASC – Adult stem cell
Bp – Base pairs
CDK – Cyclin dependant kinase
cDNA – Complementary Deoxyribonucleic acid
ChIP – Chromatin immunoprecipitation
CNV – Copy number variations
Ct – Cycle threshold
DAPI - 4',6-diamidino-2-phenylindole
dH_2O – Distilled water
DNA – Deoxyribonucleic acid
d.p.c – Days post coitum
dNTP - Deoxynucleotide
DSB – Double strand break
EDTA - Ethylenediaminetetraacetic acid
EGFP – Enhanced green fluorescent protein
ESC – Embryonic stem cell
FACS – Fluorescence assisted cell sorting
FSC – Forward scatter
G1 phase – Gap 1 phase
G2 phase – Gap 2 phase
GFP – Green fluorescent protein
GW – Gateway
Gy - Grays
HR – Homologous recombination
ICM – Inner cell mass
IgG – Immunoglobulin G
iPSC – induced pluripotent stem cell
IR – Ionizing radiation
IRES – Internal ribosome entry sequence
Kb – Kilobases
Kda - Kilodalton
LIF – Leukaemia inhibitory factor
M phase – Mitosis phase
MEF – Mouse embryonic fibroblast
MET – Mesenchymal to epithelial transition
miRNA – micro Ribonucleic acid
MOI – Multiplicity of infection
NHEJ – Non-homologous end joining
OSK - Oct4, Sox2,Klf4 and (mCherry)
OSKB – Oct4, Sox2, Klf4 and B-Myb
OSKM – Oct4, Sox2,Klf4 and c-Myc

PBS – Phosphate buffered saline
PCNA – Proliferating cell nuclear antigen
PCR – Polymerase chain reaction
PE-Cy7 - Phycoerythrin-Cychrome 7
qRT-PCR – Quantitative reverse transcription - polymerase chain reaction
Rb - Retinoblastoma
RNA - Ribonucleic acid
S phase – Synthesis phase
SD – Standard deviation
SDS-PAGE - sodium dodecyl sulphate polyacrylamide gel electrophoresis
SEM – Standard error of the mean
shRNA – Short hairpin Ribonucleic acid
siRNA – Small interfering Ribonucleic acid
SSC – Side scatter
TBS – Tris-buffered saline
TTBS - Tris-buffered saline and Tween
WT – Wild Type

CHAPTER 1: GENERAL INTRODUCTION

1.1 Myb proteins in evolution

Myb proteins are one of the largest super families of proteins that have been found in all types of life from unicellular organisms to plants, invertebrates and vertebrates (Franchini et al., 1983, Gonda and Bishop, 1983, Gonda et al., 1985, Katzen et al., 1985, Stobergrasser et al., 1992, Braun and Grotewold, 1999, Davidson et al., 2004). The ancestral member of the family, known simply as Myb, has undergone two duplication events throughout evolution leading to three members of the Myb family in vertebrates A-Myb, B-Myb and c-Myb (Nomura et al., 1988, Simon et al., 2002).

1.2 Invertebrate Myb

Invertebrates such as *Drosophila melanogaster* and *Echinoidea* (sea urchin) only have the ancestral *myb* gene that is most homologous to B-*myb* in vertebrates (Simon et al., 2002, Davidson et al., 2004).

Mutation of *myb* in *Drosophila* causes aberrant cell cycling, in particular the S to M transition, which leads to genomic instability in the form of aneuploidy and polyploidy (Fung et al., 2002, Manak et al., 2002). *Drosophila*-Myb is involved in cell cycle progression control through the induction of Cyclin B by binding directly to its promoter (Okada et al., 2002). *Drosophila*-Myb has a role in preventing salivary gland cells from endoreduplicating and in promoting S and M phase progression (Fitzpatrick et al., 2002).

In addition to binding directly to gene promoters Myb has also been shown to form complexes to regulate transcription.

In *Drosophila*, Myb has been shown to bind with mip130, mip120, mip40 and caf1 proteins in a complex named Myb-MuvB (MMB) (Beall et al., 2002, Lewis et al., 2004, Sadasivam and DeCaprio, 2013). Mip130, mip120 and mip40 are homologous to the *Caenorhabditis elegans* LIN9, LIN54 and LIN37 genes that prevent inappropriate vulva development collectively known as the Muv genes (Ferguson and Horvitz, 1989). The MMB complex binds to several members of the Retinoblastoma (Rb) family of proteins including RBF1 and RBF2 plus E2F2 and DP (Lewis et al., 2004). A comparable complex called DP, RB and MuvB (DRM) also containing the homolog of Rb was also identified in *C.elegans* (Harrison et al., 2006). The Rb family of proteins regulate E2F transcription factors which are required for cell cycle progression (Duronio et al., 1995, Lundberg and Weinberg, 1998).

The MMB complex forms part of a larger complex called the *Drosophila* Rb, E2F and Myb complex (dREAM) complex (Korenjak et al., 2004). Mammalian orthologs of the dREAM complex suggest that the complex and its role in the cell cycle are evolutionarily conserved (Korenjak et al., 2004, Litovchick et al., 2007).

B-Myb, but not A-Myb or c-Myb, has been demonstrated to be a functional ortholog of *Drosophila* Myb by rescuing the proliferation defect in *Drosophila* $myb^{-/-}$ cells through exogenous expression of B-Myb (Davidson et al., 2005). In addition, further studies in *Drosophila* showed that exogenous expression of A-Myb or c-Myb in larvae caused early lethality; however exogenous expression of B-Myb had no negative effect on larval viability (Davidson et al., 2013).

1.3 Vertebrate Myb family

The defining feature of the vertebrate Myb protein is a highly evolutionarily conserved three-repeat Myb DNA binding domain (Figure 1.1) (Davidson et al., 2004). The three vertebrate Myb proteins have a very similar structure, with a DNA binding domain at the N-terminus and a regulatory C-terminal domain (Figure 1.1) (Foos et al., 1992, McIntosh et al., 1998). The conserved DNA binding domain has been shown to bind to the DNA sequence pyAACG/TG (Biedenkapp et al., 1988). Despite structural similarities, they differ in their expression pattern as B-Myb is ubiquitously expressed (Nomura et al., 1988, Sitzmann et al., 1996), unlike A-Myb, which is expressed in some B-lymphocytes and reproductive organs (Mettus et al., 1994, Trauth et al., 1994), and c-Myb, which is expressed in the haematopoietic system and several other stem cell compartments including neural and intestinal stem cells (Sheiness and Gardinier, 1984, Duprey and Boettiger, 1985, Sitzmann et al., 1995, Malaterre et al., 2008, Cheasley et al., 2011).

Knockout mouse models have been developed for each of the genes in the family: *c-myb* knockout results in anaemic lethality due to impaired haematopoietic development at day 15 of embryonic development (Mucenski et al., 1991), A-*myb* knockout mice develop to full term but females exhibit impaired mammary gland formation and males are sterile due to flawed spermatogenesis (Toscani et al., 1997), while B-*myb* knockout is embryonic lethal at day 4.5 due to compromised inner cell mass (ICM) development (Tanaka et al., 1999).

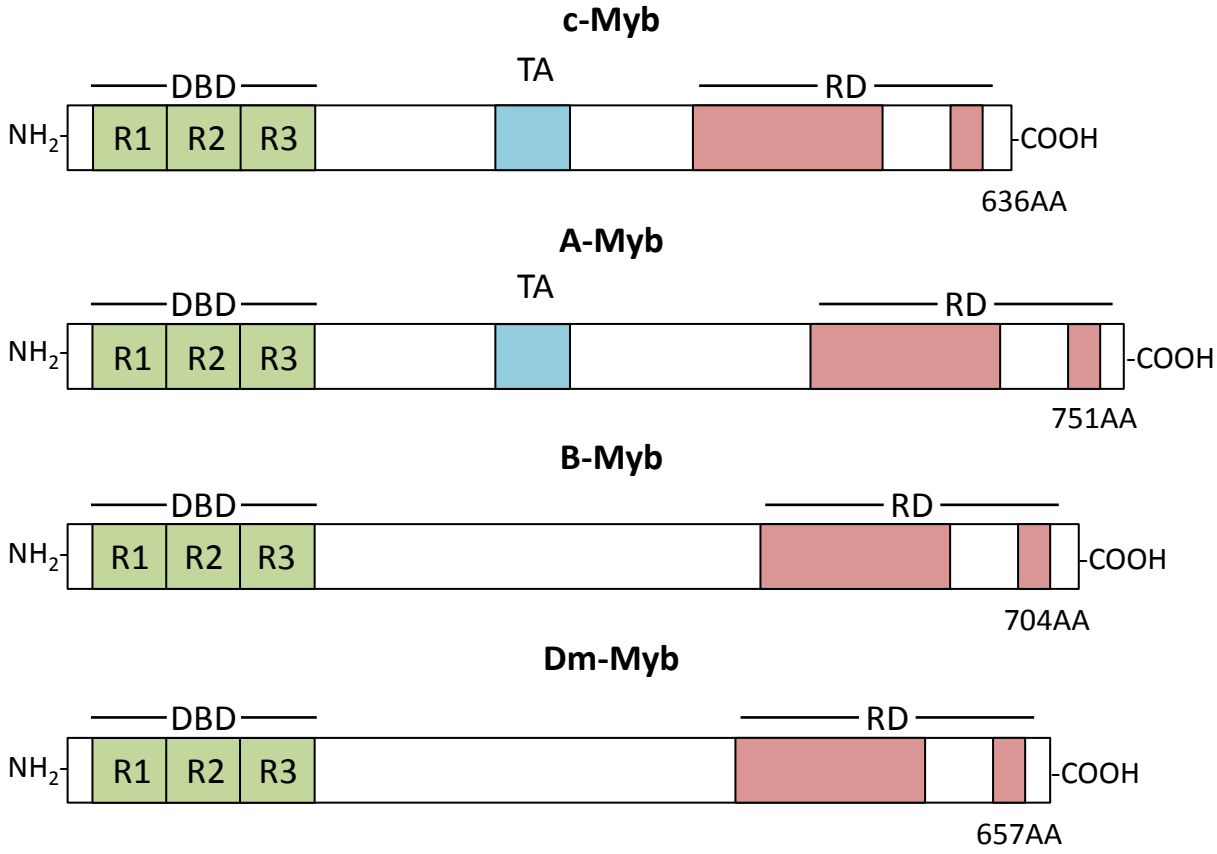


Figure 1.1: The Myb family
Schematic representing the primary protein structure of the three members of the vertebrate Myb family and *Drosophila melanogaster* Myb. Coloured sections represent conserved regions. DBD – DNA binding domain, R – Repeat, TA- Transactivation domain, RD – Regulatory domain. Adapted from (Katzen et al., 1998, Oh and Reddy, 1999, Davidson et al., 2013).

1.4 B-Myb

B-Myb is a ubiquitously expressed transcription factor that has an important role in several cellular systems, including proliferation, senescence and maintenance of genome stability.

B-Myb is highly expressed in rapidly dividing cells (Sitzmann et al., 1996), and is expressed up to 10000x more in embryonic stem cells (ESCs), embryonic germ cells and embryonic carcinoma cells compared to other somatic cell types (Tarasov et al., 2008). Experiments in fibroblasts indicate that B-Myb has a role in proliferation as inhibition slowed proliferation and over expression reduced growth factor requirements (Sala and Calabretta, 1992). B-Myb siRNA knockdown in human fibroblasts leads to cell cycle arrest in the G_2/M phase (Santilli et al., 2005).

In agreement with its role in proliferation, B-Myb expression is frequently amplified in neuroblastoma (Pomeroy et al., 2002), ovarian (Astbury et al., 2011) and breast cancer (Sorlie et al., 2001, Sotiriou et al., 2003); it is also used as a biomarker for poor prognosis in breast cancer (Oncotype DX® , Genomic Health. Inc.). B-Myb has also been implicated in prostate cancer (Bar-Shira et al., 2002), testicular cancer (Skotheim et al., 2002), and adenocarcinoma (Albrecht et al., 2004). Overexpression of B-Myb in multiple cancer cell lines blocks terminal differentiation (Raschella et al., 1995, Bies et al., 1996). Furthermore a genomic and transcriptomic analysis of 2256 human tumours from 10 types of cancer showed that B-Myb was often up regulated (Parikh et al., 2014).

Knockout of B-*myb* in mice highlights a crucial role during embryogenesis. As cells differentiate B-Myb expression decreases similarly to the essential ESC pluripotency factors: Oct4, Sox2 and Nanog (Raschella et al., 1995, Walker et al., 2007).

B-Myb has also been related to senescence/quiescence as its down regulation leads to cell senescence (Johung et al., 2007, Martineza et al., 2011). In agreement with this, B-Myb over expression is able to rescue MEFs from ras-induced senescence (Masselink et al., 2001). B-Myb expression negatively correlated with the expression of a protein involved in the cellular senescence cascade (p16) in human fibroblast cells (Huang et al., 2011).

In addition, B-Myb has been shown to be instrumental in maintaining genome integrity throughout the animal kingdom in *Drosophila* (Manak et al., 2002, Fung et al., 2002), *Danio rerio* (zebrafish) (Shepard et al., 2005), DT40 chicken B-cells (Ahlbory et al., 2005), human haemopoietic cells (Garcia and Frampton, 2006), and mouse ESCs (Lorvellec et al., 2010). Low expression of B-Myb protein in human cells results in chromosome breakage and end-to-end fusion (Garcia and Frampton, 2006). Furthermore, deletion of B-*myb* in ESCs causes an increase in double strand breaks and replication fork stalling suggesting that the genomic aberrations could be the consequence of improper genome duplication during S phase (Lorvellec et al., 2010). The group of Shunsuke Ishii discovered a complex containing B-Myb, clathrin and filamin that they termed Myb-Clafi complex which is crucial for correct formation of mitotic spindles during mitosis (Yamauchi et al., 2008). B-Myb has also been shown to form a complex with polymerase delta-interacting protein 1 (Pdip1) which interacts with proliferating cell nuclear antigen (PCNA), a protein crucial for DNA repair (Werwein et al., 2012).

1.4.1 Regulation of B-Myb during the cell cycle

B-Myb expression fluctuates during the cell cycle, with peak expression early in the S phase (Lam et al., 1992, Robinson et al., 1996), after reaching peak expression the transcription factor E2F in complex with p130 represses B-Myb expression in G0/G1 (Lam and Watson, 1993). The p130-E2F complex is disrupted at G1-S transition by phosphorylation of p130 by CDK activity. The E2F binding site in the B-*myb* promoter is conserved between mouse and humans, and its mutation leads to increased expression of B-Myb throughout the cell cycle (Lam et al., 1995).

B-Myb is phosphorylated by Cyclin A/CDK2 during the S phase increasing its transactivation activity (Robinson et al., 1996, Saville and Watson, 1998). This phosphorylation releases B-Myb from the inhibitive action of two co-repressors, N-CoR and SMRT (Li and McDonnell, 2002). Interestingly, Cyclin A also poly ubiquitinylates the c-terminus of B-Myb leading to degradation through interaction with SKP2 (Charrasse et al., 2000). During the S phase B-Myb forms a complex with MuvB and FoxM1 to progress the cell cycle by activating G2/M genes: Cyclin A, Cyclin B and CDK1 (Sala and Calabretta, 1992, Zhu et al., 2004, Pilkinton et al., 2007).

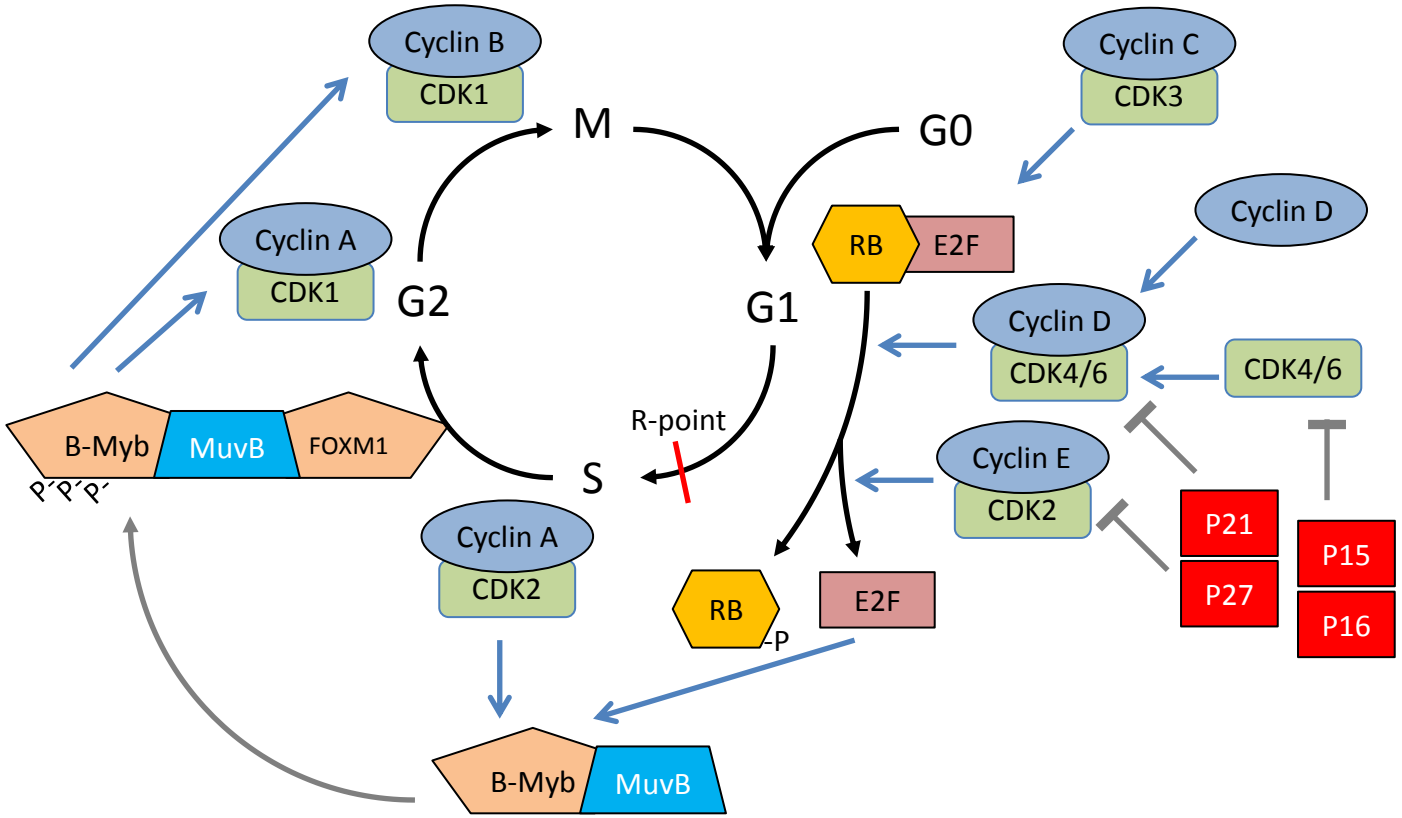


Figure 1.2: B-Myb in the cell cycle
Schematic representing B-Myb interactions during the cell cycle. M – mitosis, S- synthesis, R-point – restriction point, RB – retinoblastoma, CDK – cyclin dependent kinase. Schematic adapted from (Lundberg and Weinberg, 1999, Giacinti and Giordano, 2006, Sadasivam and DeCaprio, 2013)

1.5 Embryonic Stem cells

Embryonic stem cells (ESCs) are pluripotent cells derived from the ICM during the blastocyst stage of embryonic development. They were first isolated from mice in 1981 (Evans and Kaufman, 1981) and it was almost twenty years later that the first human ESCs were generated (Thomson et al., 1998). ESCs naturally differentiate into every cell type found in the organism from which they were derived, giving them great potential for use in regenerative medicine and gene therapy (Thomson et al., 1998, Reubinoff et al., 2000).

It is possible to grow ESCs in culture with a fibroblast feeder layer indefinitely in the presence of leukaemia inhibitory factor (LIF) due to their capacity to self-renew (Reubinoff et al., 2000). ESCs proliferate rapidly, doubling in number every 8 hours, due to a shortened G1 phase of the cell cycle which is caused by cell cycle independent activity of Cyclin A, Cyclin E and CDK2 (Stead et al., 2002, Becker et al., 2006). Despite their great potential there have been very few clinical trials with ESCs. One phase 1 trial was conducted in USA in 2009 to treat spinal cord injury by injecting ESCs into the damaged cord between 7 and 14 days after injury; phase 2 or 3 trials have yet to be conducted (http://clinicaltrials.gov/ct2/show/NCT01217008). Another trial was conducted in 2012 where retinal pigment epithelium derived from human ESCs was transplanted into patients suffering macular degeneration (Schwartz et al., 2012).

There are several problems that have hindered the use of human ESC therapy: (i) ethical issues, (ii) immune system rejection, and (iii) tumour formation that are discussed below.

1.5.1 Ethical issues

The ethical concerns over the use of ESCs in humans are due to the fact that a blastocyst, with the potential to develop into a living organism, is destroyed in the process of deriving the cells (Towns and Jones, 2004).

Although there are ethical issues, couples who are participating in *in vitro* Fertilization (IVF) therapy are given the option to donate spare blastocysts to research. These spare blastocysts can be used to generate ESC lines.

This problem led scientists to try to find other cells with as much therapeutic potential as ESCs, and to explore the use of adult stem cells (ASC) for regenerative medicine. ASCs are small populations of multipotent cells found within the adult body and are used by the organism for the maintenance and the repair of damaged tissue. Examples of ASCs include mesenchymal stem cells and neural stem cells (Caplan, 2007, Baizabal et al., 2003). The problem with the use of ASCs for therapy is that they are low in number, have restrictive differentiation potential and low proliferative rate compared to ESCs.

1.5.2 Immune rejection

Any tissue derived from ESCs that is destined to be transplanted must be tissue matched with the donor otherwise a nuclear transfer from one of the donor's cells into the ESC would need to be completed (Wilmut et al., 1997, Bajada et al., 2008). Tissue matching does not guarantee a successful transplant, an autologous transplant would be much more likely to succeed, however this is not possible as the ESCs would need to be harvested from the patient during the embryonic stages of their development.

1.5.3 Tumour formation

There are two problems that lead to tumour formation when using ESCs for therapy: (i) any tissue derived from ESCs must be free from any undifferentiated ESCs as they would lead to teratoma formation if transplanted (Thomson et al., 1998), and (ii) culturing ESCs can lead to genomic instability and altered karyotype (Amit et al., 2000, Yang et al., 2008). The formation of teratomas appears to occur more often when the injected ESCs contain chromosomal abnormalities (Moon et al., 2011). The tumourgenicity of the ESCs can be overcome by differentiating the ESCs to more mature lineages and ensuring that any transplanted tissue is free from pluripotent cells.

1.6 Somatic reprogramming

In 2006, a ground breaking discovery led to a new and exciting field of research in stem cell biology; that of induced pluripotent stem cells (iPSCs) (Takahashi and Yamanaka, 2006). This work built on the previous discoveries of somatic reprogramming demonstrated in frogs (Gurdon, 1962), sheep (Wilmut et al., 1997) and by cell fusion (Miller and Ruddle, 1976, Tada et al., 2001, Cowan et al., 2005) but refined the process to a small number of transcription factors rather than whole nuclei. iPSCs are generated by introducing the four genes, octamer-binding transcription factor 4 (Oct4), sex-determining region Y box-2 (Sox2), Krüppel-like transcription factor 4 (Klf4) and myelocytomatosis viral oncogene (c-Myc) (herein referred to as OKSM for four factor reprogramming or OSK for three factor reprogramming excluding c-Myc), into somatic cells that reprogram the cells to an ESC-like state and are able to differentiate into any cell type. Following on from his ground breaking work in mice, Yamanaka and colleagues importantly demonstrated that their reprogramming factors could be used to

generate human iPSCs (Takahashi et al., 2007) (Figure 1.3). The field of somatic cell reprogramming has advanced rapidly since the discovery in 2006. Figure 1.4 highlights some of the important discoveries that are helping push somatic reprogramming from the bench to the bedside.

The use of iPSCs in regenerative therapy circumvents the majority of limitations encountered when using ESCs.

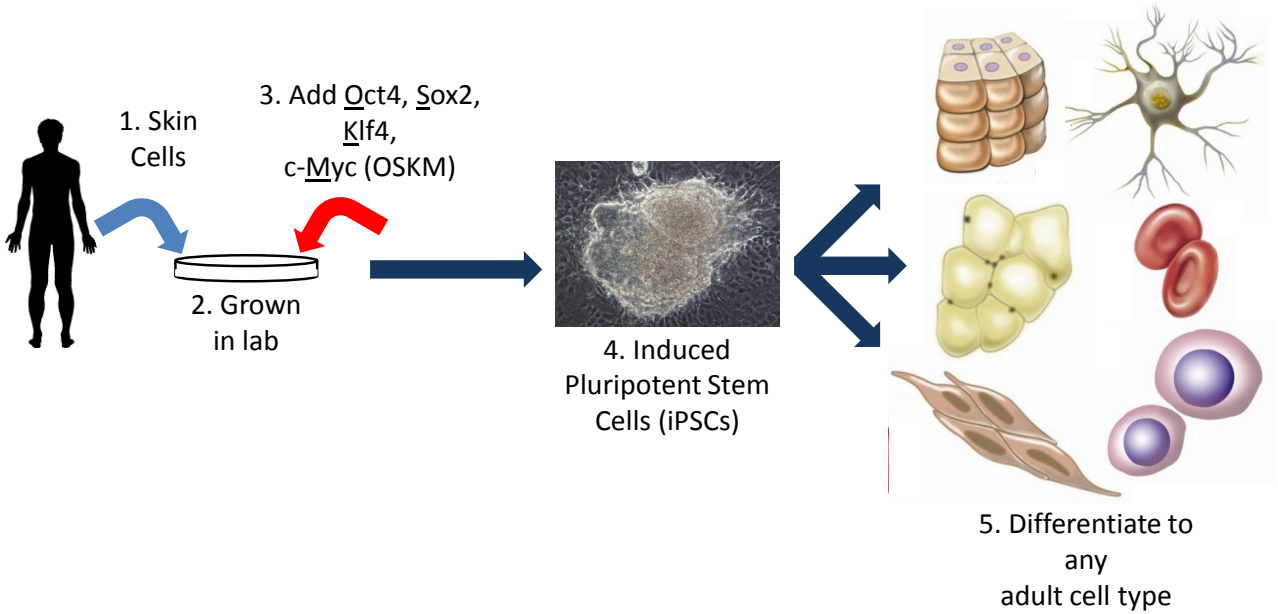


Figure 1.3: The reprogramming process
Schematic representation of the principle of somatic cellular reprogramming. Skin cells can be taken from an adult, cultured in the lab to expand the cell numbers then transduced with a virus containing four genes, Oct4, Sox2, Klf4 and c-Myc (OSKM). A small proportion of the cells transduced will reprogram to induced pluripotent stem cells (iPSCs). iPSCs can be differentiated to any other cell type as they are pluripotent. iPSCs holds great potential for use in personalised regenerative medicine.

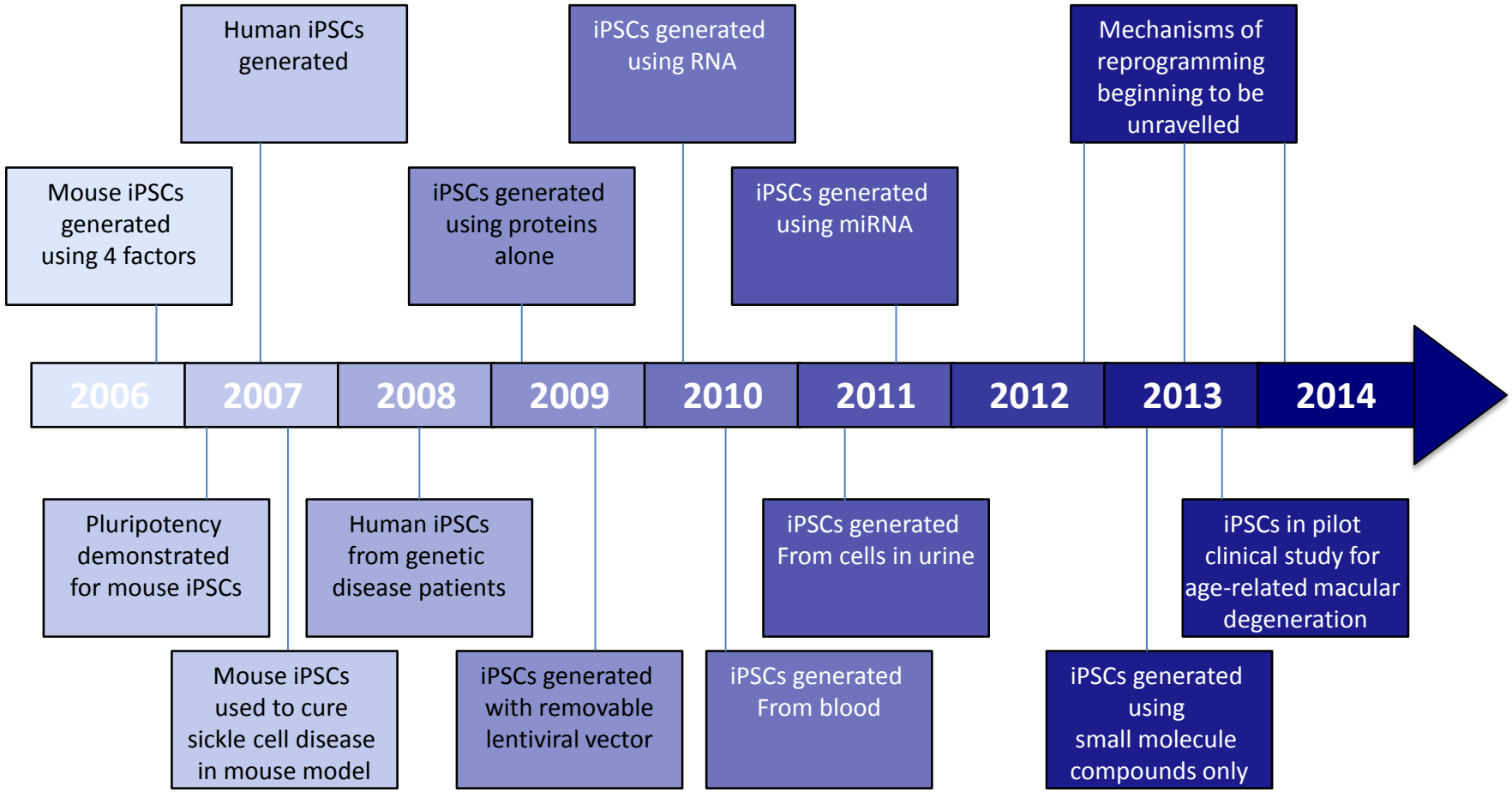


Figure 1.4: The reprogramming field timeline
Since the groundbreaking discovery in 2006, the field of somatic cellular reprogramming has advanced rapidly. Progress has been made on the methods of reprogramming, the cell types that have been reprogrammed and the underlying mechanisms of the process. An early phase clinical trial is underway in Japan only 8 years after discovery.

1.6.1 Ethical issues

Cellular reprogramming addresses the major limitations for ESC based therapies. Firstly, there are no ethical issues as there is no need to destroy a blastocyst; the cells have been generated from a range of adult somatic cells (Aoi et al., 2008, Kim et al., 2008a, Aasen et al., 2008, Staerk et al., 2010, Zhou et al., 2011). The fact that it is possible to generate patient specific iPSCs means there will be no lack of donors; the first human iPSCs were generated from human fibroblasts derived from a skin punch biopsy, a moderately invasive procedure. However, less invasive and non-invasive procedures have now been used to generate iPSCs from other cell types including blood (Staerk et al., 2010), and kidney cells found in urine (Zhou et al., 2011). These methods allow iPSCs to be generated from virtually any patient. Some limitations still need to be considered: it takes substantial time to generate the iPSCs and to fully characterise the iPSCs for pluripotency and genomic integrity. iPSCs generated from donors with different human leukocyte antigens (HLA) could be used to create a cell bank that would cover allogeneic transplantations for large populations (Taylor et al., 2012, Turner et al., 2013). Taylor *et al.* calculated that 150 selected lines with different HLA types would be able to cover 93% of the UK population for matched allograft transplantation. This task would be much easier in iPSCs compared to ESCs due to the availability of donors.

1.6.2 Immune rejection

iPSCs will be important for personalised medicine; they can be created from a patient's own cells, which in theory would not be rejected when transplanted back into the patient. This was demonstrated in a sickle cell anaemia mouse model using gene defect corrected autologous cells (Hanna et al., 2007). Many groups have now shown that iPSC

derived differentiated tissue provoke a negligible immune response when transplanted into autologous mice and monkeys (Araki et al., 2013, Guha et al., 2013, Morizane et al., 2013, Kamao et al., 2014, Hong et al., 2014). Caution will still need to be taken when transitioning into human patients, but the evidence that autologous iPSC derived tissue causes little to no immune response is encouraging.

1.6.3 Tumour formation

Unfortunately the tumourgenicity of iPSCs is similar to ESCs. Problems could arise from the formation of teratomas after the transplantation of iPSCs. Teratoma formation can be solved by purifying derived cells to be certain that no pluripotent cells are transplanted. Nevertheless, due to their rapid proliferation iPSCs can become karyotypically abnormal in the same way as ESCs and will therefore need to be screened for chromosomal changes.

1.6.4 Limitations of somatic reprogramming

There are some limitations with the cellular reprogramming technique. Firstly, the *c-Myc* gene used in the iPSC generation can become reactivated when used to generate chimeric mice, leading to tumour formation (Okita et al., 2007). Cellular reprogramming has been achieved without the addition of c-Myc, but the efficiency was significantly lower than when it was included in the reprogramming cocktail (Nakagawa et al., 2008). Secondly, the use of retroviral vectors to reprogram the cells can lead to insertional mutagenesis and potentially tumour formation (Jonkers and Berns, 1996). A number of groups have tried to deal with the efficiency and insertional mutagenesis concerns by developing new methods to reprogram which avoid integrating viral vectors, including cre-excisable lentiviral vectors (Sommer et al., 2009, Sommer et al., 2010), non-

integrating viral vectors (Stadtfeld et al., 2008, Fusaki et al., 2009), recombinant proteins (Zhou et al., 2009, Kim et al., 2009a), piggyBac transposition (Woltjen et al., 2009), synthetic mRNA (Warren et al., 2010), miRNAs (Anokye-Danso et al., 2011, Miyoshi et al., 2011) and small molecule compounds (Hou et al., 2013).

Thirdly, a problem revealed by Ramos-Mejia *et al.* is that some iPSCs do not silence the reprogramming factors and this may predispose the cells to genomic instability (Ramos-Mejia et al., 2010). This matter can be circumvented by using a non-integrating or excisable reprogramming system. Generating iPSCs with stable genomes will be crucial if iPSCs are ever to be used in regenerative medicine.

Furthermore, iPSCs have been shown to retain an epigenetic memory of the cell from which they were derived, giving them a predisposition to differentiate into lineages similar to the tissue of origin. Thus, this could cause problems with differentiation into other cell types required for transplantation (Kim et al., 2010). The group of George Daley showed that the epigenetic memory was caused by areas of the chromatin remaining methylated after the reprogramming process. These findings were also shown by the groups of Joseph Ecker and Miguel Ramalho-Santos (Lister et al., 2011, Ohi et al., 2011).

For iPSCs to ever transition from the bench to the bedside their safety will need to be determined, especially the genomic integrity of the cells, as instability is a cause of tumour formation. Laurent *et al.* used high resolution single nucleotide polymorphism analysis on human iPSCs and ESCs to show that reprogramming can cause genetic deletions. Interestingly, some of these deletions regressed from the cells during culture (Laurent et al., 2011). Prolonged culture of human ESCs and iPSCs was identified as a

cause of regional chromosomal duplications; this issue will have to be addressed in order to provide a safe supply of cells for transplantation of ESC or iPSC derived cells (Laurent et al., 2011).

Using high-resolution array-based comparative genomic hybridization and karyotyping Martins-Taylor *et al.* demonstrated some chromosomal anomalies that were only present in human iPSCs and not in the original fibroblasts. However most of the genetic alterations found in the human iPSCs tested were also found in human ESCs and likely occurred during culture of the cells (Martins-Taylor et al., 2011).

Timo Otonkoski's group analysed copy number variations (CNVs) in various passages of iPSCs and in the parental fibroblast lines from which the iPSCs were derived. They discovered that there were mutations caused by the reprogramming process but surprisingly at low passage these mutations caused a growth disadvantage to the cells. Therefore, by late passage the CNVs had been lost from the cell lines as cells without mutations gained a growth advantage (Hussein et al., 2011).

Contrary to the previous three studies, the group of Ira Hall showed that in mice, genetic alterations during the reprogramming were generally low and most alterations were also found in the parental fibroblast lines and therefore not caused by the reprogramming process (Quinlan et al., 2011). This could be due to the derivation process leading to more naïve iPSCs in mice compared to human iPSCs.

Similarly, Abzyov *et al.* discovered that half of the CNVs in the human iPSC lines that they analysed were present in the parental fibroblast lines from which the iPSCs were derived (Abyzov et al., 2012).

There is conflicting data on whether the reprogramming process causes mutations. Most of these results were gained using the iPSCs generated through retroviral transduction, other methods of iPSC generation may be less mutagenic and other reprogramming factors may also help to yield iPSCs with less DNA damage. Furthermore, altering culture conditions of the iPSCs, such as modifying oxygen tension, may also help to lower the mutations gained through culture after derivation. Care will have to be taken when generating human iPSC lines and deep sequencing will need to be carried out on the lines in order to identify any mutations. More studies will need to be undertaken to compare the levels of mutation from different reprogramming methods.

1.7 The original Yamanaka factors

24 genes were tested in the original reprogramming experiments based on their role in ESCs (Takahashi and Yamanaka, 2006). Below is a brief introduction on the four that were found to be most efficient.

1.7.1.1 Oct4

Oct4 (octamer binding factor transcription factor 4) belongs to the POU family of transcription factors encoded by the *POU5F1* gene that is expressed in early embryonic development (Scholer et al., 1989a, Scholer et al., 1989b, Scholer et al., 1990). Oct4 plays a vital role in the correct development of the embryo and also in controlling self-renewal of stem cells. *Oct4*$^{-/-}$ blastocysts do not develop past day five due to failure to develop an ICM, highlighting its importance in embryogenesis (Nichols et al., 1998). In ESCs, deregulation of Oct4 expression leads to loss of pluripotency; loss of Oct4 expression causes ESCs to differentiate into trophectoderm, while gain of Oct4 expression induces ESCs to differentiate into mesoderm or endoderm (Niwa et al., 2000). Interestingly, Oct4

was shown to form complexes with Sox2, another reprogramming factor, in embryonic carcinoma cells (Yuan et al., 1995). The groups of Richard Young and Huck-Hui Ng used genome wide ChIP approaches to identify shared binding sites for Oct4, Sox2 and Nanog of which many targets were involved in maintenance of pluripotency (Boyer et al., 2005, Loh et al., 2006). Oct4, Nanog and Sox2 have been shown to form super-enhancer domains which are essential for cell identity in ESCs (Whyte et al., 2013). Recently, it was discovered that lower expression of Oct4 in *Oct4*$^{+/-}$ ESCs leads to more homogenous expression of the core pluripotency factor Nanog (Karwacki-Neisius et al., 2013).

Kim *et al.,* illustrated the importance of Oct4 by reprogramming mouse neural stem cells with only Oct4 (Kim et al., 2009b). Furthermore, the group of Sheng Ding, showed that it is possible to reprogram human keratinocytes using just exogenous Oct4 overexpression and several chemicals, a small molecule activator of phosphoinositide-dependent kinase-1 plus small molecule inhibitors of TGFβ, MEK1 and HDAC (Zhu et al., 2010).

Even in the absence of exogenous Oct4 expression the activation of Oct4 is crucial in generating iPCSs with small molecules alone, as the small molecule, DZNep was shown to decrease methylation around the Oct4 promoter which was essential to achieve reprogramming (Hou et al., 2013).

Overall these studies highlight Oct4 as the most important reprogramming factor.

1.7.1.2 Sox2

Sox2 (Sex-determining region (sry)-related HMG box) is a member of the SOX protein family (Kamachi et al., 2000). The first member of the Sox family to be discovered was the *SRY* gene, which was mapped to the mouse and human sex-determining region on

the Y chromosome (Sinclair et al., 1990, Gubbay et al., 1990). All Sox family proteins contain a single high mobility group (HMG) motif which is a 79 amino acid evolutionarily conserved DNA binding domain (Ner, 1992, Grosschedl et al., 1994). Sox2 is required for development of the ICM and epiblast during embryonic growth, identified by day 3.5 embryonic lethality in mice with Sox2 knocked out (Avilion et al., 2003). In ESCs Oct4 and Sox2 DNA binding sites, which are termed HMG/POU cassettes, are regularly found to be adjacent (Ambrosetti et al., 1997). Increasing the distance between the HMG and POU sites in the FGF4 enhancer was shown to decrease the binding of Oct4 and Sox2 (Yuan et al., 1995, Ambrosetti et al., 1997), whereas decreasing the distance in the DPPA4 promoter was shown to increase binding (Chakravarthy et al., 2008). These studies illustrate the importance of Sox2 and Oct4 as binding partners.

Oct4 and Sox2 have been shown to be central in the transcriptional network of ESCs, interestingly co-occupying the majority of each other's target genes including *nanog* (Boyer et al., 2005, Rodda et al., 2005).

During reprogramming Sox2 is able to reduce expression of Snail, a transcription factor which regulates the mesenchymal to epithelial transition (MET) that is important during early reprogramming (Li et al., 2010b).

1.7.1.3 Klf4

Klf4 belongs to the Krüppel-like factor family of zinc finger transcriptional regulators and was first identified as being crucial for correct differentiation of cells in the epidermis (Segre et al., 1999). Klf4 was later demonstrated to play a role in cell cycle progression (Chen et al., 2001, Chen et al., 2003). Klf4 acts as a transcriptional activator and repressor of important genes that facilitate the reprogramming process. For

example, it has been shown to activate the transcription of E-cadherin, an adhesion protein important for the mesenchymal to epithelial transition (MET) that occurs in fibroblasts undergoing reprogramming (Li et al., 2010b). On the other hand, Klf4 acts as a repressor of the cell cycle regulator p53 (Rowland et al., 2005, Kawamura et al., 2009, Brosh et al., 2013) and the transcription factor Snail (a known repressor of E-cadherin) (Cano et al., 2000), further enhancing the capability of the cells to reprogram.

1.7.1.4 c-Myc

c-Myc (myelocytomatosis viral oncogene) was discovered to be the homolog of v-Myc, a retroviral oncogene which causes leukaemia in birds and cats (Donner et al., 1982). The *Drosophila* homolog Myc is crucial for cellular growth (Johnston et al., 1999). It is a transcription factor, central in the transcriptional network of many cells, which plays a role in the regulation of pluripotency and the control of the cell cycle in ESCs (Singh and Dalton, 2009). Originally thought to bind randomly, c-Myc binding targets have been mapped by genome wide ChIP with over 4000 genes potentially bound by c-Myc (Zeller et al., 2006). Ectopic expression of c-Myc is able to force fibroblasts to enter the cell cycle (Eilers et al., 1989). Interestingly, fibroblasts must be in cycle to be reprogrammed and the reprogramming process itself causes senescence through p53 activity (Banito et al., 2009). This could explain the difference in efficiency when c-Myc is omitted from the reprogramming factors (Nakagawa et al., 2008). The ability of c-Myc to block differentiation may also aid in its ability to increase reprogramming efficiency by forcing cells back towards pluripotency (Cartwright et al., 2005, Schreiner et al., 2001, Selvakumaran et al., 1996). c-Myc has been shown to regulate genes involved in proliferation in ESCs (Chen et al., 2008, Kidder et al., 2008, Kim et al., 2008b); it also regulates transcriptional pause release at its target genes increasing transcription (Rahl

et al., 2010). Furthermore, high levels of c-Myc have been shown to increase transcript abundance of its target genes, including Oct4 and Sox2, by accumulative occupancy at core promoters (Lin et al., 2012). Thus, c-Myc may be playing a role in switching on the endogenous Oct4 and Sox2 expression to establish the core pluripotency network. In addition c-Myc has a role in enhancing the binding of Oct4, Klf4 and Sox2 to chromatin (Soufi et al., 2012).

c-Myc expression, which switches fibroblasts' metabolic program to an ESC state, is only required for the first 5 days of reprogramming in order generate alkaline phosphatase positive staining colonies, illustrating its importance at the beginning of the reprogramming process (Sridharan et al., 2009, Polo et al., 2012).

1.8 The evolution of reprogramming

1.8.1 Transcription factor mediated reprogramming

Since the discovery that only four transcription factors were required to revert a terminally differentiated cell back into an pluripotent state, many researchers have been trying to find other factors that could be used to produce iPSCs.

As mentioned previously, reprogramming was shown to be possible without the oncogene c-Myc, albeit with a significant negative effect on the reprogramming efficiency (Nakagawa et al., 2008).

Nanog's role in the core transcriptional network controlling pluripotency in ESCs makes it an obvious candidate as a reprogramming factor (Boyer et al., 2005). In fact, it was soon after Yamanaka's discovery that the group of James Thomson published their strategy to reprogram human fibroblasts into iPSCs, which employed overexpression of

Oct4, Sox2, Nanog and Lin28 (Yu et al., 2007). Two years later the group of Huck-Hui Ng showed that it was possible to reprogram mouse cells to pluripotency with Oc4, Sox2 and Esrrb (Feng et al., 2009). Esrrb is a direct target of Nanog and overexpression is able to rescue pluripotency and self-renewal block after Nanog deletion in ESCs (Festuccia et al., 2012).

Reprogramming in mice was shown to be possible with several other family members of the Yamanaka transcription factors by exchanging Sox2 with Sox1 or Sox3, Klf4 with Klf2 or Klf5, and c-Myc with L-Myc or N-Myc (Nakagawa et al., 2008).

Heng *et al.* screened nuclear receptors in mice and identified orphan nuclear receptors Nr5a1 and Nr5a2 as potential substitutes for Oct4 in three or four factor reprogramming (Heng et al., 2010). The nuclear receptors in the Nr5a family are upstream activators of Oct4 and Nanog (Gu et al., 2005, Silva et al., 2009), and are able to induce pluripotency (Guo and Smith, 2010).

Due to concerns over using c-Myc in the reprogramming cocktail Yamanaka and colleagues used Glis1 in combination with Oct4, Sox2 and Klf4 to generate iPSCs from mouse and human fibroblasts. Addition of Glis1 improved efficiency of reprogramming and promoted more ESC like colonies than the original four factors (Maekawa et al., 2011). Glis1 is a transcription factor that controls gene expression during early development in mice (Kim et al., 2002, Maekawa et al., 2011).

These studies merely tweaked the original reprogramming factors, exchanging one or two with factors that were related or upstream of the substitutes. A single cell analysis of secondary reprogramming using doxycycline inducible Oct4, Sox2, Klf4 and c-Myc expression in MEFs found several alternative sets of genes that could reprogram MEFs

to pluripotency, some including the original factors and others that did not include any of the original factors (Wernig et al., 2008, Buganim et al., 2012). The group of Rudolf Jaenisch showed that the combination of Lin28, Sall4, Esrrb and Nanog or the combination of Lin28, Sall4, Esrrb and Dppa2 are able to induce reprogramming (Buganim et al., 2012). This was an important discovery as it demonstrated that there are multiple pathways to reprogramming and it reinforced the requirement to activate the core pluripotency network in the cells for them to become fully pluripotent.

1.8.2 Epigenetic regulators in reprogramming

The group of Shaorong Gao successfully reprogrammed fibroblasts by using epigenetic remodelling enzymes Rcor2 and Tet1 as an alternative to Sox2 and Oct4, respectively (Yang et al., 2011, Gao et al., 2013). Interestingly, Shinagawa *et al* replaced Sox2 and c-Myc with two histone variants that are highly expressed in oocytes. This approach attempted to harness the natural processes of development to assist the reprogramming (Shinagawa et al., 2014). Knocking down the expression of DOT1L (H3K79 histone methyltransferase) caused loss of H3K79me2 marks from pluripotency genes including Nanog and Lin28 early in the reprogramming process, leading to an increase in reprogramming efficiency, speeding up the process, and permitting reprogramming in human cells with just Oct4 and Sox2 (Onder et al., 2012).

1.8.3 P53 in reprogramming

P53 knockdown and knockout was shown to significantly increase reprogramming efficiency and enable reprogramming with just Oct4 and Sox2 in mouse cells (Kawamura et al., 2009, Marion et al., 2009). P53 expression has been shown to be a road block of reprogramming and increased expression negatively correlates with reprogramming

efficiency (González et al., 2013). Nahum Sonenberg's group knocked out p53 and eukaryotic translation initiation factor 4E (eIF4E) binding proteins in MEFs and reprogrammed mouse cells to pluripotency with exogenous expression of Oct4 alone (Tahmasebi et al., 2014). These knockouts will clearly not be useful in developing human iPSC for use in therapies as the deletions are likely to lead to tumour formation, they do however help towards elucidating the molecular mechanisms of reprograming.

1.8.4 microRNAs in reprogramming

microRNAs (miRNAs) have been shown to play a role in gene regulation throughout evolution so it is not surprising that manipulation of miRNAs has been used to affect the reprogramming process. The group of Robert Blelloch were first to harness miRNAs in reprogramming. They showed that three miRNAs that are specific to ESCs were able to replace c-Myc and produce a more homogenous population of iPSCs when combined with Oct4, Sox2 and Klf4 (Judson et al., 2009). The let-7 miRNA family was shown to lower reprogramming efficiency in human cells. Blocking let-7 miRNA during reprogramming leads to a reprogramming efficiency similar to OSKM but with only OSK (Worringer et al., 2014). These two papers revealed that reprogramming is achievable by modifying the original factors and adding or removing miRNAs. The groups of Edward Morrisey and Masaki Mori have shown that it is possible to reprogram using only miRNAs from clusters miR302 and 367 with the HDAC inhibitor valproic acid (Anokye-Danso et al., 2011), or with clusters mir-200c, 302 and 369 (Miyoshi et al., 2011).

1.8.5 Chemical reprogramming

The histone deacetylase inhibitor valproic acid has been shown to increase reprogramming efficiency and enable reprogramming in mice with OSK alone, achieving a similar efficiency as it is observed with OSKM (Huangfu et al., 2008a). It also allows reprogramming of human cells with Oct4 and Sox2 alone (Huangfu et al., 2008b). This work highlighted histone deacetylation as a potential barrier to reprogramming. Klf4 can be replaced by a small molecule called kenpaullone or bone morphogenetic proteins in reprogramming mice cells to iPSCs (Lyssiotis et al., 2009, Chen et al., 2011). Vitamin C has been shown to enhance reprogramming efficiency through prevention of senescence and demethylation of MEFs (Esteban et al., 2010, Wang et al., 2011). The groups of Kevin Eggan and Konrad Hochedlinger both showed transforming growth factor-beta (TGF-β) inhibition through small molecules was enough to substitute for Sox2 and c-Myc in the reprogramming cocktail used to produce mouse iPSCs (Ichida et al., 2009, Maherali and Hochedlinger, 2009). The most exciting development in chemical reprogramming was the discovery that it is possible to reprogram mouse cells to iPSCs with no ectopic genes at all; Hou *et al.* used four small molecule chemicals, forskolin, a TGF-β inhibitor, a glycogen synthase kinase 3 inhibitor and a S-adenosylhomocysteine hydrolase inhibitor (Hou et al., 2013). This combination was enough to reprogram mouse but not human cells to pluripotency. Exogenous Oct4 is still required for reprogramming human cells to iPSCs (Zhu et al., 2010). Human iPSCs derived through purely chemical reprogramming is an exciting prospect as there is no risk of insertional mutagenesis. There are still risks as the drugs used to reprogram the cells may be altering metabolic, DNA damage and other pathways that could modify the cells to the point that they are not useful in therapeutic treatment, so these cells will need to be screened to compare them with

iPSCs generated through other means in order to determine which method of production generates the safest cells to employ.

1.9 The mechanism of reprogramming

With the huge potential for regenerative medicine and the much simplified reprogramming strategy compared to nuclear transfer, a whole new discipline of biology has been created that is trying to unravel the molecular mechanisms of reprogramming.

The reprogramming process is able to turn a somatic genome into an ESC like genome based upon global analyses of histone modifications and methylation studies (Maherali et al., 2007, Mikkelsen et al., 2008). Histone modifications can also impair the reprogramming process, illustrated by the ability of vitamin C to overcome a pre-iPSC H3K9 methylation block (Chen et al., 2013).

Integrating the reprogramming genes into the genome of the mice allows the derivation of cells which all contain the reprogramming genes, thus avoiding the low efficiency limitations of traditional gene delivery systems. This is called secondary reprogramming. The generation of mice with the four reprogramming genes knocked into the genome under the control of a doxycycline inducible promoter has allowed the molecular mechanisms of reprogramming to be studied in much greater detail (Stadtfeld et al., 2010).

1.9.1 Tracking reprogramming through surface antigens

Extensive genome wide analysis of these secondary reprogrammable cells by Polo *et al.* showed that the reprogramming process has two distinct waves of transcription

mediated by c-Myc and Klf4 (first wave) and then Oct4, Sox2 and Klf4 (second wave). The group of Konrad Hochedlinger also identified Thy1 as a useful surface marker that is present on MEFs but is lost as pluripotency is induced. This was used in combination with SSEA1, a marker of pluripotency in mouse cells, to track the progress of reprogramming (Polo et al., 2012).

The use of surface markers to track the progress of reprogramming was refined by O'Malley *et al.* who used ICAM-1 and CD44 to track the reprogramming in secondary reprogrammable MEFs which also contained a GFP reporter gene under the control of the Nanog promoter (O'Malley et al., 2013). The group of Keisuke Kaji showed that the ICAM-1 and CD44 staining had more sensitivity in progression through the reprogramming process than Thy1 and SSEA1.

1.9.2 Epigenetic remodelling

In order for somatic cells to reprogram to iPSCs the whole epigenetic landscape must be altered, the hyper methylation of pluripotency genes typified by differentiation must be removed in order for the cells to regain a pluripotent phenotype. Overexpression of two members of the ATP-dependent BAF chromatin remodelling complex increased reprogramming efficiency with OSKM significantly, through increased and more rapid de-methylation of Oct4, Nanog and Rex1 promoters (Singhal et al., 2010). If DNA de-methylation is unsuccessful reprogramming cells can become trapped in a pre-iPSC state (Mikkelsen et al., 2008). Furthermore, the H3K27 demethylase Utx is required for reprogramming to proceed in MEFs (Mansour et al., 2012). In addition to this, H3K9 methylation was identified as a roadblock in the reprogramming process; Vitamin C

treatment lowered H3K9 methylation in pre-iPSCs and converted them to iPSCs (Chen et al., 2013).

Early in the reprogramming process over 100 promoters gain the H3K4me2 marker which is associated with actively transcribed chromatin (Koche et al., 2011). Fibroblast specific genes become marked with H3K27me3 silencing marks, whilst pluripotency genes lose H2K27me3 marks (Koche et al., 2011).

1.9.3 Models of reprogramming

The pathway from differentiated cell to reprogrammed iPSC is still not fully understood and different analyses have led to multiple models of how reprogramming proceeds. The stochastic model claims that the change for a cell to reprogram to an iPSC is a random occurrence in the cell population. By decreasing the doubling time of the cells there would be an increase in the probability that the random events that need to occur in the cells to reprogram will happen (Figure 1.5A) (Hanna et al., 2009).

Another model proposed by the group of Rudolf Jaenisch is that there is a stochastic phase at the beginning of reprogramming; once a cell has passed that phase the rest of the process is deterministic (Figure 1.5B) (Buganim et al., 2012).

The group of Konrad Hochedlinger proposed a model based on their analysis of MEFs undergoing reprogramming. They proposed the existence of two phases of transcriptional activity in the MEFs: the first wave (occurring in the first 3 days) involves the loss of MEF identity, mesenchymal to epithelial transition and a boost in proliferation; the second wave was at day 9 in which the core pluripotency network was activated and the epigenetic remodelling took place (Figure 1.5C) (Polo et al., 2012).

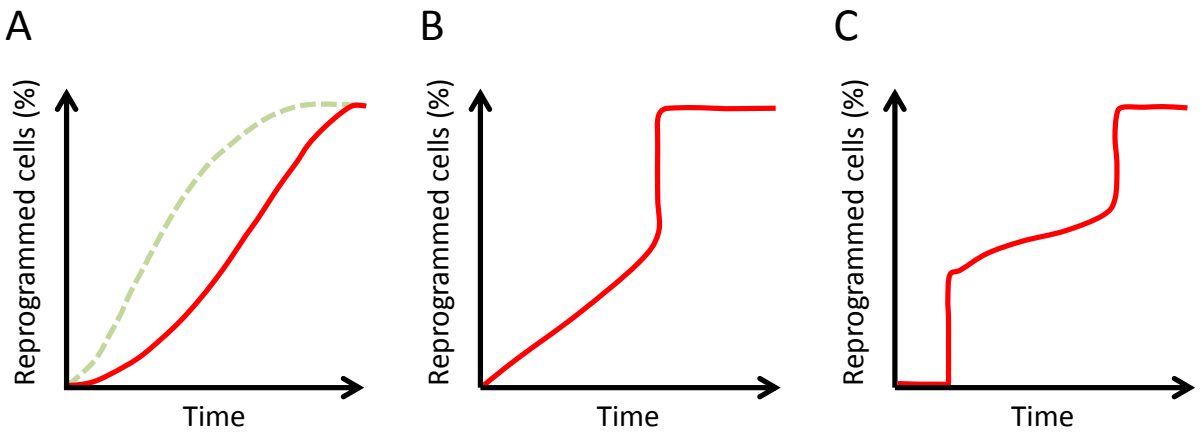


Figure 1.5: Proposed models of reprogramming
Three proposed Models of reprogramming. (A) The stochastic model (red line), which is amenable to acceleration (green line)(Hanna et al., 2009). (B) The stochastic and then deterministic model (Buganim et al., 2012). (C) Two wave of transcriptional activity model (Polo et al., 2012). Graphs adapted from (Theunissen and Jaenisch, 2014).

1.10 B-Myb transcription factor and its possible role in cellular reprogramming

Previous work done in my research group has shown the importance of B-Myb in safeguarding the integrity of the genome in ESCs through the regulation of key cell cycle genes such as c-Myc and FoxM1 (Lorvellec et al., 2010). The maintenance of genome stability and the c-Myc gene are known to have important roles for the reprogramming process (Hong et al., 2009, Kawamura et al., 2009, Kinoshita et al., 2011).

Tarasov *et al.,* presented data showing that B-Myb knockdown decreases Oct4 expression and conversely B-Myb overexpression leads to increased Oct4 expression (Tarasov et al., 2008). However, Lorvellec *et al.* showed that complete knockout of B-Myb in ESCs did not alter the expression of Oct4 (Lorvellec et al., 2010). These discrepancies could be due to the two different approaches to knockdown/knockout B-Myb.

B-Myb knockout causes c-Myc to be down regulated in ESCs. Furthermore, ectopic c-Myc expression is able to rescue stalled replication fork phenotype seen in B-*myb*$^{-/-}$ ESCs (Nakagoshi et al., 1992, Gualdrini et al., 2010, Lorvellec et al., 2010).

These previous data in combination with the facts that: (i) B-Myb expression is between 1000-10000x higher in ESCs and iPSCs compared to other somatic cells (Tarasov et al., 2008); (ii) B-Myb as well as Oct-4 and Sox2 are required for ICM formation (Tanaka et al., 1999, Niwa et al., 2000, Avilion et al., 2003); (iii) that during cellular reprogramming, B-Myb RNA levels start increasing at day 2, earlier than other pluripotent factors such as nanog (O'Malley et al., 2013), and (iv) in ESCs the technique Chromosome conformation capture combined with sequencing (4C) recently illustrated that B-Myb has more contacted active regions in chromosomes than Nanog (de Wit et al., 2013), form compelling evidence for an important role for B-Myb in cellular reprogramming.

1.11 Aims

iPSCs could be the ideal cell source for curing any disease with a degraded or damaged cellular component. Understanding the molecular mechanisms of reprogramming and improving the efficiency of reprogramming and/or producing iPSCs with greater genomic stability will be crucial if iPSCs are to be used extensively in regenerative medicine.

The aim of this project is to investigate the role of B-Myb in reprogramming and iPSC generation. The aim will be met by achieving the following objectives:

1. To generate iPSCs from MEFs harbouring modified B-*myb* alleles and from wild type MEFs.
2. To ablate B-Myb from iPSCs using cre loxP technology and to compare viability, genome instability and DNA damage markers in iPSCs with wild type, half and no B-Myb expression.
3. To determine if B-Myb expression is crucial in MEFs for reprogramming to proceed.
4. To analyse the efficiency of reprogramming with the B-*myb* gene added into the pluripotency cocktail.
5. To corroborate reprogramming studies with B-Myb overexpression in a secondary reprogramming system.

CHAPTER 2: MATERIALS AND METHODS

2.1 Cell culture and growth conditions

293T cells were grown in Dulbecco's modified eagle medium (DMEM) with 1% Penicillin/Streptomycin (5000U/ml), 2mM L-glutamine (all from Gibco) and 10% foetal bovine serum (FBS, Sigma). Referred to herein as 293T medium.

MEFs were grown in DMEM with 1% Penicillin/Streptomycin (5000U/ml), 2mM L-glutamine, 10-20% FBS and 0.1mM 2-mercaptoethanol (Sigma). Referred to herein as MEF medium.

MEFs undergoing nuclear reprogramming were grown in DMEM with 1% Penicillin/Streptomycin (5000U/ml), 2mM L-glutamine, 5% ESC qualified FBS (Hyclone, Fisher Scientific), 1% non-essential amino acids (Gibco), 0.1mM 2-mercaptoethanol and 0.01% LIF (Leukemia inhibitory factor, 10^6U/ml, Millipore). Referred to herein as iPSC medium.

iPSCs or ESCs were cultured on a feeder layer of mitotically inactivated MEFs and in Knock out-DMEM (KO-DMEM, Gibco) with 1% Penicillin/Streptomycin (5000U/ml), 2mM L-glutamine, 1% non-essential amino acids, 15% serum replacement (Gibco), 0.01% LIF (10^6U/ml), 0.1mM 2-mercaptoethanol, 3uM GSK3 inhibitor (CHIR99021, Millipore) and 1uM MEK1 inhibitor (PD0325901, Millipore). Referred to herein as ESC medium.

Cells were frozen by collecting the cells by centrifugation at 300 x g for 5 minutes, then resuspending the resultant pellet in 500µl cell specific medium then adding 500µl 2x

freezing medium (40% cell specific medium, 40% FBS/serum replacement, 20% DMSO) drop-wise. This cell suspension was then added to a 1ml cryotube (Greenier Bio One) and stored at -80°C for at least 24 hours before being transferred to liquid nitrogen storage (-150°C).

2.2 Lentiviral production

The Oct4,-Sox2-Klf4-c-Myc (OSKM), Zs-Green (GFP) and Oct4-Sox2-Klf4-mCherry (OSK) lentiviral backbone plasmids and the plasmids used for packaging the lentiviruses were generously provided by our collaborator George Murphy (Boston University, USA). The lentivirus particles used in this study were grown using a previously described method (Mostoslavsky et al., 2006). Briefly, each lentivirus was generated by combination of one backbone plasmid and all four packaging plasmids (Table 1). 90µl of Trans-IT 293T (Mirus Bio) was added to 2ml DMEM, mixed, then incubated at room temperature for 10 minutes. The plasmid mixture was added to the Trans-IT/ DMEM mixture, mixed and incubated for 15 minutes. The media on $25x10^6$ 293T in a 15cm tissue culture dish was removed and 11ml fresh 293T media was added back to the cells. The Trans-IT/DMEM/DNA mixture was added dropwise to the plate of 293T cells. The cells were incubated in a humidified atmosphere at 37°C with 5% CO_2. The following day the media on the cells was aspirated and 12.5ml fresh 293T media was added to the plate. The cells were returned to the incubator. Lentiviral supernatant was collected at 48, 60 and 72 hours after transfection. 12.5ml fresh 293T media was added back to the cells after each collection. After the final collection lentiviral supernatant was passed through a sterile 0.45µm filter and centrifuged at 35500 x g for 90 minutes. Supernatant was removed

and the pellet was rested on ice for 2 hours. The pellet was resuspended in the remaining supernatant, aliquoted and then frozen at -80°C.

Table 1: Backbone plasmids

Plasmid	**Backbone/Packaging**	**Amount per viral prep (µg)**
pHAGE-2-EF1a-mOSKM-loxP	Backbone	24
pHAGE-2-EF1a-mOSKM	Backbone	24
pHAGE-2-EF1a-mOSKM-Cherry-loxP	Backbone	24
pHAGE-2-EF1a-ZsGreen	Backbone	24
pRRL-PGK-IRES-B-*myb*	Backbone	24
pLV-CreEGFP	Backbone	24
pHAGE-2-EF1a-mOSKB	Backbone	24
pHAGE-2-EF1a-*AmCyan*	Backbone	24
pHAGE-2-EF1a-B-*myb*:*AmCyan*	Backbone	24
pHDM-tat1b	Packaging	1.2
pREV	Packaging	1.2
pHDM-Hgpm2	Packaging	1.2
pHDM-VSV-G	Packaging	2.4

2.3 Lentiviral titration

2.3.1 Flow cytometric titration

All wells of a 6 well culture plate plus one well in a second 6 well culture plate were seeded with 10^6 293T cells. The cells were incubated at 37°C overnight and the following day the medium was aspirated from each of the 6 wells and 1ml of 293T medium with 5-8µg/ml polybrene (Sigma) was added to each well. The wells were infected as shown in the following diagram that represents a 6 well culture plate:

No virus	10µl un-concentrated virus	100µl un-concentrated virus
0.01µl concentrated virus	0.1µl concentrated virus	1µl concentrated virus

The single well on the second 6 well culture plate was used to count the number of cells at the time of infection. The virally infected plate was incubated at 37°C for 24 hours. After 24 hours medium was aspirated and 2ml fresh 293T medium was added to each well. The cells were then incubated at 37°C for a further 72 hours. The titer of the virus was calculated by analysing each well for the percentage of fluorescent cells using a Beckman Coulter Cyan or BD biosciences LSRFortessa flow cytometer. The equation below was used to determine the concentration of the lentiviral preparations.

$$\text{Number of cells in the well} \times \text{percentage fluorescent positive} = \text{number of virions per volume virus added}$$

The number of virions per ml was used when determine what volume of lentivirus preparation to add to cells based on the following equation, where a multiplicity of infection (MOI) was selected between 1 and 20. MOI 1 equals a ratio of 1 virion per cell; this however does not mean all the cells will become transduced as the infectivity of the lentivirus may not be 100%.

$$\frac{\text{MOI} \times \text{number of cells to be transduced}}{\text{virions per ml in preparation}} = \text{ml of preparation required}$$

2.3.2 qPCR Titration

Viruses without fluorescent reporter genes were titrated using a Lenti-X qRT-PCR Titration Kit (Clontech). Viral RNA was isolated from 15µl of concentrated lentiviral supernatant. The viral particles were lysed by addition of 600µl of buffer RAV1 that contained carrier RNA. After mixing 600µl 100% ethanol (VWR) was added and the mixture was pipetted into a NucleoSpin RNA Virus Column inside a collection tube. RNA was bound to the column by centrifugation for 1 minute at 8000 x g. The column was placed into a new collection tube and 500µl of buffer RAW was added to the column before centrifugation at 8000 x g for 1 minute. Flow-through was discarded and 600µl of buffer RAV3 was added to the column and the tube was centrifuged for 1 minute at 8000 x g. Flow-through was discarded and 200µl of buffer RAV3 was added to the column and the tube was centrifuged at 11000 x g for 5 minutes. The column was then placed in a new collection tube and centrifuged for 3 minutes at 11000 x g. The column was then placed into a sterile 1.5ml centrifuge tube. 50µl of 70°C RNAse-free H_2O was added to the column and then incubated at room temperature for 2 minutes before centrifugation for 1 minute at 11000 x g. 12.5µl of lentiviral RNA was mixed with 2.5µl DNase I Buffer (10x), 4µ DNase I (5U/µl) and 6µl RNase-Free H_2O. The DNase I mixture was incubated

at 37°C for 30 minutes and then 70°C for 5 minutes in a thermocycler. The RNA was serially diluted by 1:10 3 times in EASY dilution buffer. The Lenti-X RNA control template was serially diluted by 1:10 4 times in EASY dilution buffer. 2µl of the diluted RNA and RNA control was pipetted in duplicated into wells of a 96 well qPCR plate (Applied Biosystems). 2µl of EASY dilution buffer was added to 6 wells as no-template control. 23µl of master mix (8µl RNase-Free H_2O, 12.5µl Quant-X Buffer (2x), 0.5µl Lenti-X Forward Primer (10µM), 0.5µl Lenti-X Reverse Primer (10µM), 0.5µl ROX reference Dye (50x), 0.5µl Quant-X Enzyme and 0.5µl RT Enzyme mix) was added to each well. The plate was sealed with a sheet of optical adhesive film (Applied Biosystems) and centrifuged at 800 x g for 2 minutes. The plate was placed in an Agilent Technologies Stratagene Mx3005P qPCR machine and the following reaction conditions were used for the reverse transcriptase reaction: 42°C for 5 minutes, 95°C for 10 seconds. The PCR reaction conditions used were: 40 cycles of 95°C for 5 seconds and 60°C for 30 seconds with SYBR green fluorescence measurement at the end of each cycle. Finally the products were dissociated with the following reaction conditions: 95°C for 15 seconds and 60°C for 30 seconds with SYBR green fluorescence measurement at each degree of dissociation. The Lenti-X control RNA template Ct values were used to calculate a lentiviral standard curve that was used to extrapolate the copy numbers per ml of the produced lentiviruses.

2.4 Primary reprogramming

MEFs were reprogrammed using lentiviral particles containing one of four backbones (pHAGE-2-E1a-mOSKM-loxP, pHAGE-2-E1a-mOSKM, pHAGE-2-E1a-mOSKM-Cherry-loxP or pHAGE-2-E1a-mOSKB). Generally reprogramming was carried out in 0.1%

gelatin coated 6 well or 12 well plates with 10^5 or 5 x 10^4 MEFs per well, respectively. MEFs were transduced in the presence of 5µg/ml polybrene (Sigma) with between 1 and 20 lentiviral particles per cell diluted in full MEF medium one day after plating. The cells were incubated at 37°C for 24 hours before the infections were stopped by aspiration of the lentivirus containing medium and addition of fresh iPSC medium. The medium on the cells was changed every 48 hours. If colonies were to be isolated the medium was changed to ESC medium when colonies were observed using an inverted microscope (Zeiss, Axiovert 25).

2.5 Secondary reprogramming

10% MEFs containing the four reprogramming factors under doxycycline control were mixed with 90% wild type MEFs and plated onto 0.1% gelatin coated six well plates at a cell density of 10^5 per well. Reprogramming was initiated by addition of 300ng/ml Doxycycline hyclate (Sigma) to the culture medium. The cells were cultured in iPSC medium with 10µg/ml vitamin C (Sigma). The cells were given fresh medium with doxycycline every 48 hours and reprogramming progress was monitored by inverted fluorescence microscopy and analysed by flow cytometry.

2.6 Individual iPSC Colony isolation

The cells were washed with PBS three times. 1ml of PBS was added to each well and a colony was identified through the 10x microscope. The identified colony was dislodged from the surrounding MEFs using a clean pipette tip cutting around the edges of the colony then withdrawing the colony into the pipette. The colony was added to 50µl Trypsin-EDTA (1x, Gibco) and incubated at 37°C for 2 minutes. 50µl of ESC medium

containing trypsin inhibitor (2X, Gibco) was added to the cells before transferring them to a 12 well tissue culture plate previously coated with mitotically inactivated MEFs.

2.7 Flow Cytometric analysis of reprogramming process

MEFs undergoing reprogramming were trypsinised to gain a single cell suspension then centrifuged at 300 x g for 5 minutes. The cell pellet was resuspended in 1ml 5% FBS/PBS then centrifuged again at 500 x g for 3 minutes. The MEFs were incubated in 100µl of anti-CD44-APC and anti-CD54-biotin antibodies (both from eBioscience) diluted 1:300 and 1:100 in 5% FBS/PBS respectively. The cells were incubated on ice for 10 minutes and then washed three times by centrifugation at 300 x g for 3 minutes, removing the supernatant and resuspending the cell pellet in 200µl of 5% FBS/PBS. The cells were then resuspended in 100µl of anti-streptavidin-PE-Cy7 antibody (Beckton Dickenson) diluted 1:1500 in 5% FBS in PBS. The sample was incubated for 5 minutes on ice then washed three times as above. Finally the cells were resuspended in 400µl of 5% FBS in PBS and passed through a 50µl Celltrics filter (Partec). The CD44 and CD54 expression was analysed by BD biosciences LSRFortessa flow cytometer.

2.8 Mice

Oct4-GFP mice (B6;129S4-*Pou5f1*$^{tm2(EGFP)Jae}$/J, The Jackson Laboratory) were crossed with B-*myb*$^{+/\Delta}$ and B-*myb*$^{+/F}$ mice (Garcia et al., 2005), for two rounds to generate B-*myb*$^{+/\Delta}$:*Oct4-GFP*^{Hm} and B-*myb*$^{+/F}$:*Oct4-GFP*^{Hm} mice. Next these mice were crossed with Cre-ER^{T2} mice (B6.129-*Gt(ROSA)26Sor*$^{tm1(cre/ERT2)Tyj}$/J , The Jackson Laboratory) to generate B-*myb*$^{+/\Delta}$:*Oct4-GFP*^{Hm}:*Cre-ER*^{T2,Hm} and B-*myb*$^{+/F}$:*Oct4-GFP*^{Hm}:*Cre-ER*^{T2,Hm} mice. These were then used to set up timed matings to obtain embryos with B-*myb*$^{F/\Delta}$:*Oct4-GFP*^{Hm}:*Cre-ER*^{T2,Ht} or B-*myb*$^{+/\Delta}$:*Oct4-GFP*^{Hm}:*Cre-ER*^{T2,Ht} to be used for experiments. *P53*$^{+/-}$

mice were a generous gift from Jorge Caamano, University of Birmingham. *P53*$^{+/-}$ mice were crossed together to generate embryos that were *P53*$^{-/-}$.

2.9 MEF derivation

Embryos were removed from the mother at 13.5 d.p.c. and placed into a 10cm dish with 10ml PBS. The foetal liver, heart and cerebellum were discarded from each embryo. A sample of the embryo gut was kept at 4°C and used for genotyping. The remaining tissue was placed into 1 well of a 24 well plate. 200µl 1x Tryspin-EDTA (Invitrogen) was added to the well and the plate was placed on an angle, to ensure the tissue was submerged in the trypsin, then placed in an incubator at 37°C for 10 minutes. 800µl complete MEF medium was added to the well and the tissue was dissociated using a 1ml pipette. The dissociated tissue was then gently added to the top of 9ml complete MEF medium in a 15ml centrifuge tube and the larger debris were allowed to settle for 2 minutes. To avoid the larger debris at the bottom of the tube 9.5ml of the MEF medium containing the dissociated cells was added to a 10cm tissue culture dish previously coated with 0.1% gelatin. The cells were incubated at 37°C for 48 hours then dissociated with 1x Trypsin-EDTA, centrifuged at 300 x g for 5 minutes and $4x10^6$ frozen in 1ml of 10% DMSO, 25% FBS in MEF medium at -80°C.

2.10 Feeder MEFs

Feeder MEFs were mitotically inactivated by irradiation or mitomycin treatment. MEFs were expanded until passage 4, and then irradiated in suspension with 20 grays of ionising radiation from a Caesium-137 source. The MEFs were then ready to be plated for use in experiments or frozen for long-term storage.

Alternatively MEFs were inactivated using mitomycin C (Sigma). 2mg of mitomycin C was dissolved in 10ml of PBS, once completely dissolved the 10ml mitomycin C was added to 190ml of complete MEF medium to give a final concentration of 10µg/ml. The medium was aspirated from the passage 4 MEFs and 10-20ml of mitomycin C was added to the plates dependant on the size of the plate. The cells were incubated at 37°C for 2 hours, and then the MEFs were washed twice with 10-20ml of PBS. The MEFs were then ready to be used in experiments or frozen for long-term storage.

2.11 Genomic DNA extraction for genotyping

DNA was extracted from mouse cells or tissue by incubating the cells at 95°C for 20 minutes in 50µl lysis buffer (25mM NaOH, 200µM EDTA). The lysis reaction was stopped by adding 50µl stop buffer (40mM Tris.HCl pH7.5). 1µl was used per PCR reaction.

DNA was extracted from iPSC colonies by picking an individual colony in 20µl of phosphate buffered saline (PBS, Gibco) and incubating at 95°C for 5 minutes. The cells were cooled on ice for 1 minute then 1µl of Proteinase K (Roche) was added and the sample was incubated at 37°C for 20 minutes. The enzyme was deactivated by incubation at 95°C for 5 minutes. 1µl of the DNA was used per PCR reaction.

2.12 Polymerase chain reaction (PCR) for genotyping

PCR was used to genotype with the following conditions: 94°C for 5 minutes, 39 x (94°C for 40 seconds, 56°C for 40 seconds, 72°C for 40 seconds). Each reaction contained 1µl DNA, 22µl PCR Reddymix (Thermo Scientific), 0.1µl forward primer and 0.1µl reverse primer (Table 2). PCR products were separated by gel electrophoresis on 2.5% agarose gels. Gels were imaged with Bio-Rad Gel Doc™ XR+ System.

Table 2: Primers used in genotyping

Primer name	Sequence	Concentration (µM)	Purpose
E2 281U	TAC TAC TTA GAG AGA CTG CC	100	B-*myb*$^{\Delta}$ allele genotyping
I5 2460U	TAA TAA AGG AGT GTC TCA GA	100	B-*myb*^{F} allele genotyping
I5 2563L	CTC TTT AGA CAG GCC ATT C	100	B-M*yb*^{F} and Δ allele genotyping
CreEx-F	GGA ACT CTT GTG CGT AAG TCG ATA G	100	Cassette excision check
CreEx-R	GGA GGC GGC CCA AAG GGA GAT CCG	100	Cassette excision check

2.13 PCR for cloning

PCR was used to clone *Sox2*, B-*myb* or *AmCyan* from plasmid DNA with the following conditions: 30 cycles of (98°C for 10 seconds, 60°C for 15 seconds, 68°C for 3 minutes). Each reaction contained 10ng of plasmid DNA (pHAGE-2-E1a-mOSKM-Cherry-loxP, pMB21 or pAmCyan respectively), 4µl dNTPs (2.5mM each, Takara Bio Inc), 1µl GXL polymerase (1.25U, Takara Bio Inc), 10µl PrimeSTAR GXL Buffer (1X, Takara Bio Inc), 0.1µl forward primer, 0.1µl reverse primer (Table 3) and dH_2O up to 50µl final volume.

Table 3: Primers used in cloning

Primer name	Sequence	Concentration (μM)	Purpose
Sox2 5' NdeI	GGT TTC TTA CAT ATG ATG TAT AAC ATG ATG GAG ACG GAG CTG AAG	100	Clone *Sox2* gene with additional NdeI site at 5' end
Sox2-E2A 3'	TTT CAA CAT CGC CAG CGA GTT TCA ACA AAG CGT AGT TAG TAC ATT GCC CAC TAC CCA TGT GCG ACA GGG GCA GTG TGC CGT TAA TGG CCG	100	Clone *Sox2* gene with additional *E2A* gene at 3' end
E2A-B-myb 5'	CTT TGT TGA AAC TCG CTG GCG ATG TTG AAA GTA ACC CCG GTC CTA TGT CTC GGC GGA CGC GCT GCG AGG ATC TGG ATG	100	Clone B-*myb* gene with additional *E2A* gene at 5' end
B-myb 3' ClaI	GGT TTA TCG ATT CAG GAC AGA ATG AGG GTC CGA GAT G	100	Clone B-*myb* gene with additional ClaI site at 3' end
5'B-myb	GGT TTG GAT CCA TGT CTC GGC GGA CGC GCT GCG AGG	100	Clone B-*myb* gene with additional BamHI site at 5' end
3'B-myb2-P2A	CTC CTC CAC GTC TCC AGC CTG CTT CAG CAG GCT GAA GTT AGT AGC TCC GCT TCC GGA CAG AAT GAG GGT CCG AGA TGT GTG GCT G	100	Clone B-*myb* gene with additional *P2A* gene at 3' end
P2A-5'AmCyan	AGC CTG CTG AAG CAG GCT GGA GAC GTG GAG GAG AAC CCT GGA CCT ATG GCT CTT TCA AAC AAG TTT ATC GGA GAT	100	Clone *AmCyan* gene with additional *P2A* gene at 5' end
3'AmCyan	GGG TTC GGC CGC TCA GAA AGG GAC AAC AGA GG	100	Clone *AmCyan* gene with additional EagI site at 3' end
5' Gateway	TCG TGA AGC GGC CGC ACA AGT TTG TAC AAA AAA GCT	100	Clone *attR* Gateway cassette plus complementary 15 bases from NcoI cut site in pHAGE-2-EF1a plasmid
3' Gateway	AGA GGT TGA TTA GGA TCA CCA CTT TGT ACA AGA AAG C	100	Clone *attR* Gateway cassette plus complementary 15 bases from BamHI cut site in pHAGE-2-EF1a plasmid

PCR was used to combine the modified *Sox2* and B-*myb* fragments or the modified *AmCyan* and B-*myb* fragments with the following conditions: 30 cycles of (98°C for 10 seconds, 60°C for 15 seconds, 72°C for 4 minutes). The reaction contained 10ng of each purified fragment, 4µl dNTPs (2.5mM each, Takara Bio Inc), 1µl GXL polymerase (1.25U, Takara Bio Inc), 10µl PrimeSTAR GXL Buffer (1X, Takara Bio Inc), 0.1µl Sox2 5'-NdeI primer, 0.1µl b-myb 3' ClaI primer (Table 3) and dH_2O up to 50µl final volume.

PCR was also used to clone a gateway cassette into the pHAGE-2-EF1a-ZsGreen-W lentiviral backbone in place of the ZsGreen gene with the following conditions: 35 cycles of (98°C for 10 seconds, 55°C for 5 seconds, 72°C for 9 seconds). Each reaction contained 200ng plasmid DNA (pMX-GW), 25µl PrimeStar Max polymerase premix (2X, Takara Bio Inc), 0.1µl forward primer. 0.1µl reverse primer (Table 3) and dH_2O up to 50µl final volume.

Cloning products were separated by gel electrophoresis on 1% agarose gels. 10% of the product was imaged on a Bio-Rad Gel Doc™ XR+ System. The remaining PCR product was excised from the gel using a clean scalpel on an UV trans-illuminator.

2.14 Agarose gel extraction

Gel bands were purified using a QIAquick Gel Extraction Kit (Qiagen). The gel band was weighed and 300µl of buffer QG was added per 1mg gel slice weight. The gel slice was incubated at 50°C for 10 minutes. 100µl isopropanol per 1mg gel slice added to dissolved gel slice. 800µl of the DNA mixture was added to a QIAquick column in a 2ml collection tube and centrifuged at 17900 x g for 1 minute. Flow through was discarded and the step was repeated if the DNA mixture was over 800µl. 500µl buffer QG was added to the column and the column was centrifuged at 17900 x g for 1 minute. The flow

through was discarded and 750µl buffer PE was added to the column to wash the DNA and the column was incubated at room temperature for 2 minutes. The column was centrifuged at 17900 x g for 1 minute and the flow through was discarded. The column was centrifuged at 17900 x g for 1 minute to remove excess ethanol. The column was then placed into a DNase free 1.5ml centrifuge tube and 30-50µl DNase free dH_2O (Sigma) was pipetted to the centre of the column, the column was incubated at room temperature for 2 minutes before centrifugation at 18000 x g for 1 minute to elute the DNA. Purified DNA concentration was measured with a Nanodrop 2000c (Thermo Scientific) spectrophotometer.

2.15 Gibson Assembly

Gibson assembly was used to combine the gateway cassette fragment cloned from the pMX-GW plasmid into pHAGE-2-EF1a plasmid linearised with NcoI and BamHI restriction enzymes. Gibson assembly reaction contents: 150ng insert (GW cassette), 50ng linearised vector (pHAGE-2-EF1a plasmid cut with NcoI and BamHI), 10µl Gibson master mix (2X, NEB) and dH_2O up to 20µl final volume. The reaction was incubated at 50°C for 1 hour. The reaction mixture was diluted 1:4 with dH_20 and then 2µl was used to transform OneShot Ccdb resistant competent bacteria (Invitrogen).

2.16 Gateway cloning

Gateway cloning was used to move genes of interest from *attL* entry vectors to the generated *attR* destination vector, pHAGE-2-EF1a-GW vector. 150ng of entry vector and 150ng of destination vector were diluted with TE buffer (10mM Tris, pH 8.0, 1mM EDTA) to a final volume of 8µl. 2µl of LR Clonase™ II enzyme mix (5x, Invitrogen) was added to the sample. The DNA and enzyme mixture was incubated for 1 hour at 25°C.

1µl of Proteinask K (Invitrogen) was added and the sample was mixed and then incubated at 37°C for 10 minutes. 1µl of the reaction was transformed into competent bacteria.

2.17 Sequencing

Any DNA that was cloned by PCR was sequenced using the primers in Table 4. Sanger sequencing was carried out by the University of Birmingham DNA sequencing service in the Biosciences department.

Table 4: Primers used for Sanger sequencing

Primer	**Sequence**	**Construct**
M13 Forward (Invitrogen)	GTA AAA CGA CGG CCA G	*Sox2-E2A*-B-*myb* and B-*myb-P2A-AmCyan* in TOPO vector
B-myb2-5'304	GCA CCA AAC AGT GGA CGC	*Sox2-E2A*-B-*myb* and B-*myb-P2A-AmCyan* in TOPO vector
B-myb-5'496	GGA GGA CGG ACA ATG CTG	*Sox2-E2A*-B-*myb* and B-*myb-P2A-AmCyan* in TOPO vector
B-myb-5'1073	GCA GTC ATC CCA GCA GGC	*Sox2-E2A*-B-*myb* and B-*myb-P2A-AmCyan* in TOPO vector
B-myb-5'1290	GCC AGC CTG TCC TTC CTG	*Sox2-E2A*-B-*myb* and B-*myb-P2A-AmCyan* in TOPO vector
B-myb-5'1783	TGG ATG AAG ATG GGA AGC	B-*myb-P2A-AmCyan* in TOPO vector
B-myb-5'2093	TCG GAC CCT CAT TCT GTC	B-*myb-P2A-AmCyan* in TOPO vector
Sox2- 5'486	GCG CAC ATG AAC GGC TGG	*Sox2-E2A*-B-*myb* in TOPO vector
Sox2-5'775	CTT CCT CCC ACT CCA GGG	*Sox2-E2A*-B-*myb* in TOPO vector
AmCyan-5'261	GCA TTT CCT GAC GGA ATG	B-*myb-P2A-AmCyan* in TOPO vector
AmCyan-5'474	TTG AAG GGT GAT GTC ACC	B-*myb-P2A-AmCyan* in TOPO vector
M13 Reverse (Invitrogen)	CAG GAA ACA GCT ATG AC	*Sox2-E2A*-B-*myb* and B-*myb-P2A-AmCyan* in TOPO vector
pHAGE-GW 3259	AGT GGG TGG AGA CTG AAG	pHAGE-2-EF1a-GW-W
pHAGE-GW 3742	AAC CAG ACC GTT CAG CTG	pHAGE-2-EF1a-GW-W
pHAGE-GW 4222	GCC GTT TGT GAT GGC TTC	pHAGE-2-EF1a-GW-W
pHAGE-GW 4678	GCC GTT ATC GTC TGT TTG	pHAGE-2-EF1a-GW-W

2.18 Competent bacteria transformation

To propagate plasmid DNA α-Select chemically competent bacteria Gold Efficiency (Bioline) or OneShot Ccdb resistant competent bacteria (Invitrogen) were used. Competent cells were thawed on ice. The cells were mixed by gently flicking the tube and then up to 5µl of DNA was added. The cells were mixed gently and then incubated on ice for 30 minutes. The cells were heat shocked for 30 seconds at 42°C and then returned to the ice for 2 minutes. 500-950µl of SOC medium (2% tryptone, 0.5% yeast extract, 10mM NaCl, 2.5mM KCl, 10mM $MgCl_2$, 10mM $MgSO_4$, and 20mM glucose, Invitrogen) was added to the cells and then the cells were incubated at 37°C for 1 hour in an orbital shaker at 200 rpm. 50-200µl of transformed cells were spread onto agar with 100µg/ml Ampicillin or Kanamycin and incubated overnight at 37°C. If the plasmid contained a lacZ reporter gene 800µg X-gal (Bioline) was spread onto the plate and allowed to dry for 30 minutes before adding the competent bacteria to enable blue/white colony screening.

2.19 Bacterial culture

Individual colonies on selective agar were used to inoculate 5ml of L-Broth with 100µg/ml Ampicillin or Kanamycin and incubated for 16 hours (miniprep) or 8 hours (maxiprep starter culture) at 37°C with vigourous shaking. After 8 hours the 500µl maxiprep starter culture was used to inoculate 250ml (maxiprep) L-Broth with 100µg/ml Ampicillin or Kanamycin and incubated for 16 hours at 37°C with vigourous shaking.

2.20 Plasmid DNA extraction

Miniprep plasmid DNA was isolated by centrifuging the culture at 6000 x g for 15 minutes at 4°C. The supernatant was removed and the pellet was resuspended in 100µl of alkaline lysis solution 1 (50mM glucose, 25mM Tris-Cl pH 8, 10mM EDTA pH 8) and transferred to a 1.5ml centrifuge tube. The tube was mixed using a vortex mixer until the pellet had completely resuspended. 200µl of freshly prepared alkaline lysis solution 2 (0.2M NaOH, 1% SDS) was added to the tube before inverting 5 times to mix. Next, 150µl of alkaline lysis solution 3 (3M Potassium Acetate pH 5) was added to the tube and its contents was mixed by inversion 7 times. The tube was incubated on ice for 5 minutes then centrifuged at 17900 x g for 5 minutes at 4°C. The supernatant was transferred to a new tube and an equal volume of phenol:chloroform (1:1) was added to the tube, mixed on a vortex mixer and centrifuged at 17900 x g for 2 minutes. The aqueous upper layer was transferred to a new tube and 2 volumes of 100% ethanol were added, then the tube was incubated at room temperature for 2 minutes. The mixture was centrifuged at 17900 x g for 5 minutes at 4°C, then the supernatant was discarded and 1ml of 70% ethanol was used to wash the DNA pellet. The tube was centrifuged at 17900 x g for 2 minutes at 4°C. The supernatant was removed and the DNA pellet was air dried for 5 minutes before being dissolved in TE (10mM Tris-Cl pH 8, 1mM EDTA pH 8) containing 20ug/ml DNase-free RNAse A (Qiagen). The purified DNA concentration was measured by using a Nanodrop 2000c (Thermo Scientific) spectrophotometer. DNA was stored at -20°C

Miniprep plasmid DNA was extracted from 16 hour cultures with QIAprep Spin Miniprep Kit (Qiagen) when the DNA was required for sequencing. Miniprep culture

was centrifuged at 6000 x g for 3 minutes at room temperature, then resuspended in 250µl buffer P1 and transferred to a 1.5ml centrifuge tube. 250µl buffer P2 was added to the tube and the tube was inverted 5 times. 350µl of N3 was added and the tube was mixed by inversion again. The tube was centrifuged at 17900 x g for 10 minutes at room temperature. The supernatant was transferred to a Qiaprep spin column and the column placed into a 2ml collection tube, then centrifuged at 17900 x g for 60 seconds. The flow through was discarded and 0.5ml buffer PB was added to the column before centrifugation at 17900 x g for 60 seconds. The flow though was again discarded and 0.75ml of buffer PE was pipetted into the column and then the column was centrifuged at 17900 x g for 60 seconds. The flow through was discarded and the column was centrifuged again to remove wash buffer. The column was then placed into a new 1.5ml centrifuge tube and 30-50µl of dH_2O was added to the centre of the column. The column was incubated at room temperature for 2 minutes and then centrifuged at 17900 x g for 1 minute. The purified DNA concentration was measured by using a Nanodrop 2000c (Thermo Scientific) spectrophotometer.

2.21 Restriction endonuclease digestion

Plasmid DNA was routinely digested with 5 units of enzyme, 1x enzyme specific buffer, 500ng-5µg DNA and up to 20µl final volume with dH_2O. The restriction enzyme reaction was incubated at the correct temperature for the specific enzyme, before electrophoretic separation.

2.22 Protein extraction

10^6 cells were centrifuged at 900 x g for 5 minutes, washed with cold PBS and resuspended in 40µl extraction buffer (RIPA) (1% Nonidet P40, 0.1% SDS, 50mM Tris-

HCl pH7.4, 0.5% Sodium-deoxycholate, 150mM NaCl, 2mM EDTA, 50mM NaF), 1mM Phenylmethanesulfonyl fluoride (PMSF), 1x protease inhibitors set I (Calbiochem), 1mM Sodium orthovanadate (Na_3VO_4)). The extraction mixture was incubated at 4°C for 20 minutes then centrifuged at 6500 x g for 10 minutes at 4°C. The supernatant was transferred to a fresh 1.5ml tube, snap frozen in a dry ice and ethanol bath and stored at -80°C until required. The concentration of the protein extract was calculated by addition of 2µl to 800µl H_2O plus 200µl Bio-Rad Protein Assay (Bio-Rad) in a 1cm cuvette then mixing and measuring absorbance at 595nm on a Nanodrop 2000c (Thermo Scientific) spectrophotometer. The absorbance was compared to a standard curve generated from known concentrations of purified BSA in 800µl H_2O plus 200µl Bio-Rad Protein Assay.

2.23 Western blotting

50µg of total protein extracts were subjected to SDS-PAGE and proteins transferred to BioTrace PVDF membranes (Bio-Rad) for 2 hours at 15V on a semidry transfer apparatus (Amersham). After blocking for 1 hour in TBS containing 0.1% Tween 20 (T-TBS) and 10% BSA, membranes were incubated with the appropriate primary antibody diluted in TTBS (Table 6) for 1 hour at room temperature or overnight at 4°C. After washing and incubation with an appropriate secondary antibody conjugated to horseradish peroxidase (Table 5), signals were detected using the Supersignal West Pico Chemiluminescence system (Thermo Scientific). The chemiluminescence was visualised by exposure on x-ray film (GE Healthcare).

Table 5: Primary antibodies used in western blotting

Antibody	Immunoglobulin	Stock concentration (µg/ml)	Dilution used	Supplier
B-Myb N19	Rabbit IgG	200	1:500	Santa Cruz
Klf4	Goat IgG	200	1:10000	Santa Cruz
Sox2 H-65	Mouse IgG	200	1:500	R&D Systems
Oct4 C-10	Mouse IgG	200	1:500	Santa Cruz
Nanog	Rabbit IgG	200	1:500	Cosmo Bio
Nucleolin	Rabbit IgG	200	1:10000	Bethyl Laboratories
HDAC1	Rabbit IgG	NA	1:1000	Turner Group, University of Birmingham

Table 6: Secondary antibodies used in western blotting

Antibody	Dilution used	Supplier
Anti-goat IgG linked to horseradish peroxidase	1:500	Santa Cruz
Anti-rabbit IgG linked to horseradish peroxidase	1:10000	GE Healthcare
Anti-mouse IgG linked to horseradish peroxidase	1:10000	GE Healthcare

2.24 Transfection

To evaluate exogenous protein expression driven by the generated Oct4-Sox2-Klf4-B-Myb (OSKB) lentiviral backbone, 293T cells were transfected with 24µg pHAGE-2-E1a-mOSKB and 2.4µg pHAGE-2-EF1a-ZsGreen-W or 24µg pHAGE-2-E1a-mOSKM-OSKM-loxP and 2.4µg pHAGE-2-EF1a-ZsGreen-W lentiviral backbones. 90µl of Trans-IT 293T (Mirus Bio) was added to 2ml DMEM, mixed then incubated at room temperature for 10 minutes. The plasmid mixture was added to the Trans-IT/ DMEM mixture, mixed and incubated for 15 minutes. The media on $25x10^6$ 293T in a 15cm tissue culture dish was removed and 11ml fresh 293T media was added back to the cells. The Trans-IT/DMEM/DNA mixture was added drop wise to the plate of 293T cells. The cells were incubated in a humidified atmosphere at 37°C with 5% CO_2. The following day the media on the cells was aspirated and 12.5ml fresh 293T media was added to the plate. The cells were returned to the incubator. At 48 hours after transfection the 293T cells were washed with PBS, then dissociated into a single cell suspension by treatment with 5ml 1X Trypsin-EDTA (Invitrogen) for 2 minutes. 5ml fresh 293T medium was added to the cells and then the suspension was centrifuged at 300 x g for 5 minutes. Supernatant was discarded and the cell pellet was resuspended in 1ml 5% FBS in PBS and passed through a 0.7µm filter into a 5ml FACS tube (BD Biosciences). 5 x 10^6 GFP positive cells were sorted and whole protein was extracted as described in section

2.25 Nucleofection

iPSCs were transfected with 5µg pCre:IRES2-EGFP using Amaxa 4D-Nucleofector (Lonza) system. 10^6 iPSCs were trypsinised to generate a single cell suspension. The trysin was inactivated by adding an equal volume of 2X trypsin inhibitor (Sigma) diluted

in ESC medium. The cells were centrifuged at 300 x g for 5 minutes and the cell pellet was washed with PBS and centrifuged again. The cell pellet was then resuspended in 100µl of supplemented Nucleofector™ solution P3 (Lonza) pre-warmed to room temperature. 10µg of pCre-IRES2-EGFP plasmid was added to the cell suspension and the combined mixture was transferred into a Nucleocuvette™. The Nucleocuvette™ was placed into the Amaxa 4D-Nucleofector and the program CG-104 was used to nucleofect the iPSCs. 500µl of ESC medium pre-warmed to 37°C was added to the Nucleocuvette™ and the cell suspension was removed using the provided Pasteur pipette. The iPSCs were then added drop wise onto a 10cm tissue culture plate previously coated with mitotically inactivated MEFs.

2.26 Karyotyping

100ng/ml of colcemid (KaryoMAX, Gibco) was added directly to cells in culture. The cells were incubated at 37°C for 2 hours. Cells were trypsinised, centrifuged at 300 x g for 5 minutes then washed twice with PBS. The cell pellet was resuspended in 1ml 0.1M KCl and incubated at room temperature for 5 minutes. Cells were counted and diluted to 10^5 per ml. 100µl was added to a cytospin funnel attached to a glass slide (Thermo Scientific). The cells were cytospun at 300 x g for 10 minutes. The glass slide was submerged in KCM buffer (120mM KCl, 20mM NaCl, 10mM Tris/HCl pH8, 0.5mM EDTA, 0.1% Triton X-100) for 8 minutes, then submerged in 4% methanol free formaldehyde in KCM buffer for 10 minutes before being washed twice with PBS. Once dry 10µl of DAPI was added to the cells and a glass coverslip was placed over them. The coverslip was sealed with clear nail varnish before being imaged at 100x magnification on a Zeiss LSM 510 Meta confocal microscope. Chromosomes of cells in metaphase were counted.

2.27 Fluorescence activated cell sorting (FACS)

Cells were sorted after viral transduction or transfection by FACS on a MoFlo XDP high speed cell sorter (Beckman Coulter). Cells were sorted for positive expression of the fluorescent reporter protein after gating for live cells and singlets.

2.28 RNA extraction

Cells were washed with PBS and then the cell pellet was lysed by pipetting up and down in 250µl Trizol Reagent (Invitrogen) and stored at -20°C until ready for extraction. The Trizol and cell solution was defrosted for 15 minutes at room temperature. 50µl of chloroform was added to the mixture and the tube was shaken vigourously by hand for 15 seconds then centrifuged at 12000 x g for 15 minutes at 4°C. The aqueous phase was extracted into a new tube and 1µl of RNase-free glycogen (Roche) was added to the extract. 125µl of 100% isopropanol was added and the mixture was incubated at room temperature. After 10 minutes the mixture was centrifuged at 12000 x g for 10 minutes at 4°C. The supernatant was discarded and the RNA pellet was washed by adding 250µl of 70% ethanol, mixing by vortex and then centrifuging at 7500 x g for 5 minutes at 4°C. The supernatant was discarded and the pellet was air dried for 5 minutes before resuspending in 20µl RNase-free dH_2O. The concentration of RNA was measured by using a Nanodrop 2000c (Thermo Scientific) spectrophotometer.

2.29 cDNA synthesis

1-5µg of RNA was mixed with 500ng of oligo $(dT)_{12\text{-}18}$ (Invitrogen), 1µl of 10mM dNTP mix (Invitrogen) and RNAse-free dH_2O to a final volume of 13µl. The mixture was incubated at 65°C for 5 minutes and then cooled on ice for 2 minutes. 1µl Superscript™

III Reverse transcriptase (Invitrogen), 1µl RNAseOUT™ (Invitrogen), 1µl 0.1M dithiothreitol (Invitrogen) and 4µl 5X First Strand Buffer (Invitrogen, 250mM Tris-HCl pH 8.3, 375mM KCl, 15mM MgCl2) were added and mixed by gentle pipetting up and down. The mixture was then incubated at 50°C for 1 hour and then 75°C for 15 minutes to deactivate the enzymes. 1-2µl was used per qPCR reaction.

2.30 TaqMan qPCR

Real time qPCR was used to analyse the cDNA produced in section 2.10. The reaction contents were 1µl TaqMan gene expression assay mix (Life Technologies, Table 7), 1µl cDNA, 10µl TaqMan PCR reaction buffer (Applied Biosystems) and 8µl H_2O. All reactions were done in triplicate. Ct values were calculated by MxPro 3000 Stratagene software. Relative expression values were calculated against β_2-microglobin using the ΔΔCt mathematical model (Livak and Schmittgen, 2001). The PCR conditions were as follows: 50°C for 2 minutes then 95°C for 10 minutes, followed by 40 cycles of (95°C for 15 seconds and 60°C for 1 minute). Fluorescence was measured at the end of each cycle.

Table 7: TaqMan oligo and primer sets used to analyse RNA expression

Gene	Assay ID
Pouf5F1(Oct4)	Mm00658129_gH
Klf4	Mm00516104_m1
Nanog	Mm02384862_g1
Myc	Mm00487804_m1
FGF4	Mm00438916_g1
Sall4	Mm01240680_m1
Cbx7	Mm00520006_m1
ETV5	Mm00465816_m1
B-myb (mybl2)	Mm00485340_m1
lin28a	Mm00524077_m1
Snai1	Mm00441533_g1
Thy1	Mm00493682_g1
Ovol1	Mm00498263_m1
Cdh1	Mm01247357_m1
Cdkn1a (P21)	Mm04205640_g1
Cdkn2a (P16)	Mm00494449_m1
Trp53 (P53)	Mm01731290_g1

2.31 Cell cycle analysis with propidium iodide

iPSCs were resuspended in 10µg/ml propidium iodide (Sigma) and incubated for 10 minutes at room temperature. Just before analysing the samples on a Beckman Coulter CyAn flow cytometer NP-40 was added to the sample to permeabilise the cells at a final concentration of 0.2%.

2.32 γ-H2AX and RAD51 immunofluorescence

iPSCs were grown on sterile glass-coverslips with mitotically inactivated MEFs for 24 hours before being fixed with 3% paraformaldehyde, 2% sucrose in PBS for 10 minutes at room temperature. Cells were permeabilised in 20mM HEPES, pH7.4, 50mM NaCl, 3mM MgCl2, 300mM sucrose, 0.5% Triton X-100 for 5 minutes at 4°C. The cells were washed with PBS then incubated with mouse anti phosphor-Histone H2A.X (Ser 139) clone JBW301 (Millipore) and rabbit anti RAD51 clone H-92 (Santa Cruz) diluted 1:100 in 5%FBS/PBS for one hour at room temperature. The cells were washed 3 times with PBS, then incubated with anti-mouse Alexa fluor 488 and anti-rabbit Alexa fluor 594 (Invitrogen) diluted 1:1000 in 5%FBS/PBS for 1 hour at room temperature. The cells were washed again 3 times in PBS and then counter stained in Vectashield with DAPI (Vector Labs). The coverslips with the cells on them were then inverted and placed onto microscope slides and sealed with clear nail varnish.

Cells were imaged as Z-stacks using an upright Zeiss 510 Laser scanning confocal Microscope.

2.33 Alkaline phosphatase staining

Medium was aspirated from the well before washing with cold PBS. The cells were fixed in 500µl cold neutral formalin buffer (0.1M Na_2HPO_4, 25mM $Na_2HPO_4.H_2O$, 4% Paraformaldehyde) for 15 minutes. The fixative was removed and the cells were rinsed once with cold dH_2O, and then left in dH_2O for 15 minutes. The dH_2O was removed and 500µl of staining solution (0.1mM Naphthol AS-MX phosphate, 27.3mM N,N-Dimethylformamide (DMF), 0.7mM Fast Red Violet LB Salt, 0.1M Tris-HCl pH 8.3) was added to the cells and then incubated at room temperature for 30 minutes. The staining solution was removed and the cells were washed once with dH_2O and then allowed to air dry. Red positively stained colonies were counted to assess the efficiency of reprogramming.

2.34 Senescence staining

Day 3 reprogramming MEFs were stained for senescence by using a Senescence β-Galactosidase Staining Kit (Cell Signalling Technology). The medium was aspirated from the MEFs before washing the cells with PBS. 500µl of 1X fixative solution (Cell Signalling Technology) was added to each well and the cells were incubated at room temperature for 15 minutes. The cells were then washed with PBS twice and 500µl of 1X β-Galactocidase staining solution (465µl 1X staining solution (Cell Signalling Technology), 5µl Staining Supplement A, 5µl Staining Supplement B, 25µl 20mg/ml X-Gal in DMF) was added to the cells. The plate was wrapped in parafilm and incubated at 37°C in a non-humidified incubator overnight. The following day the stained cells were imaged using an inverted bright field microscope at 20x magnification with an attached camera.

2.35 Apoptosis staining

An *In Situ* Cell Death Detection kit (TUNEL, Roche) was used to assess whether the viral transduction of MEFs was causing apoptosis. Day 3 reprogramming MEFs were grown on 0.1% gelatin coated 10mm coverslips in 4 well plates. Cell media was aspirated and the cells were washed with PBS and then fixed with 200µl 4% paraformaldehyde in PBS for 1 hour at room temperature. The cells were permeabilised with 0.1% Triton X-100 in 0.1% sodium citrate for 2 minutes on ice. A positive control was set up by adding 5U DNase I (Promega) and 1X DNase I buffer (10X, Promega) diluted in 50mM Tris-HCl pH7.5, 1mg/ml BSA to one of the coverslips then incubating at room temperature for 10 minutes. The cells were washed twice with PBS and then the enzyme solution was diluted 1:10 in label solution and then 20µl was applied to each coverslip, a negative control was set up with label solution without the enzyme. The coverslips were incubated at 37°C in a humidified incubator in the dark for 60 minutes. The stained cells were then washed three times with PBS and counterstained using Prolong antifade reagent with DAPI (Life Technologies). The coverslips were placed onto microscope slides and sealed with clear nail varnish. Samples were analysed on a Zeiss LSM 510 Meta confocal microscope.

2.36 Cell cycle analysis with Aminoactinomycin D (7AAD)

To analyse the cell cycle of iPSCs cells were fixed by centrifuging the cells at 300 x g for 5 minutes. The pellet was washed with 1ml of ice-cold PBS and centrifuged again at 300 x g for 5 minutes. The pellet was resuspended in 250µl of ice-cold PBS, and then 750µl of -20°C ethanol was added to the mixture drop wise whilst the tube was gently mixed on a vortex mixer. The cells were stored at -20°C for at least an hour. Cells were stained with

400µl of 20mg/ml 7AAD (Sigma) and incubated at room temperature for 30 minutes in the dark. Cell cycle profile was analysed using a Beckman Coulter CyAn flow cytometer.

2.37 Cell viability assay (Cell Quanti-Blue)

5000 iPScs were seeded per well onto mitotically inactivated MEFs in 48 well plates. After 24 hours the cells were treated with hydroxyurea (0.03, 0.06, 0,125, 0.25, 0.5 or 1mM, Sigma), PJ34 (0.1, 1, 10, 12.5, 25 or 50µM, Sigma), camptothecin (0.06, 0.125, 0.25, 0.5, 1 or 2µM, Sigma) or 0.1% saponin (Sigma). After 24 hours the medium was removed and 200µl fresh medium containing 3.75% CellQuanti-Blue™ Cell Viability assay (BioAssay Systems) was added to each well and then incubated for 30 minutes at 37°C. 200µl was transferred from each well into a black 96 well plate (Thermo Scientific) and analysed by fluorescent plate reader with excitation filter 540±25nm and emission filter 620±40nm. The remaining medium was discarded and 200µl fresh medium containing the appropriate drug was added to each well, then cultured for another 24 hours. The viability measurement was repeated at 48 and 72 hours.

CHAPTER 3: GENERATION OF IPSCS WITH MODIFIED B-MYB ALLELES

3.1 INTRODUCTION

The discovery that fully differentiated human cells could be regressed back to an embryonic like state that is pluripotent was revolutionary and a considerable achievement, with great potential for the field of regenerative medicine. iPSCs have a much greater chance of reaching the clinic compared to ESCs due to the limitations of ESCs. If iPSCs can be harnessed for use in regenerative medicine they will be an excellent resource that could potentially treat any illness or disease that involves a missing or non-functional cell type.

DNA damage is one of the controversial topics in somatic reprogramming as there is conflicting evidence over whether the process causes *de novo* mutations or if the mosaicism of the parental cell culture is the source of mutation (Abyzov et al., 2012). Either way iPSCs with normal karyotype will be essential for producing cells for regenerative medicine. Understanding genes which are known to control genome stability, such as B-*myb*, may yield methods to produce iPSCs free from chromosomal aberrations.

Previous work done in my research group showed the possibility of growing ESCs lacking B-Myb (Lorvellec et al., 2010). However, these cells had proliferation defects and showed an increase in DNA damage and chromosomal abnormalities.

By manipulating expression of B-Myb in the context of iPSCs I aim to determine how comparable iPSCs are to ESCs, if it is possible to maintain iPSCs with no B-Myb expression and if an increase in DNA damage is also observed.

In my experiments I used a polycistronic lentivirus containing the genes, *Oct4*, *Sox2*, *Klf4* and *c-Myc* (OSKM) that was kindly given to us by George Murphy from Boston University, MA, USA. The vector was designed to express all four proteins on a single backbone by including the sequence for self-cleaving peptides between *Oct4* and *Klf4* (F2A) and also between *Sox2* and *c-Myc* (E2A). The two fusion genes are separated by an internal ribosomal entry sequence (IRES). All four genes are flanked by LoxP sites once the lentiviral RNA is reverse transcribed in the cell to allow for removal of the OSKM cassette by expression of cre recombinase (Figure 3.1) (Sommer et al., 2009, Sommer et al., 2010).

A schematic of the reprogramming process is shown in Figure 3.2A. OSKM lentiviral particles are strong inducers of reprogramming. iPSC colonies with the morphology of ESC colonies begin to appear at around day 5 and are ready to be isolated at day 10-12 (Figure 3.2B). In addition to ESC-like morphology, iPSCs stain positively for alkaline phosphatase activity, a marker of pluripotency (Thomson et al., 1995, O'Connor et al., 2008). Figure 3.2C shows an example of an iPSC colony with positive red staining for alkaline phosphatase activity.

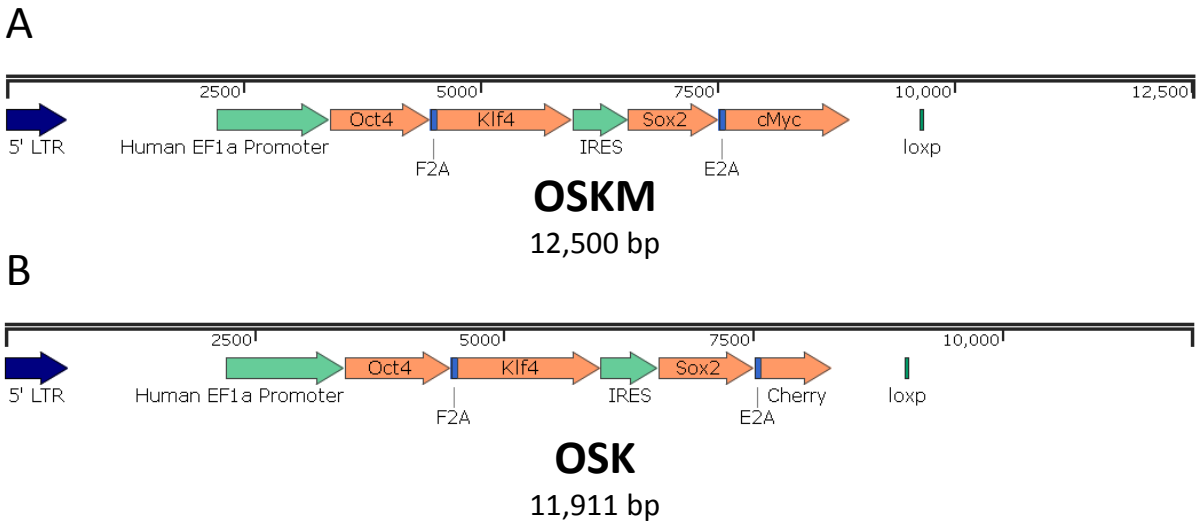


Figure 3.1: The OSKM and OSK lentiviral vectors
Schematic representation of key features of the OSKM (A) and OSK (B) lentiviral vectors. Human EF1a driven expression of *Oct4-F2A-Klf4*-IRES-*Sox2-E2A-c-Myc* fusion gene. *F2A* and *E2A* genes encode self-cleaving peptides. IRES – internal ribosome entry sequence. LTR – long terminal repeat. The single LoxP site in the vector is copied into the 5' LTR during reverse transcription resulting in flanking LoxP sites enabling cre recombinase mediated removal of the transgene cassette. The OSK vector has *mCherry* fluorophore gene in place of *c-Myc*.

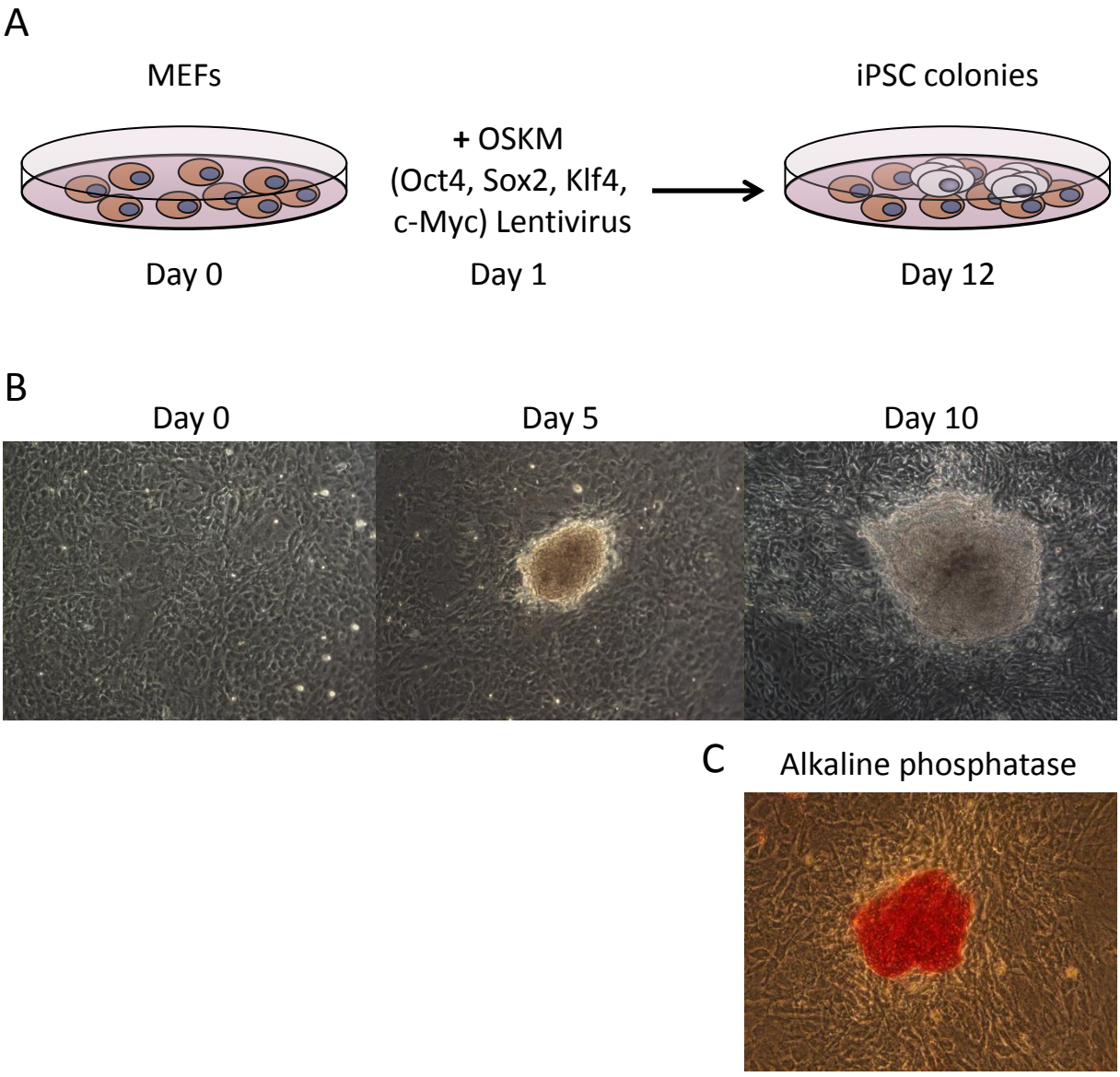


Figure 3.2: The reprogramming process

(A) Schematic representation of the reprogramming process. MEFs were transduced with a polycistronic lentivirus containing *Oct4*, *Sox2*, *Klf4* and *c-Myc* at day 1 and iPSC colonies were scored at day 10-12 (B) Phase contrast microscope images showing MEFs reprogramming at day 0, 5 and 10. Note the iPSC colony at day 5 and 10. 10x magnification. (C) Image of an iPSC colony with positive (red) alkaline phosphatase activity, a marker of pluripotency.

3.2 RESULTS

3.2.1 Generation and characterisation of B-*myb*$^{+/+}$, B-*myb*$^{+/\Delta}$ and B-*myb*$^{F/\Delta}$ iPSCs

In order to understand the role of B-Myb in iPSCs, MEFs were derived from mice with wild type B-*myb* alleles (B-*myb*$^{+/+}$), mice with one functional allele (B-*myb*$^{+/\Delta}$) or mice with one functional allele containing LoxP sites upstream of exon 2 and downstream of exon 5 (B-*myb*$^{F/\Delta}$) allowing for *in vitro* deletion through cre recombinase expression (Garcia et al., 2005). MEFs with different B-*myb* alleles where transduced with OSKM lentiviral particles and 12 days later individual iPSCs colonies were isolated from the culture and expanded by culturing on mitotically inactivated MEFs under ESC growth conditions. In this way, several iPSCs lines harbouring modified B-*myb* alleles were created.

3.2.1.1 Alkaline phosphatase staining of derived iPSC lines

B-*myb*$^{+/+}$, B-*myb*$^{+/\Delta}$ and B-*myb*$^{F/\Delta}$ iPSCs were cultured on mitotically inactivated MEFs for 24 hours and then stained for alkaline phosphatase activity. Using a phase contrast inverted microscope it was possible to see the staining of the iPSCs colonies. Figure 3.3 shows positive staining for alkaline phosphatase activity of B-*myb*$^{+/+}$ (left panel), B-*myb*$^{+/\Delta}$ (middle panel) and B-*myb*$^{F/\Delta}$ (right panel) iPSCs. The staining was consistent across the three different genotypes of iPSCs, indicating that the half expression of B-Myb in the B-*myb*$^{+/\Delta}$ and B-*myb*$^{F/\Delta}$ iPSCs did not affect pluripotency based on alkaline phosphatase staining.

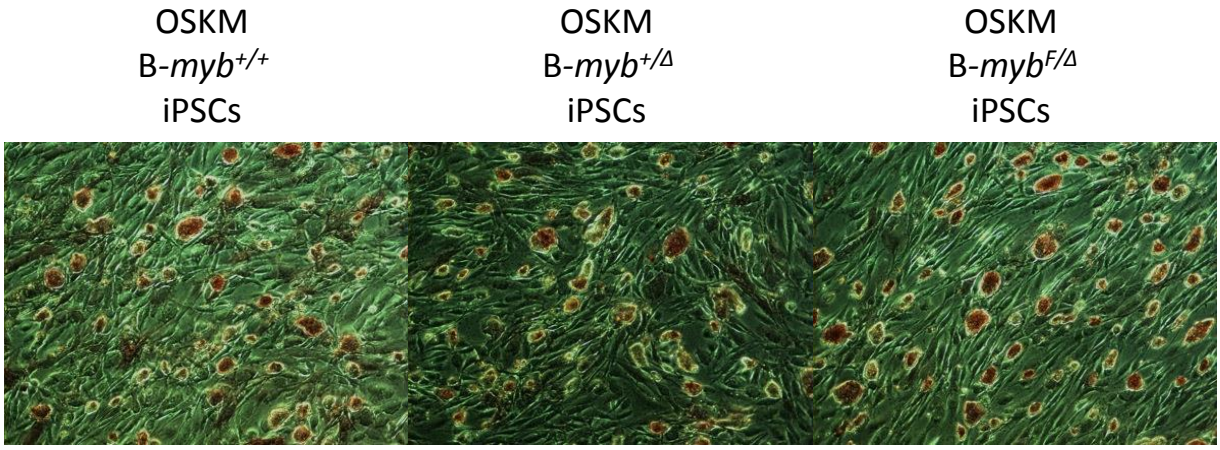


Figure 3.3: Alkaline phosphatase staining for B-*myb*$^{+/+}$, B-*myb*$^{+/\Delta}$ and B-*myb*$^{F/\Delta}$ iPSCs

Passage 6 B-*myb*$^{+/+}$, B-*myb*$^{+/\Delta}$ and B-*myb*$^{F/\Delta}$ iPSCs were grown on a mitotically inactivated MEF feeder layer for 24 hours before staining for alkaline phosphatase activity for 30 minutes. Plates showing positive AP staining at 10x magnification.

Karyotyping derived iPSC lines

From each genotype one iPSC cell line was karyotyped by counting the number of chromosomes in cells blocked at the metaphase with colcemid, a drug which depolymerises mitotic spindle. Mouse cells contain 40 chromosomes; if there are more or less than 40 chromosomes, aneuploidy may have occurred during the reprogramming process. A representative DAPI stained metaphase chromosome spread showing the correct number of chromosomes is shown in Figure 3.4A. As detailed in Figure 3.4B, the OSKM B-*myb*$^{+/+}$ iPSC line had 4% of metaphases with less than 40 chromosomes, 4% metaphases with greater than 40 chromosomes and 92% with 40 chromosomes. The OSKM B-*myb*$^{+/\Delta}$ iPSC line had 11% metaphases with less than 40 chromosomes, 4% metaphases with greater than 40 chromosomes and 85% metaphases with exactly 40 chromosomes. The OSKM B-*myb*$^{F/\Delta}$ iPSC line had 24% metaphases with less than 40 chromosomes, 3% metaphases with greater than 40 chromosomes and 72% metaphases

with 40 chromosomes. Thus, there was an increase in the percentage of metaphases with less than 40 chromosomes in both of the iPSC lines with reduced B-Myb expression, indicating that lower expression of B-Myb increases the percentage of aneuploidy cells.

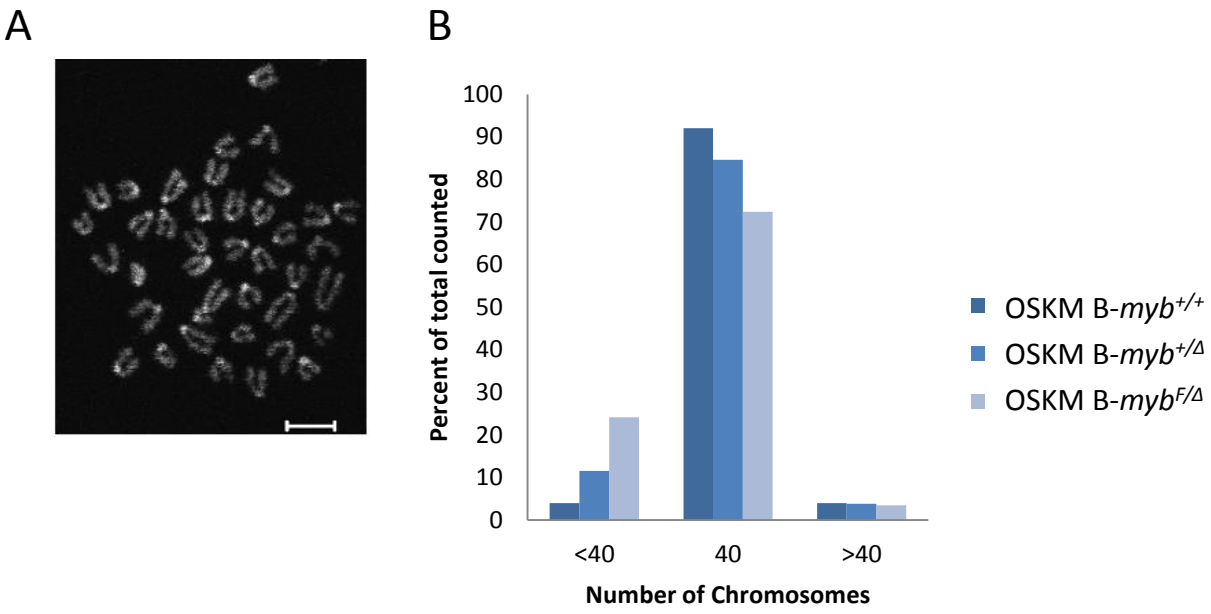


Figure 3.4: Karyotyping of three iPSC lines
$4x10^4$ B-*myb*$^{+/+}$, B-*myb*$^{+/\Delta}$ and B-*myb*$^{F/\Delta}$ iPSCs were treated with colcemid, swollen with 0.1M KCl, cytospun at 300 x g for 10 minutes onto a glass slide then stained with DAPI and imaged at 100x magnification (A) Representative metaphase spread stained with DAPI. 5µm scale bar (B) Bar graph showing the percentage of cells with <40, 40 or >40 chromosomes in each of the metaphases counted from each iPSC line. At least 25 metaphases were counted for each line.

3.2.1.2 Cell cycle analysis of iPSC lines

B-Myb has been widely reported as a cell cycle regulator. To determine whether the iPSCs with modified B-*myb* alleles have an altered cell cycle profile, iPSCs were stained with propidium iodide and analysed by flow cytometry. The cell cycle was analysed for each of the three genotypes at two different passages. Figure 3.5A shows the gating strategy as follows: cells were first selected based on their forward and side scatter (top left panel), then single cells were selected by doublet discrimination (top right panel), and finally, the percentage at each stage of the cell cycle was determined as shown by

the sectioning in the histogram (bottom panel). Figure 3.5B shows that the proportion of iPSCs in the G1 phase for B-*myb*$^{+/+}$ iPSCs was 42% compared to 29% for B-*myb*$^{+/\Delta}$ and 32% for B-*myb*$^{F/\Delta}$. Contrary to this, the proportion of iPSCs in the S phase for B-*myb*$^{+/\Delta}$ was 40% and for B-*myb*$^{F/\Delta}$ was 37% compared to B-*myb*$^{+/+}$ which was 32%. The proportion of iPSCs in the G2/M phase of the cell cycle was 35% for both B-*myb*$^{+/\Delta}$ and B-*myb*$^{F/\Delta}$ compared to 29% for B-*myb*$^{+/+}$. This data indicated that the iPSCs with only one functional allele of B-Myb have lower proportion of cells in the G1 phase and an increased proportion of cells in the S and G2/M phases.

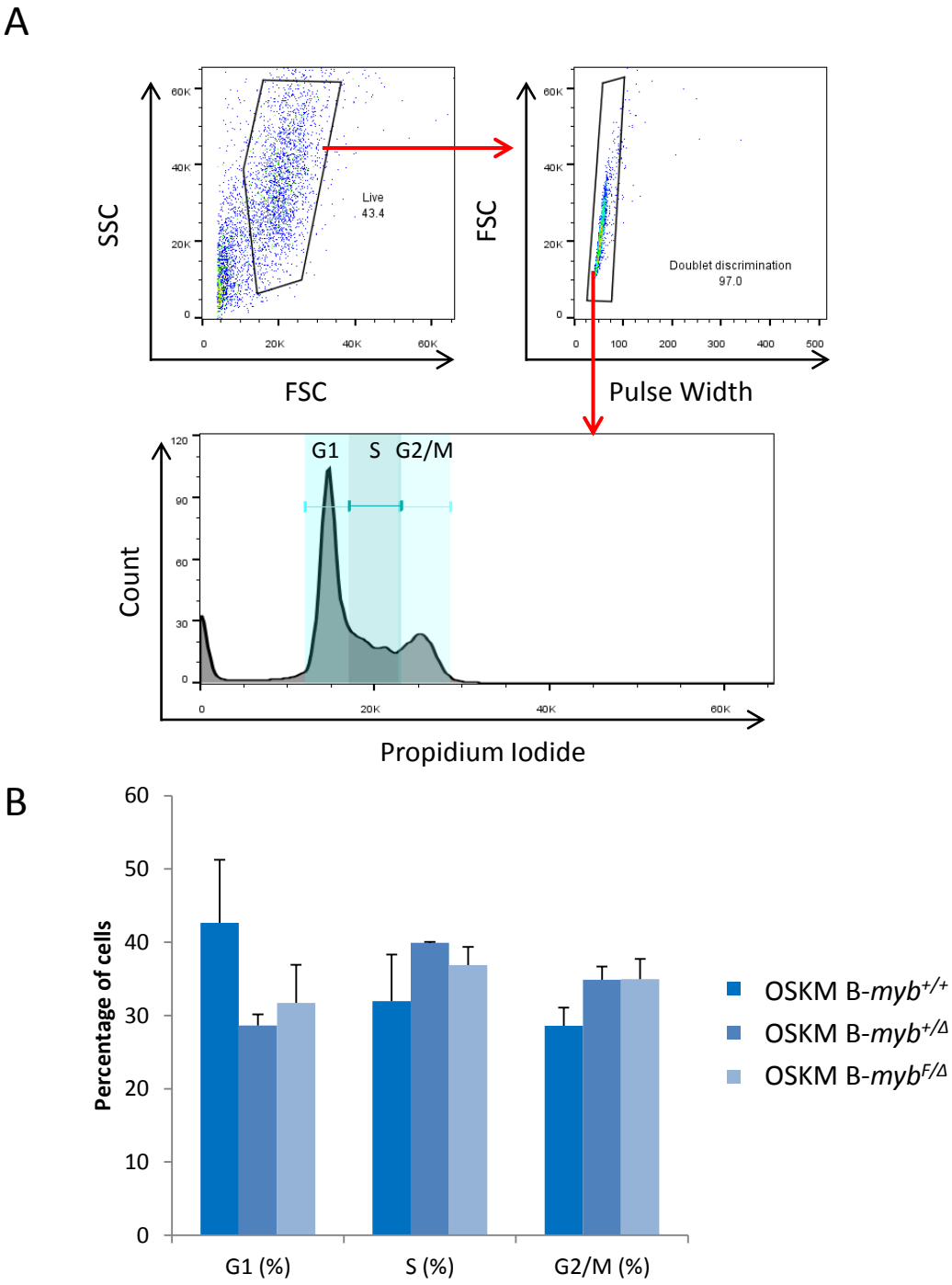


Figure 3.5: Cell cycle analysis by propidium iodide staining
(A) Gating strategy used to quantify cell cycle phases. The upper left panel shows a dot plot with the gated region (live). The upper right panel shows the dot plot for the doublet discrimination gate. Finally the double gated cells were analysed by generating a histogram representing the stages of the cell cycle, G1, S, G2/M visualised by propidium iodide incorporation (B) Bar graph representing the number of cells in each stage of the cell cycle for each of the three cell lines tested. Error bars represent SEM, N = 2.

3.2.1.3 Chimeric mouse generation with iPSC lines

The ability of iPSCs to generate chimeric animals is the gold standard for proof of pluripotency as it shows that the cells are able to generate cells from all lineages (Robertson, 1986, Tam and Rossant, 2003). To determine the pluripotency capacity *in vivo* of iPSCs that I generated, I made use of the transgenic service provided by the University of Birmingham (Andrea Bacon) to generate chimeric mice. The iPSCs were generated from C57/BL6 mice cells (black fur). These iPSCs were injected into FVB/N blastocysts (white fur); therefore it is easy to detect the percentage of chimerism by simply looking at the fur colour of the progeny. Chimeric mice were generated from three of the iPSC lines that had not yet had the pluripotency cassette excised. One chimeric mouse, one out of two littermates, was generated from a B-$myb^{+/\Delta}$ iPSC line. The chimerism observed with the B-$myb^{+/\Delta}$ iPSC line was low as the only dark patch was above the eye, but it showed that this line, even though it only had one B-*myb* allele, was able to contribute to the development of the mouse (Figure 3.6A). Also, I was able to obtain a chimeric mouse, one out of five littermates, from a B-$myb^{F/\Delta}$ iPSC line that showed a much higher contribution (40-50%) as the animal had patches of dark fur all over its body (Figure 3.6B). In another experiment, wild type iPSCs were injected into NOD-SCID blastocysts and a chimeric mouse was generated with less than 1% chimerism visible on the skin, shown in by the small patch of fur on the back of the mouse (Figure 3.6C). NOD-SCID mice do not have fur and fail to develop a thymus. Internal examination revealed the mouse had developed a thymus (Figure 3.6D), which contained functional thymic epithelial cells and was able to generate correctly selected T-cells (Song Baik, University of Birmingham, Thesis). By looking at fur appearance these iPSCs appear to have a low pluripotency capacity; hence the fact that a whole

organ could be generated was certainly unexpected. Figure 3.6E shows another example of an adult chimera generated when wild type iPSCs were injected into NOD-SCID blastocysts (centre), compared to an adult C57/BL6 mouse (left) and an adult NOD-SCID mouse (right). This highlights the variability in the percentage chimerism as both the chimera in photo E and C were generated with the same line of iPSCs.

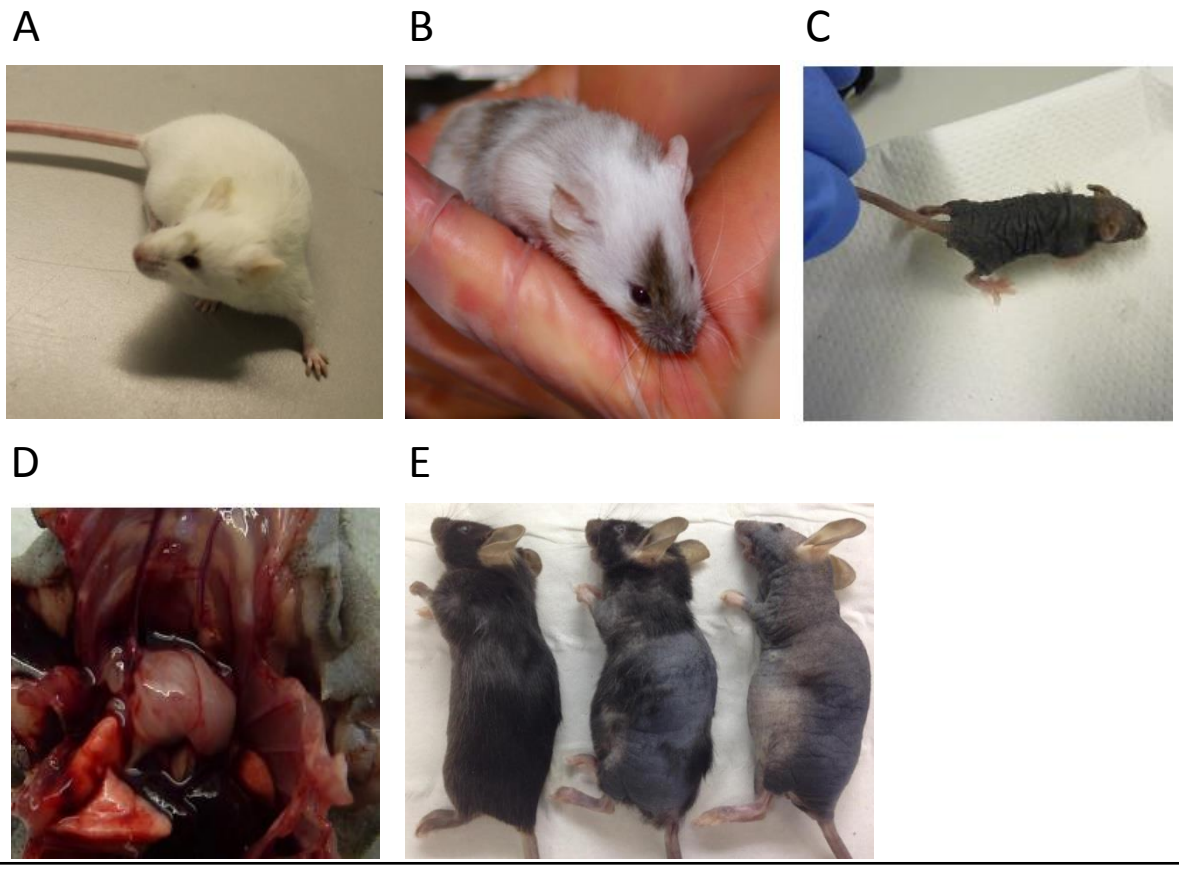


Figure 3.6: Chimeric mice
10-15 iPSCs were injected into mouse blastocysts and implanted into pseudopregnant mice by the University of Birmingham transgenic mouse facility. (A) Adult chimera generated by injection of C57/BL6 derived OSKM B-*myb*$^{+/\Delta}$ iPSCs into FVB/N blastocysts. This mouse has less than 1% chimerism as it only has a small patch above its eye. (B) Adult chimera generated by injection of C57/B6 derived OSKM B-*myb*$^{F/\Delta}$ iPSCs into FVB/N blastocysts. This mouse has 40-50% chimerism as dark fur is all over the mouse's body. (C) Adult chimera generated by injection of C57/BL6 derived OSKM B-*myb*$^{+/+}$ iPSCs into NOD-SCID blastocysts. This mouse has less than 1% chimerism shown by the patches of hair on its back and face (NOD-SCID mice are hairless). (D) Thymus examination of adult chimera. NOD-SCID mice do not develop a thymus. (E) An example of an adult C57/BL6 mouse (left). Adult chimera generated by injection of C57/BL6 derived OSKM B-*myb*$^{+/+}$ iPSCs into NOD-SCID blastocysts with 50%-60% chimerism (middle). An example of an adult NOD-SCID mouse (right).

3.2.2 Derivation of B-*myb*$^{\Delta/\Delta}$ iPSCs

In order to derive iPSCs with no B-Myb expression and at the same time remove the reprogramming cassette (OSKM) from the previously generated iPSCs, one of the B-*myb*$^{F/\Delta}$ and one of the B-*myb*$^{+/\Delta}$ iPSC lines were nucleofected with a cre-recombinase-IRES-EGFP plasmid, then live cells that were positive for GFP were sorted by FACS (Figure 3.7A). Sorted cells were plated onto mitotically inactivated MEFs and individual colonies were isolated. The red arrows in Figure 3.7B show individual iPSCs colonies as bright clusters of cells which were extracted to generate individual iPSC lines. Lines which were generated with the OSKM lentivirus that have had the pluripotency cassette removed will hence forth be designated "(OSKM)", if the pluripotency cassette is still present the line will be designated as "OSKM".

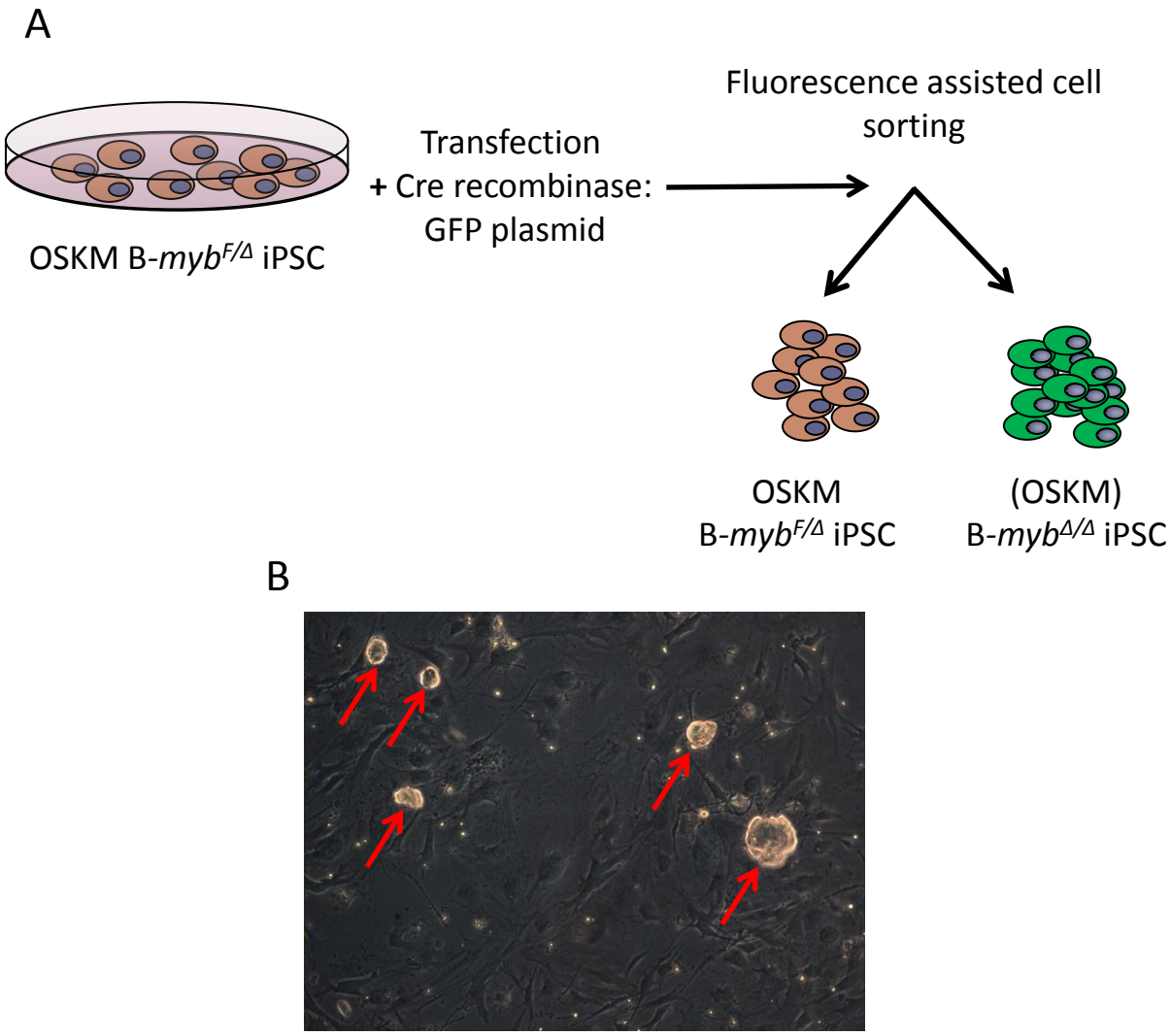


Figure 3.7: Generation of (OSKM) B-*myb*$^{\Delta/\Delta}$ iPSCs

(A) Schematic representing the experimental strategy used to generate (OSKM) B-*myb*$^{\Delta/\Delta}$ iPSCs. OSKM B-*myb*$^{F/\Delta}$ iPSCs were transfected with a Cre recombinase expression plasmid that also encoded a GFP reporter gene. Cells were then sorted based upon GFP expression. (B) GFP positive cells were plated onto mitotically inactivated MEFs; individual iPSC clones (red arrows) were isolated and expanded to generate multiple iPSC lines.

3.2.3 Confirmation of B-Myb ablation and cassette removal

A small number of cells were taken from each of the isolated colonies and genotyped by PCR to determine the loss of the B-*myb*^{F} (floxed) allele and the removal of the OSKM cassette. PCR fragments were resolved by running the samples in agarose gels. As expected, agarose gels revealed no changes on the B-*myb* alleles in the case of the B-*myb*$^{+/\Delta}$ iPSCs before and after the transfection, showing a 103bp fragment in all of the 4 lines analysed corresponding to the B-*myb*^{WT} allele (Figure 3.8A) and a 240bp fragment corresponding to the B-*myb*$^{\Delta}$ allele (Figure 3.8B).

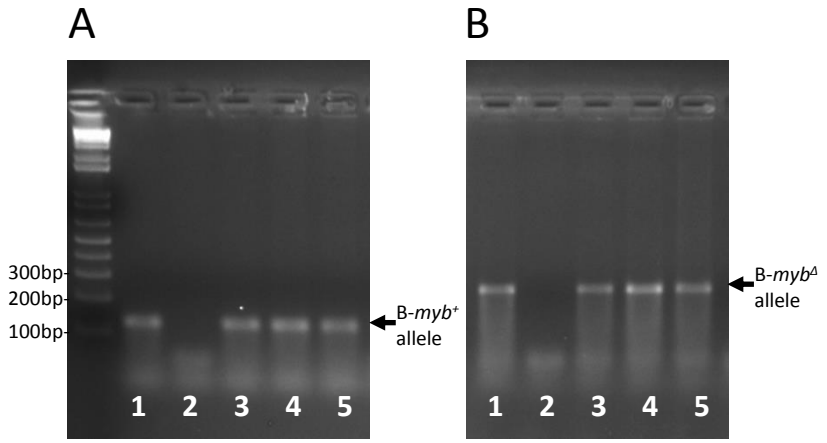


Figure 3.8: Genotyping for *B-myb*$^{+/\Delta}$ individual colonies
(A) PCR to detect B-*myb*^{WT} and B-*myb*^{F} alleles, one fragment at 103bp shows that there is a B-*myb*^{WT} allele present. (B) PCR to detect the deleted B-*myb*$^{\Delta}$ allele, one fragment at 240bp shows that there is a B-*myb*$^{\Delta}$ allele present. Lanes 1-5 correspond to individual B-*myb*$^{+/\Delta}$ iPSC lines. The relevant molecular weights are indicated on the left.

Agarose gels of PCR fragments from isolated iPSC colonies derived from B-*myb*$^{F/\Delta}$ iPSCs show that in two of the lines (Figure 3.9A, red box) the B-*myb*^{F} allele had been excised as the corresponding 103bp fragment was absent, but still had a 240bp fragment representing the B-*myb*$^{\Delta}$ allele (Figure 3.9B, red box).

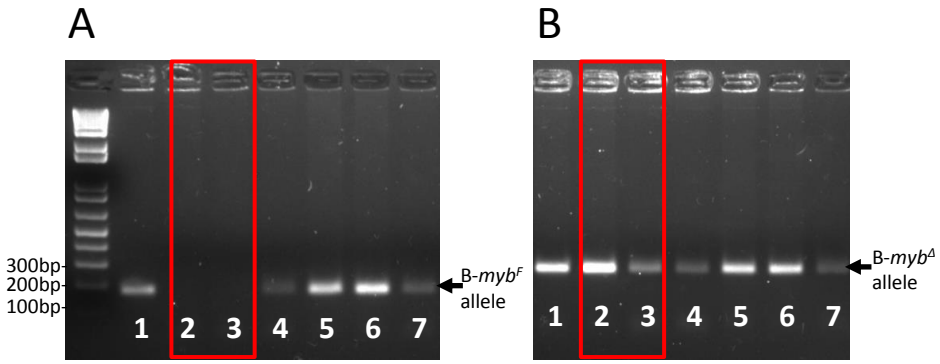


Figure 3.9: Genotyping for B-*myb*$^{\Delta/\Delta}$ individual colonies
(A) PCR to detect B-*myb*^{WT} and B-*myb*^{F} alleles, one fragment at 143bp shows that there is a B-*myb*^{F} allele present. (B) PCR to detect the deleted B-*myb*$^{\Delta}$ allele, one fragment at 240bp shows that there is a B-*myb*$^{\Delta}$ allele present. Each lane corresponds to an individual B-*myb*$^{\Delta/\Delta}$ iPSC line. The relevant molecular weights are indicated on the left.

To determine whether the pluripotency cassette had been removed, PCR was carried out with primers that were designed to amplify a 600bp fragment on the 3' end of *c-Myc* and into the WPRE region of the pluripotency cassette; therefore the clones showing a 600bp fragment on the agarose gel still contained the pluripotency cassette (Figure 3.10A). The pluripotency cassette had been removed from all five of the B-*myb*$^{+/\Delta}$ lines as there was no fragment on the gel at 600bp, the only fragment seen was in the positive control lane. I also determined whether the pluripotency cassette was still present in the B-*myb*$^{F/\Delta}$ lines or successfully removed. Only one line from the seven generated still contained the pluripotency cassette (Figure 3.10B) shown by the 600bp fragment in lane 1.

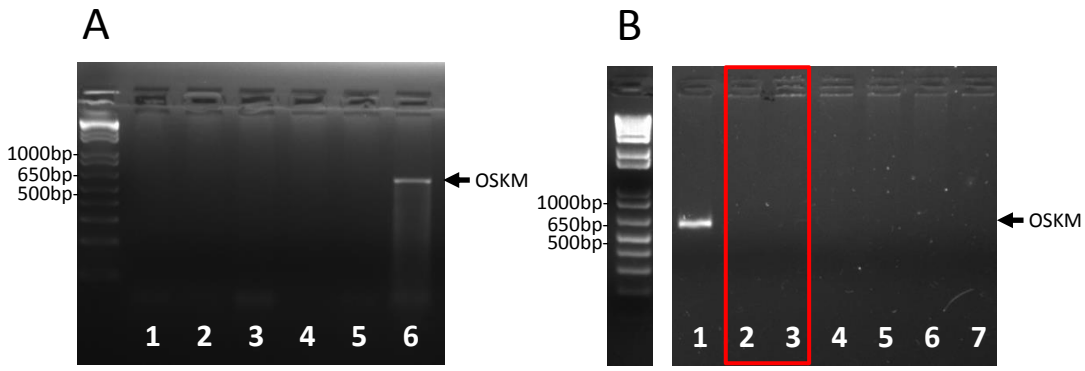


Figure 3.10: Genotyping to detect OSKM cassette
PCR to detect the presence of the OSKM cassette, a fragment at 600bp shows that there is still an OSKM cassette present. No fragment indicates that the OSKM cassette has been excised. (A) Lanes 1-5 correspond to individual B-*myb*$^{+/\Delta}$ iPSC lines, lane 6 – OSKM cassette positive control. (B) Each lane corresponds to an individual B-*myb*$^{\Delta/\Delta}$ iPSC line. The relevant molecular weights are indicated on the left.

To further confirm the deletion of the B-*myb* gene, mRNA was extracted from both B-*myb*$^{+/+}$ and B-*myb*$^{\Delta/\Delta}$ iPSCs lines, cDNA was synthesised and B-Myb expression checked by qRT-PCR. As shown in Figure 3.11, B-Myb mRNA expression in the B-*myb*$^{\Delta/\Delta}$ line is reduced by greater than 25 times compared to the wild type iPSC line.

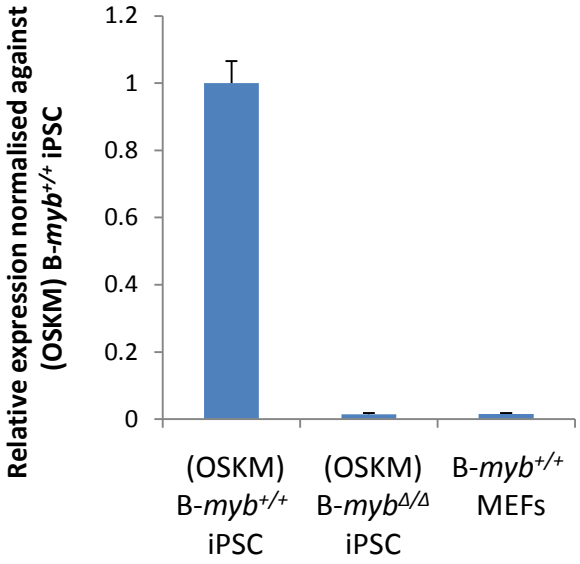


Figure 3.11: B-Myb mRNA expression in generated (OSKM) B-*myb*$^{\Delta/\Delta}$ iPSC line
(A) Histogram representing the results of qRT-PCR of iPSCs RNA from (OSKM) B-*myb*$^{+/+}$, (OSKM) B-*myb*$^{\Delta/\Delta}$ and B-*myb*$^{+/+}$ MEFs using primers designed to amplify B-*myb*. The relative expression was calculated by normalising to β_2-microglobulin housekeeping gene, then expressed relatively to (OSKM) B-*myb*$^{+/+}$ iPSC line.

Finally, B-Myb expression was also checked at the protein level by western blot. Figure 3.12A shows the absence of B-Myb protein in the (OSKM) B-*myb*$^{\Delta/\Delta}$ iPSC line. Surprisingly, this western blot showed that the B-*myb*$^{+/\Delta}$ iPSC line also had no detectible B-Myb protein expression (Figure 3.12A). The expression of pluripotent markers Oct-4 and Nanog was also analysed to determine if their expression was affected by the deletion of B-*myb*. Oct4 expression was the same on all the lines and did not appear to be affected by the level of B-Myb, mirroring what was previously described in ESCs (Lorvellec et al., 2010). The expression of Nanog was the same across all of the lines in which the pluripotency cassette had been excised but it was greater in the iPSCs that still contain the pluripotency cassette. The lack of B-Myb expression in the (OSKM) B-*myb*$^{+/\Delta}$ 1 iPSC line is un-explainable but it could be due to silencing of the remaining functional B-*myb* allele.

After finding no B-Myb expression in the (OSKM) B-*myb*$^{+/\Delta}$ 1 iPSC line, the expression of B-Myb in two further (OSKM) B-*myb*$^{+/\Delta}$ iPSC lines was checked by western blot. Figure 3.12B shows that the (OSKM) B-*myb*$^{+/\Delta}$ 2 iPSC line also had no B-Myb expression. However, the (OSKM) B-*myb*$^{+/\Delta}$ 3 iPSC line appears to express half a dose of B-Myb when compared to wild type iPSCs line expression, as was expected for iPSCs with one functional B–*myb* allele.

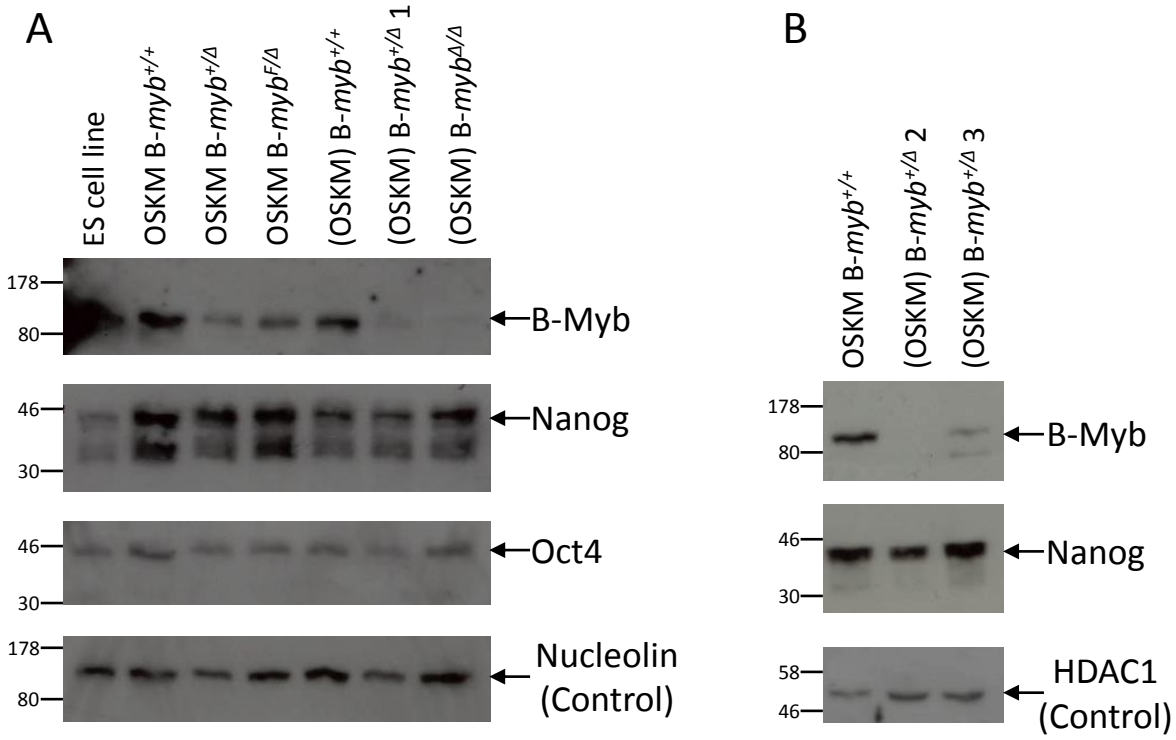


Figure 3.12: B-Myb, Nanog and Oct4 in generated iPSC lines
50μg of total protein from each of the iPSC lines and 30μg total protein from an ESC line was extracted and subjected to SDS-PAGE. Protein expression was detected by western blotting with antibodies against B-Myb, Nanog Oct4, Nucleolin or HDAC1. The position of relevant molecular weight standards is shown on the left side of the blot, and arrows on the right indicate the specific bands for each antibody.

3.3 DISCUSSION

In this chapter I described the generation and characterization of iPSCs with modified alleles of B-*myb*. iPSCs could be obtained from MEFs with one functional B-*myb* allele. Moreover, alkaline phosphatase activity was identical in the iPSCs with one functional allele compare to wild type iPSCs, showing that low levels of B-Myb does not affect basic pluripotency.

3.3.1 Chromosomal integrity

The karyotyping revealed that iPSCs with a single functional allele of B-*myb* were prone to become aneuploidy-, which may be due to the role of B-Myb in maintenance of genome integrity (Garcia and Frampton, 2006, Tarasov et al., 2008, Lorvellec et al., 2010). It would be useful to carry out a more in-depth analysis of the chromosomes through spectral karyotyping to determine if duplication or translocation of chromosomes had occurred. The karyotyping analysis was undertaken at low passage after the derivation of the iPSCs. It may also have been informative to karyotype the iPSCs at a higher passage to determine if the reduced level of B-Myb in the iPSCs led to increased chromosomal abnormalities that are normally associated with *in vitro* culturing of ESCs/iPSCs (Amps et al., 2011). Although controlling such experiments can be difficult as chromosomally abnormal pluripotent cells can often overtake a culture even with wild type cells.

3.3.2 Cell cycle changes

Unsurprisingly, due to B-Myb's role in the cell cycle, the proportion of cells in each phase of the cell cycle of the iPSCs with reduced B-Myb expression was affected. B-Myb reaches maximum expression during the S phase of the cell cycle (Lam et al., 1992, Robinson et

al., 1996) and has a role in progression from the S phase to G2/M (Sala and Calabretta, 1992, Zhu et al., 2004, Pilkinton et al., 2007). The results of the cell cycle analysis showed an increased number of cells in the S and G2/M phases; therefore the reduced B-Myb expression in these iPSCs could be delaying the progression through the cell cycle. An increase in the percentage of cells in the G2/M phase was also shown in ESCs treated with B-Myb shRNA (Tarasov et al., 2008). B-Myb activates Cyclin A, Cyclin B and CDK1 (Sala and Calabretta, 1992, Zhu et al., 2004, Pilkinton et al., 2007), which are all essential for progression through G2/M. It is conceivable that the reduced expression of B-Myb in the iPSCs is slowing cell cycle progression by affecting the expression/activity of Cyclin A, Cyclin B and CDK1.

3.3.3 Chimeric mice

An important test of a cells pluripotent capacity is their ability to contribute to chimeric mice formation (Robertson, 1986, Tam and Rossant, 2003). iPSCs with only one functional B-*myb* allele are able to form chimeric mice. There are limitations to chimera experiments as seen by the mice that I was able to generate. The percentage of chimeric fur can be very low yet whole organs not present in the non-chimeric mice can be formed, showing that the contribution to the fur is not a determinant for total contribution to the chimera. Generation of chimera using 4-N tetraploid complementation would be the ideal technique to use, as any live animal generated will be completely derived from the injected cells (Tam and Rossant, 2003). Unfortunately, this technique was not available in the Technology Hub or in the Institute of our collaborator Dr Kaji.

3.3.4 Excision of OSKM and B-*myb*

I also generated stable iPSCs with modified B-*myb* alleles in which the reprogramming cassette was excised. Interestingly, when cre recombinase was expressed in four of the generated lines the OSKM pluripotency cassette was successfully excised but the B-*myb* *floxed* allele was not removed. This could be due to different accessibility of the cre recombinase to the insertion sites of the lentivirus compared to the chromosomal position of the loxP sites in the B-myb^F allele.

Further analysis of these clones showed that the expression of the pluripotency markers, Nanog and Oct4 did not change in iPSCs with half or no B-Myb expression. This is in agreement with previous data from our lab completed in ESCs (Lorvellec et al., 2010), and contradicts data presented by Kenneth Boheler's lab in which knockdown of B-Myb in ESCs lowered expression of Oct4 (Tarasov et al., 2008).

Two of the iPSC lines that still had one functional B-*myb* allele did not appear to express any protein, this was striking but could be explained by the functional allele of B-*myb* becoming silenced in that particular line.

These data show that it is possible to maintain iPSCs which have no B-Myb expression. Moreover, cre recombinase expression not only allowed for the removal of the floxed B-*myb* allele but also for removal of the reprogramming factors from the iPSCs. There could have been multiple integrations of the polycistronic reprogramming cassette into the lines which would increase expression of the reprogramming factors in certain lines and could influence experimental results when comparing multiple cell lines. Working with factor-free iPSCs will also more closely represent ESCs (Soldner et al., 2009). These iPSCs will be a useful tool to study the effect of reduced levels of B-Myb in iPSCs.

B-Myb has been shown by our group and others to be crucial for maintenance of genome stability, so it will be interesting to use these derived iPSC lines to determine if the level of expression of B-Myb correlates with increased genome instability.

CHAPTER 4: WHAT IS THE ROLE OF B-MYB IN IPSCS?

4.1 INTRODUCTION

B-Myb has been shown to be important for proliferation and cell cycle progression.

It has been shown to be involved in maintaining genome integrity throughout the animal kingdom in *Drosophila* (Manak et al., 2002, Fung et al., 2002), *Danio rerio* (zebrafish) (Shepard et al., 2005), DT40 chicken B-cells (Ahlbory et al., 2005), human haemopoietic cells (Garcia and Frampton, 2006), and mouse ESCs (Lorvellec et al., 2010).

Previous work from my research group showed that ESCs with ablated B-Myb expression display diminished proliferation and accumulation of cells in the G2/M phase of the cell cycle. ESCs without B-Myb expression also exhibited accumulation of DNA double strand breaks (DSB) identified by detection of γ-H2AX (Lorvellec et al., 2010).

iPSCs are very similar to ESCs but a recent report shows that iPSCs are more sensitive to ionizing radiation than ESCs, claiming that the DNA repair pathways being used by the iPSCs are more similar to the pathways found in MEFs (from which the iPSCs were derived) than ESCs (Zhang et al., 2013, Tichy and Stambrook, 2008). This would potentially limit the use of iPSCs in regenerative medicine as the high proliferation rate of the cells will cause DNA damage that will not be repaired effectively if the pathway is the same as in MEFs. Understanding the pathways involved and the role of B-Myb in this process will aid in determining if iPSCs are safe for therapy.

In this chapter I attempted to determine if the absence of B-Myb in iPSCs leads to the same genome instability phenotype as previously published in ESCs.

4.2 RESULTS

4.2.1 Proliferation analysis of B-*myb*$^{\Delta/\Delta}$ iPSCs

Based on the ample literature showing the importance of B-Myb in proliferation, I decided first to determine the growth kinetics of iPSCs with ablated B-Myb compared to wild type iPSCs. 10,000 iPSCs were plated and the live cells were counted every 24 hours after plating. For this study I used iPSCs lines in which the OSKM cassette had been excised. In wild type iPSCs (B-*myb*$^{+/+}$), an exponential growth can be seen with cells tripling in number from 24 hours to 48 hours and again from 48 hours to 72 hours (Figure 4.1, blue line). This rapid proliferation has been previously described for ESCs (Chisholm et al., 1985, Thomson et al., 1998). The increase in cell number from 0 hours to 24 hours was only double which can be explained due to the passaging stress. The increase in cell number between 72 hours and 96 hours was also only 1.4 times due to the limited space in the well and the iPSCs becoming over confluent.

In contrast, the B-*myb*$^{\Delta/\Delta}$ iPSCs showed slower growth kinetics, iPSCs did not triple in number in any 24 hour period, they only doubled in number every 24 hours except between 72 hours and 96 hours in which they only increased in number by a factor of 1.2 (Figure 4.1, red line).

At 96 hours the number of wild type iPSCs was 2.7 fold higher compared to B-*myb*$^{\Delta/\Delta}$ iPSCs (P=0.0461 by unpaired two tailed Student's T-Test). Thus, this result shows that ablation of B-Myb has a negative effect on the growth of iPSCs, mirroring the proliferative defect previously shown in ESCs (Lorvellec et al., 2010).

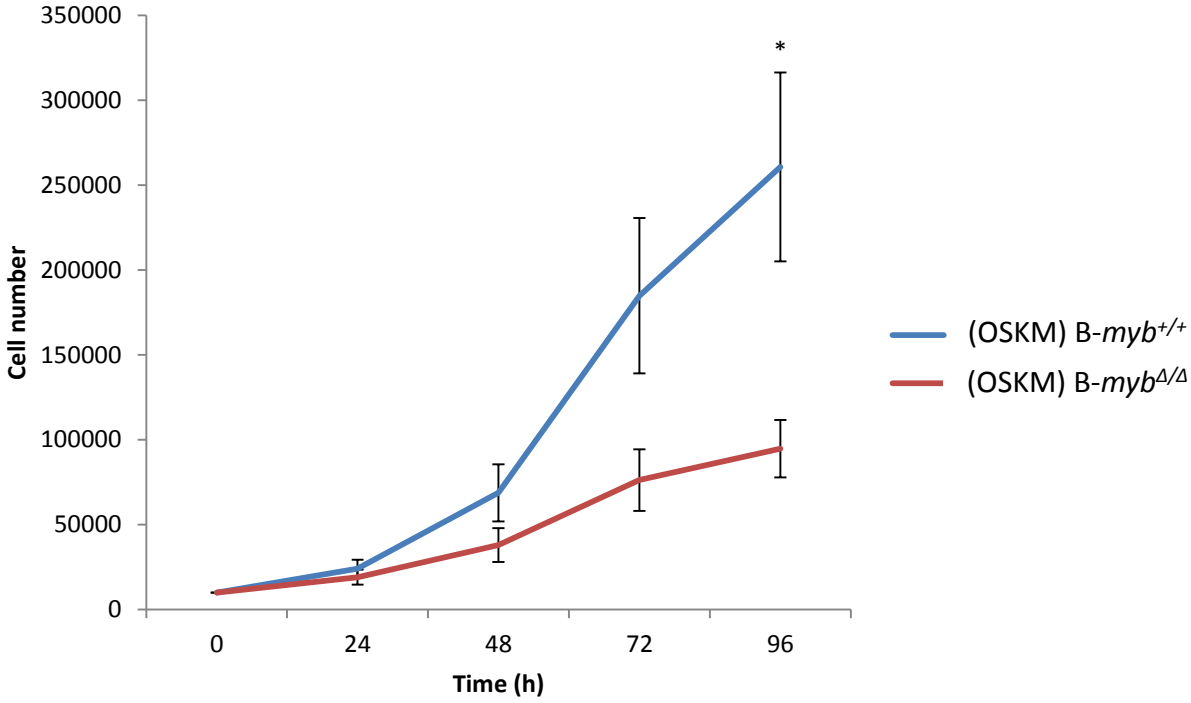


Figure 4.1: Growth rate of (OSKM) B-*myb*$^{+/+}$ or (OSKM) B-*myb*$^{\Delta/\Delta}$ iPSCs
10000 (OSKM) B-*myb*$^{+/+}$ or (OSKM) B-*myb*$^{\Delta/\Delta}$ iPSCs were plated onto mitotically inactivated MEFs then their growth was assessed every 24 hours. Error bars represent SEM, N=3, * P<0.05, by unpaired two-tailed T-Test

4.2.2 Polyploid analysis of (OSKM) B-*myb*$^{\Delta/\Delta}$ iPSCs

Downregulation of B-Myb expression in ESCs treated with B-Myb shRNA caused an increase in the number of polyploid cells after as little as 24 hours (Tarasov et al., 2008).

To determine if iPSCs in which B-Myb expression had been ablated would exhibit the same phenotype, B-*myb*$^{+/+}$, B-*myb*$^{+/\Delta}$ and B-*myb*$^{\Delta/\Delta}$ iPSCs were fixed, permeabilised and stained with DNA intercalating agent 7AAD and analysed by flow cytometry. Cells were gated based upon their FSC and SSC profile (Figure 4.2A, left panel), then gated to avoid doublets (Figure 4.2A, middle panel), and finally a histogram showing fluorescence based upon 7AAD incorporation was generated for the double gated cells (Figure 4.2A, right panel). The experiment was performed three times and the data was averaged to determine statistical significance (Figure 4.2B). Cells with higher DNA content than

G2/M are considered to be polyploid (greater than 4N). The proportion of polyploid cells in the (OSKM) B-*myb*$^{+/+}$and (OSKM) B-*myb*$^{+/\Delta}$ iPSC lines were 8.4% and 6.5% percentage, respectively. However, the percentage of polyploid cells in the (OSKM) B-*myb*$^{\Delta/\Delta}$ iPSC line was significantly higher than the (OSKM) B-*myb*$^{+/+}$ iPSCs at 19.5% (P=0.006 by unpaired two-tailed T-Test). These results indicate that iPSCs with no B-Myb expression are prone to become polyploid and thus have acquired genome instability.

4.2.3 Double strand break in (OSKM) B-*myb*$^{\Delta/\Delta}$ iPSCs

An increase in double strand breaks (DSB) formation was described in B-*myb*$^{\Delta/\Delta}$ ESCs (Lorvellec et al., 2010). To determine if more DSB could be observed in B-*myb*$^{\Delta/\Delta}$ iPSCs, I analysed phosphorylation of serine 139 of histone H2AX (γ-H2AX) and RAD51 protein expression as markers of DNA damage in cells (Rogakou et al., 1998, Paull et al., 2000, Shinohara et al., 1992, Sharan et al., 1997). B-*myb*$^{+/+}$, B-*myb*$^{+/\Delta}$ and B-*myb*$^{\Delta/\Delta}$ iPSCs were fixed, permeabilised and stained with antibodies against γ-H2AX and RAD51, then stained with appropriate fluorophore conjugated secondary antibodies and visualised by confocal microscope. Preliminary data in Figure 4.3A shows the γ-H2AX (green) and RAD51 (red) foci in unirradiated iPSCs with wild type and modified B-*myb* alleles. A cell with more than 6 H2AX-γ foci per nucleus is considered to have severe DNA damage. In this preliminary experiment, the average number of γ-H2AX and RAD51 foci per cell was above 10 regardless of whether they had wild type, half or no expression of B-Myb (Figure 4.3B and C).

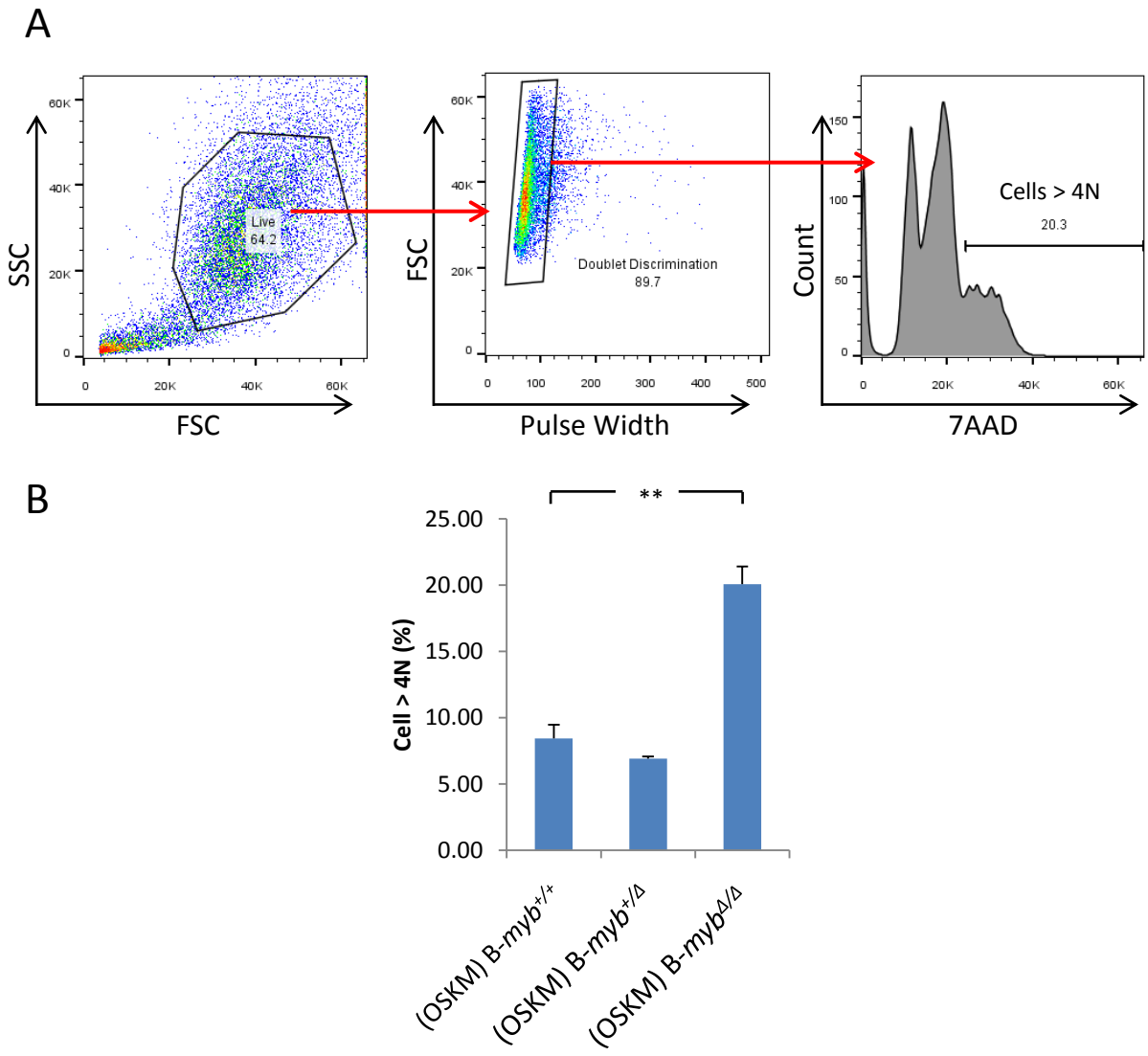


Figure 4.2: **Polyploid analysis of (OSKM) B-*myb*$^{+/+}$, (OSKM) B-*myb*$^{+/\Delta}$ or (OSKM) B-*myb*$^{\Delta/\Delta}$ iPSCs**

B-*myb*$^{+/+}$, B-*myb*$^{+/\Delta}$ and B-*myb*$^{\Delta/\Delta}$ iPSCs were fixed and permeabilised then stained with 7AAD and analysed by flow cytometry. (A) Gating strategy used to analyse cell cycle profile. Cells were gated based on FSC and SSC (left panel, live), then gated for doublet discrimination, (middle panel) finally the double gated cells were analysed by 7AAD incorporation. (B) Quantification of biological replicates. Error bars represent SEM, N = 3 ** P < 0.01 by unpaired two-tailed T-Test

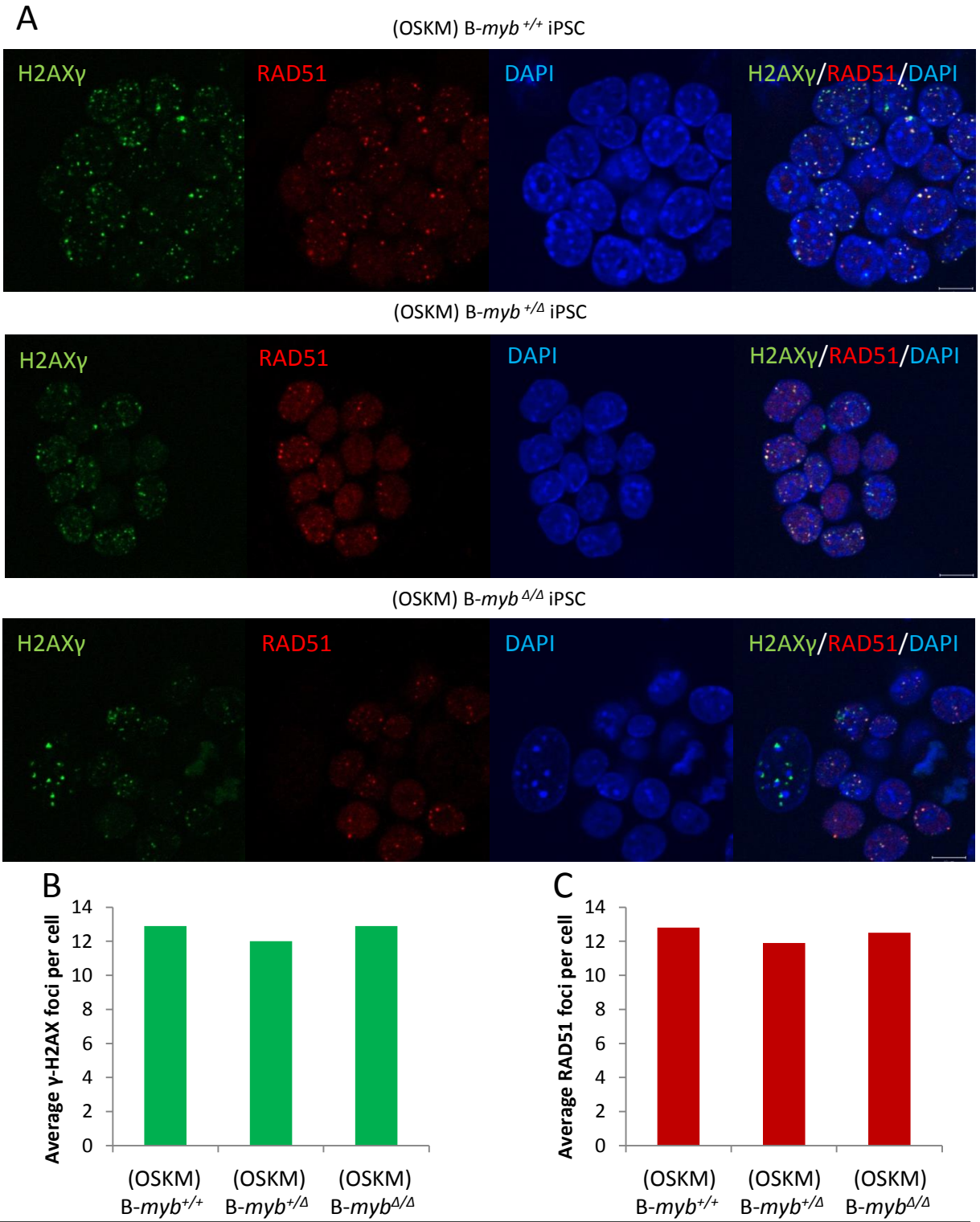


Figure 4.3: γ-H2AX and RAD51 immunofluorescence staining
(A) B-*myb*$^{+/+}$, B-*myb*$^{+/\Delta}$ and B-*myb*$^{\Delta/\Delta}$ iPSCs were grown on gelatinised coverslips with mitotically inactivated MEFs for 24 hours. They were fixed, permeabilised and then stained with primary antibodies against γ-H2AX and RAD51 raised in mouse and rabbit respectively. The cells were then stained with anti-mouse Alexa 488 and anti-mouse Alexa 594 antibodies before being counterstained with DAPI. γ-H2AX (B) and RAD51 (C) foci were counted in at least 10 nuclei per genotype.

4.2.4 Which DNA damage repair pathway is B-Myb involved in?

iPSCs with ablated B-Myb must have a defect in the cell cycle checkpoint control for cells to become polyploid. In order to gain insight on B-Myb function, iPSCs were treated with inhibitors to selective repair pathways in order to identify sensitivity.

I decided to use three different drugs for this study: Hydroxyurea, PJ34 and camptothecin.

Hydroxyurea (HU) is a drug which inhibits DNA synthesis by blocking the activity of the enzyme ribonucleotide reductase (Young and Hodas, 1964, Sinclair, 1965, Krakoff et al., 1968). Ribonucleotide reductase converts ribonucleotides into deoxynucleotides required for DNA synthesis (Lammers and Follmann, 1983), if it is blocked DNA synthesis stalls and cells will fail to replicate DNA and die (Yarbro, 1992).

To determine sensitivity to HU iPSCs with modified B-*myb* alleles were treated with increasing concentrations of HU (0.03mM-1mM) for up to 72 hours and cell viability was measured at 24, 48 and 72 hours by Cell-Quanti Blue reagent (Bio Assay Systems). Saponin treatment was used as a positive control for loss of cell viability.

At 24 hours the mean viability of B-$myb^{+/+}$ iPSCs varied between 70%-90% at each of the concentrations tested. Similar fluctuations were observed in the mean viability of B-$myb^{+/\Delta}$ and B-$myb^{\Delta/\Delta}$ iPSCs. 0.1% Saponin treatment reduced mean viability to less than 35% in each genotype of cells (Figure 4.4A).

After 48 hours of HU treatment cell viability of B-$myb^{+/+}$ iPSCs is compromised at concentrations above 0.5mM as cell viability was reduced below 50%. Cell viability was not adversely affected at lower concentrations. A similar trend was observed in B-$myb^{+/\Delta}$

iPSCs however, the B-*myb*$^{\Delta/\Delta}$ iPSCs were less sensitive and only dropped to 60% above 0.5mM HU treatment (Figure 4.4 B).

HU treatment above 0.5mM after 72 hours lowered cell viability to below 20% in B-*myb*$^{+/+}$ and B-*myb*$^{+/\Delta}$ iPSCs. B-*myb*$^{\Delta/\Delta}$ iPSCs are less sensitive to 0.5 and 1mM HU treatment as the cell viability is 31% and 45% respectively (Figure 4.4 C).

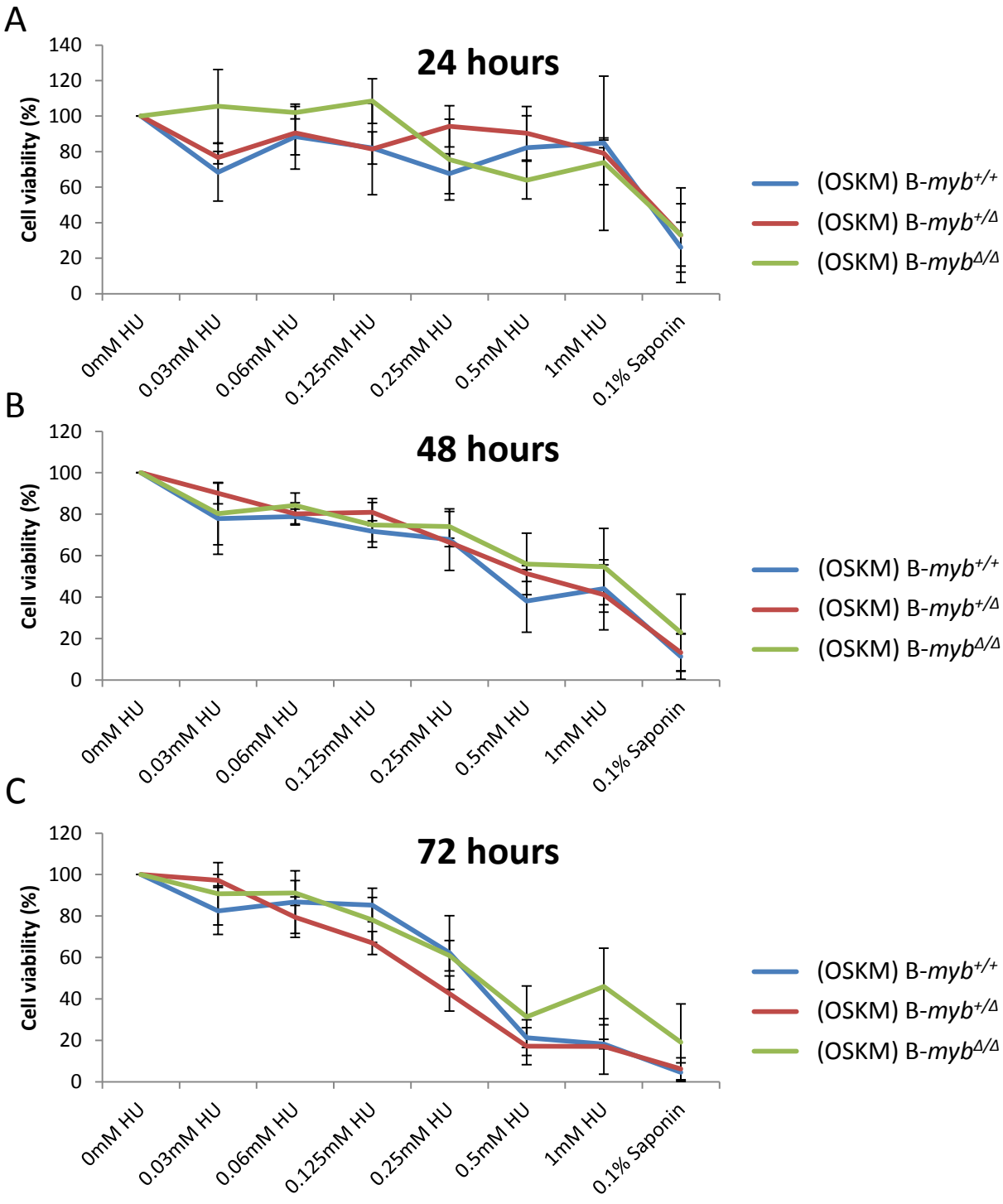


Figure 4.4: Sensitivity of iPSCs to hydroxyurea
5000 B-*myb*$^{+/+}$, B-*myb*$^{+/\Delta}$ and B-*myb*$^{\Delta/\Delta}$ iPSCs were plated onto mitotically inactivated MEFs. 24 hours after plating iPSCs were treated with serially diluted hydroxyurea (HU). 24 hours after treatment cell viability was assayed using cell quanti-blue reagent. Cell quanti-blue was removed from the cells and the cells were retreated with the same HU concentrations and then assayed again at 48 and 72 hours. The experiment was repeated at least twice with each sample analysed in triplicate. Error bars represent standard error of the mean of multiple experiments.

I also checked sensitivity to PJ34, an inhibitor of poly (ADP-ribose) polymerase 1 (PARP-1) (Abdelkarim et al., 2001). PARP-1 is involved in recruiting XRCC1, a protein which repairs single strand DNA breaks (El-Khamisy et al., 2003).

To determine sensitivity to PJ34 iPSCs with modified B-*myb* alleles were treated with increasing concentrations of PJ34 (0.1-50μM) for up to 72 hours and cell viability was measured at 24, 48 and 72 hours by Cell-Quanti Blue reagent (Bio Assay Systems). Saponin treatment was used as a positive control for loss of cell viability.

B-$myb^{+/+}$ iPSCs treated with of PJ34 for 24 hours show a gradual reduction in cell viability with a peak reduction at 50μM PJ34 reducing viability to below 60%. A similar trend was observed in B-$myb^{\Delta/\Delta}$ iPSCs. Surprisingly the B-$myb^{+/\Delta}$ iPSCs showed increased sensitivity at concentrations between 1-25μM PJ34 treatment (Figure 4.5A).

At 48 hours of PJ34 treatment B-$myb^{+/+}$ iPSCs drop below 60% viability at a lower concentration of 10μM and peak reduction of viability is below 40% at 50μM. A similar gradual decline in cell viability was observed in B-$myb^{+/\Delta}$ and B-$myb^{\Delta/\Delta}$ iPSCs, however B-$myb^{+/\Delta}$ iPSCs were more sensitive at 0.1 and 1μM PJ34 and B-$myb^{\Delta/\Delta}$ iPSCs were more resistant at 10 and 12.5μM PJ34 (Figure 4.5B).

The trend in reduction of cell viability at 72 hours is similar to 48 hours in B-$myb^{+/+}$ and B-$myb^{+/\Delta}$ iPSCs although the drop at 10μM had increased from 60% to 40% viability. Again the B-$myb^{+/\Delta}$ iPSCs showed higher sensitivity at 0.1μM PJ34. The B-$myb^{\Delta/\Delta}$ iPSCs also showed increased resistance at the 10 and 12.5μM PJ34 concentrations (Figure 4.5C).

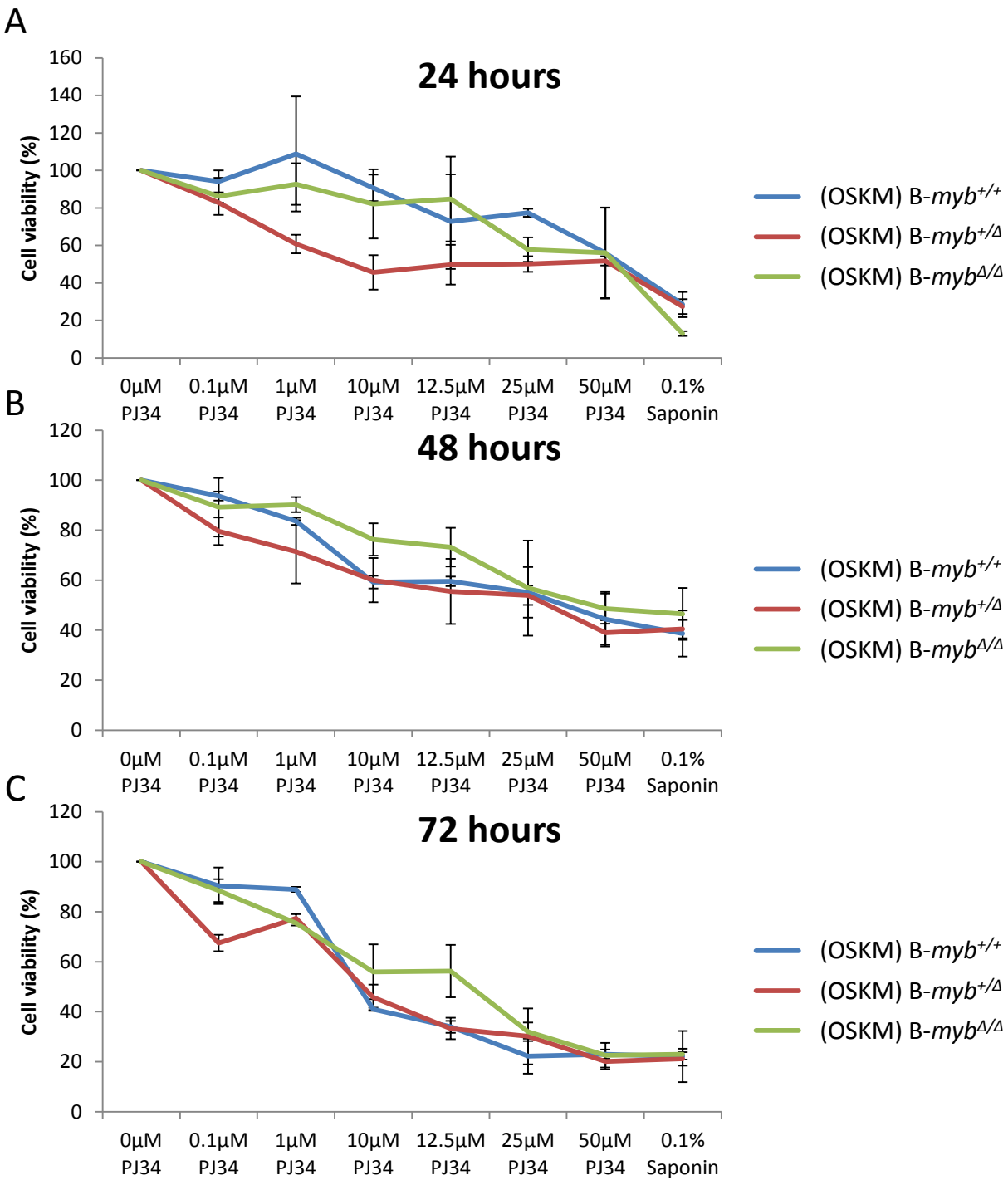


Figure 4.5: Sensitivity of iPSCs to PJ34
5000 B-*myb*$^{+/+}$, B-*myb*$^{+/\Delta}$ and B-*myb*$^{\Delta/\Delta}$ iPSCs were plated onto mitotically inactivated MEFs. 24 hours after plating iPSCs were treated with serially diluted PJ34 in full ESC medium. 24 hours after treatment cell viability was assayed using cell quanti-blue reagent. Cell quanti-blue was removed from the cells and the cells were retreated with the same PJ34 concentrations and then assayed again at 48 and 72 hours. The experiment was repeated at least twice with each sample analysed in triplicate. Error bars represent standard error of the mean of multiple experiments.

Camptothecin (CPT) is a compound with anti-tumour activity that blocks DNA repair through inhibition of DNA topoisomerase I (topo I) by forming a stable complex between topo I and DNA (Hsiang et al., 1985, Redinbo et al., 1998). Topo I is an enzyme found throughout evolution that is crucial for repair of DNA after single strand breakage (Wang, 1996).

The results in Figure 4.6 show that iPSCs with reduced or ablated expression of B-Myb are sensitive to CPT treatment at 24 hours even at the lowest dose used in this experiment (0.06μM). At 2μM CPT was toxic for B-$myb^{+/+}$ iPSCs. There is a significant difference in cell viability between the iPSCs with wild type B-Myb and iPSCs with no B-Myb when treated with 0.125μM CPT (P=0.0379 by unpaired two-tailed T-Test, Figure 4.6A).

Treating cells with CPT for 48 hours is detrimental to cell survival as a reduction in viability to below 40% is observed at 0.125μM concentration in B-$myb^{+/+}$ iPSCs. The B-$myb^{+/\Delta}$ and B-$myb^{\Delta/\Delta}$ iPSCs were less sensitive with 50% viability at the same concentration. The B-$myb^{+/+}$ iPSCs showed reduced cell viability (below 20%) at all the higher concentrations, however the B-$myb^{+/\Delta}$ and B-$myb^{\Delta/\Delta}$ iPSCs viability remained above 20% (Figure 4.6B).

72 hours of CPT treatment is toxic to the cells even at the lowest concentration tested (0.06μM) as cell viability was reduced below 55% regardless of the genotype of the iPSCs (Figure 4.6B).

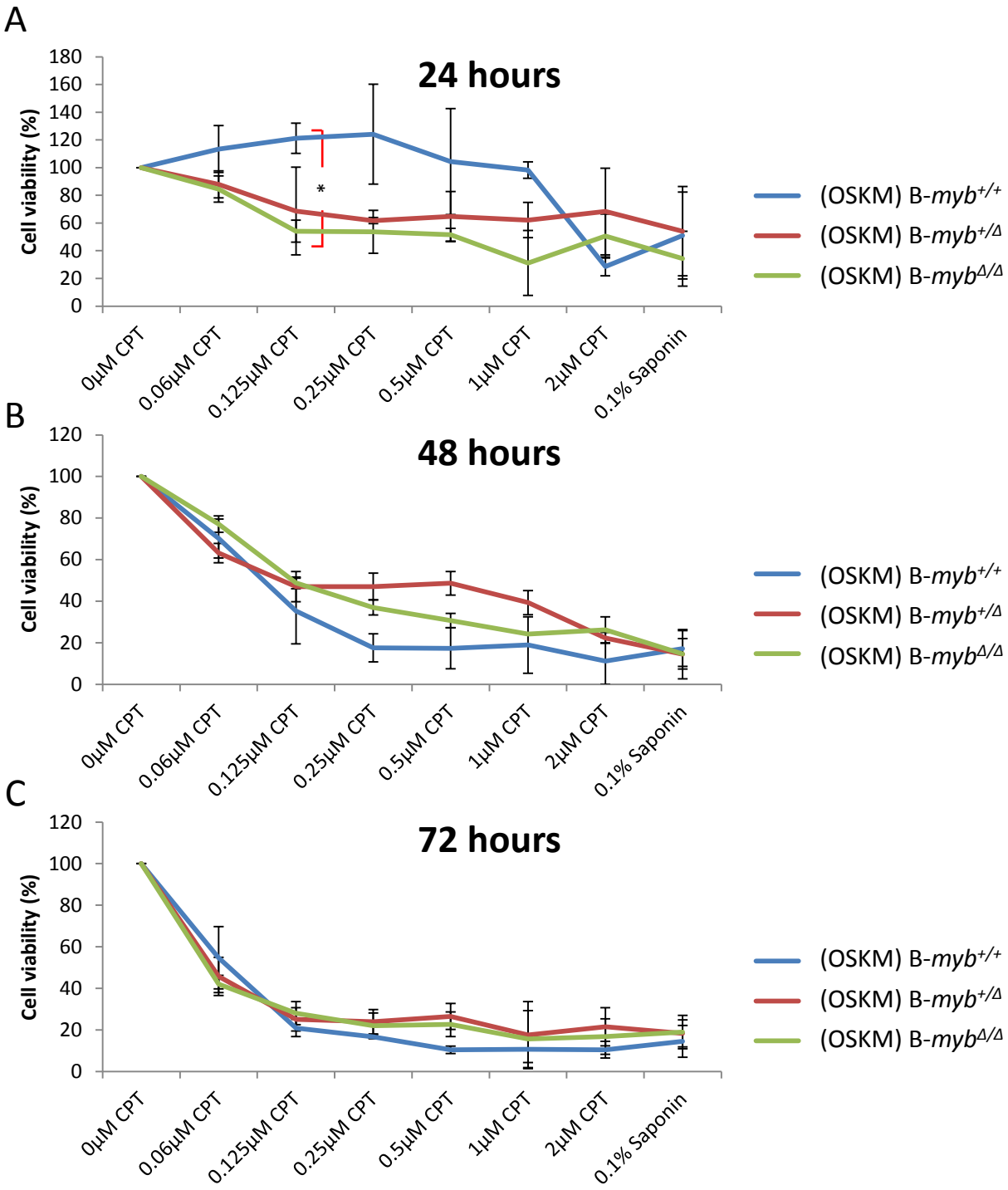


Figure 4.6: Sensitivity of iPSCs to camptothecin
5000 B-*myb*$^{+/+}$, B-*myb*$^{+/\Delta}$ and B-*myb*$^{\Delta/\Delta}$ iPSCs were plated onto mitotically inactivated MEFs. 24 hours after plating iPSCs were treated with serially diluted camptothecin (CPT) in full ESC medium. 24 hours after treatment cell viability was assayed using cell quanti-blue reagent. Cell quanti-blue was removed from the cells and the cells were retreated with the same CPT concentrations and then assayed again at 48 and 72 hours. The experiment was repeated at least twice with each sample analysed in triplicate. Error bars represent standard error of the mean of multiple experiments.

4.3 DISCUSSION

In this chapter I aimed to determine if iPSCs with no B-Myb display genome instability as previously described in ESCs (Lorvellec et al., 2010).

4.3.1 iPSC growth in the absence of B-Myb

iPSCs with no B-Myb appear to be viable, however analysis of their growth potential shows that the lack of B-Myb significantly reduces the growth of the iPSCs. This phenotype is identical to ESCs which have B-Myb ablated (Lorvellec et al., 2010). These findings indicate that B-Myb has an important role in iPSCs proliferation.

4.3.2 Lack of B-Myb leads to genomic instability

The polyploid analysis of iPSCs with ablated B-Myb compared to wild type iPSCs and iPSCs with one functional B-*myb* allele revealed double the number of polyploid cells, highlighting a role for B-Myb in maintenance of genome stability in iPSCs. The cells tested here were all of low passage (<20), so it is striking that 20% of iPSCs with ablated B-Myb contain chromosomal abnormalities. In ESCs with downregulated B-Myb levels, defects in spindle formation were attributed to the observed genomic instability (Tarasov et al., 2008). In addition to this, depletion of the B-Myb-MuvB complex in embryonal carcinoma cells led to polyploidy (Knight et al., 2009). Moreover, when looking at a single strand DNA level, B-*myb* knockout in ESCs was shown to have significantly increased replication fork stalling (Lorvellec et al., 2010). These phenotypes are not contradictory, as B-Myb regulates CDK1 and CDK1 is involved in both mitotic spindle formation and in G2/M checkpoint control (Heald et al., 1993, Blangy et al., 1995, Zhu et al., 2004). Furthermore, B-Myb is a member of the Myb-Clafi

complex which is required for assembly of clathrin in mitotic spindle formation and if impaired can lead to errors in mitosis and genomic instability (Yamauchi et al., 2008).

4.3.3 Double strand break analysis in iPSCs

The number of γ-H2AX and RAD51 foci did not change between different genotypes of iPSCs, with an average of over 10 foci per cell. At the time this study was performed, work done by others showed that healthy cells contained less than 3 foci, and cells with greater than 6 foci were considered to be damaged (Paull et al., 2000, Riballo et al., 2004, Lobrich et al., 2010). When analysing γ-H2AX and RAD51 foci in the different derived iPSC lines, I found that the majority of the cells had greater than 6 foci per cell without any irradiation or DNA damaging agent exposure. Further investigation was not continued due to the assumption that the iPSCs had become aberrant in culture.

More recently, a report was published showing that iPSCs have higher baseline γ-H2AX and RAD51 foci accountable to their high replicative activity (Felgentreff et al., 2014). The same report also showed that iPSCs had to be synchronised in order to observe DNA damage repair pathway effects (Felgentreff et al., 2014). It would be very interesting to repeat these experiments with synchronised iPSCs to determine if there is an effect on IR sensitivity when iPSCs have reduced B-Myb expression.

If reduced expression or lack of B-Myb is causing iPSCs to become sensitive to the action of drugs which block specific pathways in DNA damage repair then it is feasible that B-Myb is involved in that specific pathway.

4.3.4 DNA repair pathway analysis

Based on a possible role for B-Myb in S phase and DNA repair, I looked at the effect that different drugs which block S phase by multiple mechanisms in iPSCs with reduced or no B-Myb expression.

Reduction or lack of B-Myb expression did not cause sensitivity to hydroxyurea, a drug which depletes the deoxyribonucleotide pool, or PJ34, a PARP-1 inhibitor.

However there was an increased sensitivity to CPT treatment at 24 hours in iPSCs with reduced or no B-Myb expression. CPT inhibits DNA topoisomerase I (topo I) by binding to topo I and DNA causing formation of single strand breaks that will lead to replication fork stalling (Chen and Liu, 1994, Pommier, 2009). Stalled forks could collapse and generate DSBs in the S phase that will be sensed by the ATR/ChK1 DNA damage repair pathway activating homologous recombination (HR) repair (Flatten et al., 2005). This greater sensitivity to CPT has been reported for *BRCA2*$^{-/-}$ cells, a protein implicated in HR (Sharan et al., 1997, Rahden-Staron et al., 2003). Thus it is possible that B-Myb is involved in DNA repair.

The drop in viability when iPSCs with ablated B-Myb are treated with CPT indicates some kind of failure in the HR repair pathway. A HR defect due to lack of B-Myb could also be responsible for the increased proportion of cells observed in the S and G2/M phases, as the cells will become arrested in these phases if DNA damage is detected. Moreover, prolonged S phase arrest can lead to over replication and chromosomal instability (Bartek and Lukas, 2001, Karakaidos et al., 2004).

B-Myb suppression in Zebrafish knocks down ATR expression delaying S phase (Stern et al., 2005). This could indicate that B-Myb has a role in DNA repair though ATR/ChK1 checkpoint.

CPT also interferes with DNA resection which is required for single strand DNA repair. It could also be possible that B-Myb is playing a role in the resection process. Further investigation is required.

CHAPTER 5: IS ENDOGENOUS B-MYB REQUIRED IN THE REPROGRAMMING PROCESS?

5.1 INTRODUCTION

B-Myb is a crucial protein for proliferation (Santilli et al., 2005) and genome integrity (Garcia and Frampton, 2006, Tarasov et al., 2008, Lorvellec et al., 2010). Expression of B-Myb is high in ESCs but decreases as cells differentiate (Raschella et al., 1995). Due to the high levels expressed in ESCs and because during development the absence of B-Myb leads to early embryonic lethality due to impairment of ICM proliferation (Tanaka et al., 1999), it was hypothesised that its absence would be detrimental to ESC survival. Nevertheless we have seen that ESCs and iPSCs are able to grow in the absence of B-Myb.

Considering the many roles attributed to B-Myb we wanted to address whether the deletion of B-Myb in somatic cells blocks the reprogramming process or if on the contrary, it would increase the efficiency of reprogramming as seen in p53 knockout experiments (Kawamura et al., 2009, Marion et al., 2009).

B-Myb expression is higher in the early stages of secondary reprogramming than other pluripotency genes such as Sox2, Nanog and Lin28a (O'Malley et al., 2013). This could be due to B-Myb playing a crucial role in the reprogramming process or it could be linked to the increase in proliferation that occurs when a MEF is reprogrammed to an iPSC.

c-Myc has been shown to increase reprogramming efficiency and B-Myb has been identified as a regulator of c-Myc (Nakagawa et al., 2008, Nakagoshi et al., 1992,

Gualdrini et al., 2010, Lorvellec et al., 2010). The inclusion of c-Myc in the reprogramming factors could make endogenous B-Myb redundant and therefore not required in the reprogramming process

In this chapter, I study if B-Myb is required for cells to undergo the reprogramming process by making use of MEFs with modified B-*myb* alleles.

5.2 RESULTS

5.2.1 Deletion of B-*myb* in MEFs by exogenous expression of Cre recombinase

To determine if there is a role for B-Myb in the reprogramming process MEFs were derived from mouse embryos with wild type B-*myb* alleles (B-$myb^{+/+}$) or mouse embryos with one deleted allele and one floxed allele (B-$myb^{F/\Delta}$). This mouse model allows for the conditional deletion of B-*myb in vitro* through the expression of cre recombinase protein. MEFs were nucleofected with a plasmid that contained the cre recombinase gene followed by an internal ribosome entry sequence (IRES) linked *EGFP* reporter gene. The GFP positive cells were sorted using FACS, B-$myb^{\Delta/\Delta}$ and B-$myb^{+/+}$ MEFs were then transduced with OSKM reprogramming lentiviral particles and allowed 14 days to reprogram before being stained for alkaline phosphatase activity. This strategy is illustrated as a schematic in Figure 5.1A. Figure 5.1B (left panel) shows colonies, which stain positively (red) indicating alkaline phosphatase activity in wild type MEFs after reprogramming. In MEFs with no B-Myb (right panel) there are no positively stained colonies due to lack of colony formation during the reprogramming process.

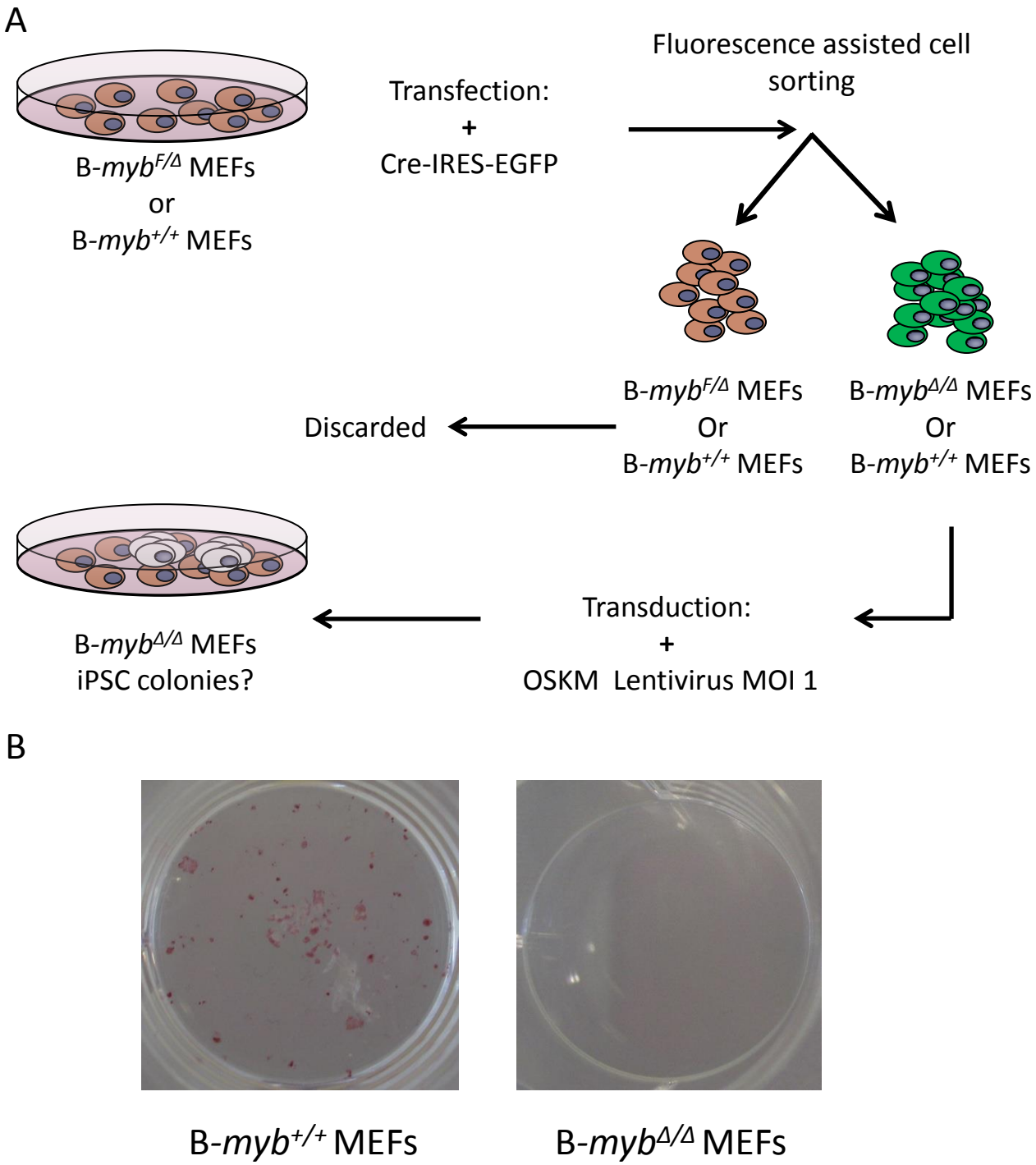


Figure 5.1: Does deletion of *B-Myb* block reprogramming?
(A) Schematic representing the experimental strategy. Briefly, MEFs with wild type of modified B-*myb* alleles were nucleofected with a plasmid that encoded *Cre-IRES-EGFP*. GFP positive MEFs were sorted, re-plated and then transduced with OSKM lentivirus to attempt to reprogram the MEFs. After 14 days the MEFs were stained for alkaline phosphatase activity. (B) Alkaline phosphatase staining, positive colonies stain red. N=1

Due to technical difficulties involving low nucleofection efficiency, low FACS purity, poor FACS yield and FACS contamination this result was only obtained from one experiment. To try to address these issues the experiment was repeated using several other transfection methods; lipofectamine, polyfectamine and electroporation were used to no avail as transfection efficiency remained low. To test if the problems were due to the plasmid being used, I generated a Cre recombinase:EGFP fusion protein expressing vector which also gave insufficient efficiency of transfection. Next, a lentiviral vector which encoded cre recombinase and GFP was used. Efficiency with the lentiviral vector was higher but there were still issues with FACS purity and contamination.

5.2.2 Deletion of B-*myb* in MEFs through endogenous expression of Cre recombinase

As a result of the difficulties of transfecting MEFs with Cre-EGFP vectors, I then decided to use an endogenous system to delete B-*myb* by crossing the B-$myb^{F/+}$ and B-$myb^{+/\Delta}$ mice with mice that express tamoxifen inducible Cre recombinase expression (Cre-ER^{T2}). B-$myb^{F/+}$:*Cre-*ER^{T2} and B-$myb^{+/\Delta}$:*Cre-*ER^{T2} were crossed to obtain B-$myb^{F/\Delta}$:*Cre-*ER^{T2} E13.5 embryos to prepare MEFs from. The efficiency of deletion in the Cre-ER^{T2} system was first determined using 4-Hydroxytamoxifen (4-OHT). MEFs were treated with 500nM 4-OHT for 24 hours then protein was extracted 48 and 96 hours after treatment. The protein was separated by SDS-PAGE and probed with antibodies against B-Myb or β-actin as a loading control. Total protein extracts from ESCs and untreated MEFs were also included as controls. Figure 5.2 shows that B-Myb expression was easily detectable in ESCs, untreated MEFs and MEFs treated with 4-OHT at 48 hours post treatment. The expression of B-Myb was not detectable in the MEFs treated with 4-OHT

at 96 hours post treatment, indicating that the deletion of B-*myb* through expression of cre recombinase after treating the MEFs with 4-OHT is sufficient to deplete protein to an undetectable level at 96 hours. The loading control was expressed at the same levels in all three lanes indicating that the same amount of protein was loaded in each well.

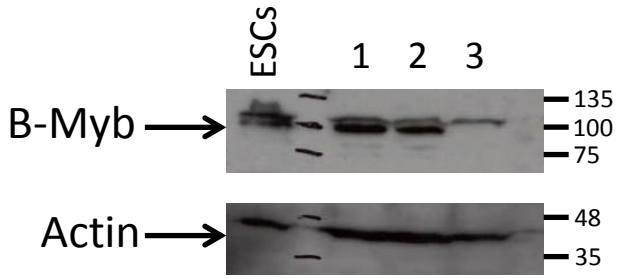


Figure 5.2: Testing Cre-ER^{T2} MEF deletion of B-*myb*
B-*myb*$^{F/\Delta}$:*Cre-ER*$^{T2+/-}$ MEFs untreated (Lane 1), B-*myb*$^{F/\Delta}$:*Cre-ER*$^{T2+/-}$ MEFs treated with 500nM 4-Hydroxytamoxifen (4OHT) for 24 hours and then protein was extracted after further 48 hours (Lane 2) or 96 hours (Lane 3). 100µg of total protein (30µg for ESCs) from each of the MEF treatments and an ESC line was extracted and subjected to SDS-PAGE. Protein expression was detected by western blotting with antibodies against B-Myb or Actin. The position of relevant molecular weight standards is shown on the right side of the blot, and arrows on the left indicate the specific bands for each antibody.

After observing that by 96 hours after 4-OHT treatment, B-Myb levels were undetectable by western blotting, I decided to use these MEFs to study the effect of B-Myb deletion during reprogramming.

B-*myb*$^{+/\Delta}$:*Cre-ER*$^{T2+/-}$ and B-*myb*$^{F/\Delta}$:*Cre-ER*$^{T2+/-}$ MEFs were treated with 500nM 4-OHT for 24 hours, grown for another 96 hours before transducing the cells with OSKM lentiviral particles at two different virus concentrations (MOI 2 and MOI 20). After 12 days the MEFs were stained for alkaline phosphatase activity. Figure 5.3 shows that there was reprogramming in the MEFs with no B-Myb expression. B-*myb*$^{+/\Delta}$:*Cre-ER*$^{T2+/-}$ MEFs had an average of 4±1 AP positive colonies compared to B-*myb*$^{\Delta/\Delta}$:*Cre-ER*$^{T2+/-}$ MEFs which had an average of 0±0 AP positive colonies. By multiplying the number of lentiviral

particles by 10 to MOI 20 the average number of AP positive colonies from B-*myb*$^{+/\Delta}$:*Cre-ER*$^{T2+/-}$ MEFs was 82±16 compared to 43±23 from B-*myb*$^{\Delta/\Delta}$:*Cre-ER*$^{T2+/-}$ MEFs.

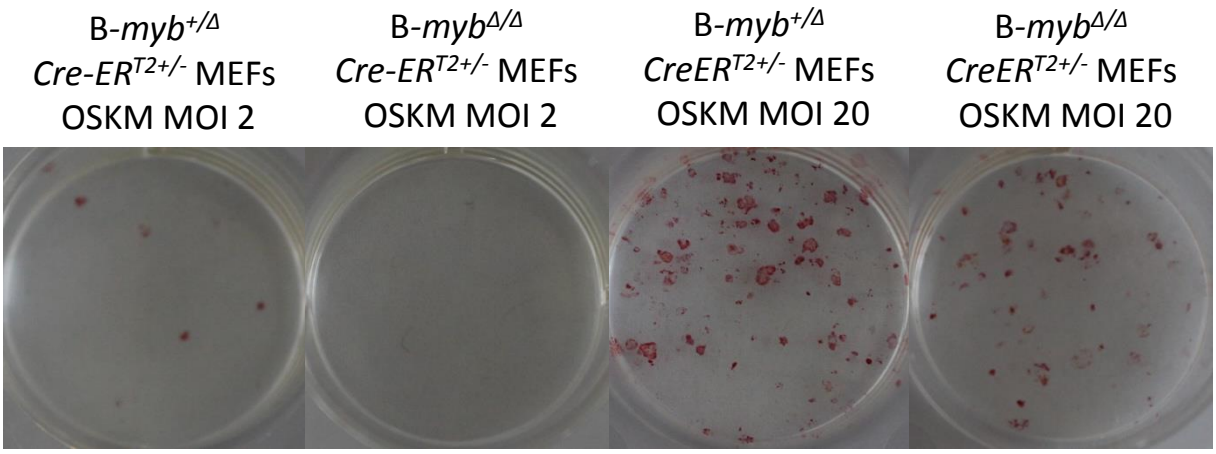


Figure 5.3: Reprogramming in the absence of B-Myb
B-*myb*$^{F/\Delta}$:*Cre-ER*$^{T2+/-}$ and B-*myb*$^{+/\Delta}$:*Cre-ER*$^{T2+/-}$ MEFs were treated with 500nm 4-OHT for 24 hours and then cultured for a further 96 hours before being transduced with OSKM lentiviral particles at MOI 2 or 20. The MEFs were cultured for 12 days before being stained for alkaline phosphatase activity. Colonies with alkaline phosphatase activity are observed as red.

One posibility is that the reprogrammed colonies seen in the B-*myb*$^{\Delta/\Delta}$ well still contained the B-*myb*^{F} allele. 18 individual colonies were picked, genomic DNA was extracted and then PCR was used to genotype the colonies for the presence of the B-*myb*^{F} allele (143bp). Figure 5.4A shows that 17 out of 18 colonies still contained the B-*myb*^{F} allele as they have a 143bp fragment on the gel image. Five B-*myb*$^{+/\Delta}$ iPSC colonies were picked as a control for the genomic extraction. To be sure that genomic DNA was extracted with enough quantity and quality; I performed PCR to determine if the B-*myb*$^{\Delta}$ allele was present. For example, cells in well 16 showed no PCR product for the B-*myb*^{F} allele that would lead to the interpretation that the clone was B-*myb*$^{\Delta/\Delta}$. This interpretation was ruled out as PCR for the B-*myb*$^{\Delta}$ allele failed to amplify any product, therefore there was not enough DNA after extraction (Figure 5.4B).

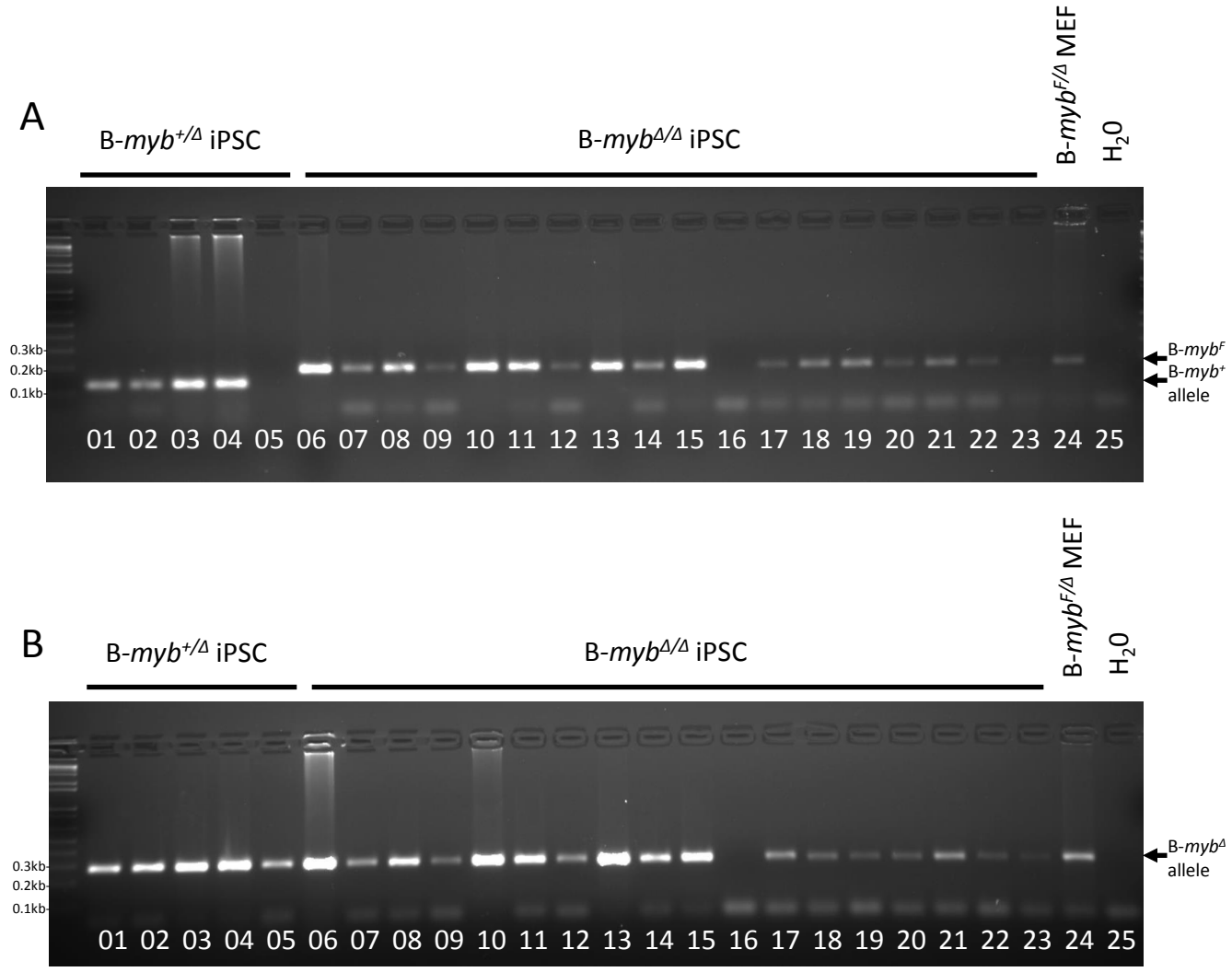


Figure 5.4: Genotyping for B-*myb*$^{\Delta/\Delta}$ *or* B-*myb*$^{+/\Delta}$ individual picked colonies generated with MOI 2 OSKM

(A) PCR to detect B-*myb*^{WT} and B-*myb*^{F} alleles, one fragment at 103bp shows that there is a B-*myb*^{WT} allele present. (B) PCR to detect the deleted *B-Myb*$^{\Delta}$ allele, one fragment at 240bp shows that there is a B-*myb*$^{\Delta}$ allele present. Lane 1-5 B-*myb*$^{+/\Delta}$ iPSC colonies, lane 6-23 B-*myb*$^{\Delta/\Delta}$ iPSC colonies, lane 24 B-*myb*$^{F/\Delta}$ control DNA, lane 25 H_2O. Size of relevant molecular weight markers are indicated on the left.

This experiment was repeated again by co-transfection of cre recombinase + EGFP plasmids at a ratio of 10:1 or pcDNA4 empty plasmid vector + EGFP at a ratio of 10:1 (as a non-deleted control transfection) in B-*myb*$^{F/\Delta}$ MEFs. MEFs positive for GFP were sorted 24 hours after transfection and then transduced with OSKM at MOI 2 or 20. Once more

iPSC colonies were observed in the "B-*myb*$^{\Delta/\Delta}$" well although in lower number than controls, with an average of 23±11 compared to an average of 70±8 in B-*myb*$^{F/\Delta}$ MEFs. All the colonies obtained in one of the wells (15 colonies) were picked from a MOI 2 OSKM well and genomic DNA was extracted to check the genotype of the cells. Figure 5.5A shows a 143bp fragment in all of the B-*myb*$^{\Delta/\Delta}$ iPSC colonies confirming the retention of the B-*myb*^{F} allele. Lanes showing faint bands for the B-*myb*^{F} allele also show faint bands for the B-*myb*$^{\Delta}$ allele (Figure 5.5B), indicating low DNA concentration. The faint bands seen in lanes 2, 5, 6, 9, 12, 13 are not seen in the H_2O control therefore ruling out the bands as contamination. There is a band in lane 7 which represents the B-*myb*$^{+}$ allele probably due to contamination with MEF DNA.

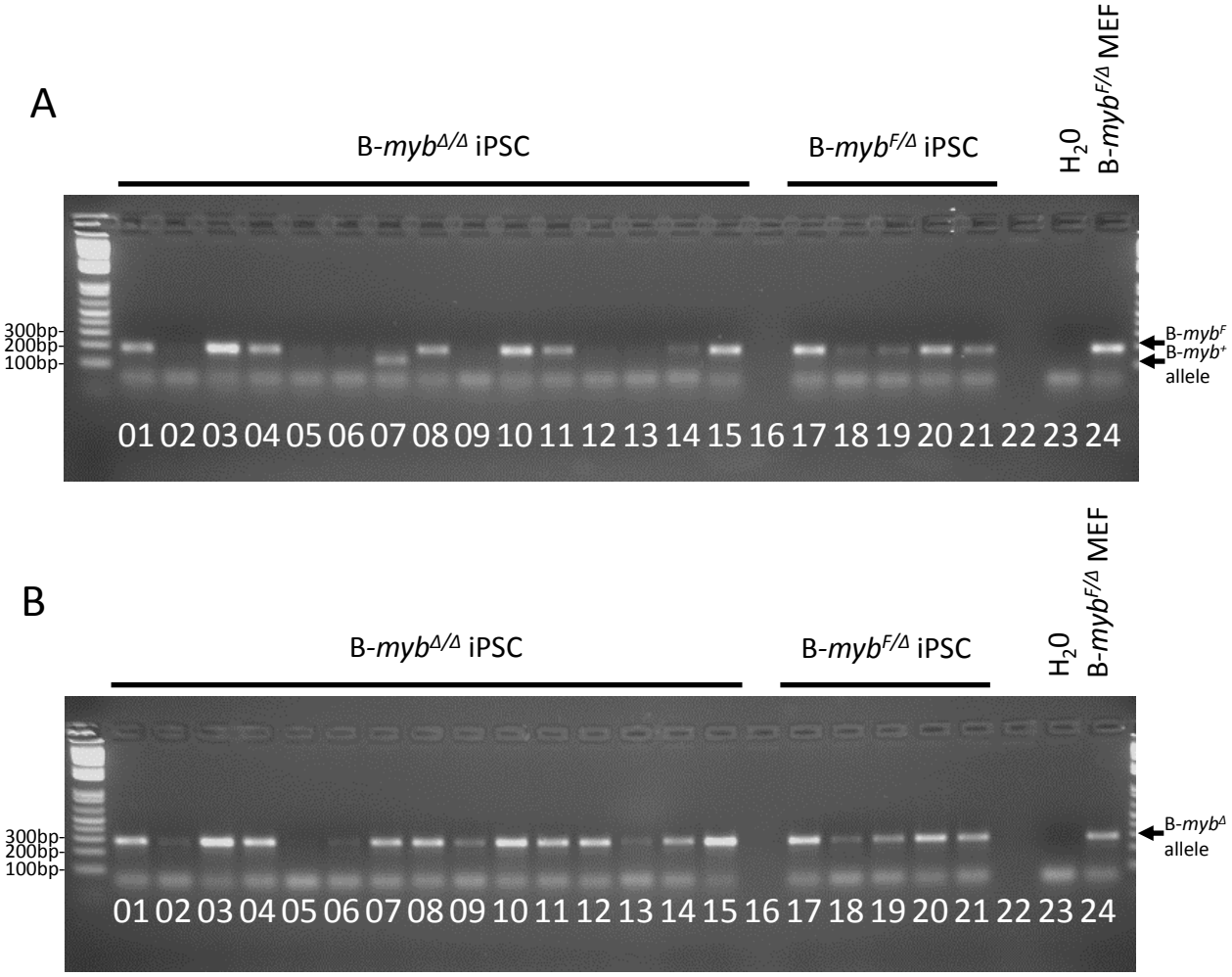


Figure 5.5: Genotyping for B-*myb*$^{\Delta/\Delta}$ *or* B-*myb*$^{F/\Delta}$ individual picked colonies
(A) PCR to detect B-*myb*^{WT} and B-*myb*^{F} alleles, one fragment at 103bp shows that there is a B-*myb*^{WT} allele present. (B) PCR to detect the deleted B-*myb*$^{\Delta}$ allele, one fragment at 240bp shows that there is a B-*myb*$^{\Delta}$ allele present. Lane 1-15 B-*myb*$^{\Delta/\Delta}$ iPSC colonies, lane 17-21 B-*myb*$^{F/\Delta}$ iPSC colonies, lane 23 H_2O, lane 24 B-*myb*$^{F/\Delta}$ control DNA lane. Size of relevant molecular weight markers are indicated on the left.

B-*myb*$^{F/\Delta}$ MEFs transduced with OSKM at MOI 20 showed an average of 96±1 colonies while in the B-*myb*$^{\Delta/\Delta}$ MEFs there was an average of 49±4 colonies. Again iPSCs were present but in a lower number. Once more, 15 colonies were picked from the OSKM MOI 20 well. Figure 5.6 confirms all of the picked colonies from the B-*myb*$^{\Delta/\Delta}$ well still contain the B-*myb*^{F} allele.

Some contamination in well 3 and 5 from wild type MEF DNA could be observed. Lane 18 had no PCR product from either PCR reaction indicating was not enough DNA was extracted from that colony.

Taken together these data indicate that reprogramming is not possible in the absence of B-Myb and the colonies that are formed come from MEFs which have not had the *B-Myb*^{F} allele deleted.

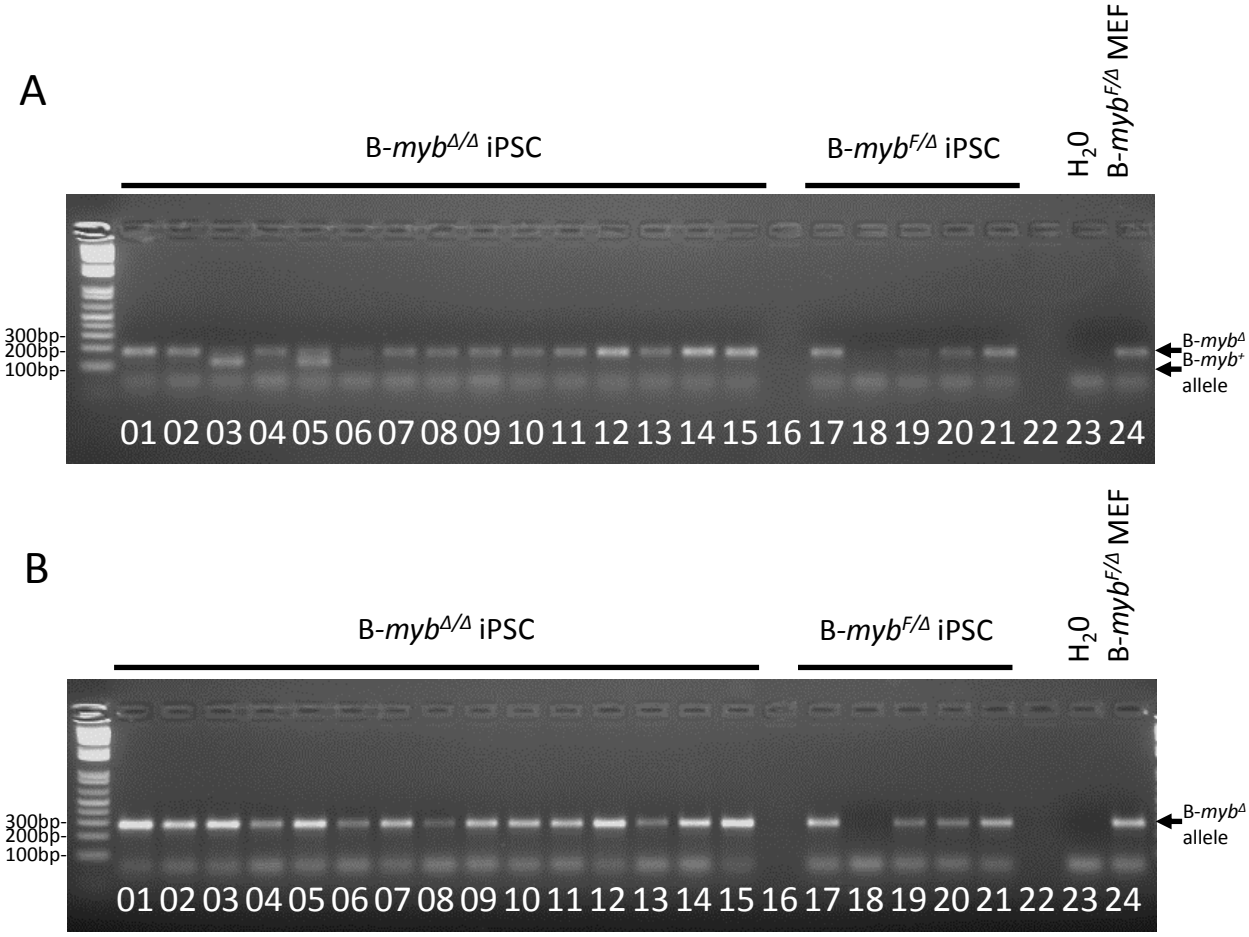


Figure 5.6: Genotyping for B-*myb*$^{\Delta/\Delta}$ or B-*myb*$^{+/\Delta}$ individual picked colonies generated with MOI 20 OSKM

(A) PCR to detect B-*myb*^{WT} and B-*myb*^{F} alleles, one fragment at 103bp shows that there is a B-*myb*^{WT} allele present. (B) PCR to detect the deleted *B-Myb*$^{\Delta}$ allele, one fragment at 240bp shows that there is a B-*myb*$^{\Delta}$ allele present. Lane 1-15 B-*myb*$^{\Delta/\Delta}$ iPSC colonies, lane 17-21 B-*myb*$^{F/\Delta}$ iPSC colonies, lane 23 H_2O, lane 24 B-*myb*$^{F/\Delta}$ control DNA. Size of relevant molecular weight markers are indicated on the left.

5.2.3 Is the block in reprogramming caused by cell cycle arrest?

B-Myb has been associated with quiescence/senescence, which is a roadblock in the reprogramming process (Zhao et al., 2008, Hong et al., 2009, Kawamura et al., 2009, Marion et al., 2009, Utikal et al., 2009). The most likely explanation for lack of reprogramming in the absence of B-Myb is a result of cells going into quiescence which may eventually lead to senescence.

To determine the molecular mechanisms responsible for the lack of reprogramming in the absence of B-Myb I determined the expression of p21 (encoded by *CDKN1A*), p16 (encoded by *CDKN2A,* also known as INK4a) and p53 (encoded by *Trp53*).

P21 is able to interact with all CDKs and its expression is growth inhibitory, it is up-regulated by p53 and is highly expressed in senescent fibroblasts (Harper et al., 1993, Eldeiry et al., 1993, Noda et al., 1994, Zhang et al., 1994, Hengst et al., 1998).

P16 causes cell cycle arrest through inhibition of CDK4 and expression increases in MEFs as they approach culture induced senescence (Serrano et al., 1993, Serrano et al., 1996, Zindy et al., 1997).

P16, p21 and p53 are all involved in promoting accelerated senescence in cells that are exposed to DNA damaging agents (Robles and Adami, 1998).

B-$myb^{F/\Delta}$ MEFs were co-transfected with cre recombinase + EGFP plasmids at a ratio of 10:1 or pcDNA4 empty plasmid vector + EGFP at a ratio of 10:1 (as a non-deleted control transfection). MEFs were sorted for GFP expression and then transduced with OSKM lentiviral particles at MOI 2 and 20. After 3 days, RNA was extracted from the MEFs, reverse transcribed and analysed for expression of p21, p16 and p53 by TaqMan qPCR. At MOI 2 the expression of p21, p16 and p53 was 3, 2 and 4 times greater in B-$myb^{\Delta/\Delta}$

MEFs compared to B-*myb*$^{F/\Delta}$ MEFs respectively (Figure 5.7). These proteins are all up-regulated at the early stages of cell cycle arrest and can lead to quiescence and senescence.

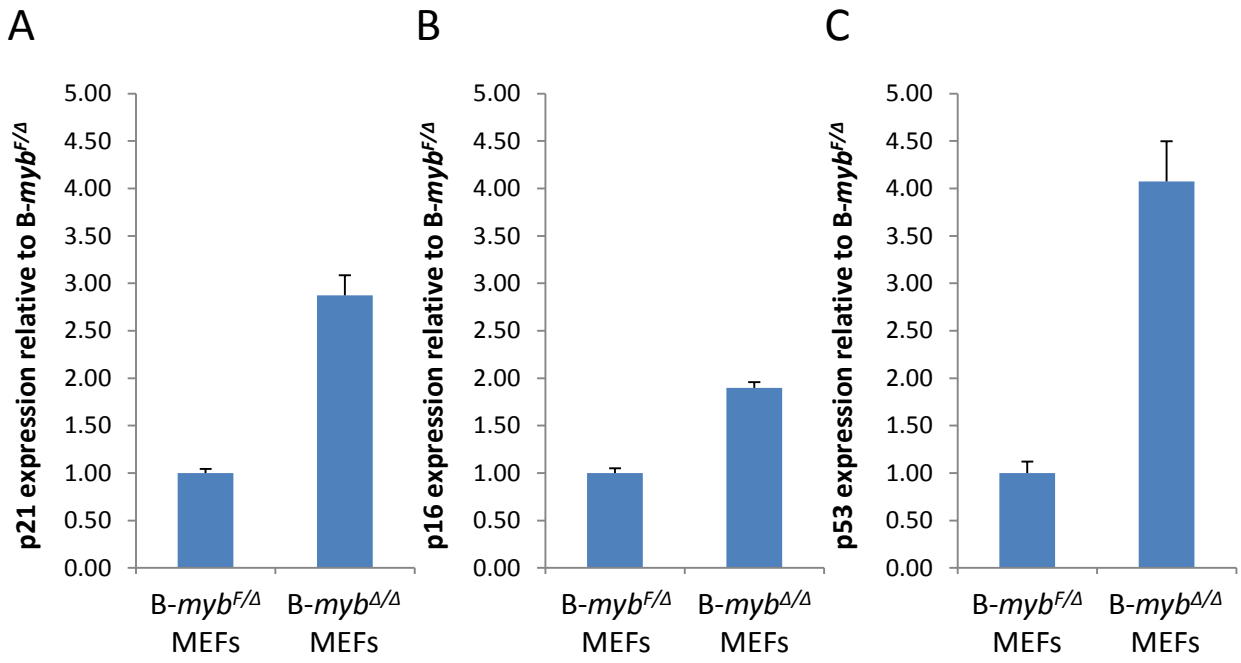


Figure 5.7: Senescence related gene expression during early reprogramming at MOI 2

RNA was extracted from B-*myb*$^{F/\Delta}$ and B-*myb*$^{\Delta/\Delta}$ MEFs transduced with OSKM MOI 2 at day 3 during reprogramming. cDNA was synthesised from the total RNA. All genes were normalized against β_2-microglobulin housekeeping gene and expressed relatively to B-*myb*$^{F/\Delta}$ MEF expression (A) P21 (*CDKN1A*) expression. (B) P16 (*CDKN2A*) expression (C) P53 (*Trp53*) expression. N=1 Error bars represent SD from three technical replicates.

At MOI 20 the expression of p21, p16 and p53 increased, but not as highly as at MOI 2: 1.7, 1.7 and 2 times greater in B-*myb*$^{\Delta/\Delta}$ MEFs compared to *B-Myb*$^{F/\Delta}$ MEFs, respectively (Figure 5.8).

Although this data is preliminary it could be an indication that the MEFs with B-Myb ablated are deficient in proliferation and therefore unable to reprogram to iPSCs.

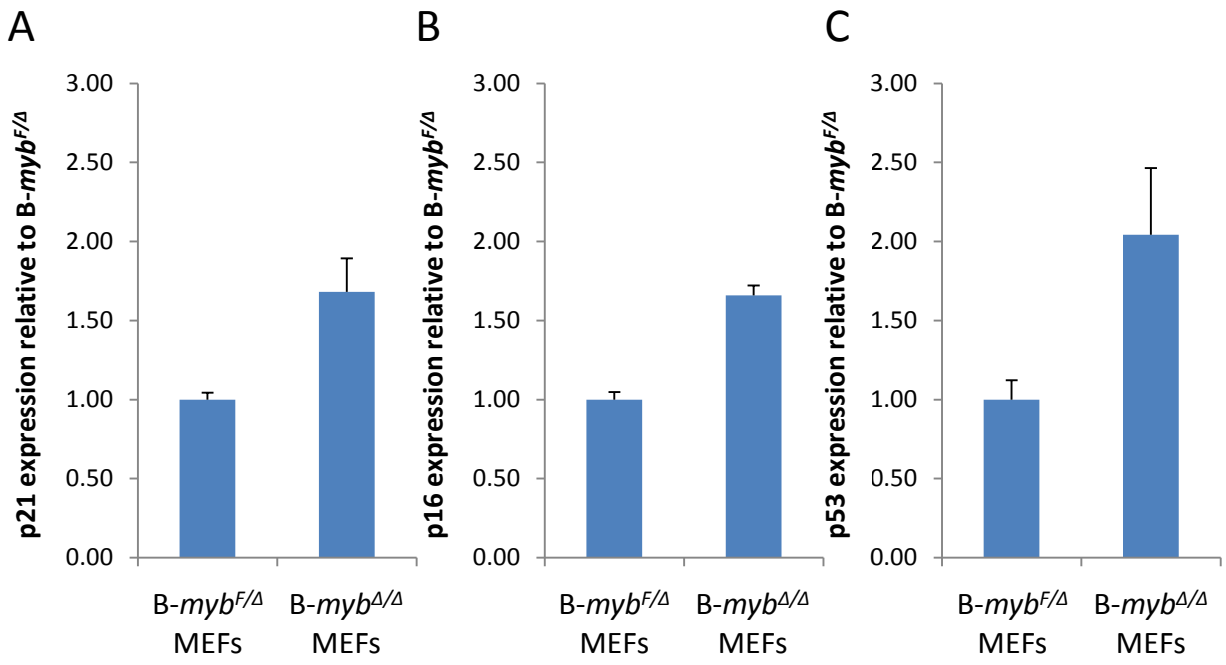


Figure 5.8: Senescence related gene expression during early reprogramming at MOI 20

RNA was extracted from B-$myb^{F/\Delta}$ and B-$myb^{\Delta/\Delta}$ MEFs transduced with OSKM MOI 20 at day 3 during reprogramming. cDNA was synthesised from the total RNA. All genes were normalized against β_2-microglobulin housekeeping gene and expressed relatively to B-$myb^{F/\Delta}$ MEF expression (A) P21 (*CDKN1A*) expression. (B) P16 (*CDKN2A*) expression (C) P53 (*Trp53*) expression. N=1 Error bars represent SD from three technical replicates.

5.3 DISCUSSION

5.3.1 Removal of B-Myb in MEFs

In this chapter, I aimed to study the effect that ablation of B-Myb would have in reprogramming. My results indicate that MEFs without B-Myb are unable to reprogram to iPSCs; however, attempts to repeat this result were hampered by poor transfection efficiency of the Cre recombinase-IRES-EGFP plasmid. It has been described that the gene following the IRES may be weakly expressed (Mizuguchi et al., 2000). Therefore cells could be expressing Cre recombinase but not the EGFP, lowering the perceived transfection efficiency. To address the low transfection efficiency, I generated an EGFP: Cre recombinase fusion plasmid, thus expressing EGFP and Cre recombinase in the same quantities.

Several gene delivery methods were tested in order to optimise the delivery of cre recombinase. AMAXA nucleofection system gave poor transfection efficiency (<1%) with the pCre-IRES-EGFP plasmid or an EGFP fusion cre plasmid. Lipofectamine and turbofect transfection reagents were also tested but gave similarly low transfection efficiency (<5%). Only transduction with lentivirus Cre-IRES-EGFP gave between 10-20% efficiency, thus allowing a much larger number of cre recombinase positive MEFs to be sorted and used in reprogramming experiments. Unfortunately, using an integrating cre lentivirus led to the problem that the cre recombinase in the cells would also excise the OSKM vector and prevent reprogramming. To solve this problem we obtained the OSKM vector without the loxP sites from our collaborator George Murphy, Boston Medical School.

Additional problems were encountered when this experiment was scaled up in order to get enough cells for subsequent reprogramming studies. The number of cells recovered after FACS was often too low to set up any experiments, the cells did not recover after the sorting, or cells were contaminated with bacteria after plating. The experiment was repeated once successfully recovering enough cells to perform the reprogramming study using this method. However there were colonies present in the wells. These colonies were analysed by PCR and appeared to still contain the B-*myb*^{F} allele. This is likely due to FACS purity, another technical difficulty with these experiments.

5.3.2 Endogenous system

In order to deal with these technical difficulties B-*myb*$^{F/\Delta}$:*Cre-ER*^{T2} mice were derived, which have the cre recombinase fused to a mutated ligand binding domain of the human estrogen receptor (ER). The ER can be activated by ectopic tamoxifen administration and cre recombinase expressed. These MEFs were first tested to determine what concentration of 4OHT (4-hydroxytamoxifen), was required to ablate B-Myb expression. The results show that B-Myb ablation is complete by 96 hours after 4OHT treatment. Surprisingly, when the cells were used for reprogramming, colonies were generated from the B-Myb ablated MEFs. Again when the colonies were isolated and PCR was used to determine the genotype of the cells the B-*myb*^{F}-allele was still present in all of the colonies checked, demonstrating that the efficiency of the deletion was not 100%.

When Cre recombinase is expressed in B-*myb*$^{F/\Delta}$ MEFs the B-Myb protein is ablated and the MEFs stop cycling. This is in agreement with previous reports describing that B-Myb is crucial for correct cell cycling and has been shown to severely limit mitosis in MEFs (Yamauchi et al., 2008). As mentioned earlier, reprogramming is sensitive to the cell

cycle (Hanna et al., 2009). If B-Myb deletion is not achieved in the whole culture, cells still containing B-Myb will overtake the culture and will be able to reprogram.

All in all, I was unable to get any iPSC colonies from MEFs with the B-*myb* gene deleted; indicating that absence of B-Myb is detrimental for the reprogramming process. It has been shown that tumour suppressor p53 plays an important role in mammalian cells by protecting the genome against accumulation of mutations (Vousden and Prives, 2009). Manipulation of p53 through knockout, knockdown and deregulation enables cellular reprogramming to occur with just Oct4 and Sox2 expression (Kawamura et al., 2009, Marion et al., 2009). It would be interesting to determine whether the reprogramming in the absence of B-Myb, can be rescued in a $p53^{-/-}$ background.

CHAPTER 6: COULD B-MYB INCREASE EFFICIENCY OF REPROGRAMMING?

6.1 INTRODUCTION

One of the major goals in the reprogramming field is the improvement of the low efficiency of the technique so that iPSCs can be used for regenerative medicine.

The low efficiency of primary reprogramming can also lead to selection of cells which may be more susceptible to the reprogramming, such as cells with low p53 expression. In fact, iPSC lines generated from cells with low or no p53 expression could present a risk of tumour formation if the low p53 expression were to be passed to all daughter iPSCs.

The goal of increased efficiency of reprogramming must be achieved whilst maintaining genomic integrity. The reprogramming efficiency can be improved dramatically in the absence of p53 in knockout mouse models (Kawamura et al., 2009, Marion et al., 2009). Knocking out p53 to boost reprogramming will not be acceptable for regenerative medicine due to risk of tumour formation.

B-Myb has been shown to be important in maintaining genomic stability throughout the animal kingdom (Manak et al., 2002, Fung et al., 2002, Shepard et al., 2005, Ahlbory et al., 2005, Garcia and Frampton, 2006, Lorvellec et al., 2010). It has also been shown to regulate c-Myc (Nakagoshi et al., 1992, Gualdrini et al., 2010, Lorvellec et al., 2010), one of the Yamanaka factors commonly used in reprogramming (Takahashi and Yamanaka, 2006). c-Myc improves the efficiency of reprogramming but at a cost of producing iPSCs

which are much less likely to produce live offspring by 4N tetraploid complementation experiments in mice, compared to iPSCs reprogrammed with only OSK (Buganim et al., 2014).

B-Myb expression also increases at day 2 of reprogramming, earlier than other pluripotency markers such as Nanog and Esrrb (O'Malley et al., 2013). Expression of B-Myb is up to 10,000 times higher in ESCs compared to somatic cells (Tarasov et al., 2008). In addition, 4C experiments have shown that B-Myb has more contacted active regions in the chromosomes of ESCs than Nanog (de Wit et al., 2013). These data provide compelling evidence that B-Myb has an important role in pluripotency.

In this chapter, I will try to determine if inclusion of B-Myb in the reprogramming factors could increase the efficiency of reprogramming without having a detrimental effect on genomic stability.

6.2 RESULTS

6.2.1 Testing the B-*myb* lentivirus

To determine if B-Myb overexpression influences reprogramming I made use of a B-*myb-IRES-EGFP* lentiviral backbone. First the B-*myb-IRES-EGFP* lentivirus was tested by transducing wild type MEFs at a MOI of 1 and analysing the GFP expression by flow cytometry, and by measuring the mRNA expression of B-Myb by qRT-PCR after 7 days. Figure 6.1A shows expression of GFP in the MEFs transduced with the B-*myb IRES EGFP* lentivirus (referred to herein as B-*myb* lentivirus). The expression of B-Myb mRNA was shown to be 23 times higher in wild type MEFs transduced with B-*myb* lentivirus (Figure 6.1B). This indicated that the lentivirus was correctly expressing B-Myb in the MEFs.

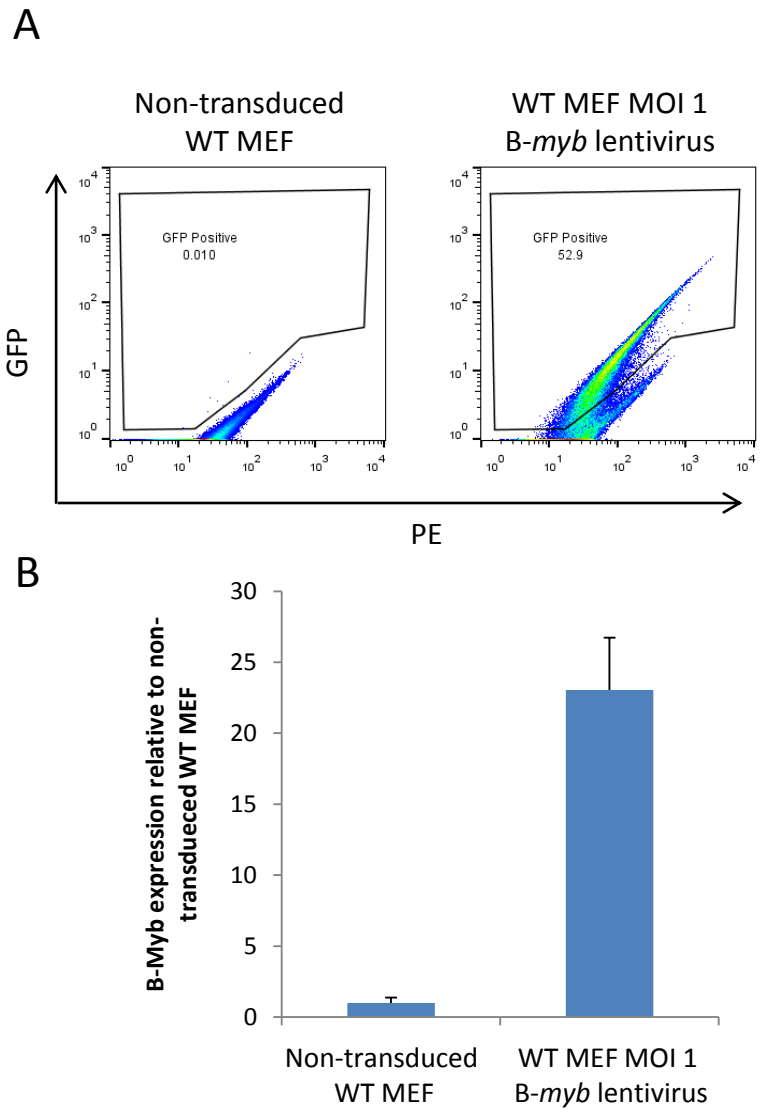


Figure 6.1: B-Myb overexpression analysis in wild type MEFs
(A) Dot plots showing expression of GFP against PE in WT MEFs (left panel) and WT MEFs transduced with MOI 1 B-*myb-IRES-EGFP* lentivirus (right panel). (B) Histogram representing the expression of B-Myb in wild type MEFs and wild type MEFs transduced with MOI 1 B-*myb-IRES-EGFP* lentivirus, N = 1 error bars represent SD of 3 technical replicates

6.2.2 The effect of additional B-Myb in reprogramming

Previous work from our lab showed that B-Myb regulates one of the genes used in the reprogramming cocktail, *c-Myc* (Lorvellec et al., 2010). As mentioned previously, the efficiency of reprogramming is compromised when c-Myc is omitted from the reprogramming factors (Nakagawa et al., 2008). Furthermore, B-Myb expression increases at the early stages of reprogramming before other pluripotency factors, such as Nanog and Lin28a (O'Malley et al., 2013). In addition to its possible role in pluripotency, B-Myb's role in maintenance of genome integrity may protect MEFs from DNA damage and p53 mediated apoptosis during reprogramming. To determine if (i) B-Myb could be a substitute for c-Myc in reprogramming and (ii) whether B-Myb would enhance the efficiency of reprogramming, the B-*myb* lentivirus was used together with the OSKM or OSK lentivirus.

Figure 6.2A shows the experimental strategy used. Briefly, wild type MEFs were transduced at MOI 1 with OSKM virus alone, OSK virus alone, OSKM + B-*myb* lentiviruses or MOI 2 OSK + MOI 1 B-*myb* lentiviruses, and reprogramming efficiency was measured by alkaline phosphatase (AP) staining. The cells were stained for AP activity after 10 or 14 days. Surprisingly, it was visually clear that addition of B-Myb to the reprogramming factors lowered the number of alkaline phosphatase positive colonies (Figure 6.2B). When colonies were counted a 2.7 fold reduction in the number of colonies was observed when B-Myb was added. (OSKM 470±5 colonies vs 169±14 colonies when reprogramming with OSKM + B-*myb* lentivirus, P=0.0008 by unpaired two-tailed T-Test, Figure 6.2C). When reprogramming was done in the absence of c-Myc, using the OSK lentiviral vector, a 2 fold reduction was observed when B-Myb was added (OSK 1154±67

colonies compared to 554±6 when reprogramming with OSK+B-*myb* lentivirus), (P=0.012 by unpaired two-tailed T-Test), Figure 6.2D).

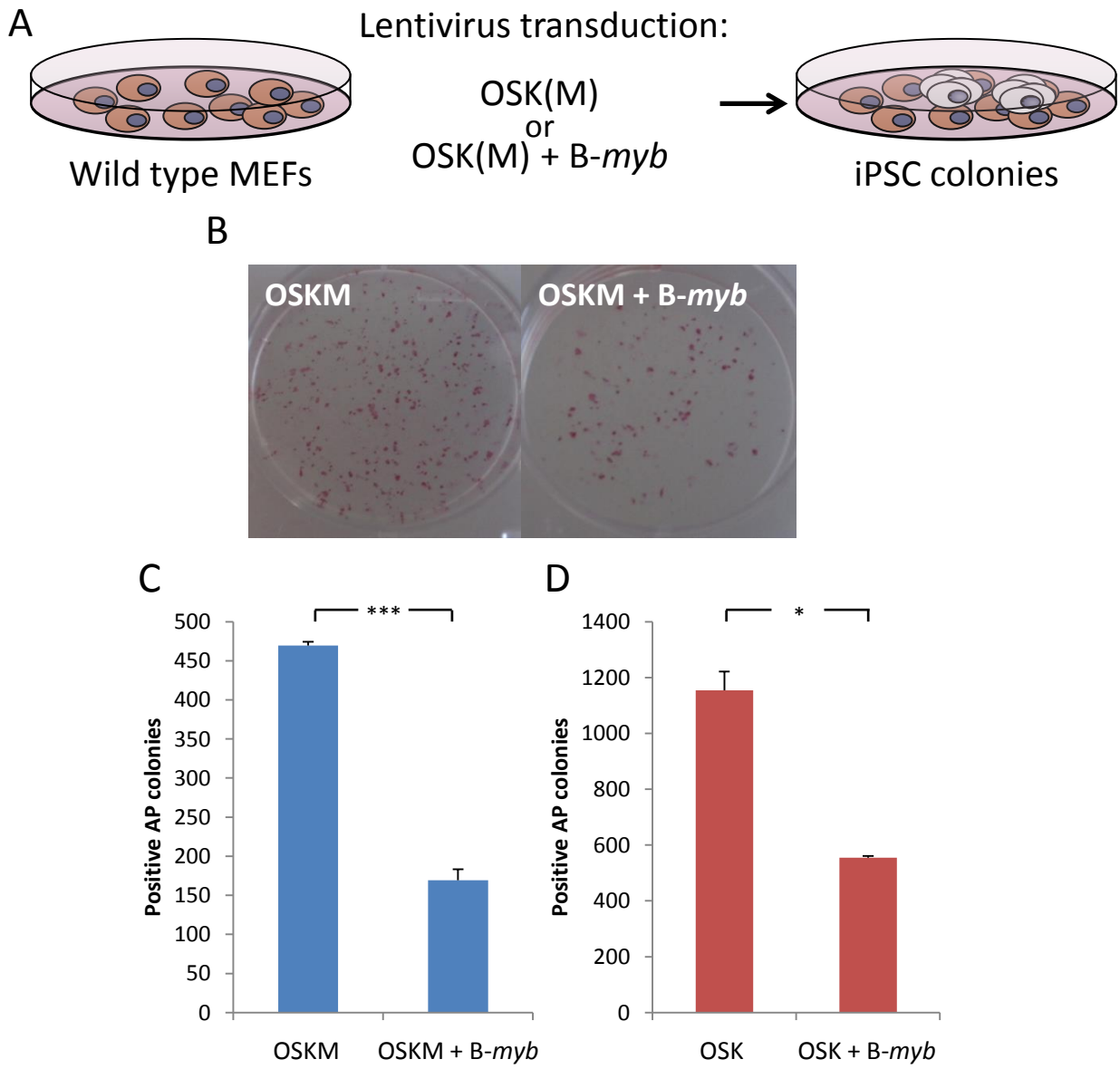


Figure 6.2: Alkaline phosphatase staining for MEFs reprogrammed with OSKM or OSKM + B-*myb* lentivirus

(A) Schematic representing the experimental procedure. (B) 10^5 MEFs were infected with OSKM virus MOI 1, OSKM plus B-*myb* virus both MOI 1, allowed to reprogram for 10 days then stained for alkaline phosphatase activity for 30 minutes. Plates showing positive AP stained colonies (red) OSKM (left panel) and OSKM + B-*myb* (right panel). (C) Graph representing the positive colony counts when reprogramming with OSKM +/- B-*myb* virus. (D) Graph representing the positive colony counts when reprogramming with MOI 2 OSK +/- MOI 1 B-*myb* virus. N=3 Error bars represent SEM. *P<0.05, ***P<0.001 by unpaired two-tailed T-Test

To identify if the lower reprogramming efficiency observed when combining the OSKM and B-*myb* lentiviruses was due to the transduction of two different lentiviruses simultaneously, the experiment was repeated with a control virus (*Zs-Green* virus) which is similar in size to the B-*myb* virus (Figure 6.3A). As in the previous experiment, it was clear that additional B-Myb resulted in a reduction in the number of AP positive colonies (Figure 6.3B). The number of colonies generated with the OSKM + B-*myb* was 115±6 compared to 183±13 colonies when reprogramming with OSKM + *Zs-Green* viruses. The number of colonies generated with OSKM lentiviral particles alone was 254±3 (P=0.02 by unpaired two-tailed T-Test, Figure 6.3C). Thus, a negative effect on the colony number was observed when adding a second virus during the reprogramming process, but there was a further negative effect when the lentivirus encoded B-Myb. This effect appears to be linked to the expression of B-Myb and therefore I investigated this result further.

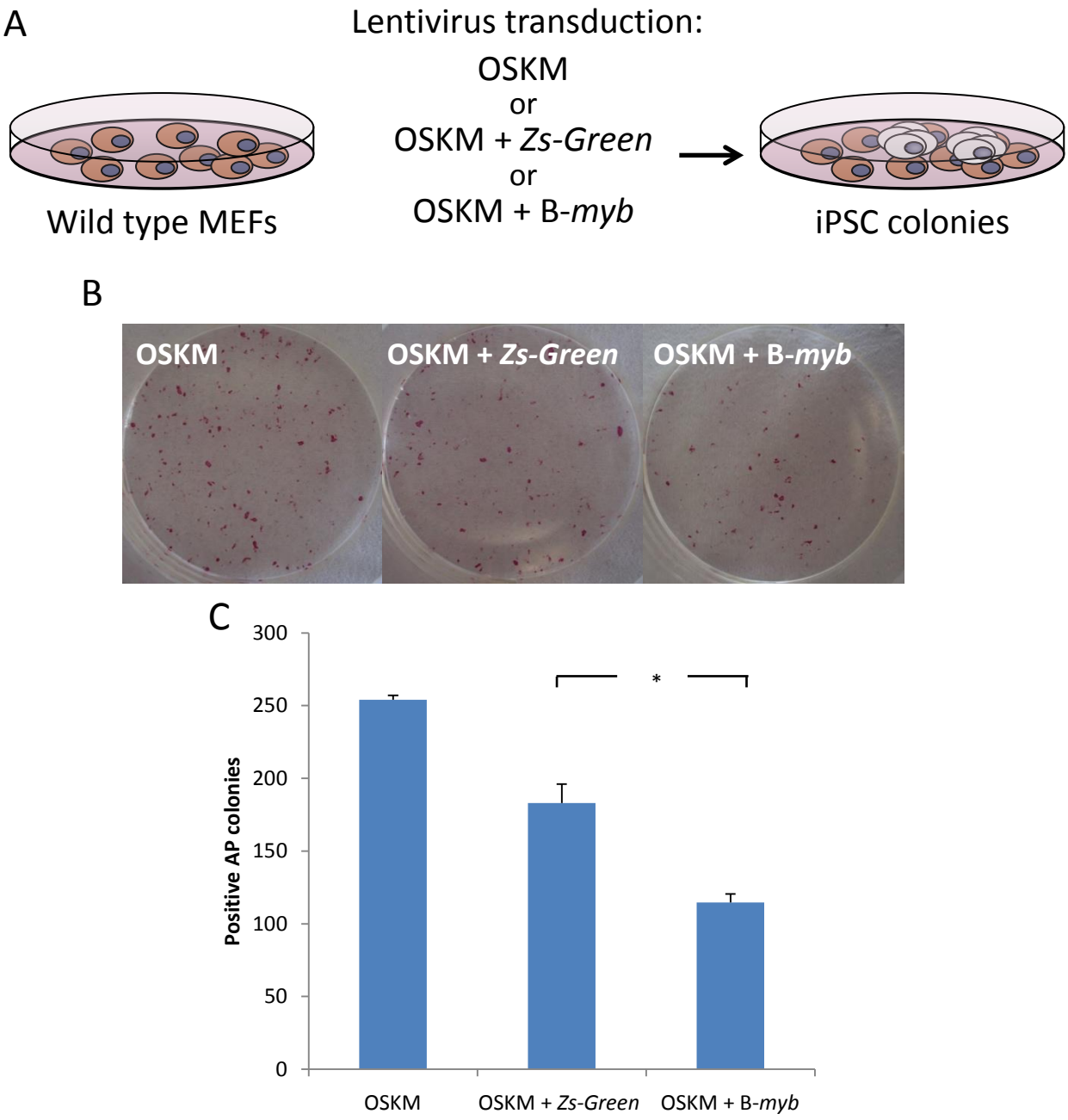


Figure 6.3: Alkaline phosphatase staining of reprogrammed MEFs

(A) Schematic representing the experimental procedure (B) 10^5 MEFs were transduced with OSKM (left panel), OSKM + *Zs-Green* (middle panel) or OSKM + B-*myb* (right panel) lentiviral particles (all MOI 1), then tested for pluripotency by alkaline phosphatase staining at day 10. Plates showing positive AP staining (red). (C) Graph representing the positive colony counts. N=3 Error bars represent SEM *P<0.05 by unpaired two-tailed T-test

6.2.3 Generation of the Oct4, Sox2, Klf4 and B-Myb (OSKB) lentivirus

Based on the results from the co-transduction of OSK(M) and B-*myb* lentiviruses, a polycistronic lentivirus vector that had the B-*myb* gene incorporated together with the reprogramming genes was designed and constructed. This way, I could discern whether the lowered efficiency observed was due to the additional B-Myb expression or due to the double lentiviral transduction.

The strategy used to generate the lentiviral backbone is shown as a schematic in Figure 6.4. First, the *Sox2* gene was amplified from a plasmid by PCR using primers (Table 3) that were designed to add an additional 5' NdeI restriction site and a 3' *E2A* gene. The *E2A* gene encodes a self-cleaving peptide which will enable the fusion gene to be cleaved into two separate proteins after translation (Ryan et al., 1991, Szymczak and Vignali, 2005, Kim et al., 2011). An *E2A* gene was selected as it is the same peptide that combines the *Sox2* and *c-Myc* genes in the OSKM vector. The B-*myb* gene was amplified from a plasmid by PCR using primers (Table 3) that were designed to add an additional 3' ClaI restriction site and a 5' E2A gene. Figure 6.5A shows the 2.2kb B-*myb* and the 1kb *Sox2* PCR products. Both PCR products were purified and a small amount of each was mixed together to be used as template for a second round of PCR which fused the two products together to generate a 3.2kb *Sox2-E2A*-B-*myb* PCR product (Figure 6.5B).

The *Sox2-E2A*-B-*myb* fragment was purified from the agarose gel and then incubated with Taq DNA polymerase to generate adenine overhangs to facilitate ligation into TOPO® TA (Invitrogen) bacterial expression vector. This vector was used to transform competent E.coli and plasmid DNA was extracted from 12 individual overnight cultures. Each plasmid DNA extract was digested with SacI restriction enzyme to check for

colonies that had incorporated the correct plasmid (Figure 6.5C). Plasmid DNA from overnight culture number 6 had bands of 0.5kb and 5.6kb which was expected from the *Sox2*-E2A-B-*myb* fragment being properly ligated into TOPO vector with the correct orientation. This plasmid DNA was sent for Sanger sequencing. The sequencing data revealed a single point mutation at base 108 from G to A; fortunately this mutation did not affect the amino acid sequence (Figure 6.6).

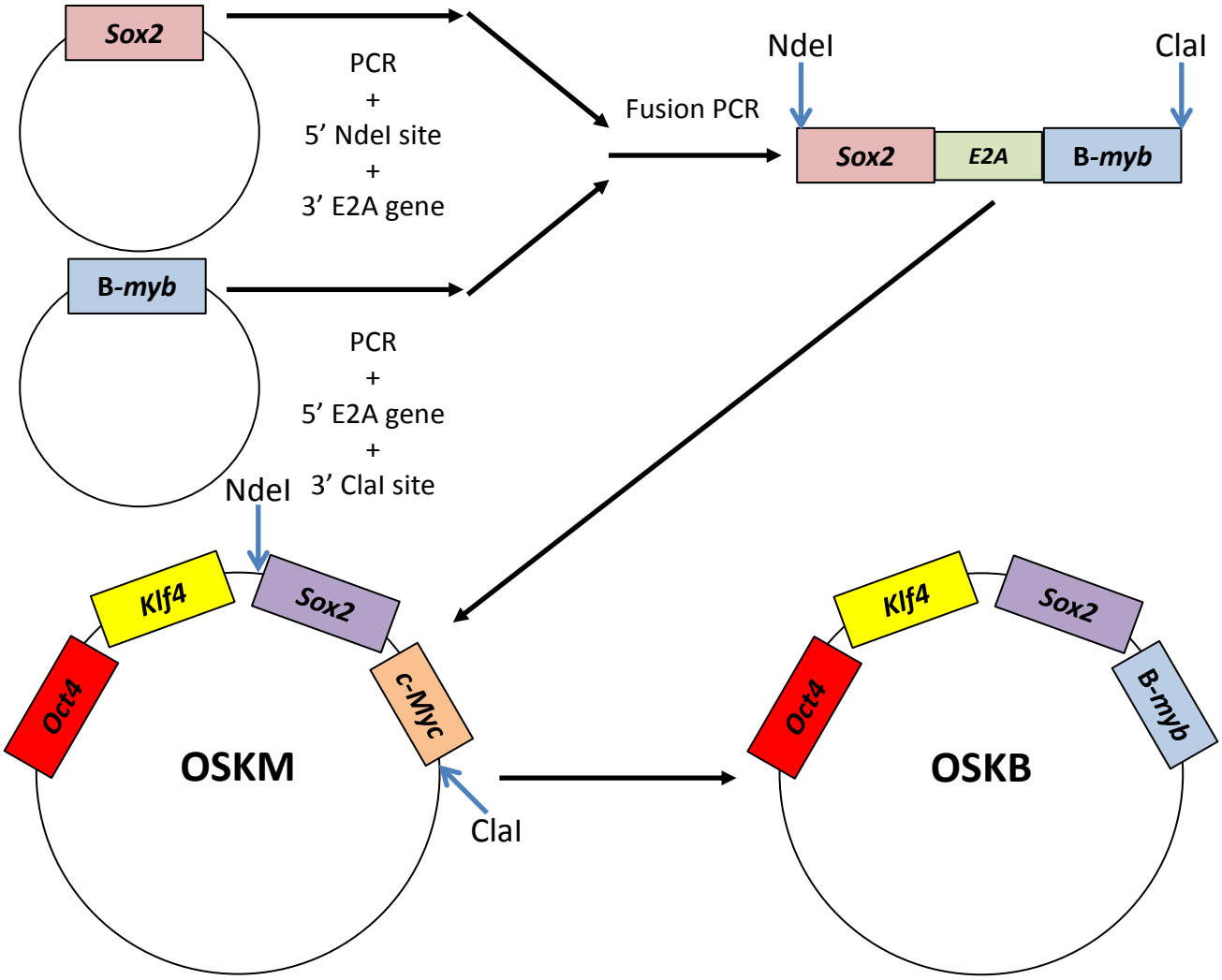


Figure 6.4: Generation of the OSKB lentiviral backbone
The B-*myb* and *Sox2* genes were amplified by PCR from separate plasmids with primers that contained flanking restriction sites and an internal *E2A* gene sequence. The cloned genes were mixed and fused together with a second round of PCR. The resultant fusion gene was transferred into the lentiviral backbone using the flanking restriction sites.

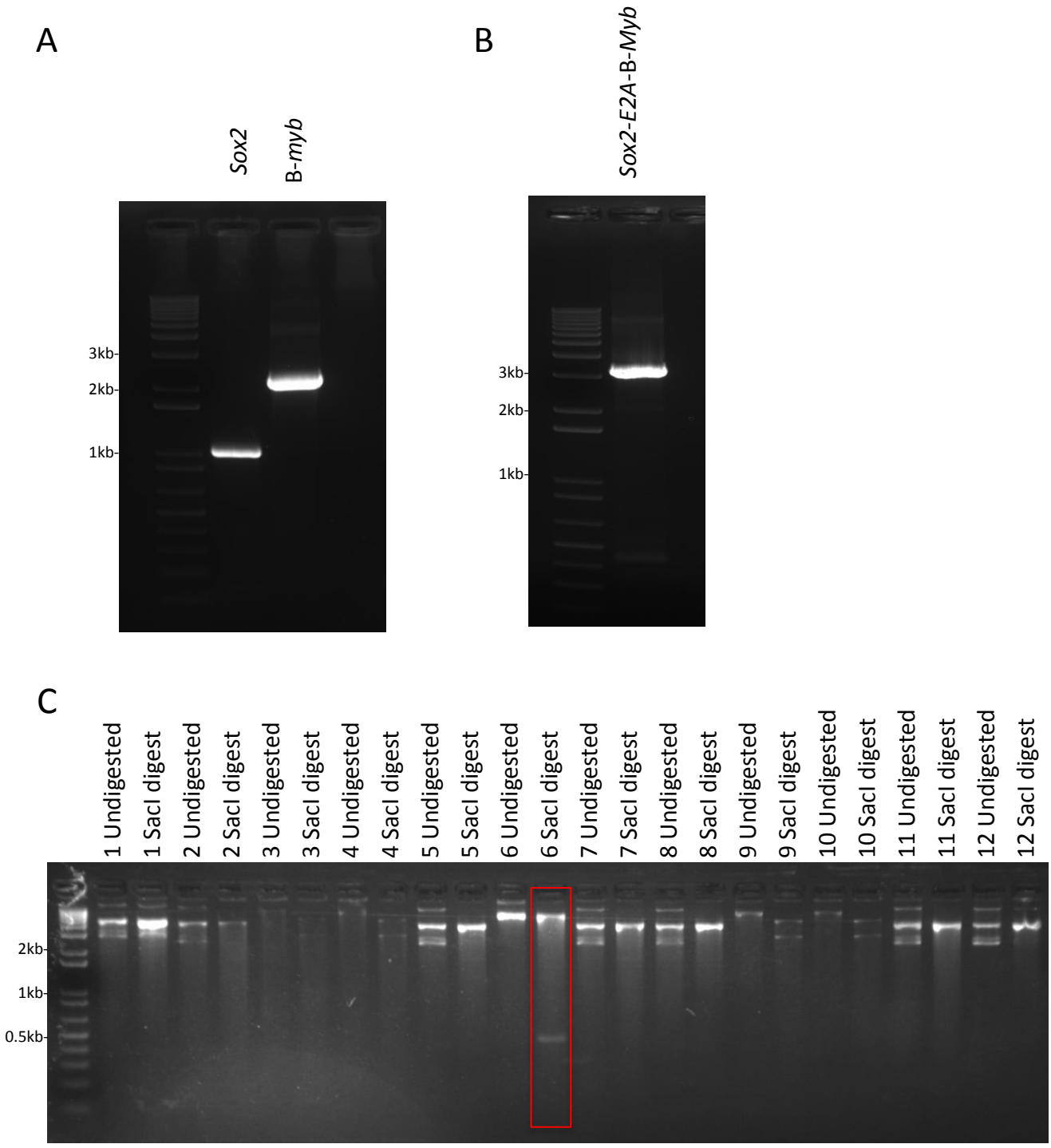


Figure 6.5: Cloning the *Sox2-E2A*-B-*myb* fusion gene

(A) *Sox2* and B-*myb* genes were amplified from separate plasmids by PCR. PCR products were separated by agarose gel electrophoresis. The bands seen at 1kb and 2.2kb correspond to *Sox2* and B-*myb* respectively. (B) The single band at 3.2kb corresponds to the successfully generated *Sox2-E2A*-B-*myb* fragment. (C) Agarose gel showing undigested and SacI digested plasmid DNA from 12 individual E.coli colonies. Colony 6 (red box) digested with SacI gave two bands (0.5kb and 5.6kb) corresponding to the *Sox2-E2A*-B-*myb* fragment being correctly ligated into the TOPO vector. Size of relevant molecular weight markers are shown on the left.

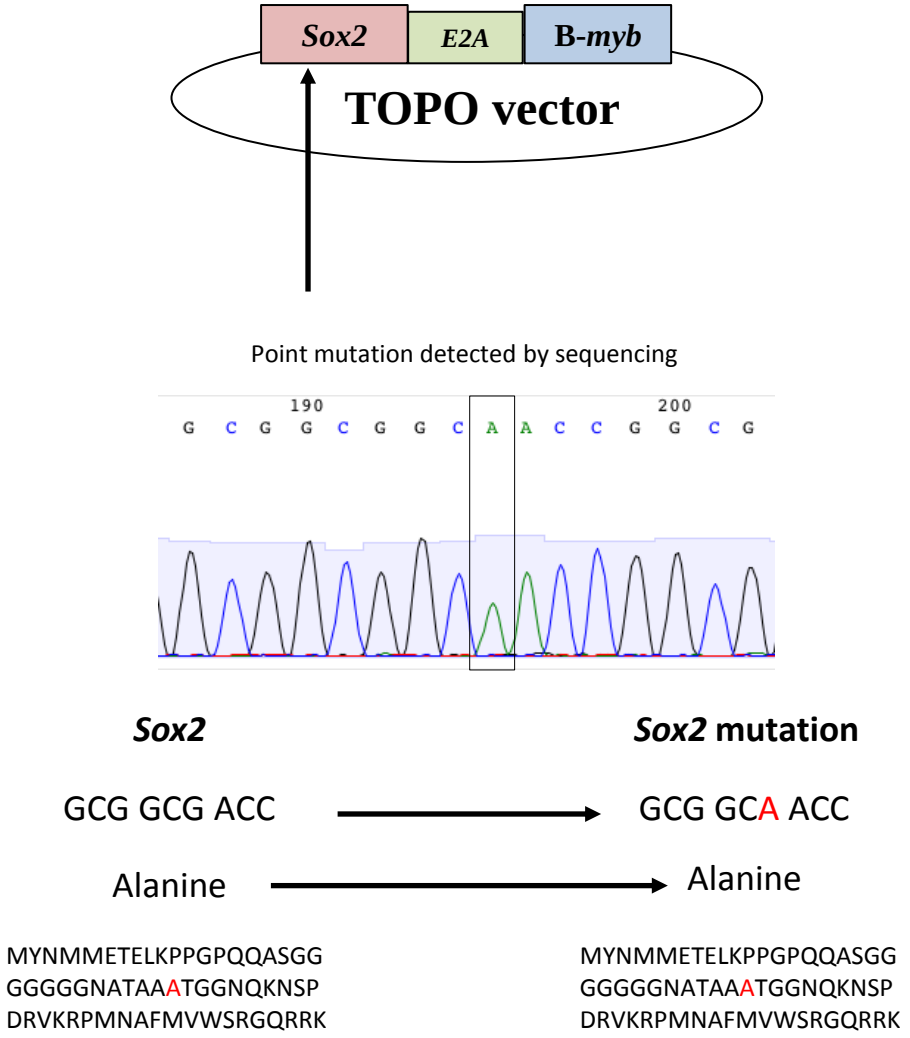


Figure 6.6: Sanger sequencing for cloned *Sox2-E2A*-B-*myb* fusion gene
The *Sox2-E2A*-B-*myb* fusion gene previously ligated into the TOPO cloning vector was sent for Sanger sequencing using primers complementary to the TOPO vector flanking the fusion gene and four primers complementary to internal regions 500 base pairs apart within the fusion gene. The sequencing revealed that the nucleotide at position 108 in the fusion gene was mutated from guanine to adenine. This mutation did not alter the amino acid sequence.

The sequenced *Sox2-E2A*-B-*myb*/TOPO plasmid and the pHAGE-2-EF1a-mOSKM-Cherry-loxP backbone plasmid were digested with NdeI and ClaI. Then the 3.2kb *Sox2-E2A*-B-*myb* (insert) and the 11kb pHAGE-2-E1a-mOSKM-Cherry-loxP (vector) were excised from the gel and purified (Figure 6.7A, red boxes). This insert and vector were ligated and used to transform E.coli competent bacteria. 29 colonies were picked from this

ligation and 27 of them contained the insert in the correct orientation. The extracted plasmid DNA was checked by digestion with three sets of restriction enzymes (Figure 6.7B), that would cut twice in the OSKB vector generating two fragments of the following sizes: AgeI - 5491bp and 7824bp, ClaI and BamHI - 6199bp and 7116bp, Eco47III - 2556bp and 10759bp. The restriction digestion confirmed that the OSKB vector was successfully generated.

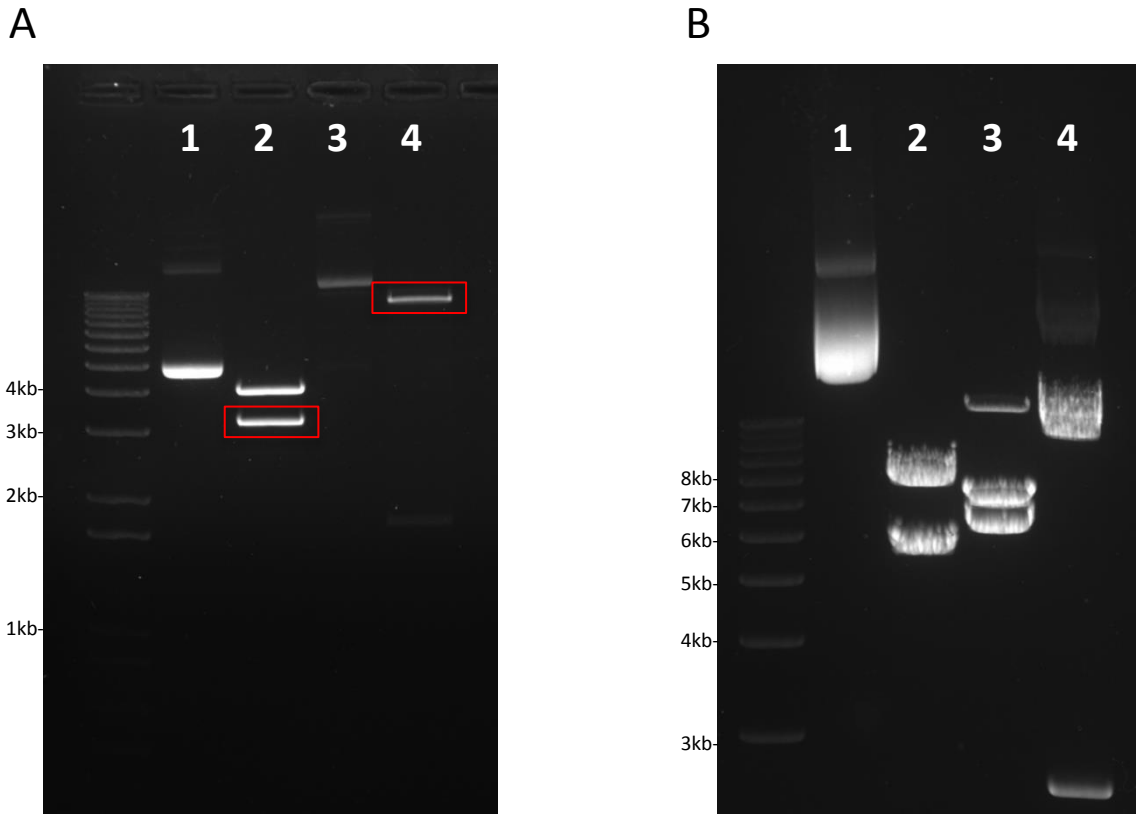


Figure 6.7: Digestion of *Sox2-E2A*-B-*myb* fragment and confirmation of OSKB plasmid
(A) Agarose gel showing *Sox2-E2A*-B-*myb*/TOPO vector (lane 2) and pHAGE-2-E1a-mSTEMCCA-Cherry-loxP vector (lane 4) digested with ClaI and NdeI, with non-digested controls (lane 1 and 3). The 3.2kb *Sox2-E2A*-B-*myb* (red box, lane 2) and the 11kb pHAGE-2-E1a-mSTEMCCA-Cherry-loxP (red box, lane 4) bands were excised and used for ligation. (B) Agarose gel showing OSKB plasmid DNA digested with AgeI (lane 2), Eco47III (lane 4) and ClaI/BamHI (lane 3) and non-digested OSKB (lane 1). The expected products were as follows AgeI - 5491bp and 7824bp, ClaI and BamHI - 6199bp and 7116bp, Eco47III - 2556bp and 10759bp. The additional band in lane 3 is single cut, linearised plasmid. This banding pattern shows that the plasmid is correct.

To test that the *Oct4, Sox2, Klf4* and B-*myb* genes present in the construct could be expressed correctly as proteins, the OSKB or the OSKM plasmids were transfected into 293T cells and 2 days later whole protein was extracted. Proteins were separated by SDS-PAGE and transferred to PVDF membranes to perform western blots. As shown in Figure 6.8 the expression of the four proteins could be detected. The level of expression of Oct4 and Klf4, shown by bands at 45 and 50kda, respectively, was exactly the same in the OSKB and OSKM transfected 293T cells, which is not surprising as the vectors are both controlled by the same promoter and are very similar in size. The Sox2 expression, shown by a band at 30kda, was slightly lower in the OSKB vector transfected 293T cells compared to the OSKM. This could be due to the larger size of the B-Myb, which would be translated along with the Sox2 due to the E2A peptide. B-Myb expression, shown by the band at 95kda, was only observed in the OSKB transfected 293T cells as there is no B-*myb* gene on the OSKM vector, and the endogenous expression of B-Myb in 293T cells is very low.

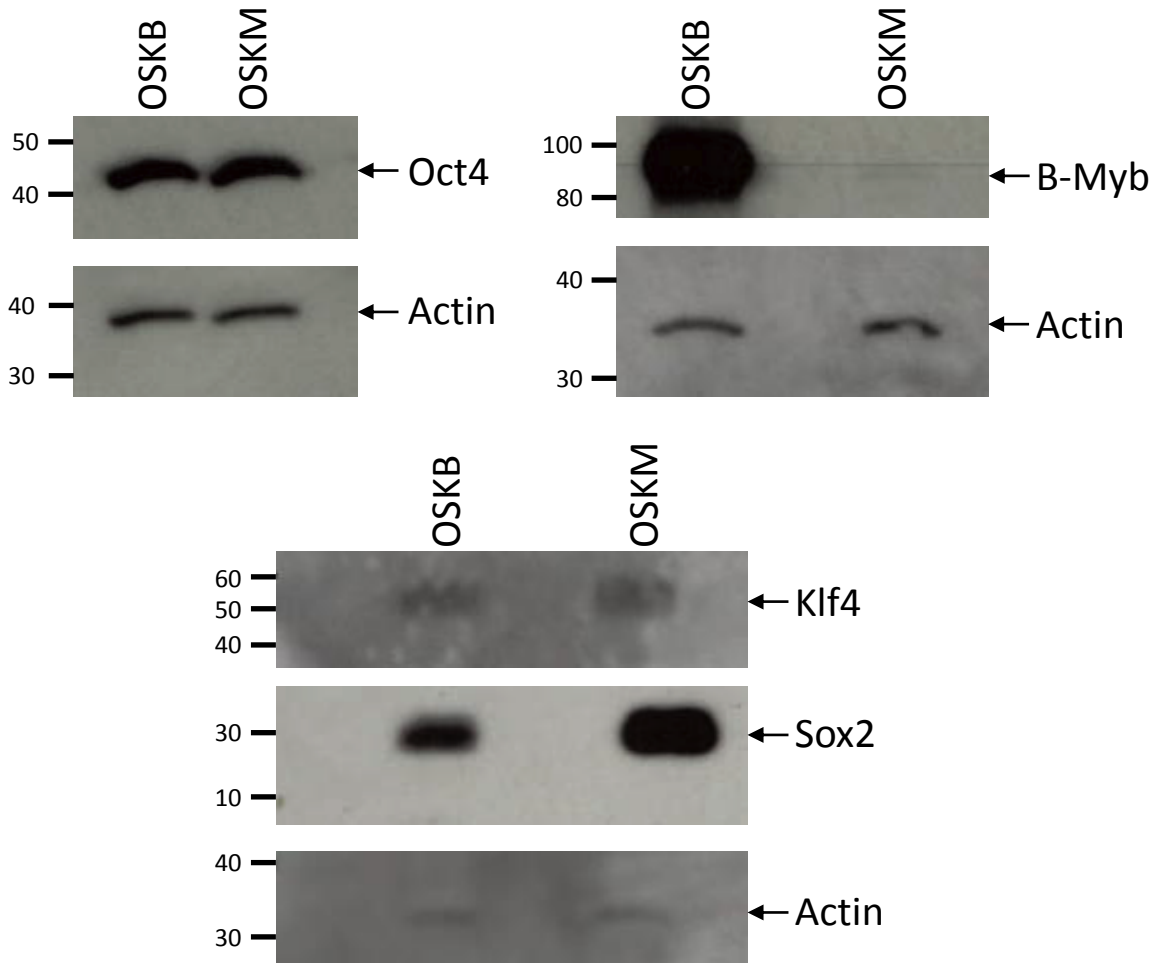


Figure 6.8: Protein expression of OSKB and OSKM lentiviral backbones in transfected 293T cell line

2.5 x 10^7 293T were transfected with either OSKB or OSKM lentiviral backbone. 50µg of total protein was extracted and subjected to SDS-PAGE. Protein expression was detected by western blotting with antibodies against B-Myb, Oct4, Klf4, Sox2 or Actin. The position of relevant molecular weight (kda) standards is shown on the left side of the blot, and arrows on the right indicate the specific bands for each antibody.

6.2.4 Reprogramming with OSKB lentivirus

MEFs were derived from mice with an *IRES-EGFP* fusion cassette downstream of the stop codon of the endogenous *Oct4* gene (referred to herein as Oct4-GFP MEFs) and transduced with OSKM, OSK or OSKB lentiviruses at MOI 2 (Figure 6.9A). 14 days after transduction the GFP positive colonies were counted using an inverted fluorescent microscope and then the colonies were stained for alkaline phosphatase activity. As expected, the number of alkaline phosphatase positive colonies were lower in OSK transduced MEFs compared to OSKM transduced MEFs (Figure 6.9B). Surprisingly, a very striking result was observed in MEFs transduced with OSKB, with only one single AP positive colony present (Figure 6.9B). Quantification of the ESC-like colonies showed that the mean number of iPSC colonies with OSKM was 226±15, 72±16 with OSK and 1±0 with OSKB. There was a statistically significant difference in reprogramming using the OSKB lentivirus compared to using the OSKM lentivirus (P=0.009 tested using unpaired two-tailed T-Test) (Figure 6.9C). This is the same effect that was observed when reprogramming was perfomed with OSKM + B-*myb* lentiviruses (Figure 6.2 and Figure 6.3). I also took advantage of the Oct4-GFP knock-in MEFs and determined the expression of GFP in the iPSCs generated. Only truly pluripotent iPSCs will be GFP positive as the GFP expression is driven by the endogenous Oct4 promoter. The mean percentage of GFP positive colonies were highest in the OSKB transduced MEFs (100±0%), followed by OSK transduced MEFs (79±4%) and OSKM transduced MEF (57±6%). These data indicate that B-Myb overexpression is detrimental for the reprogramming process.

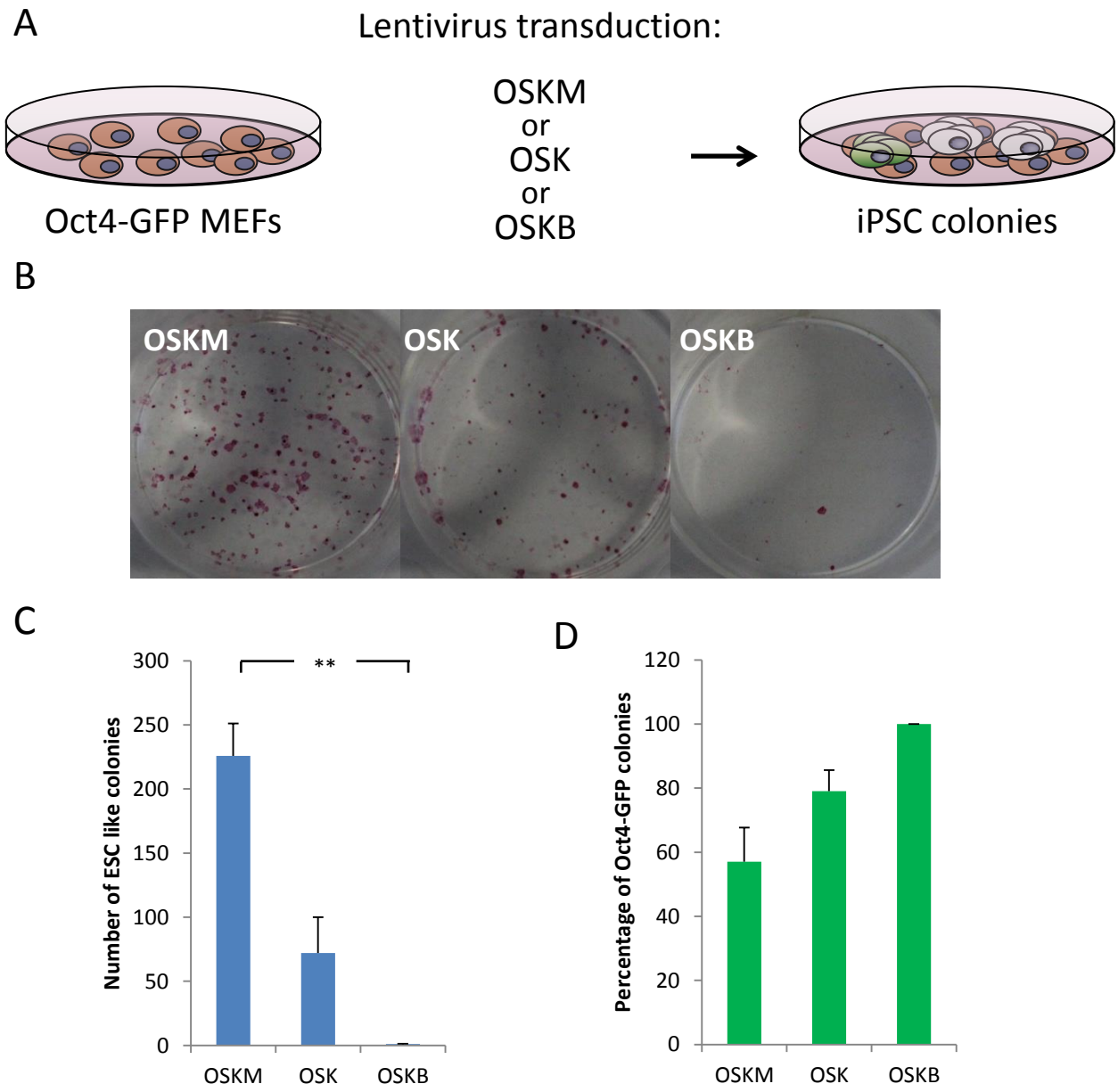


Figure 6.9: Reprogramming with OSKB lentivirus at MOI 2
(A) Schematic of the experimental strategy. Oct4-GFP MEFs were transduced with MOI 2 OSKM, OSK or OSKB lentiviral particles and allowed to reprogram for 14 days before GFP positive colonies were counted and the cells were stained for alkaline phosphatase activity. (B) Alkaline phosphatase staining of MEFs at day 14. OSKM (left panel), OSK (middle panel) and OSKB (right panel). Plates showing positive staining (red). (C) Graph representing the number of ESC like colonies based on morphology. Error bars represent SEM, N=3, ** P<0.01 by two-tailed Student's T-Test. (D) Graph representing the percentage ESC like colonies that also expressed GFP. Error bars represent SEM, N=3

To determine if by increasing the number of viral particles the number of MEFs that reprogram would increase, I repeated the experiment with a MOI of 20. Figure 6.10A shows that at MOI 20 there was in increase in the number of colonies with each of the different lentiviruses but still the number of colonies was much lower when reprogramming was performed with OSKB lentivirus. The mean number of ESC-like colonies when reprogramming was performed with OSKM lentivirus was 333±72, compared to 347±68 when reprogramming with OSK and 62±14 when reprogramming with the OSKB lentivirus (Figure 6.10B). By analysing the expression of GFP driven by the endogenous *Oct4* promoter I determined that the percentage of GFP positive iPSC colonies generated through reprogramming with OSKB was higher (72±3%) than for OSK (47±9%) and OSKM (52±8%, Figure 6.10C).

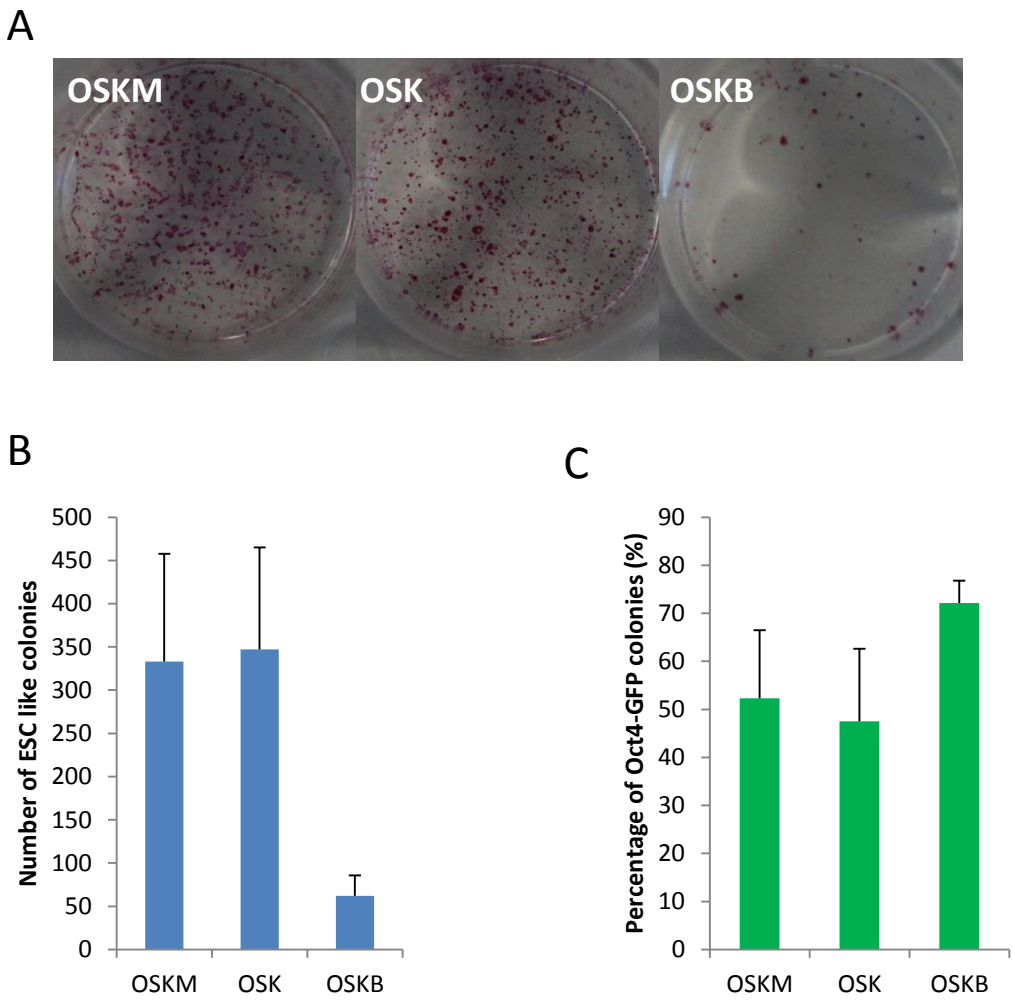


Figure 6.10: Reprogramming with OSKB lentivirus at MOI 20
Oct4-GFP MEFs were transduced with MOI 20 OSKM, OSK or OSKB lentiviral particles and allowed to reprogram for 14 days before GFP positive colonies were counted and then the cells were stained for alkaline phosphatase activity. (A) Alkaline phosphatase staining of MEFs at day 14. OSKM (left panel), OSK (middle panel) and OSKB (right panel). Plates showing positive staining (red). (B) Graph representing the ESC like colonies based on morphology. Error bars represent SEM, N=3 (C) Graph representing the percentage of the ESC like colonies that also expressed GFP. Error bars represent SEM, N=3

6.2.5 The reduced reprogramming efficiency is not caused by quiescence/ senescence in the MEFs.

I then wanted to determine the cause of the lack of reprogramming observed when B-Myb is overexpressed. One possibility is that the lower reprogramming efficiency observed when using the OSKB lentivirus compared to the OSK lentivirus was due to cell cycle arrest. Two approaches were taken. First, I checked for β-galactosidase activity, as it has been shown to be a marker for senescent cells that is not present in normal, quiescent or immortalised cells (Dimri et al., 1995). I did not detect β-galactosidase activity in MEFs transduced with either OSK or OSKB lentiviral particles compared to the negative control (non-transduced MEFs), indicating that the MEFs are not becoming senescent as a result of the viral transduction (Figure 6.11).

Bearing in mind that β-galactosidase activity could be a later event during senescence, I decided to look at the expression of p21, p16 and p53 (As mentioned in section 5.2.3 these genes have all been shown to have roles in promoting cell senescence.).

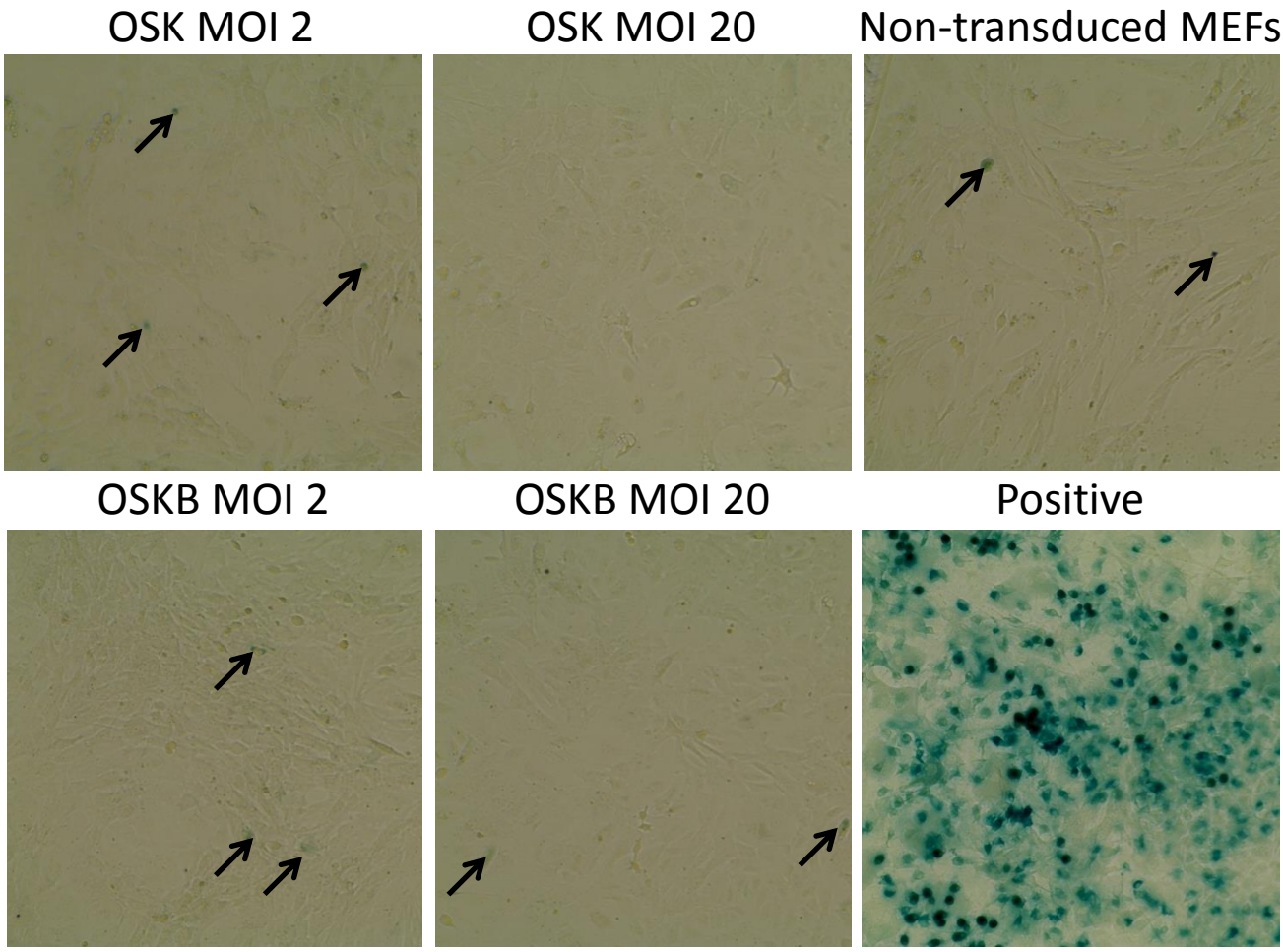


Figure 6.11: **β-galactosidase staining in MEFs transduced with OSK or OSKB**
MEFs were transduced with OSKB or OSK lentiviral particles at MOI 2 or 20. After 3 days the cells were fixed and stained for β-galactosidase activity, a marker of senescent cells. Representative image from 20x magnification inverted bright field microscope. Positively stained are cells highlighted by black arrows. Positive – MEFs cultured for 10 days without passage. N=2

RNA was extracted from the MEFs that were transduced with OSKM, OSKB or OSK lentiviral particles three days after transduction. The RNA was used as a template to synthesise cDNA which was analysed for expression of p21, p16 and p53. As shown in Figure 6.12A the mean expression of p21 in MEFs reprogrammed with OSKM, OSK or OSKB at MOI 2 was similar to non-transduced MEFs (1.06, 0.9 and 0.74, respectively). At MOI 20 the mean expression of p21 increased only when MEFs were transduced with

OSKM (2.18 fold) but not when MEFs were transduced with either OSK or OSKB lentiviral particles compared to non-transduced MEFs (Figure 6.12B). These results indicate that the early senescence marker p21 is not upregulated in the MEFs transduced with OSKB virus.

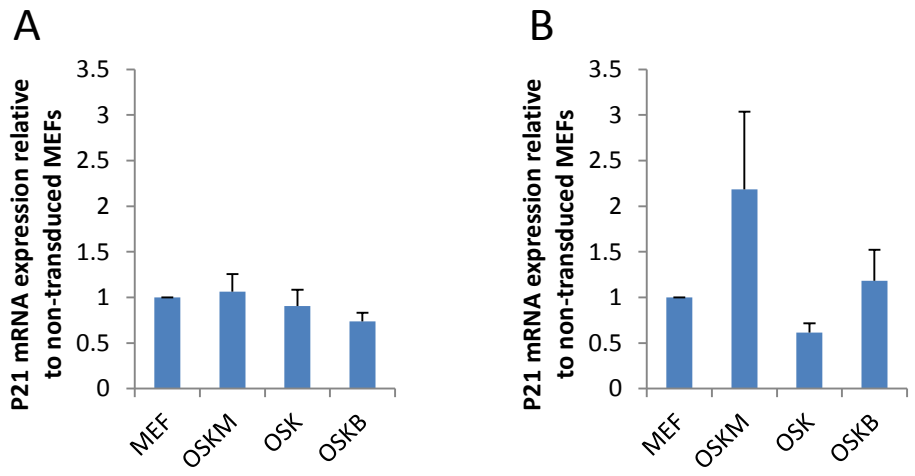


Figure 6.12: P21 mRNA expression
RNA was extracted from wild-type MEFs at day 3 during reprogramming using OSKM, OSK or OSKB at MOI 2 (A) or MOI 20 (B). cDNA was reverse transcribed from total RNA and expression of p21 was measured by qPCR, normalized against β_2-microglobulin housekeeping gene and expressed relatively to non-transduced MEFs. N=3

In addition, the expression of p16 was analysed in reprogramming MEFs at day 3. The mean expression of p16 was increased compared to non-transduced MEFs when reprogramming with OSKM and OSKB at MOI 2 by a factor of 2.76 and 1.89, respectively, but it did not increase in MEFs transduced with OSK (Figure 6.13A). At MOI 20, OSKM and OSKB transduced MEFs also showed an upregulation of p16 by a factor of 2.99 and 1.4, respectively, however, expression did not increase in MEFs transduced with OSK (Figure 6.13B).

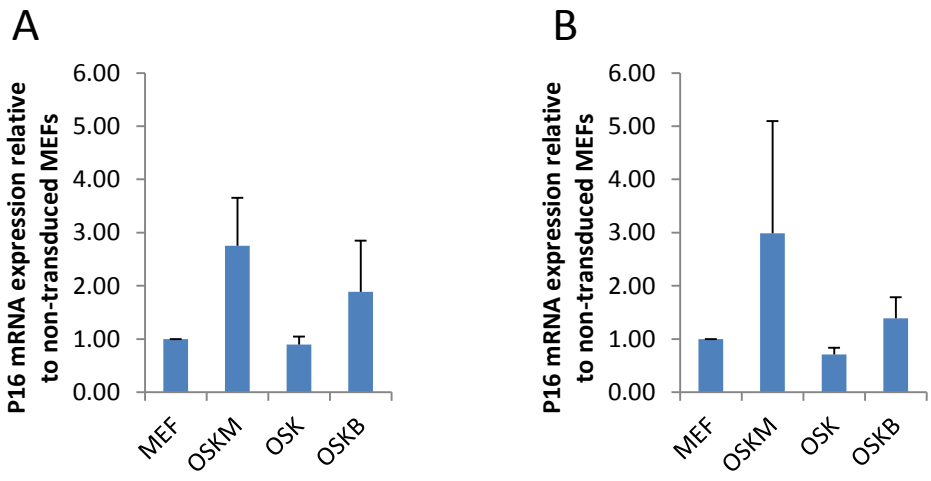


Figure 6.13: P16 mRNA expression
RNA was extracted from wild-type MEFs at day 3 during reprogramming using OSKM, OSK or OSKB at MOI 2 (A) or MOI 20 (B). cDNA was reverse transcribed from total RNA and expression of p16 was measured by qPCR and normalized against β_2-microglobulin housekeeping gene and expressed relatively to non-transduced MEFs. N=3, error bars represent SEM.

P53 expression was measured at day 3 during reprogramming. The expression of p53 in MEFs transduced with OSKM, OSK or OSKB at MOI 2 did not increase when compared to non-transduced MEFs (Figure 6.14A). At MOI 20, p53 expression increased in MEFs transduced with OSKM by a factor of 1.4 compared to non-transduced MEFs (Figure 6.14B). On the contrary, p53 expression decreased in MEFs transduced with OSK or OSKB at MOI 20 by a factor of 0.5 compared to non-transduced MEFs (Figure 6.14B). The difference between OSK MOI 20 and non-transduced MEFs was statistically significant when tested with an unpaired two-tailed T-Test (P=0.02).

All three senescence related gene expression were only observed to increase in MEFs treated with OSKM at MOI 20.

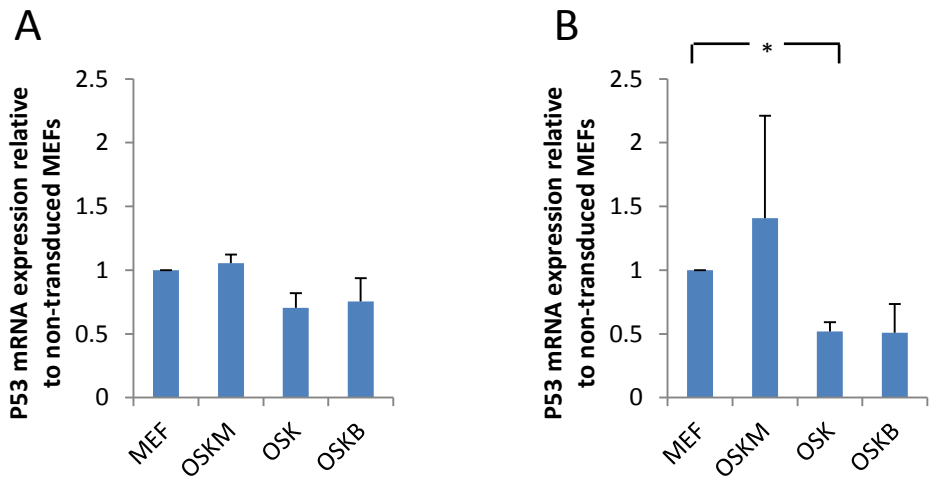


Figure 6.14: P53 mRNA expression
RNA was extracted from wild-type MEFs at day 3 during reprogramming using OSKM, OSK or OSKB at MOI 2 (A) or MOI 20 (B). cDNA was reverse transcribed from total RNA and expression of p53 was measured by qPCR and normalized against β_2-microglobulin housekeeping gene and expressed relatively to non-transduced MEFs. N=3 * P <0.05 by unpaired two-tailed T-Test, error bars represent SEM.

6.2.6 The reduced reprogramming efficiency is not caused by apoptosis in the MEFs

The reprogramming process causes apoptosis through DNA damage activation of p53 (Kawamura et al., 2009), and activation of caspase 3 and 8 (Li et al., 2010a). The level of p53 expression is also a factor affecting the reprogramming efficiency (Kawamura et al., 2009, Marion et al., 2009). The p53 upregulated modulator of apoptosis (PUMA) was shown to inhibit reprogramming (Li et al., 2013). Interestingly PUMA is able to induce apoptosis independently of p53 and therefore apoptosis could be occurring in iPSCs even if p53 expression is lower (Yu and Zhang, 2008).

To determine if the reduced reprogramming efficiency observed when using the OSKB lentivirus was due to an increase in the cells undergoing apoptosis MEFs were stained for fragmentation of genomic DNA by terminal deoxynucleotidyl transferase dUTP nick

end labelling (TUNEL). The TUNEL staining employed a red fluorochrome and the MEFs were also counterstained with DAPI (blue), apoptotic nuclei are shown in pink on a merged confocal image. MEFs that were treated with DNase I to cut the genomic DNA served as a positive control (Figure 6.15A). When MEFs were transduced with MOI 2 OSKM, OSK or OSKB the percentage of apoptotic nuclei were 5±5, 2±2 and 4±4, respectively, indicating that each lentiviral vector caused a similar amount of apoptosis (Figure 6.15B). At MOI 20, the transduction with OSKM, OSK or OSKB led to 5±5, 5±5 and 4±4 percent apoptotic nuclei, respectively, indicating that increasing the MOI of the transduction did not increase the apoptosis and that the apoptosis caused by each lentiviral vector was very similar (Figure 6.15C).

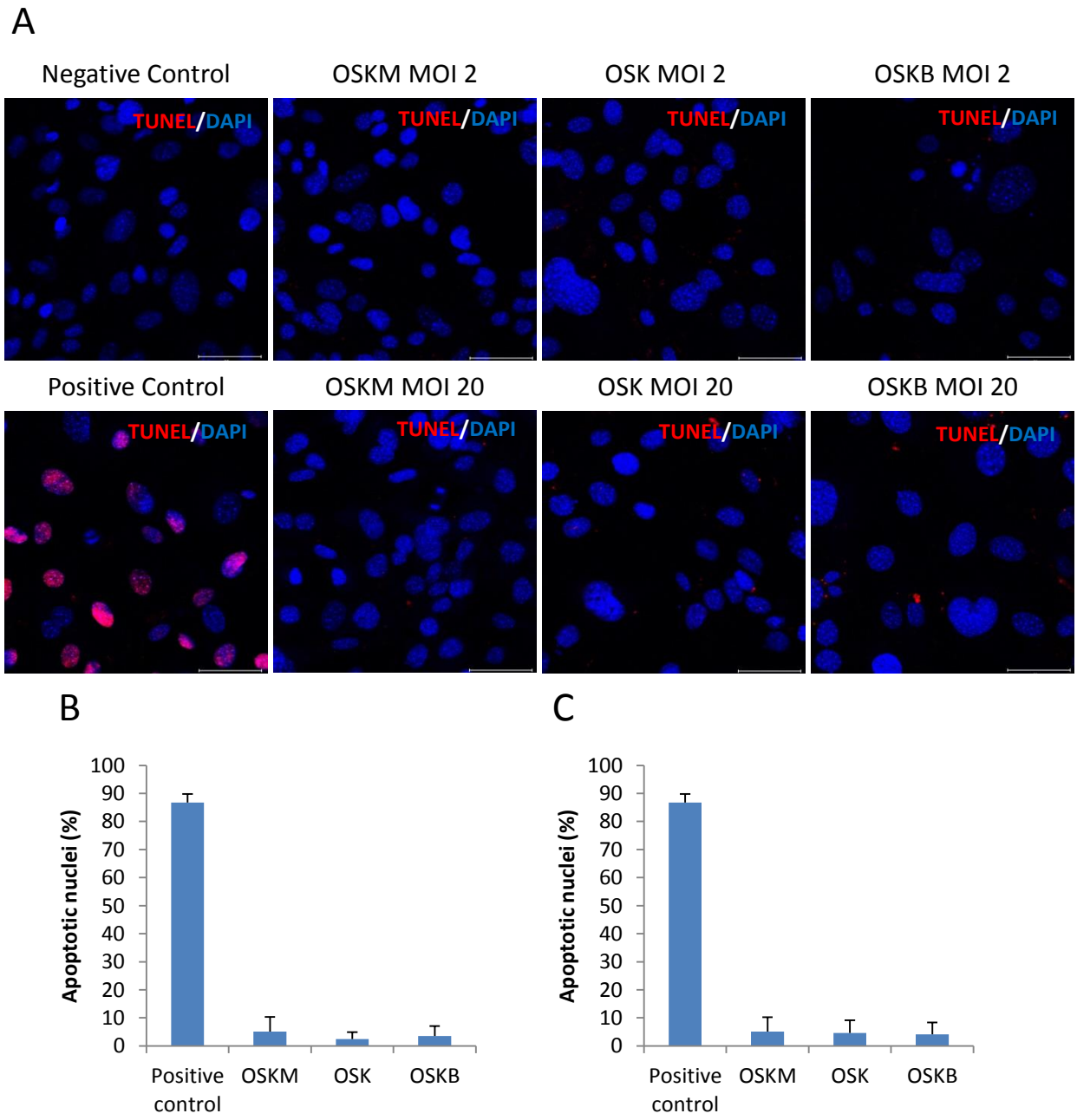


Figure 6.15: TUNEL staining in MEFs
Wild type MEFs were grown on gelatin coated glass coverslips and then transduced with OSKM, OSK or OSKB at MOI 2 or 20. After 3 days MEFs were stained for genomic DNA fragmentation with TUNEL assay. (A) Representative merged images at 40x magnification from confocal microscope show TUNEL staining (red) and DAPI (blue). Scale bar = 50µm. Positive control - MEFs treated with DNase I, negative control –non-transduced MEFs. (B&C) Quantification of apoptotic nuclei counts from each condition MOI 2 (B) and MOI 20 (C). N=2

Results in section 6.2.5 show that p53 expression did not increase when transducing MEFs with the OSKB lentivirus compared to non-transduced MEFs. To be sure that p53

is not involved in the reduction in reprogramming efficiency, *p53*$^{-/-}$ MEFs were transduced with OSK or OSKB lentiviral particles at MOI 20 and then stained for AP activity after 14 days (Figure 6.16A). Surprisingly, there were positively stained cells in the no virus control wells (Figure 6.16B), these cells were however not counted as they did not have an ESC like morphology (Figure 6.16C). As in previous experiments there was visibly more AP positive colonies in the OSK transduced MEFs compared to OSKB transduced MEFs (Figure 6.16B). There were significantly more AP positive colonies in OSK transduced MEFs (1152±121) compared to OSKB (88±2) transduced MEFs (P=0.012 by unpaired two-tailed T-Test, Figure 6.16D). Knockout of *p53* in MEFs has been reported to increase OSK reprogramming by a factor of 4 (Marion et al., 2009). When compared to the mean number of ESC like colonies in Figure 6.10B the number of colonies in *p53*$^{-/-}$ MEFs transduced with OSK increased by a factor of 3.3. On the other hand, the number of colonies in *p53*$^{-/-}$ MEFs transduced with OSKB only increased by a factor of 1.4. This data seem to indicate that the reduced efficiency observed when transducing MEFs with the OSKB lentivirus is not due to the activation of p53 pathways. Thus, B-Myb must have additional role/s during reprogramming other than in cell cycle progression.

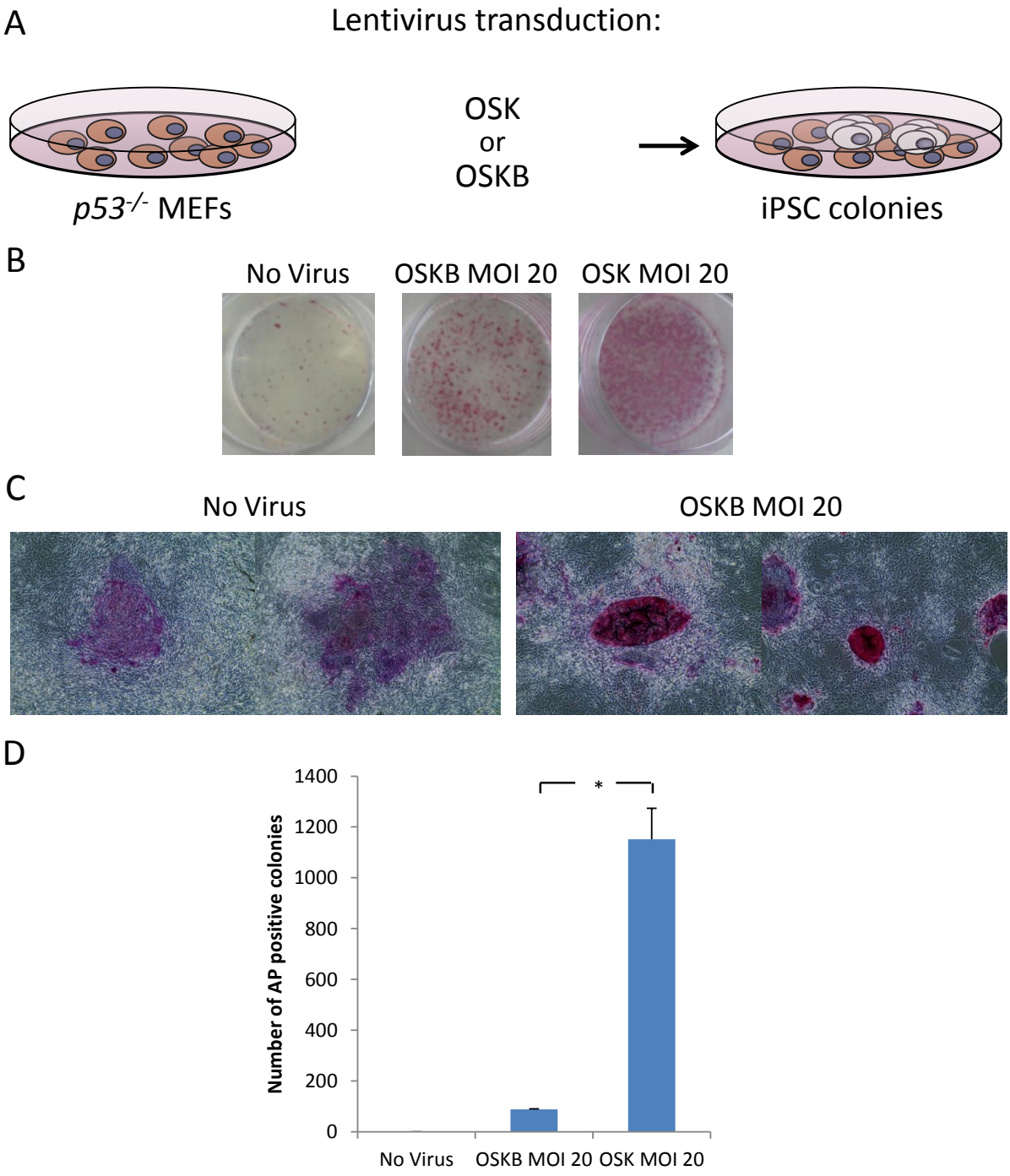


Figure 6.16: Reprogramming in *p53*$^{-/-}$ MEFs
(A) Schematic of the experimental strategy. (B) *P53*$^{-/-}$ MEFs were transduced with OSK or OSKB lentiviral particles at MOI 20 and allowed to reprogram for 14 days before staining for AP activity. (C) Example of positive stained cells that are not considered colonies (left panel) or that are considered colonies (right panel) 10x magnification. (D) Quantification of alkaline positive colonies. N = 3, Error bars represent SEM.* P<0.05 by unpaired two-tailed T-Test.

6.2.7 Reprogramming kinetics are slower in OSKB reprogramming

Next, I aimed to identify when during reprogramming the addition of B-Myb was affecting the process. MEFs were transduced with OSKM, OSK or OSKB lentiviral particles and tracked throughout the reprogramming process using flow cytometry to measure the expression of surface antigens CD44 and CD54 (ICAM1)(O'Malley et al., 2013). MEFs that are reprogramming change in morphology becoming smaller and less granular which is reflected in their FSC/SSC profile (Figure 6.17A). Untransduced MEFs express both CD44 and CD54 surface markers (Figure 6.17B, left panel). As MEFs reprogram towards iPSCs their surface antigen expression inevitably changes, firstly their expression of CD54 is lost (cells in Q3), then expression of CD44 is lost (cells in Q4), and finally, iPSC regain expression of CD54 (cells in Q1). This approach was first validated using Oct4-GFP MEFs. When the GFP positive cells (Figure 6.17C) were presented as a dot plot of CD44 against CD54 (Figure 6.17D) it showed that the expression of Oct4-GFP correlated with cells that had reached the final two stages of reprogramming (pre-iPSCs and iPSCs) based on CD44 and CD54 expression (Q4 and Q1).

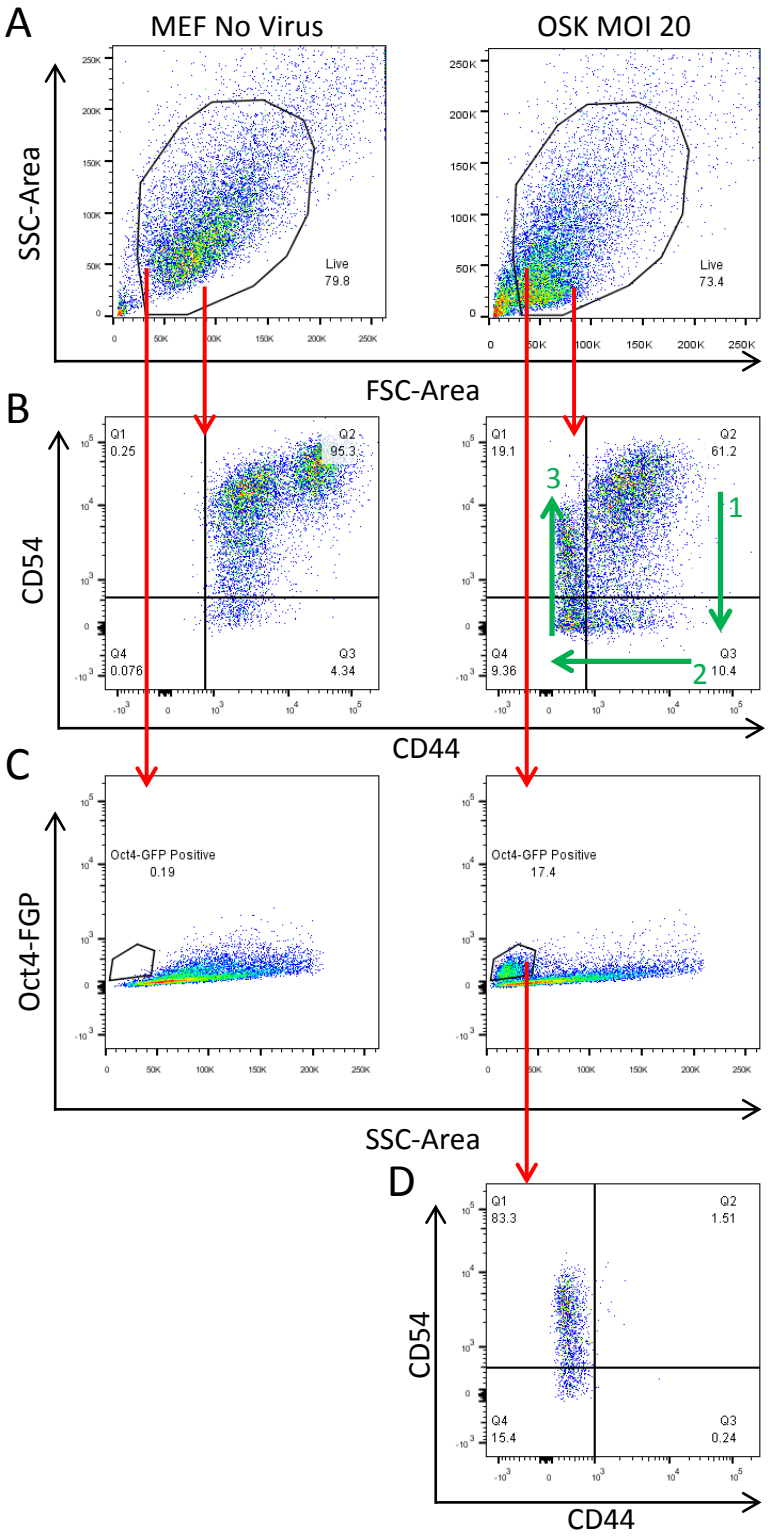


Figure 6.17: Schematic to show gating strategy used in flow cytometry
Cell were gated based on their size and granularity (A, Live), then shown as dot plots representing their expression of CD44 and CD54. Green arrows show progression of CD44/CD54 expression during reprogramming (B). Reprogramming MEFs were gated for GFP expression driven by endogenous Oct4 promoter (C, GFP positive population). (D) Dot plot showing CD44/CD54 expression in GFP positive pre-iPSCs and iPSCs.

MEFs were tracked through reprogramming at day 6, 9, 12 and 16 after being transduced with OSKM, OSK or OSKB lentiviral particles at MOI 2. The mean percentage of cells in the quadrant (Q1, CD54+, CD44-) that corresponds to the fully reprogrammed iPSCs at day 6 was 2.68%, 0.81% and 0.76% for OSKM, OSK and OSKB reprogramming MEFs, respectively (Figure 6.18A). The mean percentage of fully reprogrammed MEFs at day 9 increased to 5.04% for OSKM reprogramming, but remained comparable to non-transduced MEFs at 1.62% and 0.99% for OSK and OSKB reprogramming MEFs, respectively (Figure 6.18B). At day 12, the percentage of cells in this quadrant had increased to 12.6% and 5% for OSKM and OSK reprogrammed MEFs, respectively, but only 1.7% for OSKB reprogrammed MEFs (Figure 6.18C). Finally, at day 16, the mean percentage of fully reprogrammed iPSCs further increased to 17% and 8% for OSKM and OSK reprogrammed MEFs, respectively. OSKB reprogrammed MEFs remained at 1.48% which is comparable to non-transduced MEFs (0.5%, Figure 6.18D).

The mean percentage of the fully reprogrammed iPSCs is significantly less in MEFs reprogrammed with OSKB compared to OSKM at each of the four time points (P=0.021, 0.0346, 0.0218 and 0.0185, respectively by unpaired two-tailed T-Test). It also shows that at day 16, the percentage of fully reprogrammed iPSCs when reprogramming is done using the OSKB lentivirus is significantly lower than when using the OSK lentivirus (P=0.0033 by unpaired two tailed T-Test).

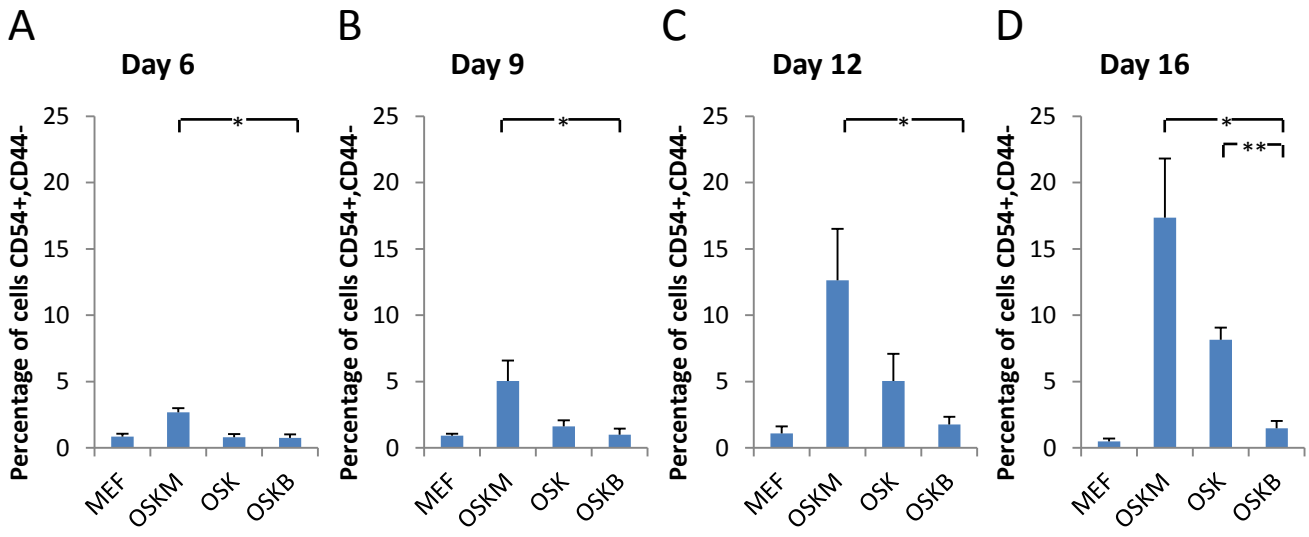


Figure 6.18: Fully reprogramed (CD54+,CD44-) iPSC quantification for OSKM, OSK or OSKB at MOI 2

MEFs were transduced with OSK, OSKM or OSKB lentiviral particles at MOI 2 then cultured up to 16 days. At day 6, 9, 12 and 16 MEFs were stained with CD44-APC and CD54-PE-Cy7 antibodies and reprogramming kinetics were analysed by flow cytometry. Graphs represent percentage of cells in the CD54+, CD44- quadrant. Error bars represent SEM, N=3, * P<0.05, ** P<0.01 by unpaired two-tailed T-Test.

The experiment was also conducted at MOI 20 with OSKM, OSK or OSKB. Figure 6.19A shows that the mean percentage of fully reprogrammed iPSCs at day 6 was 5.45% for OSKM. This rapid reprogramming was contrary to OSK and OSKB which had 0.61% and 1.1% fully reprogrammed iPSCs, values comparable to the non-transduced MEFs (0.85%). At day 9, the mean percentage of fully reprogrammed iPSCs was 4.4%, 2.2% and 1.6% for OSKM, OSK and OSKB reprogramming MEFs, respectively; once more levels achieved by OSKB transduction were similar to the non –transduced MEFs (0.9%, Figure 6.19B). At day 12, the mean percentage of fully reprogrammed iPSCs in OSKM and OSK reprogramming MEFs was 6.4% and 8.2%, respectively. OSKB transduced MEFs showed a greater percentage of fully reprogrammed iPSC at 3.78%; the first time a percentage was considered greater than background (Figure 6.19C). Finally, the graphs in Figure 6.19D illustrate that all three conditions were able to achieve reprogramming

at day 16, although the efficiency was different with 13.6%, 14.6% and 5.27% in OSKM, OSK and OSKB reprogramming MEFs, respectively.

At this MOI, the reduction in cells reaching the fully reprogrammed quadrant with OSKB reprogramming was only statistically significantly lower than OSKM and OSK reprogramming at day 16 (P=0.0089 and 0.0016, respectively, by unpaired two-tailed T-Test). This data corroborates the colony count data as it is possible to reprogram with OSKB at MOI 20 but at a reduced level compared to OSKM and OSK reprogramming.

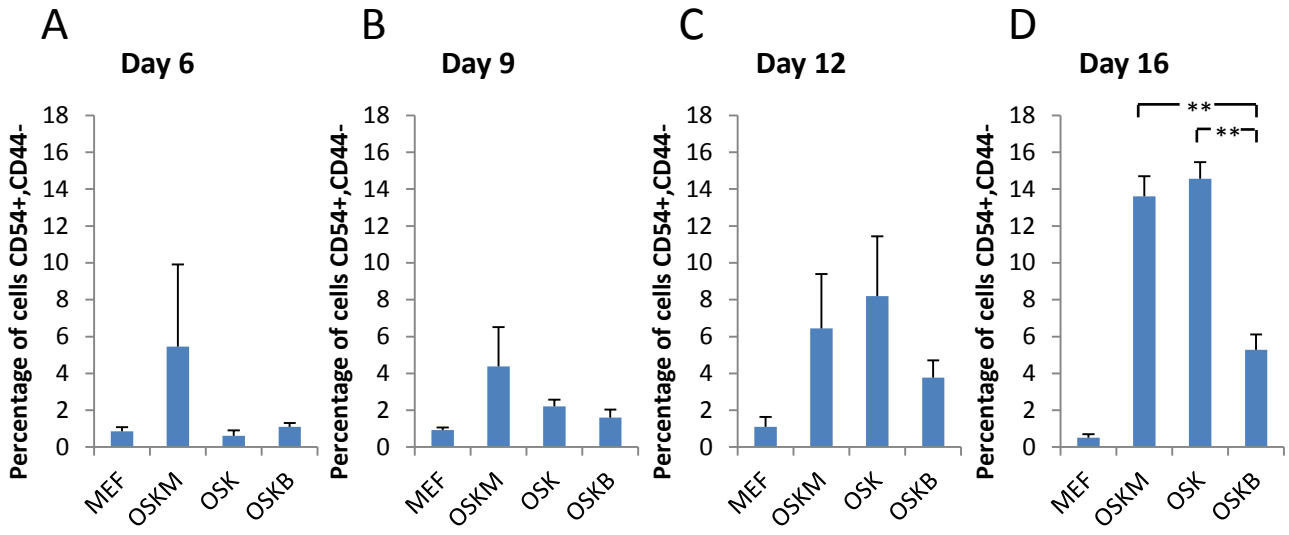


Figure 6.19: Fully reprogramed (CD54+,CD44-) iPSC quantification for OSKM, OSK or OSKB at MOI 20

MEFs were transduced with OSK, OSKM or OSKB lentiviral particles at MOI 20 then cultured up to 16 days. At day 6, 9, 12 and 16 MEFs were stained with CD44-APC and CD54-PE-Cy7 antibodies and reprogramming kinetics were analysed by flow cytometry. Graphs represent percentage of cells in the CD54+, CD44- quadrant. Error bars represent SEM,N=3, ** P<0.01 by unpaired two-tailed T-Test

One advantage of tracking iPSCs with CD44 and CD54 expression markers is that there are multiple stages that can be analysed during the process. I decided to quantify the percentage of cells that are in the quadrant (Q3, CD54-, CD44-) corresponding to the population of partially reprogrammed iPSCs (pre-iPSCs). Figure 6.20A shows that the mean percentage of pre-iPSCs was 6.1%, 0.3% and 0.2% in OSKM, OSK and OSKB reprogramming MEFs, respectively at day 6. At day 9, the mean percentage of pre-iPSCs had increased to 9.9% in OSKM; while very little increase was observed for OSK and OSKB (Figure 6.20B). Figure 6.20C shows that the mean percentage of pre-iPSCs at day 9 remained the same for OSKM at 9.4%, while a small increase to 3.4% was observed in OSK transduced MEFs. However, the OSKB transduced MEFs remained at a percentage comparable to non-transduced MEFs. Finally, at day 16, the mean percentage of pre-iPSCs were, 5.9%, 5.2% and 0.9% in OSKM, OSK and OSKB reprogramming MEFs, respectively (Figure 6.20D). The drop in the percentage of pre-iPSCs in OSKM and OSK occurs as a result of pre-iPSCs becoming fully reprogrammed iPSCs, thus the cells gain expression of CD54 and consequently moved into the fully reprogrammed iPSC quadrant.

When reprogramming was done at a MOI of 2, there were significantly less pre-iPSCs when comparing OSKM and OSKB at day 6, 9, 12 and 16 (P= 0.003, 0.0003, 0.0004 and 0.0096, respectively, by unpaired two-tailed T-Test). There was also a lower percentage of pre-iPSCs when comparing OSK to OSKB at all four time points, however it was only significantly lower at day 12 (P=0.0321 by unpaired two-tailed T-Test).

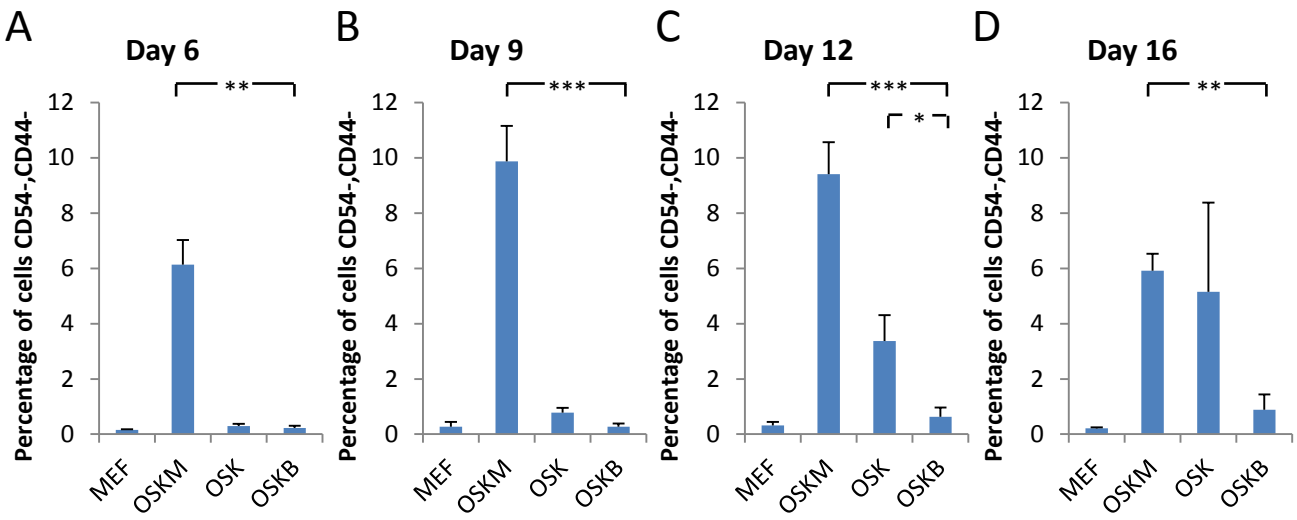


Figure 6.20: Partially reprogramed (CD54-,CD44-) iPSC quantification for OSKM, OSK or OSKB at MOI 2

MEFs were transduced with OSK, OSKM or OSKB lentiviral particles at MOI 2 then cultured up to 16 days. At day 6, 9, 12 and 16 MEFs were stained with CD44-APC and CD54-PE-Cy7 antibodies and reprogramming kinetics were analysed by flow cytometry. Graphs represent percentage of cells in the CD54+, CD44- quadrant. Error bars represent SEM, N=3 * P<0.05, ** P<0.01, *** P <0.001 by unpaired two-tailed T-Test

A similar pattern was observed when the MOI of the reprogramming lentiviruses was increased to 20. The mean percentage of pre-iPSCs at day 6 was already 13.7% for OSKM reprogrammed MEFs while in OSK and OSKB reprogramming MEFs it was 0.2% and 0.3%, respectively, equivalent to the non-transduced MEFs (0.2%, Figure 6.21A). At day 9, the mean percentage of pre-iPSCs decreased in OSKM reprogramming MEFs to 8%, while in OSK reprogramming MEFs there was a modest increase to 1.5%, which is greater than the percentage in non-transduced MEFs. However, the mean percentage of pre-iPSCs was 0.6% in OSKB reprogrammed MEFs, a value still comparable to non-transduced MEFS (0.2%, Figure 6.21B). Figure 6.21C shows that the mean percentage of pre-iPSCs was 9.9%, 5% and 2.3% for OSKM, OSK and OSKB reprogramming MEFs, respectively, at day 12. Finally, at day 16, the mean percentage of pre-iPSCs was 5.9%, 6.6% and 3.2% for OSKM, OSK and OSKB reprogramming MEFs, respectively (Figure 6.21D).

The percentage of pre-iPSCs was lower in OSKB compared to OSKM at all four time points and significantly lower at day 9 and day 12 (P=0.0002 and 0.0004, respectively, by unpaired two-tailed T-Test). The percentage of pre-iPSCs was also lower in OSKB compared to OSK at day 9 and 16 and was significantly lower at day 12 (P=0.0392 by unpaired two-tailed T-Test).

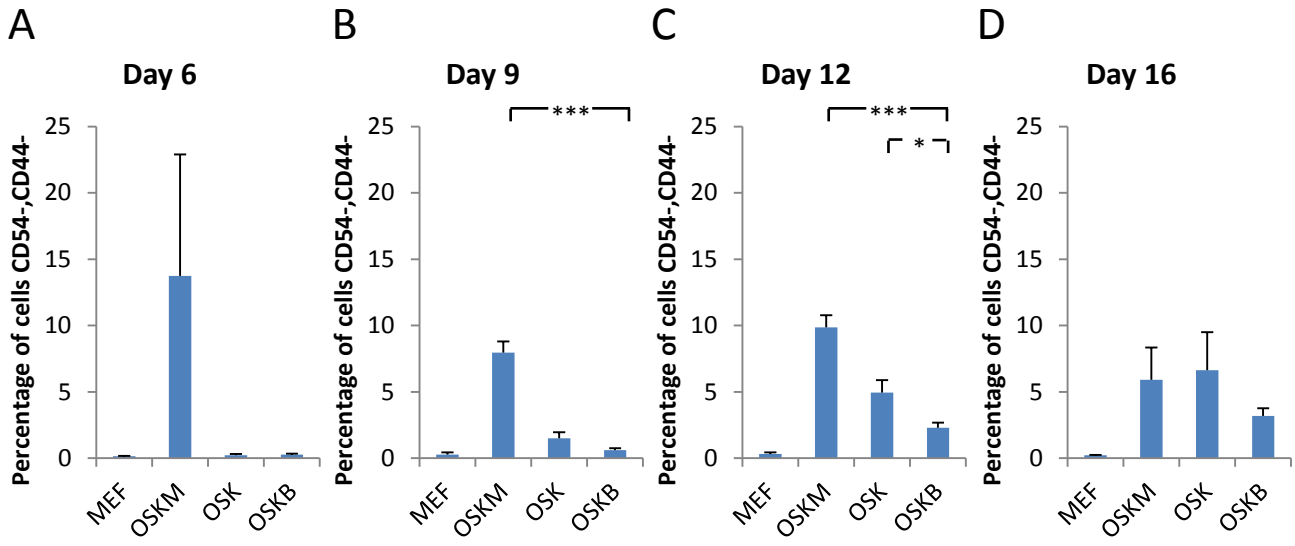


Figure 6.21: Partially reprogramed (CD54-,CD44-) iPSC quantification for OSKM, OSK or OSKB at MOI 20

MEFs were transduced with OSK, OSKM or OSKB lentiviral particles at MOI 20 then cultured up to 16 days. At day 6, 9, 12 and 16 MEFs were stained with CD44-APC and CD54-PE-Cy7 antibodies and reprogramming kinetics were analysed by flow cytometry. Graphs represent percentage of cells in the CD54+, CD44- quadrant. Error bars represent SEM, N=3 * P<0.05, *** P <0.001 by unpaired two-tailed T-Test

6.2.8 RNA analysis of MEFs undergoing reprogramming

6.2.8.1 Early pluripotency gene expression at MOI 2

From previous results it became clear that the OSKB transduction affected the kinetics of reprogramming based on CD44/CD54 expression. I therefore decided to study whether the expression of 14 genes involved in pluripotency, cell proliferation or mesenchymal to endothelial transition (MET) were affected.

RNA was extracted from MEFs at day 3, 6 and 9 during reprogramming with OSK or OSKB at MOI 2 and 20. OSK was compared to OSKB because they have more similar reprogramming kinetics due to the omission of the *c-Myc* gene. Expression was calculated as relative to the highest expression observed for each gene, which was generally day 9 for the pluripotency genes, as they become up regulated as the MEFs reprogrammed to iPSCs. This leads to a problem when analysing the statistical significance in experiments when each of the biological replicates have the same time point set to 100%, as the standard deviation is zero, and therefore, there is no standard error of the mean and the P value is much lower than expected. Thus, I did not report significance or P value when all three biological replicates had the same peak expression point.

As mentioned previously, Oct4 is a key pluripotency factor and the most difficult to replace of the factors used to reprogram. Figure 6.22A shows that the mean expression of Oct4 increased in both OSKB and OSK reprogrammed MEFs at day 3 to 7% and 21%, respectively. The mean expression of Oct4 continued to increase for both OSKB and OSK reprogrammed MEFs reaching 13% and 30%, respectively at day 6. At day 9, the mean expression of Oct4 in OSKB and OSK reprogramming MEFs peaked at 35% and 100%,

respectively. The large increase in Oct4 expression from day 6 to 9 corresponds to the higher percentage of reprogramming cells observed in OSK transduced MEFs compared to OSKB transduced MEFs, as the endogenous Oct4 will be activated by day 9.

Klf4 was shown to be important in the early stages of reprogramming as it plays a role in the MET, which must take place for MEFs to become iPSCs (Polo et al., 2012).

Figure 6.22B shows the expression of Klf4 at day 3, 6 and 9 in MEFs transduced with either OSKB or OSK lentiviral particles at MOI 2. The mean expression of Klf4 increased at day 3 in MEFs reprogrammed with OSKB or OSK to 26% and 45%, respectively. At day 6 the mean expression remained similar to day 3 at 23% and 49% in MEFs reprogrammed with OSKB or OSK, respectively. The mean expression then increased to 60% and 90% at day 9 for MEFs reprogramming with OSKB or OSK, respectively.

Ets Variant 5 (ETV5(also known as Ets-Related Molecule (ERM)) is a transcription factor belonging to the ETS family (Monte et al., 1994). It has an essential role in maintenance of the spermatogonial stem cell niche (Chen et al., 2005), regulation of the actin cytoskeleton (Tsukita et al., 1994) and has been reported to be involved in metastasis in cancer (Monge et al., 2007). ETV5 is up-regulated during the reprogramming (O'Malley et al., 2013).

Figure 6.22C shows that the mean expression of ETV5 in MEFs undergoing reprogramming with MOI 2 OSKB increased to 20% at day 3; while in OSK reprogramming MEFs the expression increased more rapidly to 37%. At day 6, the mean expression of ETV5 in the OSK reprogramming MEFs continued to increase steadily to 61%; in contrast the mean expression of ETV5 in MEFs reprogramming with OSKB increased slightly to 25%. At day 9, the OSK reprogramming MEFs mean expression of

ETV5 continued to rise to 100%, however the OSKB reprogramming MEF mean expression decreased to 24%. The difference in expression of ETV5 was statistically significant at day 6 in MEFs reprogrammed with OSKB or OSK when using an unpaired two-tailed T-Test (P=0.0109).

Splat-like transcription factor 4 (Sall4) is a zinc-finger transcription factor essential for maintenance of pluripotency in ESCs and in early embryonic cell-fate decisions (Zhang et al., 2006). Sall4 expression is upregulated during the reprogramming process similarly to other pluripotency factors (Xu et al., 2009, Samavarchi-Tehrani et al., 2010, O'Malley et al., 2013).

Figure 6.22D shows that the mean Sall4 expression began to rise at day 6 in OSK reprogramming MEFs to 7%. By day 9, the Sall4 expression in OSK reprogramming had greatly risen to 100%, whereas in OSKB reprogramming the expression of Sall4 had risen to only 3%. The difference in expression at day 6 was statistically significant (P=0.032) by unpaired two-tailed T-Test.

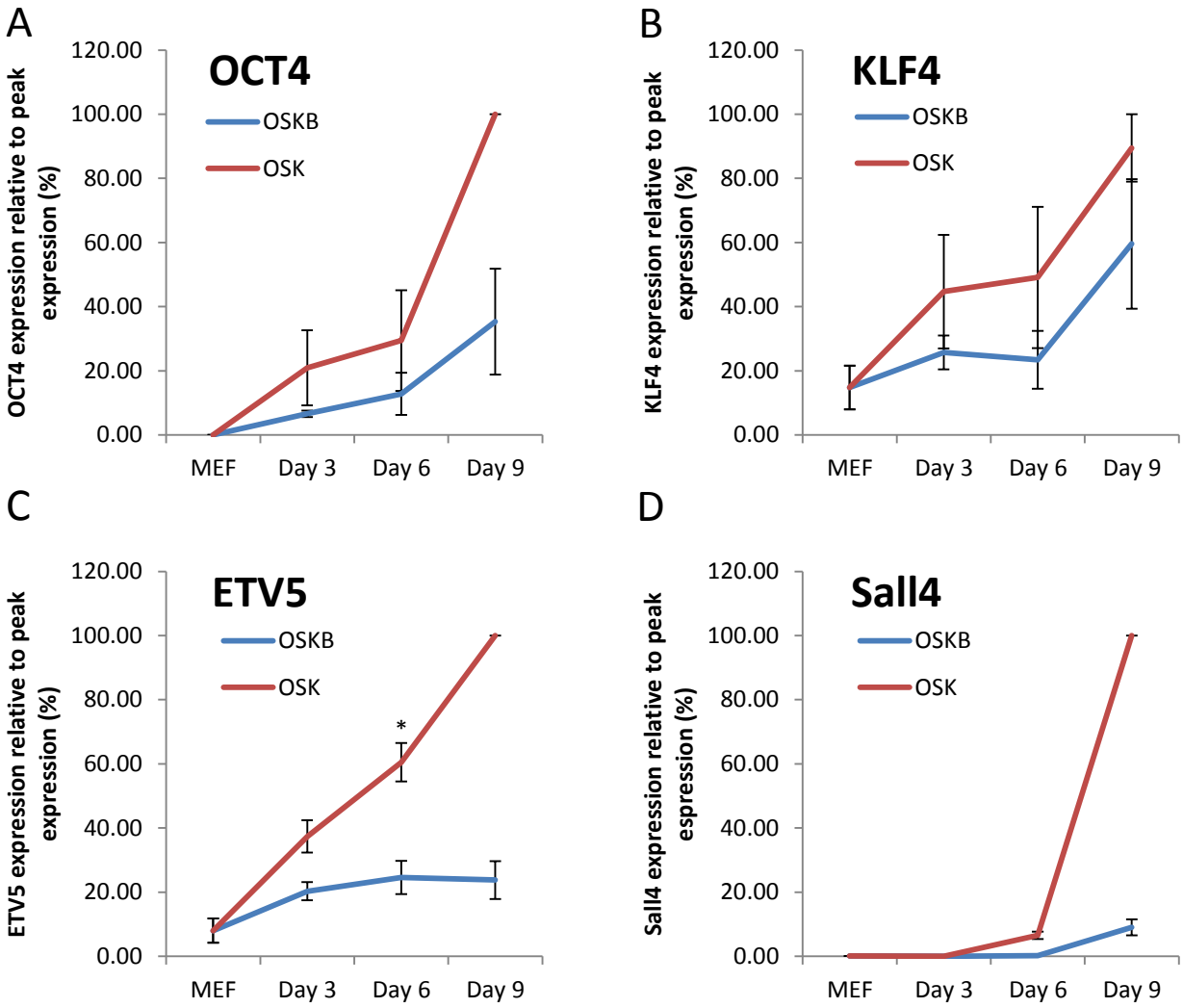


Figure 6.22: RNA expression of early pluripotency genes during reprogramming with OSKB or OSK at MOI 2

Wild type MEFs were reprogrammed with MOI 2 OSKB or OSK lentiviral particles. At day 3, day 6 or day 9 RNA was extracted from the MEFs, reverse transcribed to generate cDNA, then expression of (A) Oct4, (B) KLF4, (C) ETV5 or (D) Sall4 was measured using qPCR. Expression was normalized against β_2-microglobulin housekeeping gene, and then expressed relatively to peak expression of each gene. N= 3 error bars represent standard error of the mean * $P<0.05$ by two tailed unpaired T-Test

6.2.8.2 Early pluripotency gene expression at MOI 20

The experiment was also performed with OSKB and OSK lentiviral particles at a MOI of 20, as previous experiments showed that it was possible to reprogram MEFs with the OSKB lentiviral vector at this higher MOI, albeit with a much lower efficiency compared to OSK reprogramming.

Figure 6.23A shows the mean Oct4 expression in MEFs undergoing reprogramming with MOI 20 OSKB or OSK lentiviral particles at day 3, 6 and 9. At day 3, the expression of Oct4 had increased to 14% in OSKB reprogramming while the expression had increased to 29% in OSK reprogramming MEFs, more than double compared to OSKB. Both OSKB and OSK showed a small increase in Oct4 expression at day 6 (19% and 42%, respectively). By day 9, the Oct4 expression increased sharply in both OSKB and OSK reprogramming MEFs (77% and 92%, respectively).

Klf4 expression rose in both OSKB and OSK transduced MEFs to 13% and 21%, respectively, at day 3. The expression of Klf4 then dropped to 12% at day 6 in OSKB transduced MEFs, in contrast to OSK transduced MEFs in which the expression rose slightly to 28%. Both OSKB and OSK transduced MEFs expression of Klf4 rose sharply to 73% and 100% by day 9 (Figure 6.23B).

Figure 6.23C shows the mean increase of ETV5 expression when reprogramming with either OSKB or OSK lentiviral particles at MOI 2. The expression of ETV5 increased in both OSKB and OSK transduced MEFs to 14% and 17%, respectively, at day 3. At day 6, there was then a sharp increase in ETV5 expression in both OSKB and OSK transduced MEFs to 54% and 65%, respectively. The expression then increased less sharply to 81% for both OSKB and OSK transduced MEFs at day 9.

Expression of Sall4 started to increase in both conditions at day 6 with OSKB transduced MEFs reaching 2% in contrast to OSK transduced MEFs, which increased to 16% expression (Figure 6.23D). The expression of Sall4 then increased sharply at day 9 in both OSKB and OSK transduced MEFs to 73% and 76%, respectively. The difference in expression of Sall4 between OSK and OSKB transduced MEFs at day 6 was significant by unpaired two-tailed T-Test (P=0.038).

In summary, the fluctuations in expression of the pluripotency genes when reprogramming with OSK and OSKB are much more similar at MOI 20 compared to MOI 2, indicating that it is possible to overcome the B-Myb block by increasing the expression of the reprogramming factors and thus the factor/target ratio.

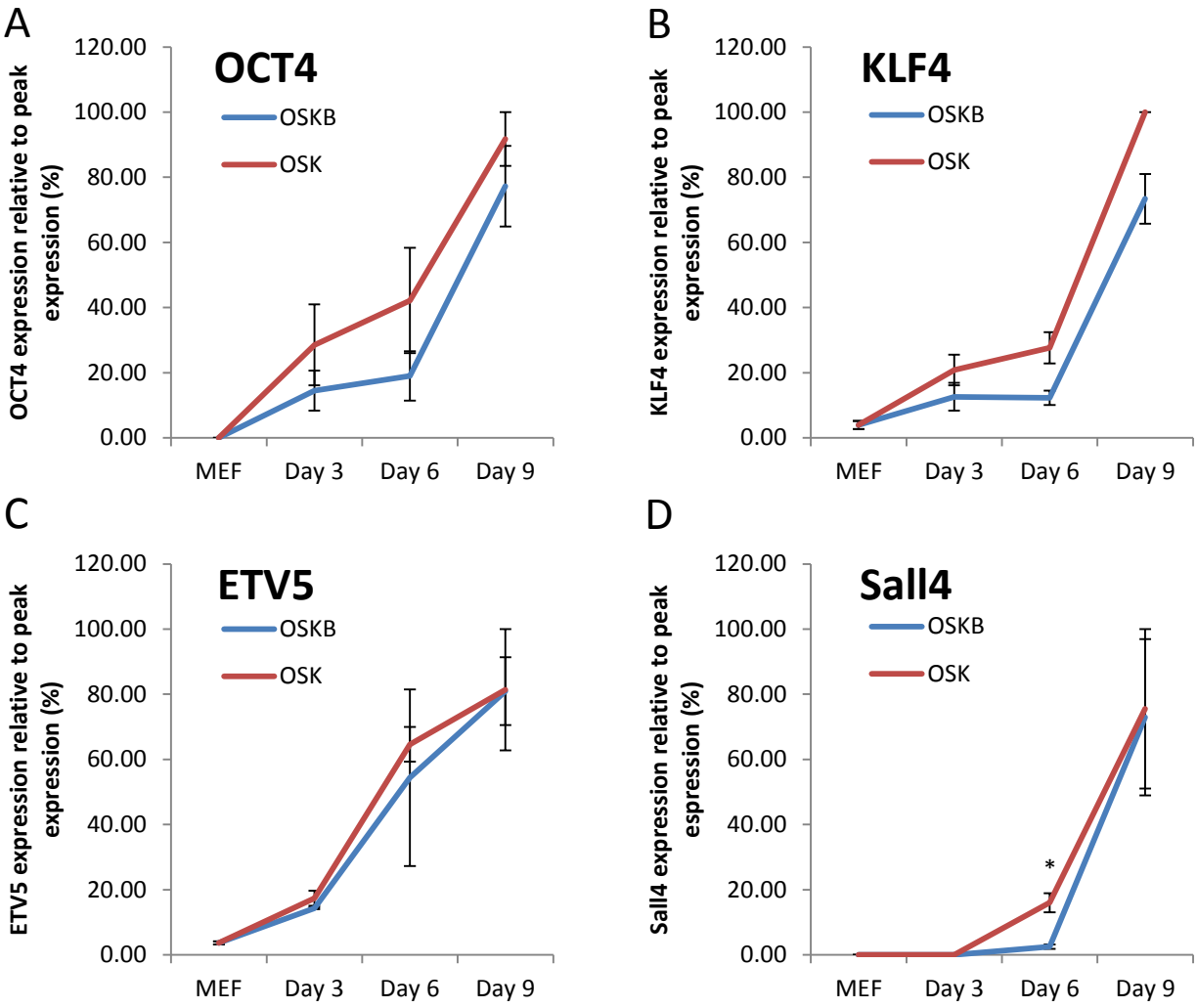


Figure 6.23: RNA expression of early pluripotency genes during reprogramming with OSKB or OSK at MOI 20

Wild type MEFs were reprogrammed with MOI 20 OSKB or OSK lentiviral particles. At day 3, day 6 or day 9 RNA was extracted from the MEFs, reverse transcribed to generate cDNA, then expression of (A) Oct4, (B) Klf4, (C) ETV5 or (D) Sall4 was measured using qPCR. Expression was normalized against β_2-microglobulin housekeeping gene, and then expressed relatively to peak expression of each gene. N= 3 error bars represent standard error of the mean * $P<0.05$ by unpaired two tailed T-Test

6.2.8.3 Late pluripotency gene expression at MOI 2

B-Myb is highly expressed in ESCs (Tarasov et al., 2008) and its expression has been shown to increase in the early stages of secondary reprogramming (O'Malley et al., 2013) hinting at a role for B-Myb in reprogramming.

B-Myb expression at day 3 rose rapidly in OSKB transduced MEFs to 73%, which was expected as the OSKB vector contained the B-*myb* gene. On the other hand, in the OSK transduced MEFs B-Myb expression only increased to 3% Figure 6.24A. The expression of B-Myb dropped at day 6 in the OSKB transduced MEFs to 62%, while its expression in OSK transduced MEFs remained unchanged at 3%. B-Myb expression increased again in OSKB transduced MEFs at day 9 to 100% compared to 19% in OSK transduced MEFs. The difference in expression of B-Myb in OSKB compared to OSK transduced MEFs at day 3 was significant by unpaired two-tailed T-Test (P=0.044).

Nanog is a transcription factor that is found at the core of the pluripotency factor network (Boyer et al., 2005, Rodda et al., 2005), and expression of Nanog is one of the hallmarks of fully reprogrammed iPSCs (Takahashi and Yamanaka, 2006).

Expression of Nanog began to increase at day 6 for both OSKB and OSK transduced MEFs to 1% and 6%, respectively (Figure 6.24B). At day 9, the expression of Nanog rose sharply in OSK transduced MEFs to 100% whilst in contrast the OSKB transduced MEFs expression only increased to 8%. The difference in Nanog expression between OSKB and OSK reprogrammed MEFs was statistically significant at day 6 (P=0.014) when tested with an unpaired two-tailed T-Test.

Lin28a is a RNA binding protein that is highly expressed during embryogenesis with expression decreasing after differentiation (Yang and Moss, 2003). Lin28a has been

identified as a factor which can induce pluripotency in combination with Nanog, Oct4 and Sox2 (Yu et al., 2007). Expression of Lin28a increases as reprogramming proceeds (O'Malley et al., 2013).

Similarly to Nanog expression, Lin28a expression only began to rise at day 6 in OSK and OSKB transduced MEFs to 0.5% and 2%, respectively (Figure 6.24C). The Lin28a expression then rose rapidly in OSK transduced MEFs to 100% while it only increased to 7% in OSKB transduced MEFs at day 9.

Fibroblast growth factor 4 (FGF4) is important for embryonic development as knockout mouse models are embryonic lethal due to impaired ICM formation (Feldman et al., 1995). FGF4 expression is restricted to embryonic and embryonal carcinoma cells and it forms complexes with Sox2 and Oct4 (Yuan et al., 1995).

At day 3, FGF4 expression increased sharply to 55% in OSK transduced MEFs, while it only rose to 13% in OSKB transduced MEFs (Figure 6.24D). Expression of FGF4 then dropped slightly in both OSK and OSKB transduced MEFs to 48% and 11%, respectively, at day 6. There was then a sharp increase in FGF4 expression in OSK treated MEFs at day 9 to 100%, whereas in contrast, there was only a minor increase in FGF4 expression in OSKB transduced MEFs to 13%. The difference in expression of FGF4 between OSK and OSKB reprogramming MEFs was statistically significant at day 6 ($P=0.047$ by unpaired two-tailed T-Test).

Chromobox homolog 7 (CBX7) is a polycomb group protein which can immortalise MEFs by down regulating p16 and p53 induced senescence (Gil et al., 2004). CBX7 has been identified as a controller of early-lineage commitment in ESCs (Morey et al., 2013).

Expression of CBX7 increases as MEFs are reprogrammed to iPSCs (O'Malley et al., 2013).

The expression of CBX7 increased in both OSKB and OSK transduced MEFs to 6% and 11%, respectively, at day 3 (Figure 6.24E). At day 6, the OSKB transduced MEF expression of CBX7 had increased to 23% while the CBX7 expression in OSK transduced MEFs had increased to 43%. By day 9, the CBX7 expression in OSKB transduced MEFs only increased to 28% while the expression in OSK transduced MEFs sharply increased to 100%.

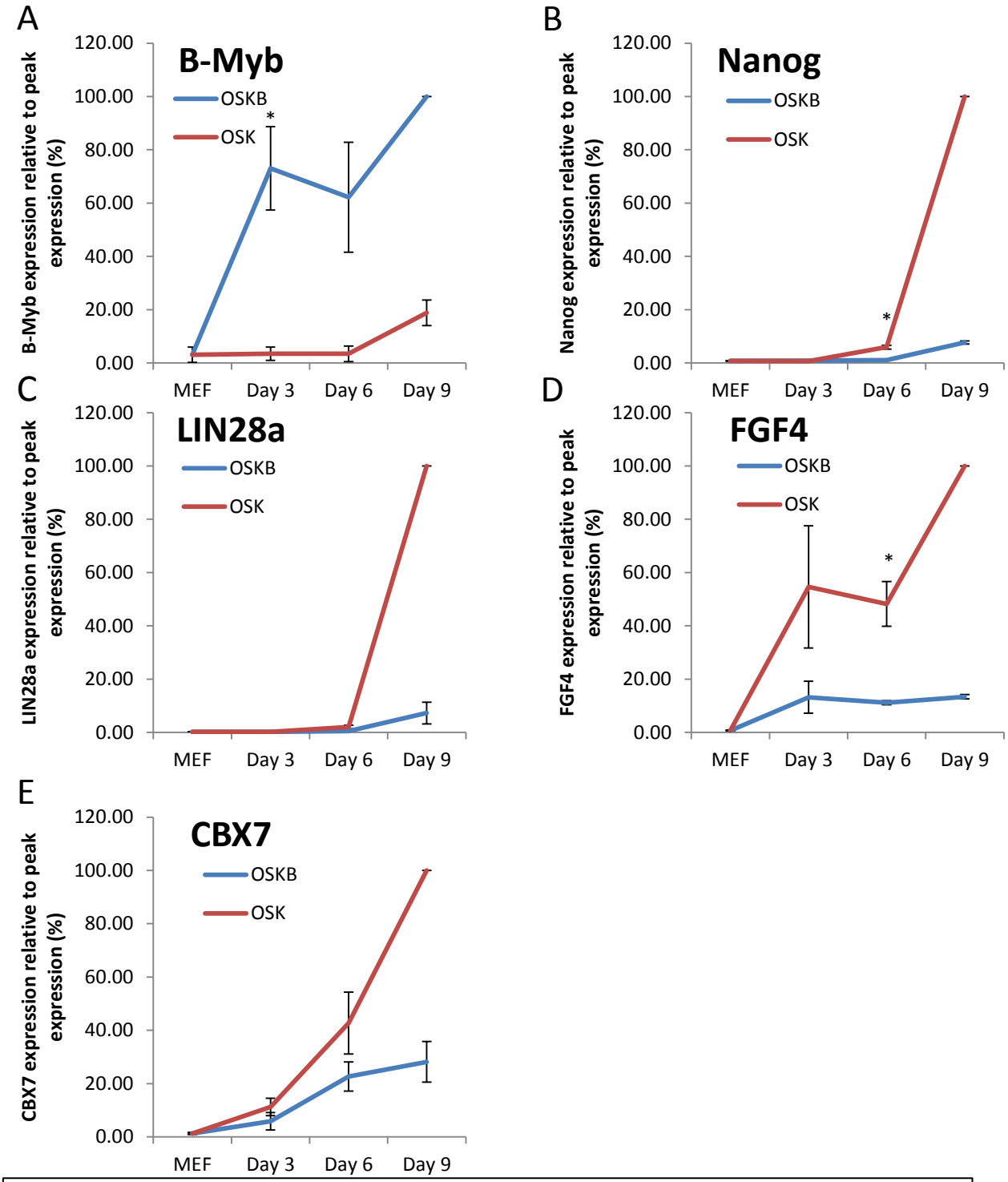


Figure 6.24: RNA expression of late pluripotency genes during reprogramming with MOI 2 OSKB or OSK

Wild type MEFs were reprogrammed with MOI 2 OSKB or OSK lentiviral particles. At day 3, day 6 or day 9 RNA was extracted from the MEFs, reverse transcribed to generate cDNA then expression of (A) B-Myb, (B) Nanog, (C) Lin28a, (D) FGF4 or (E) CBX7 was measured using qPCR. Expression was normalized against β_2-microglobulin housekeeping gene, and then expressed relatively to peak expression of that gene. N= 3 error bars represent standard error of the mean * P<0.05 by two tailed unpaired T-Test

6.2.8.4 Late pluripotency gene expression at MOI 20

The experiment was repeated with OSKB and OSK lentiviral particles at a MOI 20 to boost the reprogramming efficiency.

The mean expression of B-Myb rose in the OSKB transduced MEFs to 18% at day 3; in contrast the expression dropped in OSK transduced MEFs to 2%, which was lower than non-transduced MEF expression (6%). At day 6, the B-Myb expression remained the same in OSKB transduced MEFs (19%) but rose back to 6% in OSK transduced MEFs. The expression of B-Myb rose sharply at day 9 in the OSKB MEFs to 100% corresponding with the expression of endogenous B-Myb as iPSCs are being generated. The expression of B-Myb in the OSK transduced MEFs only increased to 14% at day 9 (Figure 6.25A).

The mean expression of Nanog began to rise at day 6 in the OSK transduced MEFs to 9%. At day 9, the expression of Nanog sharply rose in both OSK and OSKB transduced MEFs, to 100% and 79%, respectively (Figure 6.25B). The difference between Nanog expression in OSKB and OSK reprogramming MEFs was statistically significant at day 6 (P=0.015) when tested with an unpaired two-tailed T-Test.

Similarly to Nanog, expression of Lin28a was undetectable until day 6 at which point it was 2% for OSK transduced MEFs and 0.5% for OSKB transduced MEFS. Expression then increased rapidly to 85% and 54% for OSK and OSKB transduced MEFs, respectively, at day 9 (Figure 6.25C).

The mean expression of FGF4 rose steadily in both OSK and OSKB transduced MEFs to 31% and 24%, respectively, at day 3. The expression continued to rise to 68% and 55% for OSK and OSKB transduced MEFs, respectively, at day 6. The expression began to

plateau in both OSK and OSKB transduced MEFs at day 9 reaching 75% and 64% expression, respectively (Figure 6.25D).

CBX7 expression rose at day 3 to 2% and 4% in OSK and OSKB transduced MEFs, respectively. At day 6, the CBX7 expression increased to 18% in OSK transduced MEFs, but only increased to 7% for OSKB transduced MEFs. By day 9, the difference between the expression in OSK and OSKB transduced MEFs had widened to 100% and 40%, respectively (Figure 6.25E).

In summary, at MOI 2 late pluripotency genes failed to be upregulated when cells are reprogrammed with OSKB. Nonetheless, at MOI 20, by increasing the number of viral particles, some degree of reprogramming is achieved and the pluripotent genes are upregulated.

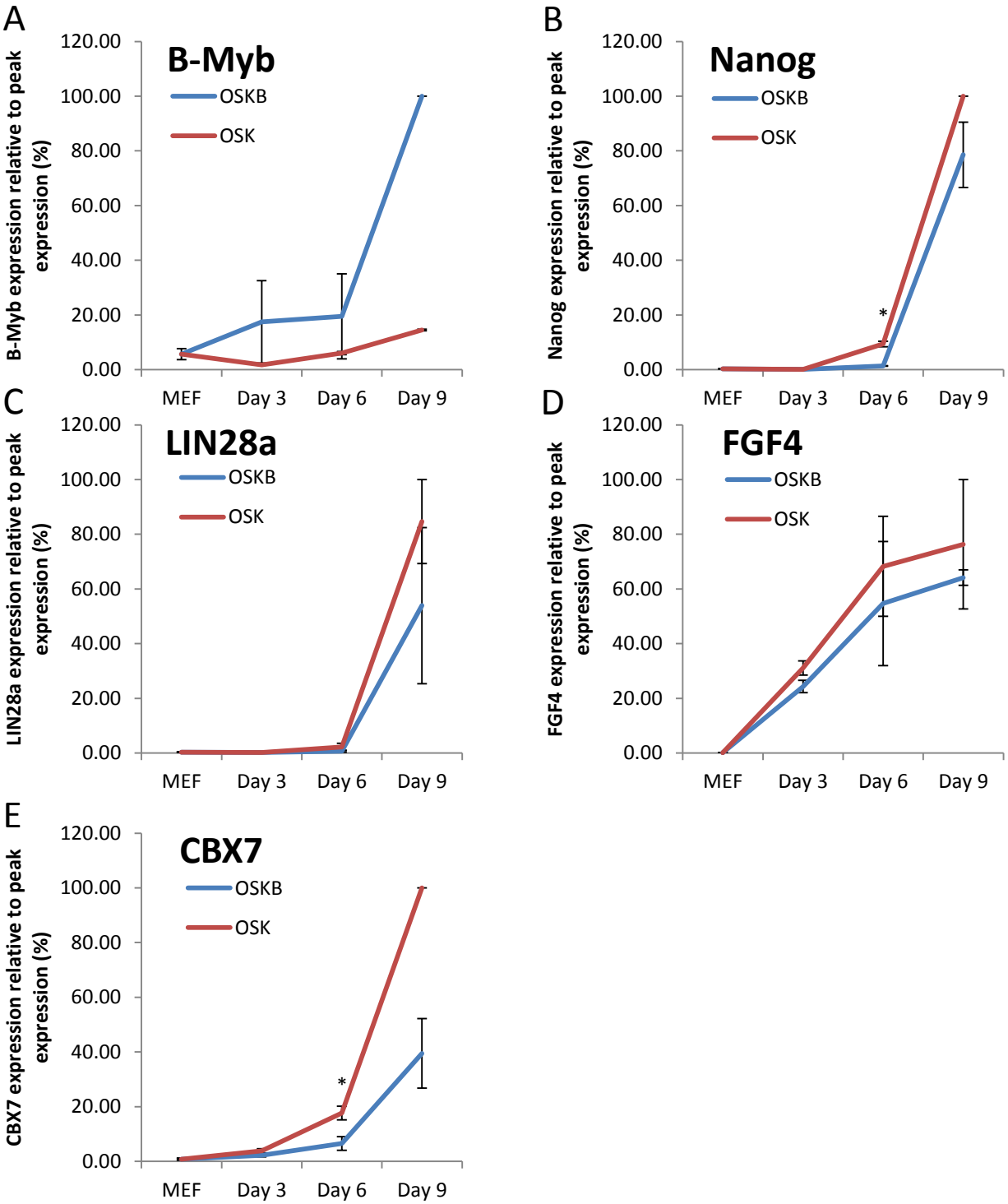


Figure 6.25: RNA expression of late pluripotency genes during reprogramming with MOI 20 OSKB or OSK

Wild type MEFs were reprogrammed with MOI 20 OSKB or OSK lentiviral particles. At day 3, day 6 or day 9 RNA was extracted from the MEFs, reverse transcribed to generate cDNA then expression of (A) B-Myb, (B) Nanog, (C) Lin28a, (D) FGF4 or (E) CBX7 was measured using qPCR. Expression was normalized against β_2-microglobulin housekeeping gene, and then expressed relatively to peak expression for each gene. N= 3 error bars represent standard error of the mean **P<0.01 by two tailed unpaired T-Test

6.2.8.5 MET and proliferative gene expression at MOI 2

Snai1 encodes the transcription factor Snail which controls epithelial to mesenchymal transitions through regulation of E-cadherin (Batlle et al., 2000, Cano et al., 2000, Mani et al., 2008). It was shown to be down-regulated in cells undergoing reprogramming where a mesenchymal to epithelial transition must take place in a secondary reprogramming system (Polo et al., 2012).

Mean Snai1 expression in untransduced MEFs was 59% (Figure 6.26A). Initially, Snai1 dropped in both OSK and OSKB transduced MEFs to 32% and 36%, respectively, at day 3. Then expression of Snai1 increased back to 58% in both OSK and OSKB transduced MEFs, matching pre-transduction expression. Finally, at day 9, the expression of Snai1 increased to 84% and 75% in OSK and OSKB transduced MEFs, respectively.

Cdh1 is the gene which encodes E-Cadherin, a member of the cadherin family of calcium dependent cell adhesion proteins which have an important role in maintaining cell to cell contact (Takeichi, 1991). E-Cadherin is required for early embryogenesis; mouse embryos with no expression have impaired formation of trophectodermal epithelium and fail to implant (Larue et al., 1994). *Cdh1* knockout ESCs cannot differentiate to tissues with organised structure and lose self-renewal capacity (Larue et al., 1996, Soncin et al., 2009). E-Cadherin expression is required in MEFs to reprogram to iPSCs and E-Cadherin can replace Oct4 in the Yamanaka factors to produce iPSCs. (Redmer et al., 2011).

The mean expression of Cdh1 RNA started to escalate at day 6 in both OSK and OSKB transduced MEFs, increasing to 15% and 3%, respectively (Figure 6.26B). The Cdh1

expression then increased rapidly to 100% in OSK transduced MEFs, while in OSKB transduced MEFs it only increased to 6%.

Thymocyte differentiation antigen 1 (Thy1) was first discovered as surface antigen present on T-cells (Reif and Allen, 1964). It is also expressed on the surface of cells from the mesenchymal lineage, including fibroblasts, yet it is not expressed on the surface of iPSCs (Hoppo et al., 2004, Polo et al., 2012). The group of Konrad Hochedlinger showed that MEFs that continued to expressing Thy1 after induction of reprogramming were unable to become iPSCs (Polo et al., 2012).

Thy1 expression initially decreased from 91% in MEFs to 61% and 82% in OSK and OSKB transduced MEFs, respectively, at day 3. At day 6, the expression then rose back to 83% in OSK transduced MEFs, however in OSKB transduced MEFs it continued to decrease down to 72%. The expression of Thy1 then decreased in both OSK and OSKB transduced MEFs to 70% and 52%, respectively, at day 9 (Figure 6.26C).

Ovol1 is the mammalian homolog to the *Ovo* gene in *Drosophila* (Chidambaram et al., 1997). Ovol1 expression is low in MEFs but then increases during reprogramming with peak expression at day 11 before expression drops to half of peak expression in iPSCs (O'Malley et al., 2013). This peak expression coincides with the proposed second wave of transcriptional activity during the reprogramming process (Polo et al., 2012). Expression of Ovol1 decreases histone acetylation, a histone marker of poor reprogramming prognosis (Nair et al., 2007).

Expression of Ovol1 did not increase above background levels until day 9 in OSK and OSKB transduced MEFs, at which point it increased to 100% and 8%, respectively (Figure 6.26D).

c-Myc is a well-studied oncogene and was included in the original reprogramming factors employed by Shinya Yamanaka and colleagues (Evan and Vousden, 2001, Takahashi and Yamanaka, 2006). c-Myc also plays an important role in cell cycling and proliferation.

The mean expression of c-Myc was highest in non-transduced MEFs (90%). It dropped to 55% and 67% in OSK and OSKB transduced MEFs, respectively, at day 3 (Figure 6.26E). In OSK transduced MEFs the expression dropped marginally to 50% while in OSKB transduced MEFs the expression dropped sharply to 30% at day 6. At day 9, the expression of c-Myc increased in both OSK and OSKB transduced MEFs to 71% and 41%, respectively.

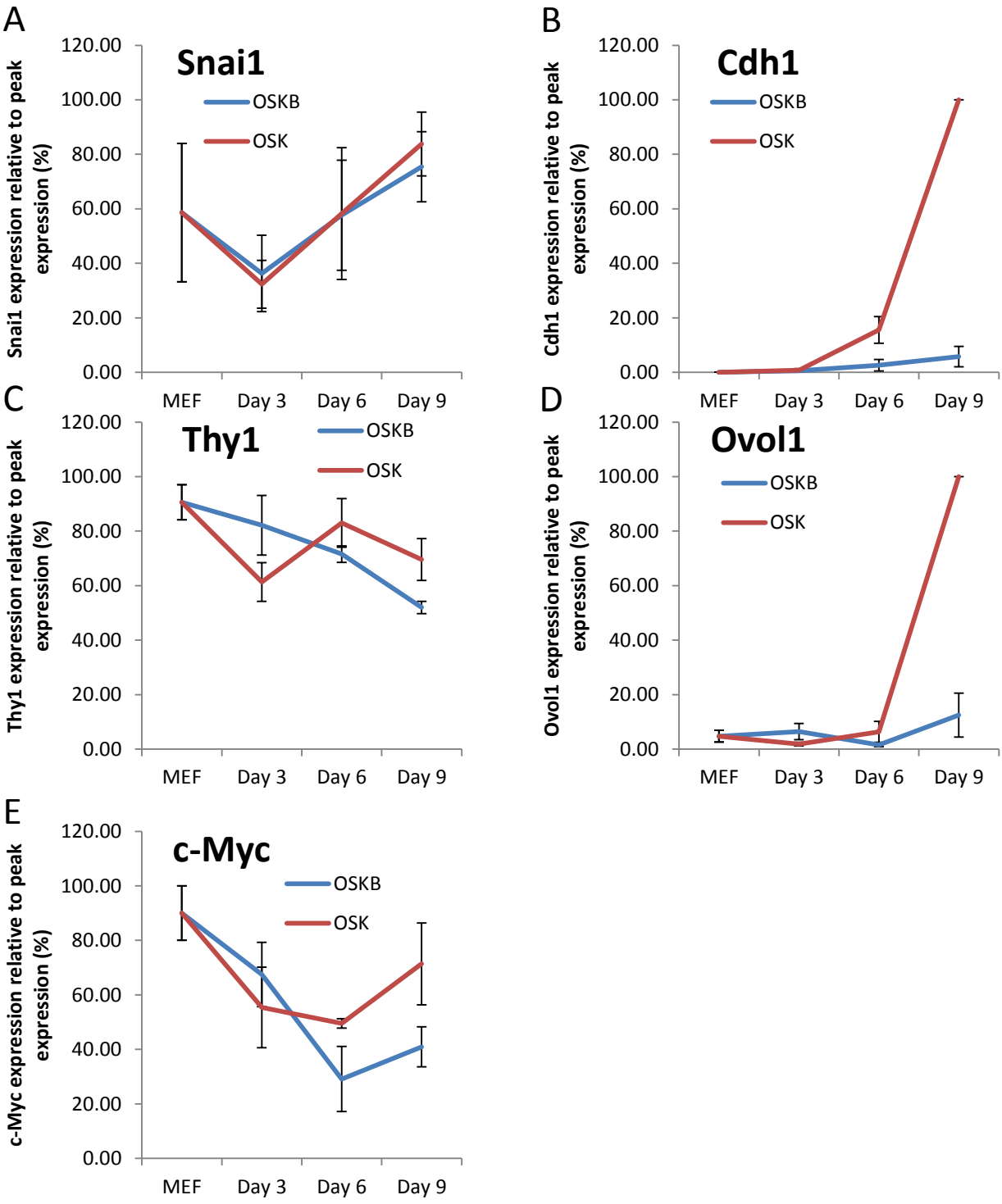


Figure 6.26: RNA expression of MET genes and c-Myc during reprogramming with MOI 2 OSKB or OSK

Wild type MEFs were reprogrammed with MOI 2 OSKB or OSK lentiviral particles. At day 3, day 6 or day 9 RNA was extracted from the MEFs, reverse transcribed to generate cDNA then expression of (A) Snai1, (B) Cdh1, (C) Thy1, (D) Ovol1 or (E) c-Myc was measured using qPCR. Expression was normalized against β_2-microglobulin housekeeping gene, and then expressed relatively to peak expression for each gene. N= 3 error bars represent standard error of the mean.

6.2.8.6 MET and proliferative gene expression at MOI 20

This analysis was repeated at a MOI 20.

Snai1 expression profile was similar to the MOI 2 experiments. Expression was 60% in non-transduced MEFs. At day 3 after transduction with OSK the Snai1 expression had dropped to 6% and 7% in OSK and OSKB transduced MEFs, respectively. The expression then rose to 25% and 34% in OSK and OSKB transduced MEFs, respectively, at day 6. The OSK transduced MEFs expression of Snai1 then rose sharply to 100% at day 9, while the OSKB transduced MEF expression rose more gradually to 50% (Figure 6.27A).

Expression of Cdh1 did not increase until day 6, as seen in the MOI 2 experiments. The expression rose to 24% in OSK transduced MEFs but only 5% in OSKB transduced MEFs, this difference was statistically significant (P=0.028 by unpaired two-tailed T-Test). Finally, the expression increased rapidly in both OSK and OSKB transduced MEFs at day 9 to 85% and 65%, respectively (Figure 6.27B). The expression of Cdh1 at this increased MOI in OSKB and OSK transduced MEFs is much closer compared to the MOI 2 experiment.

The expression of Thy1 in non-transduced MEFs was 73% (Figure 6.27C). The expression dropped to 19% and 30% in OSK and OSKB transduced MEFs, respectively, at day 3. Thy1 expression then returned to 70% and 73% in OSK and OSKB transduced MEFs, respectively, at day 6. The expression then remained almost constant with OSK transduced MEFs at 73% and OSKB transduced MEFs 62% at day 9.

The Ovol1 expression initially dropped from 5% in non-transduced MEFs to 1 and 0.5% in OSK and OSKB transduced MEFs, respectively, at day 3. The OSKB transduced MEF expression of Ovol1 then rose very slightly to 2% at day6, in contrast to the OSK

transduced MEF expression which increased to 13%. The expression of Ovol1 in OSK transduced MEFs continued to increase steadily at day 9 to 43%, while the OSKB transduced MEFs expression increased more dramatically to 100% (Figure 6.27D).

The expression of c-Myc started at 79% in non-transduced MEFs. c-Myc expression in OSK and OSKB transduced MEFs dropped at day 3 to 38% and 34%, respectively. The expression then increased in both OSK and OSKB transduced MEFs to 71% and 52%, respectively, at day 6. Finally, at day 9 the expression of c-Myc dropped in both OSK and OSKB transduced MEFs to 49% and 33%, respectively (Figure 6.27E).

Overall the results from the MOI 20 experiment show that the expression levels of the genes in the OSKB transduced MEFs are more similar to the expression observed in OSK transduced MEFs, which matches the colony counting experiments as the reprogramming does occur at this MOI, albeit at lower efficiency.

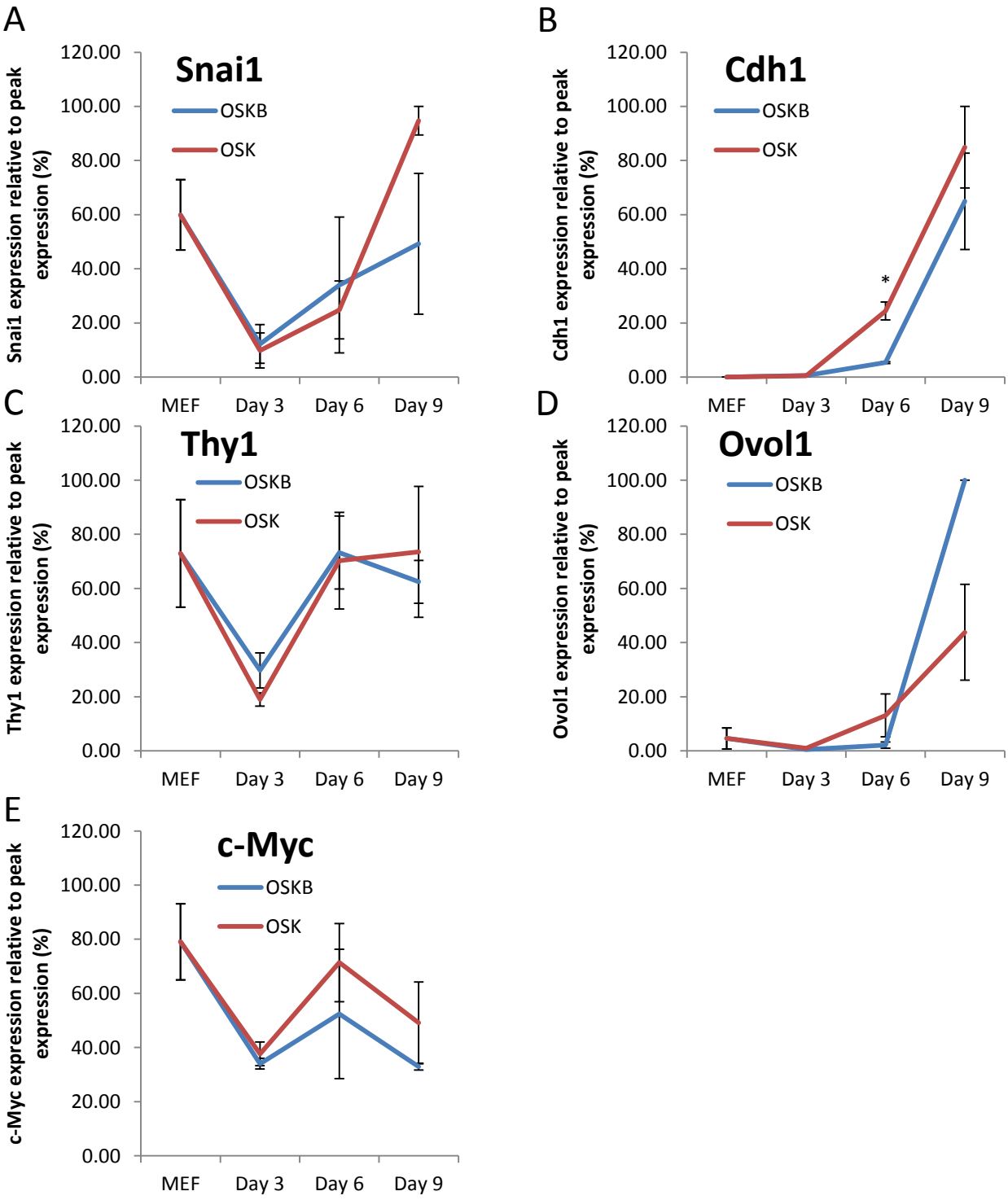


Figure 6.27: RNA expression of MET genes and c-Myc during reprogramming with MOI 20 OSKB or OSK

Wild type MEFs were reprogrammed with MOI 20 OSKB or OSK lentiviral particles. At day 3, day 6 or day 9 RNA was extracted from the MEFs, reverse transcribed to generate cDNA then expression of (A) Snai1, (B) Cdh1, (C) Thy1, (D) Ovol1 or (E) c-Myc was measured using qPCR. Expression was normalized against β_2-microglobulin housekeeping gene, and then expressed relatively to peak expression for each gene. N= 3 error bars represent standard error of the mean.

6.2.9 Do OSKB reprogrammed iPSCs have lower DNA damage?

I have seen that overexpression of B-Myb is detrimental for reprogramming. It could be possible that this effect is a reflection of B-Myb's role in safe guarding genome integrity. Thus, OSKB could lead to better iPSCs (based on GFP and morphology) but with lower efficiency because iPSCs with high DNA damage are being eliminated. Thus, I decided to test if iPSCs generated by transducing MEFs with OSKB had lower DNA damage.

iPSCs were generated using OSKM, OSK or OSKB lentiviral particles, individual iPSC colonies were isolated and expanded to generate iPSC lines. At passage 2, these iPSC lines were stained for γ-H2AX and analysed by flow cytometry. Preliminary results in Figure 6.28A show that there was a lower amount of γ-H2AX in the two iPSC lines generated with OSKB compared to the two lines generated with OSKM. However the preliminary results in Figure 6.28B show that the amount of γ-H2AX in the OSKB and OSK derived iPSC lines were very similar. These experiments need to be repeated with a greater number of individual colonies to gain further insight into the γ-H2AX. It would also be useful to analyse γ-H2AX foci by confocal microscopy to determine the size of the foci as that data is lost in flow cytometric analysis.

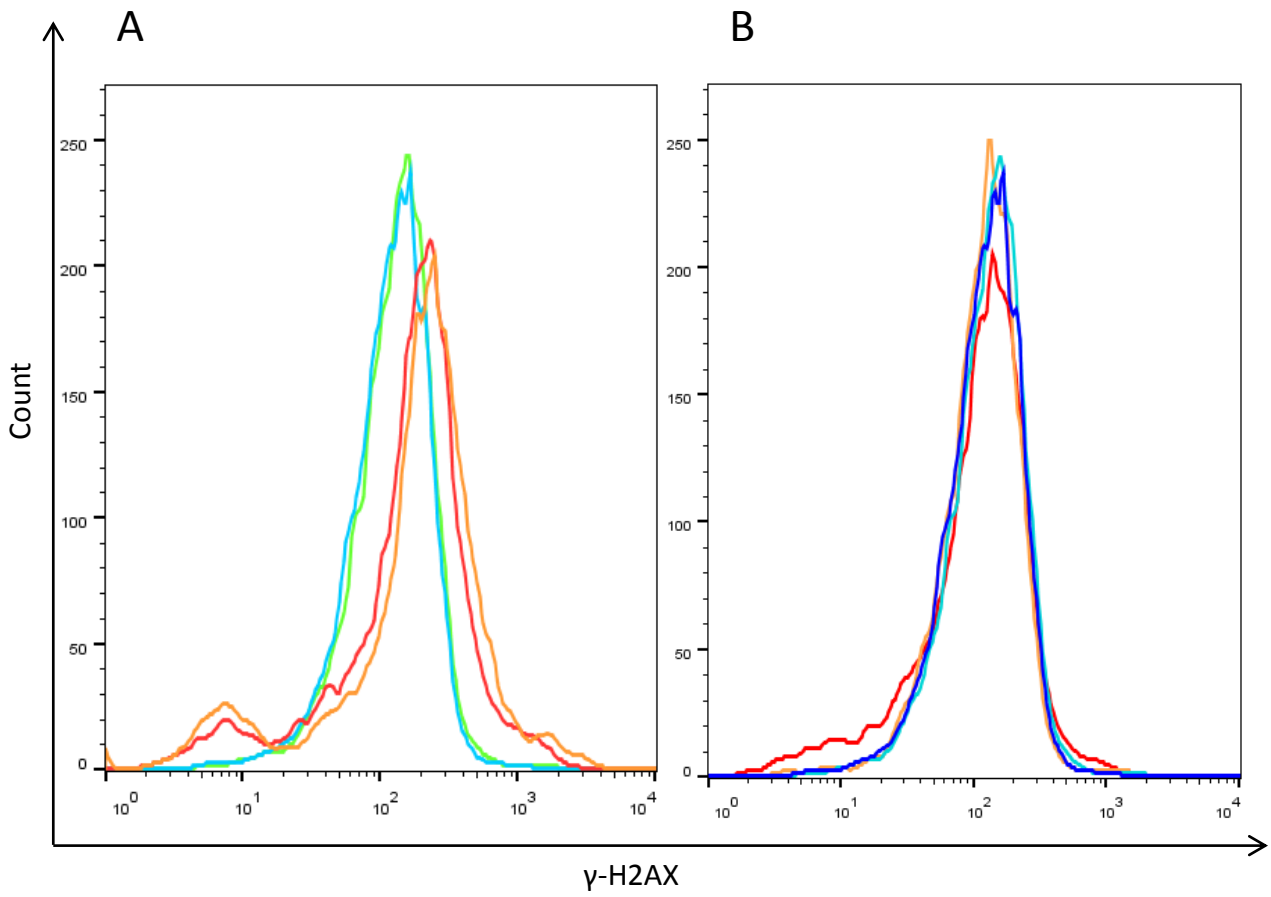


Figure 6.28: γ-H2AX in early passage iPSCs
Early passage iPSCs derived using OSKM, OSK or OSK lentiviral particles were stained with anti-γ-H2AX-FITC antibody then analysed by flow cytometry. Cells were gated based on size and granularity to exclude debris and then gated for singlets before analysing γ-H2AX counts.(A) OSKB iPSC line 1 (Blue), OSKB iPSC line 2 (Green), OSKM iPSC line 1 (Red), OSKM line 2 (Orange).(B) OSKB iPSC line 1 (Blue), OSKB iPSC line 2 (Teal), OSK iPSC line 1 (Red), OSK iPSC line 2 (Orange)

6.3 DISCUSSION

In this chapter, I aimed to determine whether B-Myb overexpression would lead to an increase in reprogramming efficiency using multiple methods of B-Myb overexpression.

Co-transduction of B-*myb* and OSKM or OSK lentiviral particles leads to a lower efficiency of reprogramming compared to OSKM or OSK alone; however, the alkaline phosphatase staining was identical and the colonies were morphologically similar. To control for the fact that the cells were being transduced with two viruses instead of one, the experiment was repeated including the control *Zs-Green* virus in the OSKM. Co-transduction may have caused the lower efficiency but the results of the second experiment show that the OSKM + B-*myb* transduced cells still had a lower reprogramming efficiency than the OSKM + *Zs-Green* transduced cells.

To confirm that the results with co-transduction were not an artefact of the multiple lentiviral transductions (Walker et al., 1996), the OSK backbone was re-engineered to contain the B-*myb* gene in place of the mCherry fluorophore. With this new OSKB vector I could be certain that B-Myb is being overexpressed in each transduced cell along with the reprogramming factors. This is an improvement over the co-transduction as it was not possible to determine which MEFs had been transduced with both the lentiviral particles or if the iPSCs generated contained both viruses. Only the OSK genes were included due to the size constraints of the lentiviral delivery system, as the originally theorised OSKMB backbone would be too large and the lentiviral particles would not have packaged correctly.

At a low MOI the OSKB failed to reprogram MEFs to iPSCs, but it was possible to reprogram with the OSKB vector at 10 times the original MOI. The reprogramming

efficiency of the OSKM and OSK vectors was higher at every MOI tested. One possibility is that the titration of the virus was wrong. To overcome this possibility lentiviral particles were titrated through qPCR as the OSKB vector contained no reporter gene. At this point the OSKM and OSK were routinely titrated with qPCR too, to ensure that identical numbers of lentiviral particles were used in each comparison experiment. This result confirms that B-Myb is detrimental for reprogramming.

6.3.1 Role of B-Myb in cell cycle arrest

Due to B-Myb's role in the cell cycle (Santilli et al., 2005), and evidence that changes in B-Myb expression can affect senescence (Johung et al., 2007), the senescence of MEFs during reprogramming was analysed by β-galactosidase staining and by analysis of expression of factors involved in senescence. This would be a plausible explanation as reprogramming has been shown to activate p53, which is detrimental to reprogramming. Both analyses revealed that the OSKB vector was not responsible for an increase in cell cycle arrest compared to OSKM or OSK reprogramming MEFs. To gain further insight into whether the cells are cycling at the same rates BrdU incorporation assays would be carried out as part of future work.

6.3.2 The OSKB vector is not inducing additional apoptosis

Apoptosis was also analysed in the MEFs during reprogramming. The levels of apoptosis in the OSKB reprogramming MEFs were no higher than OSKM or OSK reprogramming MEFs. Thus, I ruled out the possibility that the transduction with OSKB was leading to apoptosis in the MEFs.

6.3.3 OSKB vector is detrimental to kinetics of reprogramming

I also employed surface antigen expression as a marker of reprogramming progress detailed in a recent report (O'Malley et al., 2013). The number of MEFs which reach the final stages of reprogramming based on their CD44 and CD54 expression is significantly lower when reprogramming with OSKB compared to OSKM or OSK. This analysis also revealed that the number of MEFs which reach the pre-iPSC stage of reprogramming is significantly lower when reprogramming with OSKB compared to OSKM or OSK, indicating that correct levels of B-Myb are required at the early stage of the reprogramming process. One possibility is that a there is problem with viral particle concentration or the infectivity of the OSKB particles is lower than OSK and OSKM. This possibility was addressed and is presented in the following chapter using a secondary reprogramming system.

6.3.4 OSKB reprogrammed MEFs fail to activate pluripotency genes at low MOI

The RNA expression analysis of the MEFs undergoing reprogramming shows that the early and late pluripotency genes are not being expressed when using the OSKB lentiviral particles at MOI 2. However, when the number of viral particles is increased by 10 fold, the expression of the early and late pluripotency markers is recovered, with similar kinetics as described when reprogramming with OSK lentiviral particles. However the OSK reprogrammed MEFs have higher expression of most of the early and late pluripotency genes analysed.

The MET gene expression data also showed more similar trends when comparing OSK and OSKB reprogramming at MOI 20. Indicating that increased expression of Oct4, Sox2

and Klf4 may be able to overcome the blockage in reprogramming caused by B-Myb overexpression.

The limitation of this study was that RNA was extracted from the total population of MEFs including MEFs that were not undergoing reprogramming. For example, it has been reported that Thy1 expression decreases during reprogramming (Polo et al., 2012, O'Malley et al., 2013), however I observed a drop in expression and then a return to non-transduced MEF level, possibly due to the expression of Thy1 in the many MEFs that were not undergoing reprogramming.

It would be useful to use a secondary reprogramming system in which there is a reporter gene for the expression of the Yamanaka factors. This would allow me to FACS sort only MEFs which were undergoing reprogramming at multiple time points during the reprogramming. This selection would lower the background expression from non-reprogramming MEFs.

B-Myb has been shown to be important in cell cycle regulation (Lam et al., 1992, Lam and Watson, 1993, Tanaka et al., 1999) and the reprogramming process is sensitive to the cell cycle (Hanna et al., 2009). Therefore, the additional B-Myb could be altering the cell cycle of the cells to a point in which they are not able to reprogram. Over-expression of B-Myb in ESCs leads to an increase in the production of Oct4 and Sox2 proteins (Tarasov et al., 2008) and increasing the levels of Sox2 in the reprogramming cocktail has been shown to lower the efficiency of reprogramming (Yamaguchi et al., 2011). The comparative levels of each of the reprogramming factors are important in generation of hiPSCs (Papapetrou et al., 2009). It is possible that B-Myb over expression could have a negative effect on reprogramming by up regulating the levels of Sox2.

CHAPTER 7: DOES B-MYB OVEREXPRESSION AFFECT SECONDARY REPROGRAMMING?

7.1 INTRODUCTION

Secondary reprogramming offers a powerful system for studying the effect of additional factors during reprogramming. The four reprogramming genes are incorporated into the genome of the mouse cells under drug inducible promoters, ensuring high efficiency of reprogramming (Wernig et al., 2008). The secondary reprogramming MEF system was kindly provided by our collaborator Keisuke Kaji, University of Edinburgh. Dr Kaji engineered secondary reprogramming MEFs with a doxycycline inducible promoter controlling the expression of OSKM. The construct also contains a *mOrange* reporter gene to enable flow cytometric analysis of only MEFs which have activated the reprogramming genes. Due to the high reprogramming efficiency and the ability to gate only cells that are actively producing the reprogramming factors, it is easier to detect changes in the reprogramming process. This is an ideal system to examine the effect of overexpression of B-Myb during reprogramming.

7.2 RESULTS

7.2.1 Generating a lentiviral backbone with a gateway destination cassette

Lentiviral transduction is a powerful tool for gene expression and knockdown. I decided to modify the ZsGreen lentiviral backbone to include a Gateway acceptor (GW) sequence which would facilitate swapping the gene of interest in the lentiviral backbone through a simple *in vitro* reaction (Hartley et al., 2000).

In order to do so, a GW sequence was cloned into the pHAGE-EF1a lentiviral backbone to enable simple *in vitro* transfer of genes from entry vectors. The strategy used is summarised as a schematic in Figure 7.1.

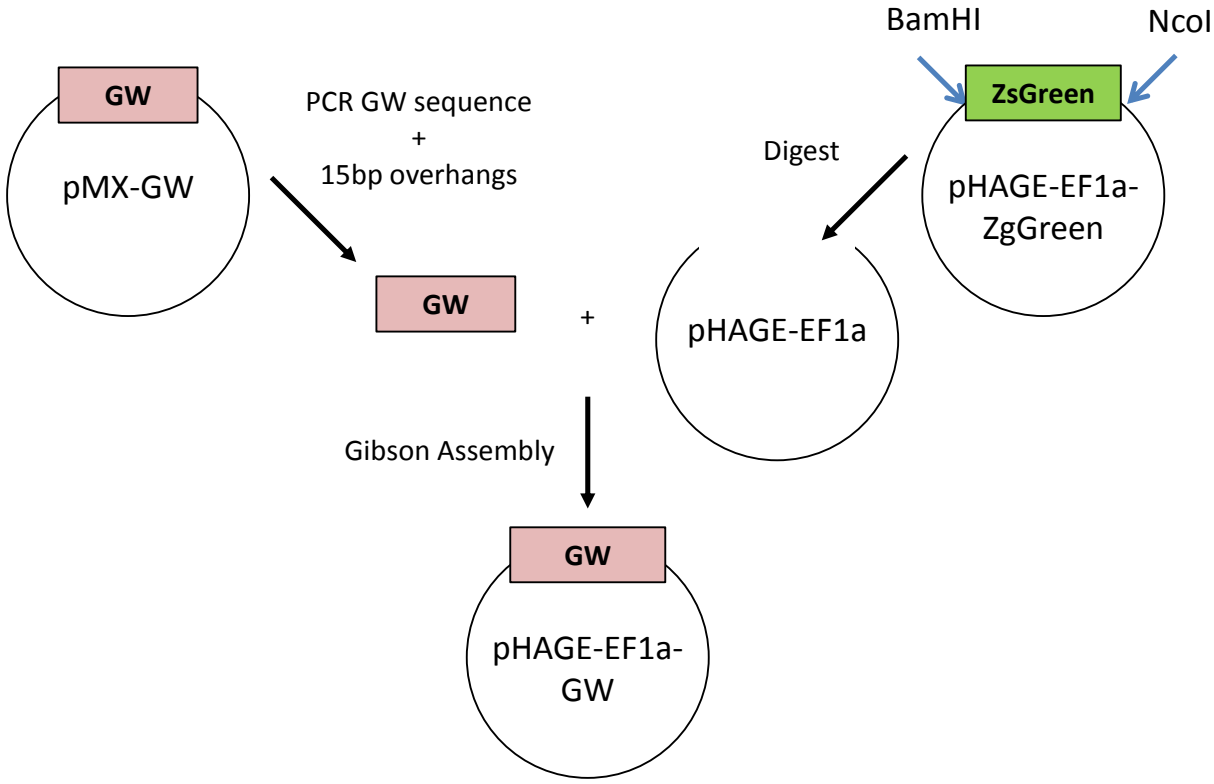


Figure 7.1: Generation of the lentiviral backbone with a Gateway® acceptor site
The Gateway® acceptor site was cloned from the pMX-GW retroviral backbone with primers that added 15 base overhangs corresponding to the regions flanking the ZsGreen gene in the pHAGE-EF1a-ZsGreen plasmid sequence. This PCR product was purified and cloned into linearised pHAGE-EF1a using Gibson Assembly®.

The gateway acceptor site sequence was cloned from pMX-GW retroviral plasmid with primers that contained 15bp overhangs that match the 15bp flanking the *ZsGreen* gene in pHAGE-EF1a-ZsGreen. The results of the PCR reaction can be seen in Figure 7.2A (lane1-4). The 1.7k amplicon was obtained in all four PCR reactions; the DNA was extracted and purified. Meanwhile the pHAGE-EF1a-ZsGreen plasmid was digested with BamHI and NcoI restriction endonucleases to remove the *ZsGreen* gene. Figure 7.2A shows in lane 6 the expected 9kb linearised pHAGE-EF1a plasmid that was extracted and purified. Due to two BamHI sites located within the GW sequence Gibson Assembly® was used to assemble the final construct (Gibson et al., 2009). Briefly a 5' exonuclease creates an overhang on each of the DNA fragments allowing the complementary sequence added to the GW sequence to anneal to a pHAGE-EF1a linearised plasmid when incubated with DNA polymerase and DNA ligase. The assembled plasmid was transformed into E.coli and single colonies were isolated and expanded to yield plasmid DNA. Extracted plasmid DNA was digested with EcoRI restriction endonuclease to determine if the assemble had succeeded. Figure 7.2B lane 1 shows that the assembly was successful as the expected digestion pattern was 6851bp and 1829bp DNA fragments. The inserted region of the plasmid was checked for mutations by Sanger sequencing, one mutation was found but it was in a non-coding region of the plasmid.

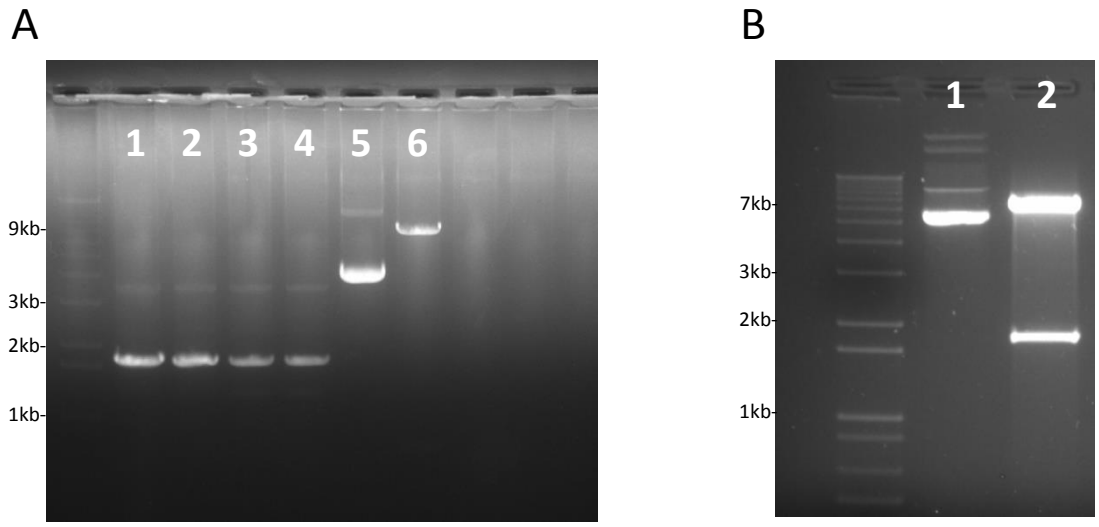


Figure 7.2: Cloning the Gateway® acceptor site, removing *ZsGreen* gene and assembling construct
The Gateway® acceptor site (GW) was cloned from the pMX-GW retroviral backbone with primers that added 15 base overhangs corresponding to the regions flanking the *ZsGreen* gene in the pHAGE-EF1a-ZsGreen plasmid sequence. (A) Lane 1-4 individual PCR reactions to clone GW sequence. The size of the site is 1.7kb. Lane 5 non-digested pHAGE-EF1a-ZsGreen plasmid, Lane 6 pHAGE-EF1a-ZsGreen plasmid digested with BamHI and NcoI, the linearised pHAGE-EF1a is 9kb.(B) The GW sequence was cloned into the linearised pHAGE-EF1a plasmid using Gibson Assembly, then transformed into E.coli to propagate. DNA extracted from E.coli was digested with EcoRI to determine if the cloning had succeeded, the expected fragments were 6851 and 1829bp. Lane 1 undigested extracted plasmid DNA, lane 2 EcoRI digested plasmid DNA. The relevant molecular weights are indicated on the left.

7.2.2 Generating B-Myb-AmCyan lentiviral backbone

The B-*myb* gene was cloned from plasmid DNA using primers designed to add a 5' BamHI restriction enzyme site and a self-cleaving peptide gene, *P2A* on the 3' end of the gene. A *P2A* gene was selected due to it having more efficient cleavage than the other *2A* peptide genes (Kim et al., 2011). The *AmCyan* gene was cloned from plasmid DNA with primers designed to add a *P2A* gene on the 5' end of the gene and an EagI restriction enzyme site on the 3' end. Figure 7.3A shows the PCR products *AmCyan* (750bp) and B-*myb* (2.2kb) separated by electrophoresis. The two products were then combined by a second round of PCR to create a 2.9kb B-*myb-P2A-AmCyan* fusion gene (Figure 7.3B).

The PCR product was purified and A-tailed using Taq polymerase before being ligated into TOPO expression vector. Plasmid DNA was expanded in E.coli and the plasmid was confirmed by restriction digest. Figure 7.3C shows confirmation of successful ligation of the fusion gene into the TOPO vector as digestion with PstI was expected to yield 1.2kb, 1.8kb and 3.8kb fragments that were seen in DNA extracted from colony 1 (red box).

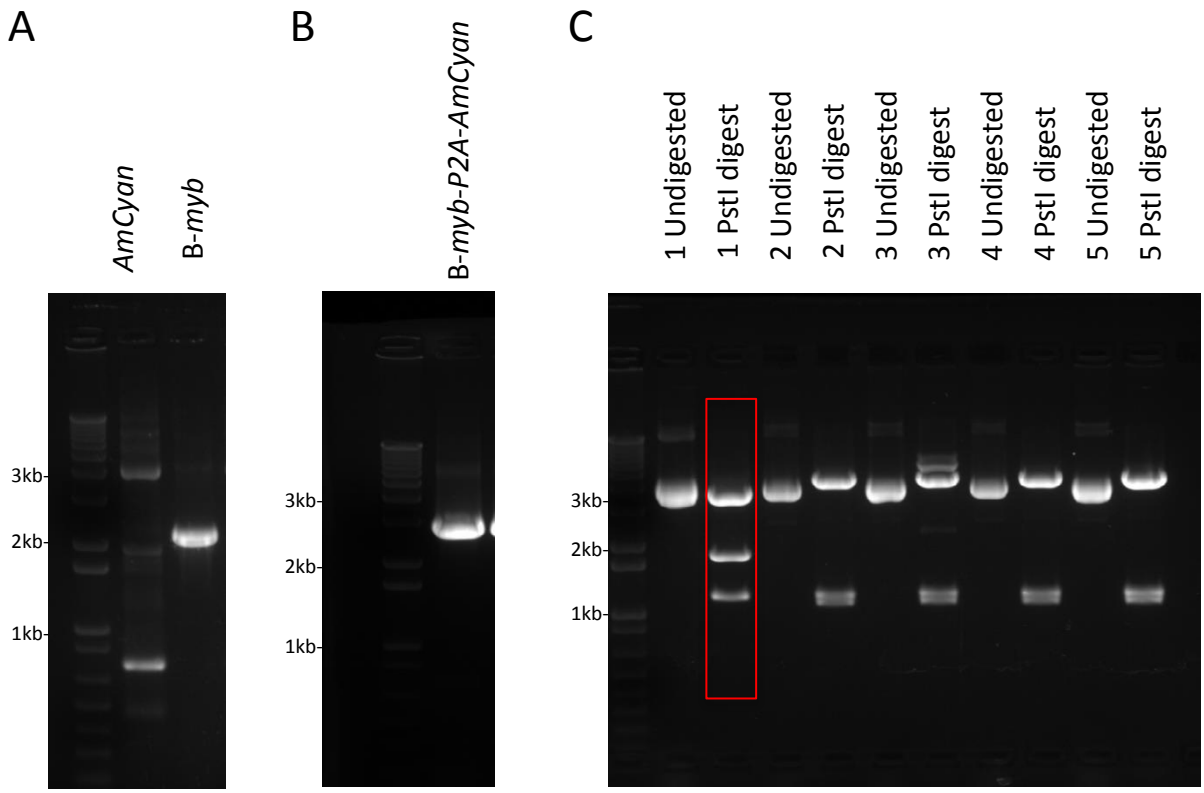


Figure 7.3: **Generation of the B-*myb-P2A-AmCyan* fusion gene**
(A) *AmCyan* and B-*myb* genes were amplified from separate plasmids by PCR. PCR products were separated by agarose gel electrophoresis. The fragments seen at 750bp and 2.2kb correspond to *AmCyan* and B-*myb* respectively. (B) The single fragment at 2.9kb corresponds to the successfully generated B-*myb-P2A-AmCyan* fragment. (C) Agarose gel showing undigested and PstI digested plasmid DNA from 5 different E.coli colonies. Colony 1 (red box) digested with PstI gave three fragments (1.2kb, 1.8kb and 3.8kb) corresponding to the B-*myb-P2A-AmCyan* fragment being correctly ligated into the TOPO vector.

Using the engineered restriction sites, the B-*myb-P2A-AmCyan* fragment was cut from the TOPO vector and ligated into the corresponding sites on the pENTR plasmid to

generate pENTR-B-*myb-P2A-AmCyan* plasmid. This plasmid was checked by restriction digestion using PstI restriction endonuclease which was expected to yield 1.9 and 3.2kb fragments as shown in Figure 7.4A (colonies 1, 2 and 3). The insert was also sequenced to check for DNA mutations during PCR errors. No mutations were detected by Sanger sequencing. The entry vector was then used to shuttle the B-*myb-P2A-AmCyan* fragment into the pHAGE-EF1a-GW destination vector to generate pHAGE-EF1a-B-*myb-P2A-AmCyan*. This vector was checked by restriction endonuclease digestion using SmaI and ClaI with an expected digestion pattern of 8467bp and 1450bp fragments in the correctly oriented insert in the pHAGE-EF1a vector. Figure 7.5 lane 4 shows that the plasmid was successfully generated as it contains the expected fragments after digestion.

pHAGE-EF1a-*AmCyan* was also generated to use as a control vector by cutting *AmCyan* from p*AmCyan* using BamHI and NotI and ligated into the corresponding sites of the pENTR vector. This vector was checked by restriction digestion with ClaI and PstI, where the expected digestion pattern for the correctly oriented insert ligated into the pENTR vector was 2382bp and 611bp fragments as shown in Figure 7.4B (colonies 1-4). The *AmCyan* was then shuttled into the pHAGE-EF1a-GW vector to generate pHAGE-EF1a-*AmCyan*. This vector was digested with SmaI to determine if the insert had been successfully recombined into the final vector in the correct orientation as the expected digestion pattern was 6107bp and 1682bp fragments. Figure 7.5 lane 2 shows the expected digestion pattern and therefore confirms that the final plasmid was successfully generated.

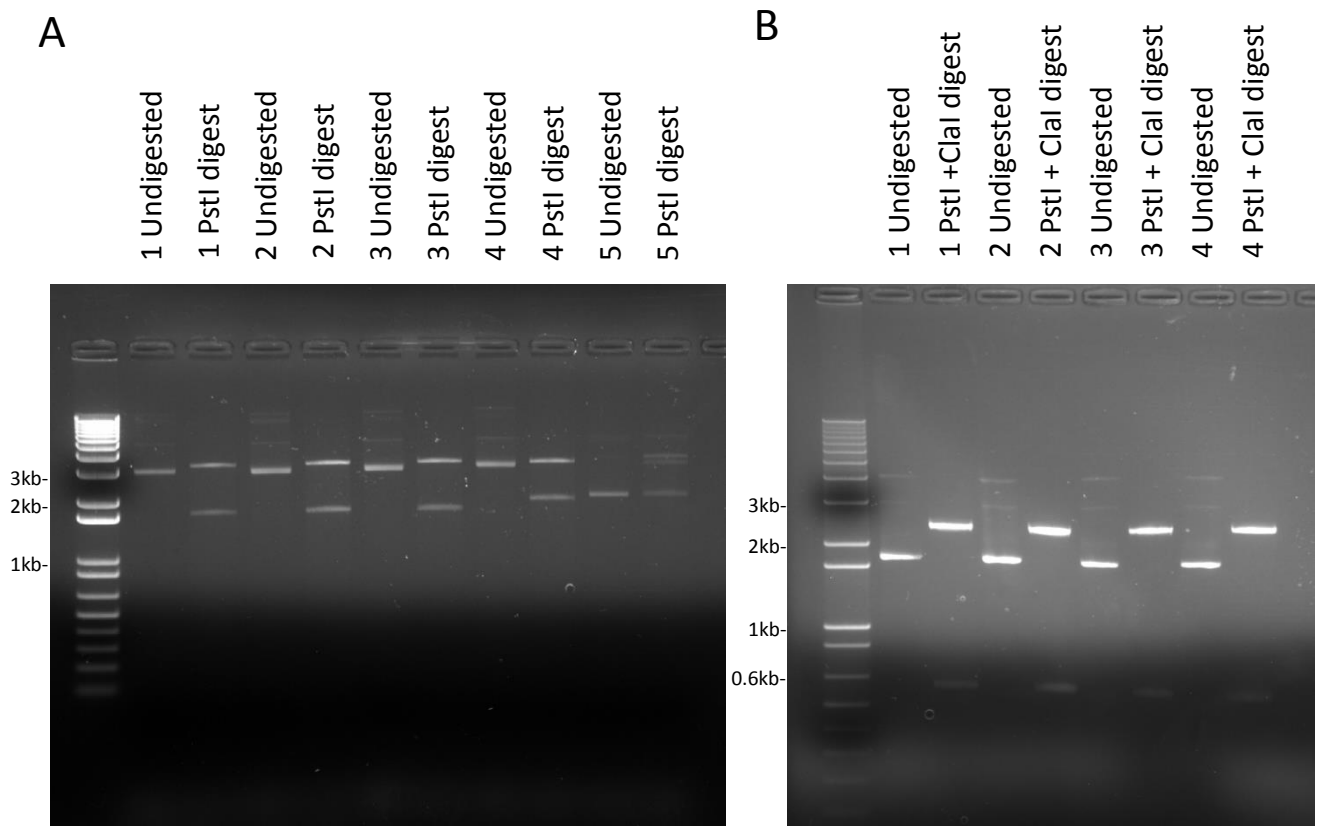


Figure 7.4: Confirmation of ligation into entry plasmids
(A)The B-*myb-P2A-AmCyan* fusion gene was ligated into the pENTR vector and propagated in E.coli, individual colonies were isolated and plasmid DNA was extracted. The extracted DNA was digested with PstI restriction endonuclease. The expected digestion fragments for the correctly oriented ligated insert were 3.2kb and 1.9kb. Colonies 1, 2 and 3 contain the ligation in the correct orientation. (B) The AmCyan fluorescent protein gene was ligated into the pENTR vector, then propagated in E.coli, individual colonies were isolated and plasmid DNA was extracted. The extracted DNA was digested with PstI and ClaI. The expected digestion fragments for the correctly orientated AmCyan gene in the pENTR vector were 2382bp and 611bp. All four colonies contain the correct plasmid.

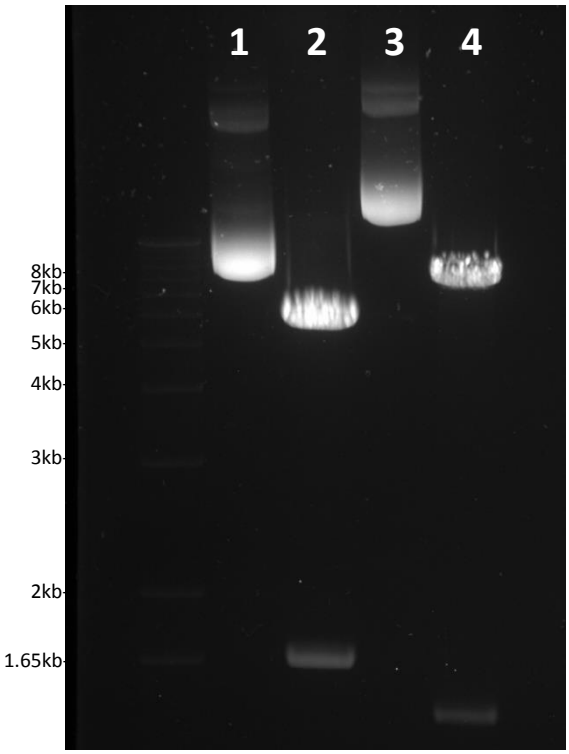


Figure 7.5: Confirmation of recombination into pHAGE-EF1a destination plasmids

The *AmCyan* gene or the B-*myb-P2A-AmCyan* fusion gene was shuttled from pENTR vectors into pHAGE-EF1a-GW using LR clonase enzyme. The recombined DNA was transformed into E.coli and individual colonies were isolated and expanded. DNA was extracted from bacterial cultures and then digested with SmaI (pHAGE-EF1a-*AmCyan,* Lane 2) or SmaI + ClaI (pHAGE-EF1a-B-*myb-P2A-AmCyan*, Lane 4) and then separated by electrophoresis compared to non-digested control DNA (Lane 1 and 3). The expected fragments for lane 2 were 6107bp and 1682bp, and lane 4 were 8497bp and 1450bp.

To confirm that the subcloning of B-*myb* in this vector was successful and that B-Myb could be overexpressed, I transfected 293T cells with the vector and after 48 hours extracted total protein from the 293T cells. The total protein was separated by SDS-PAGE and transferred to PVDF membranes to perform western blots. As shown in Figure 7.6 the expression of the B-Myb protein could be detected.

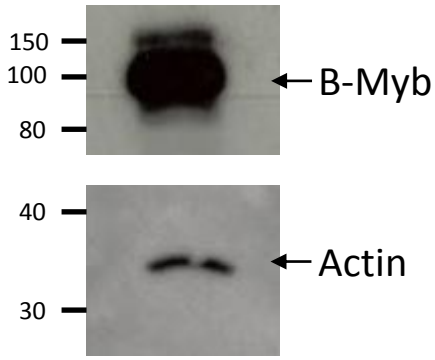


Figure 7.6: Confirmation of B-Myb expression
293T cells were transfected with the pHAGE-EF1a-B-*myb-P2A-AmCyan* lentiviral backbone, sorted by FACS based on AmCyan expression. Protein was extracted from AmCyan positive 293T cells and 50µg of protein was separated by SDS-PAGE. Protein expression was detected by western blotting with antibodies against B-Myb or Actin. The position of relevant molecular weight standards is shown on the left side of the blot, and arrows on the right indicate the specific bands for each antibody.

7.2.3 B-Myb overexpression lowers secondary reprogramming efficiency

Secondary reprogramming (MKOS) MEFs express the OSKM reprogramming factors endogenously under the control of the inducible TetO doxycycline promoter. They have been engineered to contain a *mOrange* reporter gene downstream of the reprogramming factors to identify cells which are expressing the reprogramming factors. These secondary reprogramming MEFs were kindly provided by our collaborator Keisuke Kaji, University of Edinburgh. MKOS MEFs were mixed with wild type MEFs at a ratio of 1:9, and then transduced at MOI 10 with lentiviral particles encoding B-*myb-AmCyan* or *AmCyan*. Secondary reprogramming was initiated by addition of doxycycline and reprogramming was tracked by flow cytometry using CD44 and CD54 antigen expression. Gating strategy was as follows: first live cells were gated based on their FSC/SSC profile (Figure 7.7A), next cells were gated based on positive mOrange expression compared to untreated MEFs (Figure 7.7B), then cells were gated based on positive AmCyan expression compared to non-transduced MEFs (Figure 7.7C), and finally, the expression of CD44 and CD54 was analysed (Figure 7.7D).

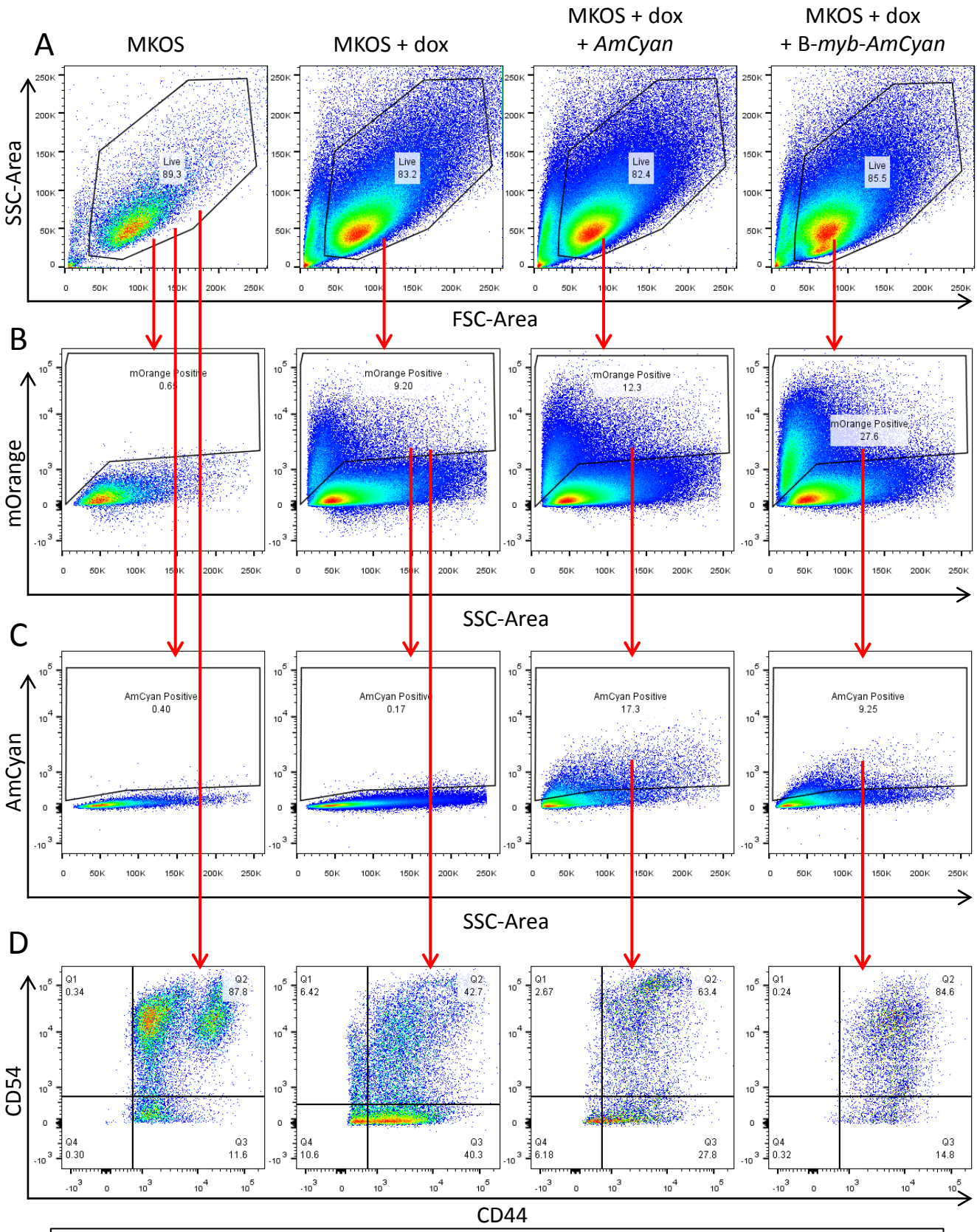


Figure 7.7: Gating strategy used to track secondary reprogramming
Cells were gated based on size and granularity to exclude debris (A), then gated for mOrange expression (B), then AmCyan expression (C) and finally shown as a dot plot representing CD44 and CD54 expression (D).

Figure 7.8 shows that the mean percentage of fully reprogrammed iPSCs (Q1, CD54+, CD44-) at day 9 was similar (10% and 8%) in non-transduced MKOS MEFs and MKOS MEFs transduced with *AmCyan* lentivirus. This was in clear contrast to MKOS MEFs transduced with B-*myb*-*AmCyan* lentivirus which did not reprogram at all (0.3% in Q1, identical to non-transduced MEFs). At day 12, the mean percentage of fully reprogrammed iPSCs was 6% and 9% in non-transduced MKOS MEFs and MKOS MEFs transduced with *AmCyan* lentivirus, respectively. There was a slight increase in reprogramming in MKOS MEFs transduced with B-*myb*-*AmCyan* lentivirus. At day 16, the mean percentage of fully reprogrammed iPSCs was the same for non-transduced MKOS MEFs and MKOS MEFs transduced with *AmCyan* lentivirus (9%). MKOS MEFs transduced with B-*myb*-*AmCyan* lentivirus did not show any reprogramming (0.6%).

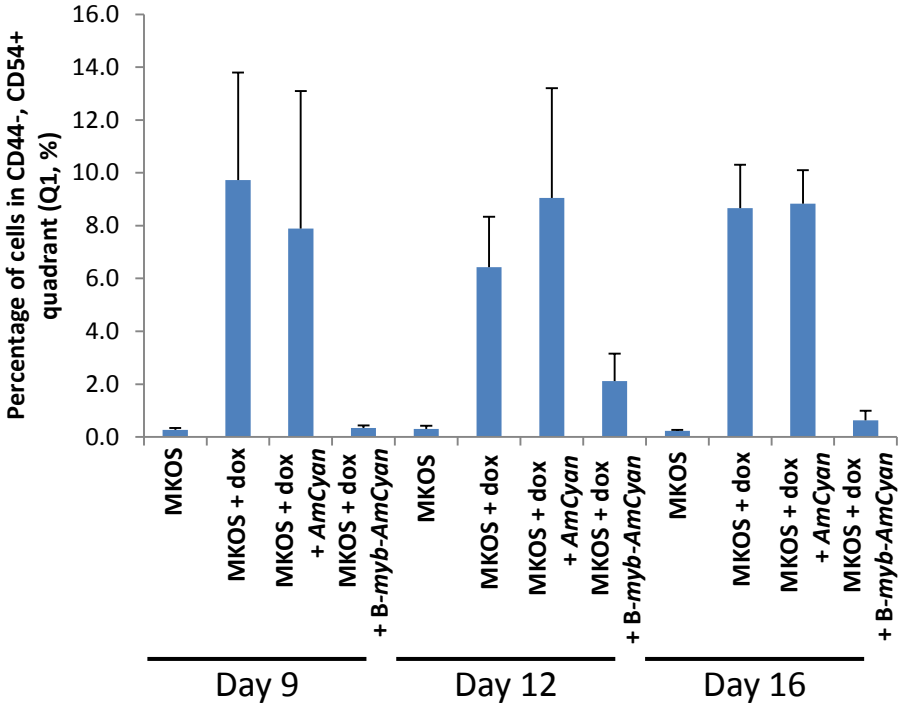


Figure 7.8: Fully reprogramed (CD54+,CD44-) iPSC quantification for MKOS MEFs transduced with B-*myb-AmCyan* or *AmCyan*

MKOS MEFs mixed with WT MEFs (1:9) were transduced with B-*myb-AmCyan* or *AmCyan* lentiviral particles at MOI 10. CD44 negative and CD54 positive expression was quantified for the live population (MKOS), which are mOrange positive (MKOS + dox) and mOrange/AmCyan double positive (*AmCyan* and B-*myb*-AmCyan) N=2

Figure 7.9 shows that the mean percentage of pre-iPSCs (Q4, CD54-, CD44-), at day 9, was 13% and 7% in non-transduced MKOS MEFs and MKOS MEFs transduced with *AmCyan* lentivirus, while MKOS MEFs transduced with B-*myb-AmCyan* lentivirus had not been able to progress to this stage (0.8%). At day 12, the mean percentage of pre-iPSCs was 6%, 1% and 1% in non-transduced MKOS, MKOS MEFs transduced with *AmCyan* lentivirus and MKOS MEFs transduced with B-*myb-AmCyan* lentivirus, respectively. Finally, at day 16, the mean percentage of pre-iPSCs was 3%, 2% and 0.3% in non-transduced MKOS, MKOS MEFs transduced with *AmCyan* lentivirus and MKOS MEFs transduced with B-*myb-AmCyan* lentivirus, respectively. The percentage of cells in the non-transduced MKOS and MKOS transduced with *AmCyan* is lower at this time point as

most of the cells are fully reprogrammed. In the case of the MKOS MEFs transduced with B-*myb-AmCyan* lentivirus the low percentage of cells at this stage is due to a block in reprogramming.

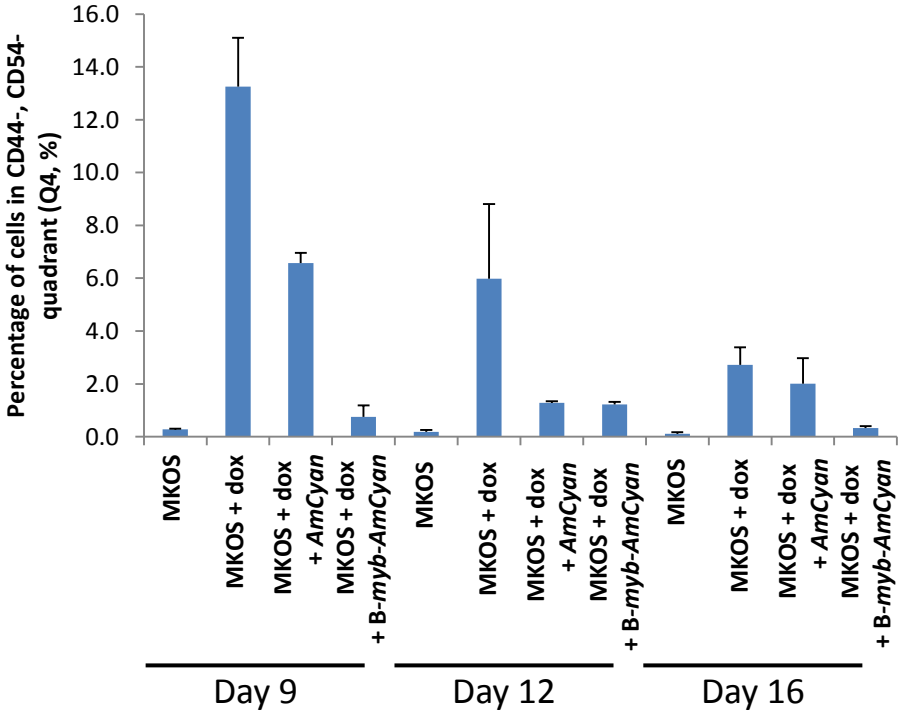


Figure 7.9: Partially reprogramed (CD54-, CD44-) iPSC quantification for MKOS MEFs transduced with B-*myb* or *AmCyan*
MKOS MEFs mixed with WT MEFs (1:9) were transduced with B-*myb-AmCyan* or *AmCyan* lentiviral particles at MOI 10. CD44 negative and CD54 negative expression was quantified for the live population (MKOS), which are mOrange positive (MKOS + dox) and mOrange/AmCyan double positive (*AmCyan* and B-*myb*-AmCyan) N=2

7.2.4 Reduced efficiency of secondary reprogramming is not due to senescence in the MEFs

To determine if the block in reprogramming observed when over expressing B-Myb in the secondary reprogramming system was due to the cells becoming arrested in the cell cycle, I decided to stain reprogramming MEFs for β-galactosidase activity and measure expression of cell cycle arrest associated factors p21, p16 and p53. MKOS MEFs were mixed with wild-type MEFs are a ratio of 1:9, plated, and then transduced with MOI 10

AmCyan or B-*myb-AmCyan* lentiviral particles. Doxycycline was added to the MEFs to initiate reprogramming, and 3 days later the MEFs were fixed, permeabilised and stained for β-galactosidase activity. Figure 7.10 shows that the levels of β-galactosidase are not increased when the MEFs are transduced with either of the lentiviral constructs.

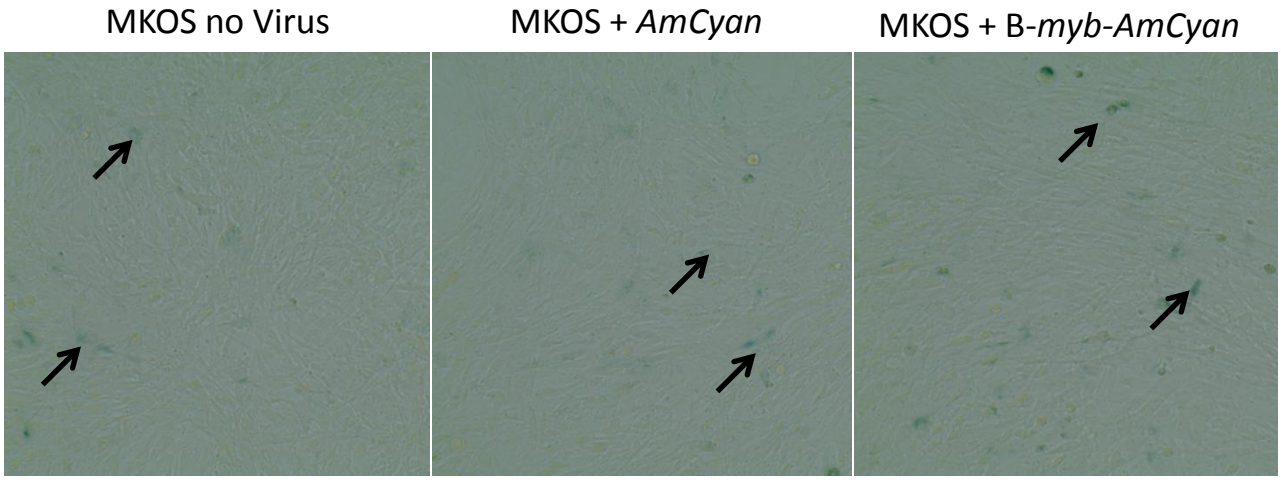


Figure 7.10: β-galactosidase staining in the MKOS MEFs
MKOS MEFs mixed with WT MEFs (1:9) were transduced with *AmCyan* or B-*myb-AmCyan* lentiviral particles at MOI 10. The following day doxycycline was added to initiate reprogramming. After 3 days the cells were fixed and stained for β-galactosidase activity, a marker of senescent cells. Representative image from 20x magnification inverted bright field microscope. Positively stained cells highlighted by black arrows. N=2

Due to difficulty quantifying the β-galactosidase staining and because it is considered a late marker of senescence (Lee et al., 2006), RNA was also extracted from the same MEFs at day 3 to analyse expression of quiescence/senescence related factors p21, p16 and p53.

Figure 7.11 shows that the mean expression of p21 did not increase in MKOS MEFs transduced with either B-*myb-AmCyan* or *AmCyan*. On the contrary, p21 expression decreased in the *AmCyan* transduced MEFs to 79% and to 70% in the B-*myb-AmCyan* transduced MEFs when compared to non-transduced MEFs.

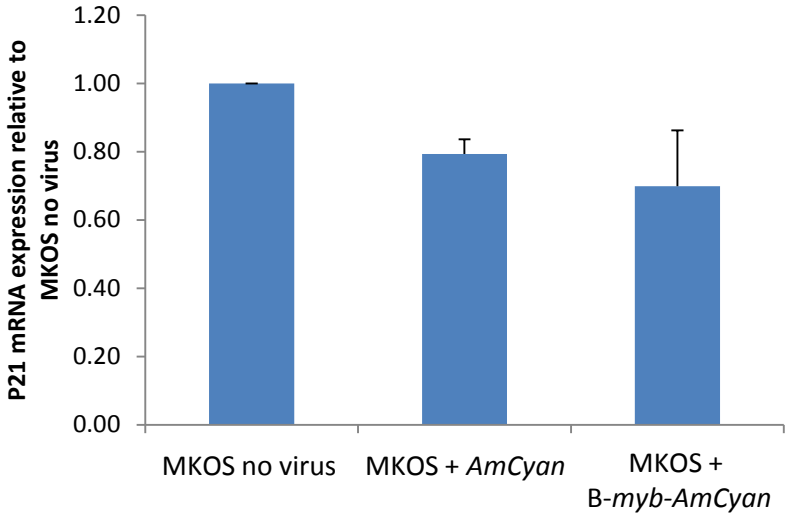


Figure 7.11: P21 mRNA expression in MKOS
10% MKOS MEFs mixed with 90% WT MEFs were transduced with MOI 10 *AmCyan* or B-*myb-AmCyan* lentiviral particles. The following day doxycycline was added to initiate reprogramming. After three days mRNA was extracted, reverse transcribed to cDNA, and analysed for expression of p21. Expression was normalised against β_2-microglobulin and then shown as relative to the MKOS no virus control. N=2, error bars represent SEM.

The expression of p16 also did not increase in the MKOS transduced with either B-*myb-AmCyan* or *AmCyan*. Surprisingly the p16 expression in the MKOS MEFs transduced with B-*myb-AmCyan* lentivirus dropped to 73% (Figure 7.12).

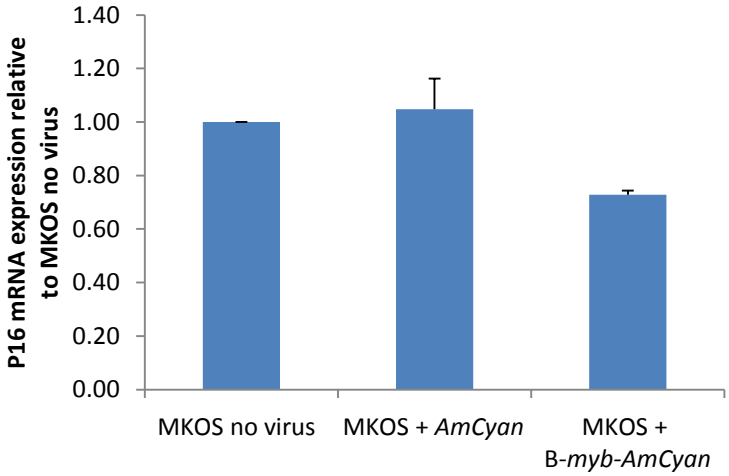


Figure 7.12: P16 mRNA expression in MKOS
10% MKOS MEFs mixed with 90% WT MEFs were transduced with MOI 10 *AmCyan* or B-*myb-AmCyan* lentiviral particles. The following day doxycycline was added to initiate reprogramming. After three days mRNA was extracted, reverse transcribed to cDNA, and analysed for expression of p16. Expression was normalised against β_2-microglobulin and then shown as relative to the MKOS no virus control. N=2, error bars represent SEM.

The expression of p53, a known roadblock in the reprogramming process, surprisingly decreased in both *AmCyan* and B-*myb-AmCyan* transduced MKOS MEFs to 75% and 60%, respectively, compared to non-transduced MEF expression (Figure 7.13).

The decreased expression of p21, p16 and p53 in B-*myb-AmCyan* transduced MKOS MEFs could therefore not explain the reduced reprogramming efficiency.

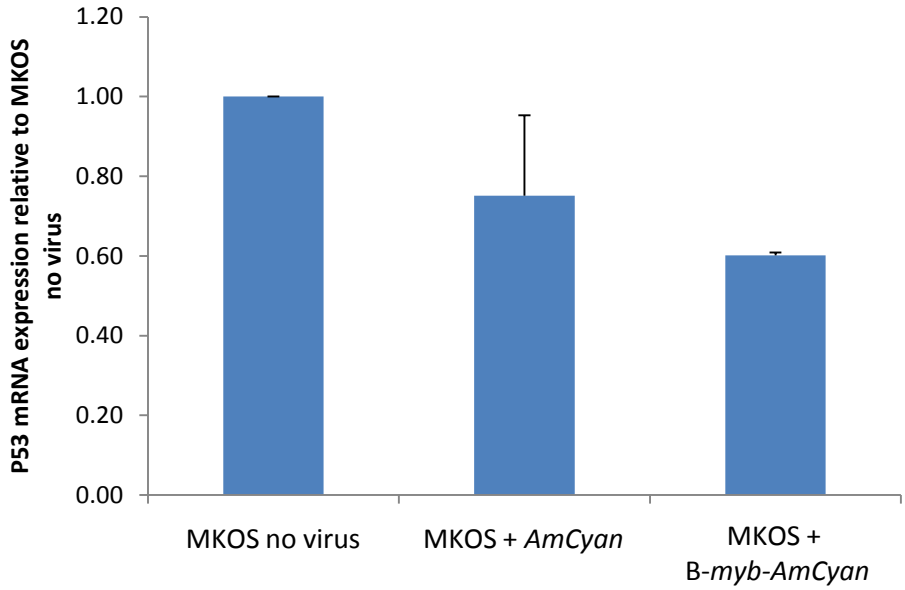


Figure 7.13: P53 mRNA expression in MKOS
10% MKOS MEFs mixed with 90% WT MEFs were transduced with MOI 10 *AmCyan* or B-*myb-AmCyan* lentiviral particles. The following day doxycycline was added to initiate reprogramming. After three days mRNA was extracted, reverse transcribed to cDNA, and analysed for expression of p53. Expression was normalised against β_2-microglobulin and then shown as relative to the MKOS no virus control. N=2, Error bars represent SEM

7.2.5 Reduced efficiency of secondary reprogramming is not due to apoptosis in the MEFs

Apoptosis, mediated through p53 activation, causes a block of reprogramming (Kawamura et al., 2009, Marion et al., 2009). My previous results using a primary reprogramming system showed lower levels of p53, which could not explain a defect in reprogramming due to p53-mediated apoptosis; however apoptosis could still be the cause of lower reprogramming efficiency through p53 independent apoptosis (Yu and Zhang, 2008, Li et al., 2013).

To determine if the reduced reprogramming efficiency observed when transducing MKOS MEFs with the B-*myb-AmCyan* lentivirus was due to an increase in the cells

undergoing apoptosis during the reprogramming process, MEFs were stained for fragmentation of genomic DNA by TUNEL. The TUNEL staining employed a red fluorochrome and the MEFs were also counterstained with DAPI, giving a DNA damaged pink nuclei on a merged confocal image. MEFs treated with DNase I to cut the genomic DNA was used as a positive control (Figure 7.14A). MKOS MEFs and wild type MEFs were mixed at a ratio 1:9, and then transduced with *AmCyan* or B-*myb*-*AmCyan* lentiviral particles at MOI 10. Reprogramming was initiated by addition of doxycycline and after 3 days the cells apoptosis was measured (Figure 7.14A). I could conclude that there was no increase in the number of apoptotic nuclei when comparing the B-*myb*-*AmCyan* transduced MKOS MEFs and the non-transduced control MEFs (Figure 7.14B).

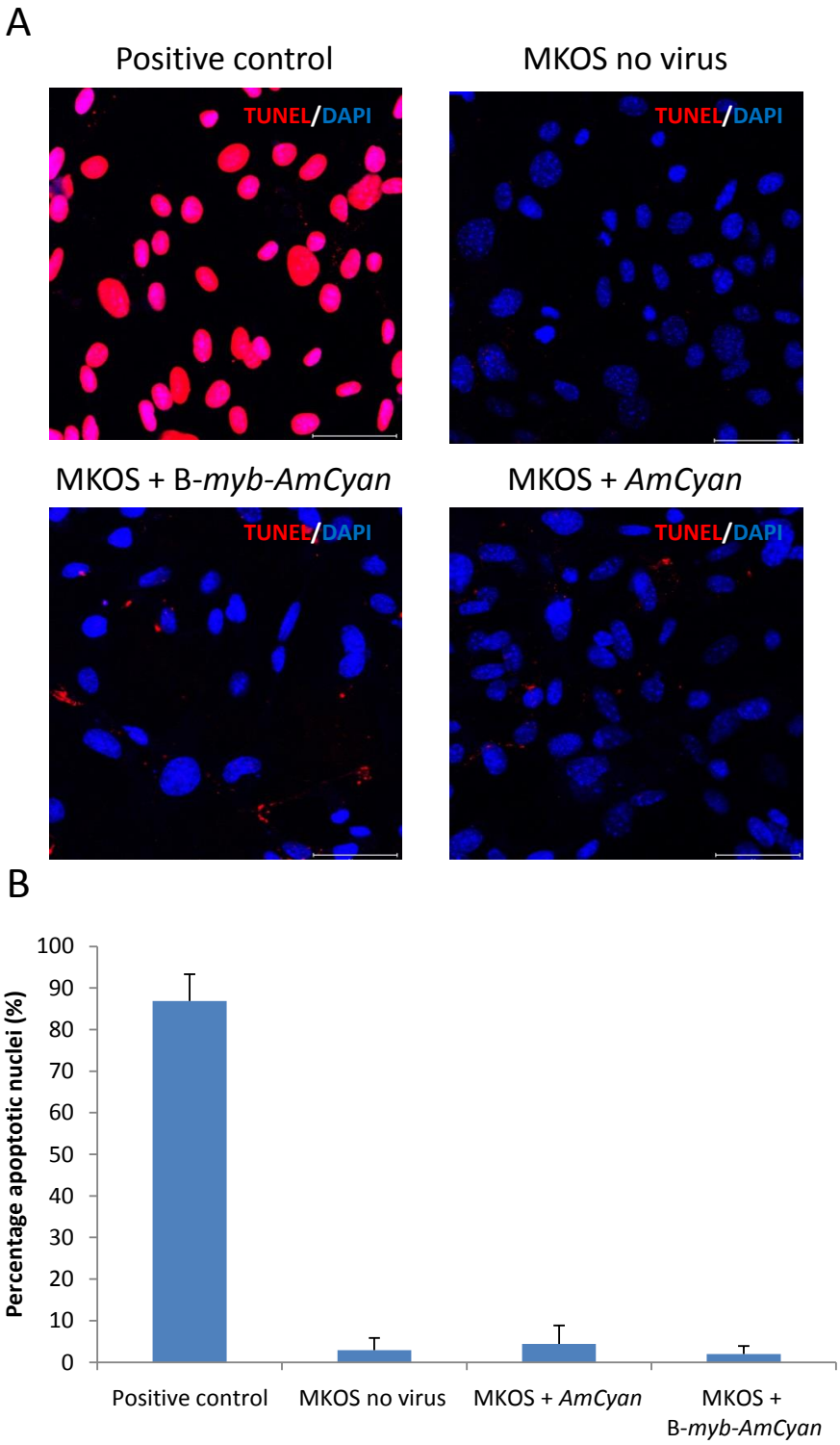


Figure 7.14: TUNEL assay in the MKOS MEFs

MKOS MEFs were grown on gelatin coated glass coverslips and then transduced with *AmCyan* or B-*myb-AmCyan* lentiviral particles at MOI 10. The following day doxycycline was added to initiate reprogramming. After 3 days MEFs were stained for genomic DNA fragmentation with TUNEL assay (A) Representative merged images at 40x magnification from confocal microscope show TUNEL staining (red) and DAPI (blue). Scale bar = 50µm. (B) Quantification of apoptotic nuclei counts from each condition. N=2

7.3 DISCUSSION

7.3.1 Secondary reprogramming

In this chapter, I aimed to determine if the phenotype observed when comparing the generated OSKB reprogramming vector with the traditional OSKM and OSK vectors was due to the additional expression of B-Myb or some kind of viral artefact. To enable this, a secondary reprogramming system was employed. The advantage of secondary reprogramming is that the four reprogramming genes are already incorporated into the MEFs genome under control of a doxycycline driven promoter, thus they are a useful tool for studying how addition of extra factors affect the reprogramming process (Wernig et al., 2008).

7.3.2 Generating a B-*myb-AmCyan* expression vector

Two lentiviral vectors were designed and generated to allow for expression of a B-Myb-P2A-AmCyan fusion protein which would separate after translation due to a linking self-cleaving peptide. The AmCyan reporter protein was selected so that it could be used alongside Nanog or Oct4 GFP expressing MEFs. However when analysed, the AmCyan fluorescence was too bright in the GFP channel and therefore could not be used in combination with GFP, thus, secondary reprogramming MEFs without the Nanog-GFP reporter gene were used for the experiments. This was unfortunate as the endogenous expression of Nanog is a hallmark of fully reprogrammed iPSCs. Fortuitously O' Malley *et al.* showed that during the reprogramming process with secondary reprogrammable MEFs (MKOS-TNG) CD44 negative and CD54 positive expression correlates significantly with Nanog-GFP expression (O'Malley et al., 2013). This was also observed in primary

reprogramming using Oct4-GFP MEFs, so I was confident that CD44/CD54 analysis of the reprogramming process was accurate.

7.3.3 B-Myb over expression inhibits reprogramming

My data shows that overexpression of B-Myb during the reprogramming process severely blocks progression to partially or fully reprogrammed iPSCs. This phenotype is identical to the phenotype described with primary lentiviral reprogramming using the OSKB lentiviral particles. Other factors have been shown to reduce reprogramming efficiency when over expressed at the same time as reprogramming. The group of Rong-Fu Wang identified Jmjd3 as an inhibitor of reprogramming through up regulation of p21 (Zhao et al., 2013). The *let-7* miRNA family was also shown to block reprogramming when fibroblasts were transfected with a *let-7* mimic (Worringer et al., 2014). Mbd3 a subunit of the nucleosome remodelling and deacetylation (NuRD) complex has also been identified as a roadblock in the reprogramming process when overexpressed (Rais et al., 2013, Luo et al., 2013). Overexpression of Gata4 during reprogramming reduced reprogramming efficiency through a down regulation of endogenous Nanog expression (Serrano et al., 2013). These four identified factors were all shown to reduce reprogramming through different mechanisms; it would be extremely interesting to elucidate the molecular mechanisms behind the reduced reprogramming efficiency when B-Myb is overexpressed.

7.3.4 Reprogramming inhibition is not due to cell cycle arrest or apoptosis

The B-*myb-AmCyan* lentivirus is not causing senescence of the MEFs as there was not an increase in β-galactosidase staining or increases in the senescence related gene expression. In fact the expression of p16 and p53 were both lower in the MKOS MEFs

transduced with the B-*myb-AmCyan* lentivirus. Low p53 expression has been shown to promote reprogramming (Zhao et al., 2008, Hong et al., 2009, Kawamura et al., 2009, Marion et al., 2009, Utikal et al., 2009), yet the B-*myb-AmCyan* transduced MEFs do not reprogram as efficiently. Furthermore, analysis of the MKOS MEFs during reprogramming showed that the percentage of MEFs expressing the mOrange reporter protein was consistently higher in the MEFs transduced with the B-*myb-AmCyan* lentivirus compared to the *AmCyan* and the non-transduced MEFs. This could indicate increased proliferation when MEFs are overexpressing B-Myb. This effect in proliferation has been reported previously (Masselink et al., 2001). This is consistent with the lower p53 expression in the MKOS MEFs transduced with B-*myb-AmCyan* lentivirus. Higher proliferation increases reprogramming efficiency hence the inclusion of c-Myc in the original reprogramming cocktail (Takahashi and Yamanaka, 2006). So it is interesting that the MKOS MEFs transduced with B-*myb-AmCyan* have lower p53 expression and higher proliferation yet are unable to reprogram. Thus, the block in reprogramming is not due to cell cycle arrest or apoptosis and must be due to a negative effect on one of the molecular events required for reprogramming to take place such as MET, epigenetic reorganization or activation of endogenous pluripotency genes. It would be useful to use the secondary reprogramming system to analyse RNA expression of the same 14 genes that were analysed in the OSKB reprogramming experiments. This experiment would be much more informative as it would be possible to sort the mOrange positive and AmCyan positive cells during the reprogramming process to extract RNA from. This would ensure that all the cells that are analysed for RNA expression would be reprogramming and have B-Myb over expressed, compared to the RNA analysis in Chapter 6.

CHAPTER 8: GENERAL DISCUSSION AND PERSPECTIVES

The molecular mechanisms that regulate somatic cellular reprogramming are rapidly being deciphered in the reprogramming field. Several genes have been identified as regulators for the reprogramming process such as p53 (Kawamura et al., 2009, Marion et al., 2009), Mbd3 (Rais et al., 2013, Luo et al., 2013), Jmjd3 (Zhao et al., 2013), and Gata4 (Serrano et al., 2013). The common feature of these genes is that their overexpression blocks reprogramming and knockdown or knockout increase reprogramming efficiency. Thus, these genes are categorised as roadblocks for reprogramming.

I was able to show that deletion of B-*myb* impaired reprogramming (Chapter 5). Several approaches to delete B-*myb* in MEFs were followed to have consistent results. Nonetheless, even using genetic models (Cre-ER^{T2} transgenic mice) to circumvent poor transfection efficiency, failed to give a clear picture. The crossings to get embryos which were B-*myb*$^{F/D}$*:Oct-4GFP:Cre-ER*^{T2} took a considerable amount of time. Just recently, a new mouse strain containing a floxed mTomato fluorescent reporter gene upstream of an EGFP gene was imported to the lab. It would have been ideal to get mice B-*myb*$^{F/\Delta}$*:Oct-4GFP:Cre-ER*^{T2}*:mTmG* . This would have enable FACS sorting of a pure population of MEFs which had ablated B-Myb expression.

I also showed that overexpression of B-Myb negatively affects reprogramming efficiency in both primary and secondary reprogramming systems (Chapter 6 and 7). Moreover, by

increasing the number of viral particles, and thus the factor/target ratio, the reprogramming process occurs with reduced efficiency but yields higher "quality" iPSCs based on morphology and GFP expression driven by endogenous Oct4 promoter (Chapter 6.2.4). It would be interesting to reveal the exact mechanism behind the block in reprogramming when B-Myb is over expressed and also to determine how much B-Myb is "too much" for reprogramming to occur. To do this a Human influenza hemagglutinin (HA) tag will be added to B-*myb-AmCyan* in an expression vector with a doxycycline controlled promoter. This will then allow MEFs to be transduced and sorted based on their AmCyan expression to obtain a pure population of MEFs. MEFs will be transduced with the OSKM reprogramming vector and B-Myb expression will be increased at different time points and different concentrations based on the concentration of doxycycline used. This approach would yield information about the exact time during the reprogramming process that the overexpression of B-Myb is causing the block. Once a time point has been determined more data could be gained by using the HA tag on the overexpressed B-Myb protein to determine what DNA or proteins B-Myb is interacting with through ChIP and Co-IP experiments.

This doxycycline inducible system could also be used to determine the minimum B-Myb expression required for reprogramming to proceed by transducing B-$myb^{F/\Delta}$ MEFs before knocking out the B-*myb* gene with cre recombinase and adding different concentrations of doxycycline to induce B-Myb expression.

I showed that the lack of reprogramming in the absence of B-Myb could be due to cells becoming quiescent (Chapter 5.2.3). Nevertheless, lack of reprogramming when B-Myb

was overexpressed at MOI 2 could not be explained by cells becoming quiescent (Chapter 6.2.5 and 7.2.4).

It would also be interesting to determine if the inclusion of B-Myb in the reprogramming factors is reducing the DSBs. My preliminary data seems to indicate that reprogramming in the presence of B-Myb gives rise to iPSCs with less DNA damage measured by γ-H2AX staining (Chapter 6.2.9). To confirm this result, many more individual iPSCs colonies would need to be analysed. These results could be of extreme importance for reprogramming as obtaining iPSCs with reduced DNA damage is a major goal of the iPSC field. Recently, the group of Rudolf Jaenisch showed that by using the four factors Sall4, Nanog, Esrrb, and Lin28 (SNEL) they were able to produce iPSCs with greater genomic stability and that these were more likely to produce live mice in 4N tetraploid complementation assays; they did however report a much reduced reprogramming efficiency compared to OSKM or OSK reprogramming (Buganim et al., 2014). I also saw a lower reprogramming efficiency compared to OSK and OSKM reprogramming when using the OSKB lentivirus. It would be very interesting to perform 4N complementation assays with iPSCs generated with the OSKB lentivirus and to further analyse their genomic instability and DNA damage.

It may also be fascinating to try to reprogram with SNEL plus B-Myb to determine if the SNEL iPSCs can be improved further with inclusion of B-Myb.

In summary, I was able to show that both deletion of B-Myb and overexpression of B-Myb during reprogramming is detrimental for reprogramming (Chapter 0, 6 and 7), Thus, timing and level of B-Myb expression are crucial for reprogramming, indicating

that B-Myb does not act as a roadblock but as a gatekeeper for the reprogramming process. This work places B-Myb as a key protein for somatic reprogramming.

The work presented in this thesis shows that the mechanisms by which B-Myb affects reprogramming are much more complicated than expected and to elucidate the precise role of B-Myb during reprogramming would require further work.

During my PhD, I also studied whether iPSCs lacking B-Myb display a replication phenotype as previously observed in ESCs (Lorvellec et al., 2010). I generated, validated, and characterised several clones before and after excision of the reprogramming cassette (Chapter 3.2.1). I was able to show that B-Myb deficient iPSCs display growth kinetics defects (Chapter 4.2.1) and loss of genome integrity with a high percentage of cells becoming polyploid (Chapter 4.2.2). Due to the results obtained in the absence of DNA damage agents (Chapter 4.2.3), this part of the project was discarded and I focussed on the role of B-Myb during the reprogramming process. Nonetheless, just three months ago, an article was published showing that iPSCs have a greater level of basal DNA damage (Felgentreff et al., 2014), meaning that the number of γ-H2AX and RAD51 foci I observed was not due to an artefact of the technique or due to bad iPSC generation. Moreover, my preliminary data showing that B-Myb ablated iPSCs display a greater sensitivity to CPT (Chapter 4.2.4), even at low concentrations is quite promising and could point to a role for B-Myb in DNA repair. Further work to determine the kinetics of DNA repair in these iPSCs in the presence of damaging agents will be followed up in the lab.

REFERENCES

AASEN, T., RAYA, A., BARRERO, M. J., GARRETA, E., CONSIGLIO, A., GONZALEZ, F., VASSENA, R., BILIC, J., PEKARIK, V., TISCORNIA, G., EDEL, M., BOUE, S. & BELMONTE, J. C. I. 2008. Efficient and rapid generation of induced pluripotent stem cells from human keratinocytes. *Nature Biotechnology,* 26**,** 1276-1284.

ABDELKARIM, G. E., GERTZ, K., HARMS, C., KATCHANOV, J., DIRNAGL, U., SZABO, C. & ENDRES, M. 2001. Protective effects of PJ34, a novel, potent inhibitor of poly(ADP-ribose) polymerase (PARP) in in vitro and in vivo models of stroke. *International Journal of Molecular Medicine,* 7**,** 255-260.

ABYZOV, A., MARIANI, J., PALEJEV, D., ZHANG, Y., HANEY, M. S., TOMASINI, L., FERRANDINO, A. F., BELMAKER, L. A. R., SZEKELY, A., WILSON, M., KOCABAS, A., CALIXTO, N. E., GRIGORENKO, E. L., HUTTNER, A., CHAWARSKA, K., WEISSMAN, S., URBAN, A. E., GERSTEIN, M. & VACCARINO, F. M. 2012. Somatic copy number mosaicism in human skin revealed by induced pluripotent stem cells. *Nature,* 492**,** 438-+.

AHLBORY, D. R., APPL, H., LANG, D. & KLEMPNAUER, K. H. 2005. Disruption of B-myb in DT40 cells reveals novel function for B-Myb in the response to DNA-damage. *Oncogene,* 24**,** 7127-7134.

ALBRECHT, B., HAUSMANN, M., ZITZELSBERGER, H., STEIN, H., SIEWERT, J. R., HOPT, U., LANGER, R., HOFLER, H., WERNER, M. & WALCH, A. 2004. Array-based comparative genomic hybridization for the detection of DNA sequence copy number changes in Barrett's adenocarcinoma. *Journal of Pathology,* 203**,** 780-788.

AMBROSETTI, D. C., BASILICO, C. & DAILEY, L. 1997. Synergistic activation of the fibroblast growth factor 4 enhancer by Sox2 and Oct-3 depends on protein-protein interactions facilitated by a specific spatial arrangement of factor binding sites. *Molecular and Cellular Biology,* 17**,** 6321-6329.

AMIT, M., CARPENTER, M. K., INOKUMA, M. S., CHIU, C. P., HARRIS, C. P., WAKNITZ, M. A., ITSKOVITZ-ELDOR, J. & THOMSON, J. A. 2000. Clonally derived human embryonic stem cell lines maintain pluripotency and proliferative potential for prolonged periods of culture. *Developmental Biology,* 227**,** 271-278.

AMPS, K., ANDREWS, P. W., ANYFANTIS, G., ARMSTRONG, L., AVERY, S., BAHARVAND, H., BAKER, J., BAKER, D., MUNOZ, M. B., BEIL, S., BENVENISTY, N., BEN-YOSEF, D., BIANCOTTI, J. C., BOSMAN, A., BRENA, R. M., BRISON, D., CAISANDER, G., CAMARASA, M. V., CHEN, J., CHIAO, E., CHOI, Y. M., CHOO, A. B., COLLINS, D., COLMAN, A., CROOK, J. M., DALEY, G. Q., DALTON, A., DE SOUSA, P. A., DENNING, C., DOWNIE, J., DVORAK, P., MONTGOMERY, K. D., FEKI, A., FORD, A., FOX, V., FRAGA, A. M., FRUMKIN, T., GE, L., GOKHALE, P. J., GOLAN-LEV, T., GOURABI, H., GROPP, M., LU, G., HAMPL, A., HARRON, K., HEALY, L., HERATH, W., HOLM, F., HOVATTA, O., HYLLNER, J., INAMDAR, M. S., IRWANTO, A. K., ISHII, T., JACONI, M., JIN, Y., KIMBER, S., KISELEV, S., KNOWLES, B. B., KOPPER, O., KUKHARENKO, V., KULIEV, A., LAGARKOVA, M. A., LAIRD, P. W., LAKO, M., LASLETT, A. L., LAVON, N., LEE, D. R., LEE, J. E., LI, C., LIM, L. S., LUDWIG, T. E., MA, Y., MALTBY, E., MATEIZEL, I., MAYSHAR, Y., MILEIKOVSKY, M., MINGER, S. L., MIYAZAKI, T., MOON, S. Y.,

MOORE, H., MUMMERY, C., NAGY, A., NAKATSUJI, N., NARWANI, K., OH, S. K., OH, S. K., OLSON, C., OTONKOSKI, T., PAN, F., PARK, I. H., PELLS, S., PERA, M. F., PEREIRA, L. V., QI, O., RAJ, G. S., REUBINOFF, B., ROBINS, A., ROBSON, P., ROSSANT, J., SALEKDEH, G. H., et al. 2011. Screening ethnically diverse human embryonic stem cells identifies a chromosome 20 minimal amplicon conferring growth advantage. *Nat Biotechnol,* 29**,** 1132-44.

ANOKYE-DANSO, F., TRIVEDI, C. M., JUHR, D., GUPTA, M., CUI, Z., TIAN, Y., ZHANG, Y. Z., YANG, W. L., GRUBER, P. J., EPSTEIN, J. A. & MORRISEY, E. E. 2011. Highly Efficient miRNA-Mediated Reprogramming of Mouse and Human Somatic Cells to Pluripotency. *Cell Stem Cell,* 8**,** 376-388.

AOI, T., YAE, K., NAKAGAWA, M., ICHISAKA, T., OKITA, K., TAKAHASHI, K., CHIBA, T. & YAMANAKA, S. 2008. Generation of pluripotent stem cells from adult mouse liver and stomach cells. *Science,* 321**,** 699-702.

ARAKI, R., UDA, M., HOKI, Y., SUNAYAMA, M., NAKAMURA, M., ANDO, S., SUGIURA, M., IDENO, H., SHIMADA, A., NIFUJI, A. & ABE, M. 2013. Negligible immunogenicity of terminally differentiated cells derived from induced pluripotent or embryonic stem cells. *Nature,* 494**,** 100-104.

ASTBURY, K., MCEVOY, L., BRIAN, H., SPILLANE, C., SHEILS, O., MARTIN, C. & O'LEARY, J. J. 2011. MYBL2 (B-MYB) in Cervical Cancer Putative Biomarker. *International Journal of Gynecological Cancer,* 21**,** 206-212.

AVILION, A. A., NICOLIS, S. K., PEVNY, L. H., PEREZ, L., VIVIAN, N. & LOVELL-BADGE, R. 2003. Multipotent cell lineages in early mouse development depend on SOX2 function. *Genes & Development,* 17**,** 126-140.

BAIZABAL, J. M., FURLAN-MAGARIL, M., SANTA-OLALLA, J. & COVARRUBIAS, L. 2003. Neural stem cells in development and regenerative medicine. *Archives of Medical Research,* 34**,** 572-588.

BAJADA, S., MAZAKOVA, I., RICHARDSON, J. B. & ASHAMMAKHI, N. 2008. Updates on stem cells and their applications in regenerative medicine. *Journal of Tissue Engineering and Regenerative Medicine,* 2**,** 169-183.

BANITO, A., RASHID, S. T., ACOSTA, J. C., LI, S., PEREIRA, C. F., GETI, I., PINHO, S., SILVA, J. C., AZUARA, V., WALSH, M., VALLIER, L. & GIL, J. 2009. Senescence impairs successful reprogramming to pluripotent stem cells. *Genes & Development,* 23**,** 2134-2139.

BAR-SHIRA, A., PINTHUS, J. H., ROZOVSKY, U., GOLDSTEIN, M., SELLERS, W. R., YARON, Y., ESHHAR, Z. & ORR-URTREGER, A. 2002. Multiple genes in human 20q13 chromosomal region are involved in an advanced prostate cancer xenograft. *Cancer Research,* 62**,** 6803-6807.

BARTEK, J. & LUKAS, J. 2001. Mammalian G1- and S-phase checkpoints in response to DNA damage. *Current Opinion in Cell Biology,* 13**,** 738-747.

BATLLE, E., SANCHO, E., FRANCI, C., DOMINGUEZ, D., MONFAR, M., BAULIDA, J. & DE HERREROS, A. G. 2000. The transcription factor Snail is a repressor of E-cadherin gene expression in epithelial tumour cells. *Nature Cell Biology,* 2**,** 84-89.

BEALL, E. L., MANAK, J. R., ZHOU, S., BELL, M., LIPSICK, J. S. & BOTCHAN, M. R. 2002. Role for a Drosophila Myb-containing protein complex in site-specific DNA replication. *Nature,* 420**,** 833-837.

BECKER, K. A., GHULE, P. N., THERRIEN, J. A., LIAN, J. B., STEIN, J. L., VAN WIJNEN, A. J. & STEIN, G. S. 2006. Self-renewal of human embryonic stem cells is supported by a shortened G1 cell cycle phase. *Journal of Cellular Physiology,* 209**,** 883-893.

BIEDENKAPP, H., BORGMEYER, U., SIPPEL, A. E. & KLEMPNAUER, K. H. 1988. VIRAL MYB ONCOGENE ENCODES A SEQUENCE-SPECIFIC DNA-BINDING ACTIVITY. *Nature,* 335**,** 835-837.

BIES, J., HOFFMAN, B., AMANULLAH, A., GIESE, T. & WOLFF, L. 1996. B-Myb prevents growth arrest associated with terminal differentiation of monocytic cells. *Oncogene,* 12**,** 355-363.

BLANGY, A., LANE, H. A., DHERIN, P., HARPER, M., KRESS, M. & NIGG, E. A. 1995. Phosphorylation by p34(cdc2) regulates spindle association of human Eg5, a kinesin-related motor essential for bipolar spindle formation in vivo. *Cell,* 83**,** 1159-1169.

BOYER, L. A., LEE, T. I., COLE, M. F., JOHNSTONE, S. E., LEVINE, S. S., ZUCKER, J. R., GUENTHER, M. G., KUMAR, R. M., MURRAY, H. L., JENNER, R. G., GIFFORD, D. K., MELTON, D. A., JAENISCH, R. & YOUNG, R. A. 2005. Core transcriptional regulatory circuitry in human embryonic stem cells. *Cell,* 122**,** 947-956.

BRAUN, E. L. & GROTEWOLD, E. 1999. Newly discovered plant c-myb-like genes rewrite the evolution of the plant myb gene family. *Plant Physiology,* 121**,** 21-24.

BROSH, R., ASSIA-ALROY, Y., MOLCHADSKY, A., BORNSTEIN, C., DEKEL, E., MADAR, S., SHETZER, Y., RIVLIN, N., GOLDFINGER, N., SARIG, R. & ROTTER, V. 2013. p53 Counteracts reprogramming by inhibiting mesenchymal-to-epithelial transition. *Cell Death and Differentiation,* 20**,** 312-320.

BUGANIM, Y., FADDAH, D. A., CHENG, A. W., ITSKOVICH, E., MARKOULAKI, S., GANZ, K., KLEMM, S. L., VAN OUDENAARDEN, A. & JAENISCH, R. 2012. Single-Cell Expression Analyses during Cellular Reprogramming Reveal an Early Stochastic and a Late Hierarchic Phase. *Cell,* 150**,** 1209-1222.

BUGANIM, Y., MARKOULAKI, S., VAN WIETMARSCHEN, N., HOKE, H., WU, T., GANZ, K., AKHTAR-ZAIDI, B., HE, Y., ABRAHAM, BRIAN J., PORUBSKY, D., KULENKAMPFF, E., FADDAH, DINA A., SHI, L., GAO, Q., SARKAR, S., COHEN, M., GOLDMANN, J., NERY, JOSEPH R., SCHULTZ, MATTHEW D., ECKER, JOSEPH R., XIAO, A., YOUNG, R. A., LANSDORP, PETER M. & JAENISCH, R. 2014. The Developmental Potential of iPSCs Is Greatly Influenced by Reprogramming Factor Selection. *Cell Stem Cell,* 15**,** 295-309.

CANO, A., PEREZ-MORENO, M. A., RODRIGO, I., LOCASCIO, A., BLANCO, M. J., DEL BARRIO, M. G., PORTILLO, F. & NIETO, M. A. 2000. The transcription factor Snail controls epithelial-mesenchymal transitions by repressing E-cadherin expression. *Nature Cell Biology,* 2**,** 76-83.

CAPLAN, A. I. 2007. Adult mesenchymal stem cells for tissue engineering versus regenerative medicine. *Journal of Cellular Physiology,* 213**,** 341-347.

CARTWRIGHT, P., MCLEAN, C., SHEPPARD, A., RIVETT, D., JONES, K. & DALTON, S. 2005. LIF/STAT3 controls ES cell self-renewal and pluripotency by a Myc-dependent mechanism. *Development,* 132**,** 885-896.

CHAKRAVARTHY, H., BOER, B., DESLER, M., MALLANNA, S. K., MCKEITHAN, T. W. & RIZZINO, A. 2008. Identification of DPPA4 and other genes as putative Sox2 : Oct-3/4 target genes using a combination of in silico analysis and transcription-based assays. *Journal of Cellular Physiology,* 216**,** 651-662.

CHARRASSE, S., CARENA, I., BRONDANI, V., KLEMPNAUER, K. H. & FERRARI, S. 2000. Degradation of B-Myb by ubiquitin-mediated proteolysis: involvement of the Cdc34-SCFp45Skp2 pathway. *Oncogene,* 19**,** 2986-2995.

CHEASLEY, D., PEREIRA, L., LIGHTOWLER, S., VINCAN, E., MALATERRE, J. & RAMSAY, R. G. 2011. Myb Controls Intestinal Stem Cell Genes and Self-Renewal. *Stem Cells,* 29**,** 2042-2050.

CHEN, A. Y. & LIU, L. F. 1994. DNA TOPOISOMERASES - ESSENTIAL ENZYMES AND LETHAL TARGETS. *Annual Review of Pharmacology and Toxicology,* 34**,** 191-218.

CHEN, C., OUYANG, W., GRIGURA, V., ZHOU, Q., CARNES, K., LIM, H., ZHAO, G. Q., ARBER, S., KURPIOS, N., MURPHY, T. L., CHENG, A. M., HASSELL, J. A., CHANDRASHEKAR, V., HOFMANN, M. C., HESS, R. A. & MURPHY, K. M. 2005. ERM is required for transcriptional control of the spermatogonial stem cell niche. *Nature,* 436**,** 1030-1034.

CHEN, J., LIU, H., LIU, J., QI, J., WEI, B., YANG, J., LIANG, H., CHEN, Y., CHEN, J., WU, Y., GUO, L., ZHU, J., ZHAO, X., PENG, T., ZHANG, Y., CHEN, S., LI, X., LI, D., WANG, T. & PEI, D. 2013. H3K9 methylation is a barrier during somatic cell reprogramming into iPSCs. *Nature Genetics,* 45**,** 34-U62.

CHEN, J. K., LIU, J., YANG, J. Q., CHEN, Y., CHEN, J., NI, S., SONG, H., ZENG, L. W., DING, K. & PEI, D. Q. 2011. BMPs functionally replace Klf4 and support efficient reprogramming of mouse fibroblasts by Oct4 alone. *Cell Research,* 21**,** 205-212.

CHEN, X., XU, H., YUAN, P., FANG, F., HUSS, M., VEGA, V. B., WONG, E., ORLOV, Y. L., ZHANG, W. W., JIANG, J. M., LOH, Y. H., YEO, H. C., YEO, Z. X., NARANG, V., GOVINDARAJAN, K. R., LEONG, B., SHAHAB, A., RUAN, Y. J., BOURQUE, G., SUNG, W. K., CLARKE, N. D., WEI, C. L. & NG, H. H. 2008. Integration of external signaling pathways with the core transcriptional network in embryonic stem cells. *Cell,* 133**,** 1106-1117.

CHEN, X. M., JOHNS, D. C., GEIMAN, D. E., MARBAN, E., DANG, D. T., HAMLIN, G., SUN, R. G. & YANG, V. W. 2001. Kruppel-like factor 4 (Gut-enriched Kruppel-like factor) inhibits cell proliferation by blocking G(1)/S progression of the cell cycle. *Journal of Biological Chemistry,* 276**,** 30423-30428.

CHEN, X. M., WHITNEY, E. M., GAO, S. Y. & YANG, V. W. 2003. Transcriptional profiling of Kruppel-like factor 4 reveals a function in cell cycle regulation and epithelial differentiation. *Journal of Molecular Biology,* 326**,** 665-677.

CHIDAMBARAM, A., ALLIKMETS, R., CHANDRASEKARAPPA, S., GURU, S. C., MODI, W., GERRARD, B. & DEAN, M. 1997. Characterization of a human homolog (OVOL1) of the Drosophila ovo gene, which maps to Chromosome 11q13. *Mammalian Genome,* 8**,** 950-951.

CHISHOLM, J. C., JOHNSON, M. H., WARREN, P. D., FLEMING, T. P. & PICKERING, S. J. 1985. DEVELOPMENTAL VARIABILITY WITHIN AND BETWEEN MOUSE EXPANDING BLASTOCYSTS AND THEIR ICMS. *Journal of Embryology and Experimental Morphology,* 86**,** 311-336.

COWAN, C. A., ATIENZA, J., MELTON, D. A. & EGGAN, K. 2005. Nuclear reprogramming of somatic cells after fusion with human embryonic stem cells. *Science,* 309**,** 1369-1373.

DAVIDSON, C., RAY, E. & LIPSICK, J. 2004. Evolution of Myb Proteins. *In:* FRAMPTON, J. (ed.) *Myb Transcription Factors: Their Role in Growth, Differentiation and Disease.* Kluwer Academic Publishers.

DAVIDSON, C. J., GUTHRIE, E. E. & LIPSICK, J. S. 2013. Duplication and maintenance of the Myb genes of vertebrate animals. *Biology open,* 2**,** 101-10.

DAVIDSON, C. J., TIROUVANZIAM, R., HERZENBERG, L. A. & LIPSICK, J. S. 2005. Functional evolution of the vertebrate Myb gene family: B-Myb, but neither A-Myb nor C-Myb, complements drosophila Myb in hemocytes. *Genetics,* 169**,** 215-229.

DE WIT, E., BOUWMAN, B. A. M., ZHU, Y., KLOUS, P., SPLINTER, E., VERSTEGEN, M. J. A. M., KRIJGER, P. H. L., FESTUCCIA, N., NORA, E. P., WELLING, M., HEARD, E., GEIJSEN, N., POOT, R. A., CHAMBERS, I. & DE LAAT, W. 2013. The pluripotent genome in three dimensions is shaped around pluripotency factors. *Nature,* 501**,** 227-+.

DIMRI, G. P., LEE, X. H., BASILE, G., ACOSTA, M., SCOTT, C., ROSKELLEY, C., MEDRANO, E. E., LINSKENS, M., RUBELJ, I., PEREIRASMITH, O., PEACOCKE, M. & CAMPISI, J. 1995. A BIOMARKER THAT IDENTIFIES SENESCENT HUMAN-CELLS IN CULTURE AND IN AGING SKIN IN-VIVO. *Proceedings of the National Academy of Sciences of the United States of America,* 92**,** 9363-9367.

DONNER, P., GREISERWILKE, I. & MOELLING, K. 1982. NUCLEAR-LOCALIZATION AND DNA-BINDING OF THE TRANSFORMING GENE-PRODUCT OF AVIAN MYELOCYTOMATOSIS VIRUS. *Nature,* 296**,** 262-266.

DUPREY, S. P. & BOETTIGER, D. 1985. DEVELOPMENTAL REGULATION OF C-MYB IN NORMAL MYELOID PROGENITOR CELLS. *Proceedings of the National Academy of Sciences of the United States of America,* 82**,** 6937-6941.

DURONIO, R. J., OFARRELL, P. H., XIE, J. E., BROOK, A. & DYSON, N. 1995. THE TRANSCRIPTION FACTOR E2F IS REQUIRED FOR S-PHASE DURING DROSOPHILA EMBRYOGENESIS. *Genes & Development,* 9**,** 1445-1455.

EILERS, M., PICARD, D., YAMAMOTO, K. R. & BISHOP, J. M. 1989. CHIMERAS OF MYC ONCOPROTEIN AND STEROID-RECEPTORS CAUSE HORMONE-DEPENDENT TRANSFORMATION OF CELLS. *Nature,* 340**,** 66-68.

EL-KHAMISY, S. F., MASUTANI, M., SUZUKI, H. & CALDECOTT, K. W. 2003. A requirement for PARP-1 for the assembly or stability of XRCC1 nuclear foci at sites of oxidative DNA damage. *Nucleic Acids Research,* 31**,** 5526-5533.

ELDEIRY, W. S., TOKINO, T., VELCULESCU, V. E., LEVY, D. B., PARSONS, R., TRENT, J. M., LIN, D., MERCER, W. E., KINZLER, K. W. & VOGELSTEIN, B. 1993. WAF1, A POTENTIAL MEDIATOR OF P53 TUMOR SUPPRESSION. *Cell,* 75**,** 817-825.

ESTEBAN, M. A., WANG, T., QIN, B. M., YANG, J. Y., QIN, D. J., CAI, J. L., LI, W., WENG, Z. H., CHEN, J. K., NI, S., CHEN, K. S., LI, Y., LIU, X. P., XU, J. Y., ZHANG, S. Q., LI, F., HE, W. Z., LABUDA, K., SONG, Y. C., PETERBAUER, A., WOLBANK, S., REDL, H., ZHONG, M., CAI, D. Z., ZENG, L. W. & PEI, D. Q. 2010. Vitamin C Enhances the Generation of Mouse and Human Induced Pluripotent Stem Cells. *Cell Stem Cell,* 6**,** 71-79.

EVAN, G. I. & VOUSDEN, K. H. 2001. Proliferation, cell cycle and apoptosis in cancer. *Nature,* 411**,** 342-348.

EVANS, M. J. & KAUFMAN, M. H. 1981. ESTABLISHMENT IN CULTURE OF PLURIPOTENTIAL CELLS FROM MOUSE EMBRYOS. *Nature,* 292**,** 154-156.

FELDMAN, B., POUEYMIROU, W., PAPAIOANNOU, V. E., DECHIARA, T. M. & GOLDFARB, M. 1995. REQUIREMENT OF FGF-4 FOR POSTIMPLANTATION MOUSE DEVELOPMENT. *Science,* 267**,** 246-249.

FELGENTREFF, K., DU, L. K., WEINACHT, K. G., DOBBS, K., BARTISH, M., GILIANI, S., SCHLAEGER, T., DEVINE, A., SCHAMBACH, A., WOODBINE, L. J., DAVIES, G., BAXI, S. N., VAN DER BURG, M., BLEESING, J., GENNERY, A., MANIS, J., PAN-HAMMARSTROM, Q. & NOTARANGELO, L. D. 2014. Differential role of nonhomologous end joining factors in the generation, DNA damage response, and myeloid differentiation of human induced pluripotent stem cells. *Proceedings of the National Academy of Sciences of the United States of America,* 111**,** 8889-8894.

FENG, B., JIANG, J. M., KRAUS, P., NG, J. H., HENG, J. C. D., CHAN, Y. S., YAW, L. P., ZHANG, W. W., LOH, Y. H., HAN, J. Y., VEGA, V. B., CACHEUX-RATABOUL, V., LIM, B., LUFKIN, T. & NG, H. H. 2009. Reprogramming of fibroblasts into induced pluripotent stem cells with orphan nuclear receptor Esrrb. *Nature Cell Biology,* 11**,** 197-U193.

FERGUSON, E. L. & HORVITZ, H. R. 1989. THE MULTIVULVA PHENOTYPE OF CERTAIN CAENORHABDITIS-ELEGANS MUTANTS RESULTS FROM DEFECTS IN 2 FUNCTIONALLY REDUNDANT PATHWAYS. *Genetics,* 123**,** 109-121.

FESTUCCIA, N., OSORNO, R., HALBRITTER, F., KARWACKI-NEISIUS, V., NAVARRO, P., COLBY, D., WONG, F., YATES, A., TOMLINSON, S. R. & CHAMBERS, I. 2012. Esrrb Is a Direct Nanog Target Gene that Can Substitute for Nanog Function in Pluripotent Cells. *Cell Stem Cell,* 11**,** 477-490.

FITZPATRICK, C. A., SHARKOV, N. V., RAMSAY, G. & KATZEN, A. L. 2002. Drosophila myb exerts opposing effects on S phase, promoting proliferation and suppressing endoreduplication. *Development,* 129**,** 4497-4507.

FLATTEN, K., DAI, N. T., VROMAN, B. T., LOEGERING, D., ERLICHMAN, C., KARNITZ, L. M. & KAUFMANN, S. H. 2005. The role of checkpoint kinase 1 in sensitivity to topoisomerase I poisons. *Journal of Biological Chemistry,* 280**,** 14349-14355.

FOOS, G., GRIMM, S. & KLEMPNAUER, K. H. 1992. FUNCTIONAL ANTAGONISM BETWEEN MEMBERS OF THE MYB FAMILY - B-MYB INHIBITS V-MYB-INDUCED GENE ACTIVATION. *Embo Journal,* 11**,** 4619-4629.

FRANCHINI, G., WONGSTAAL, F., BALUDA, M. A., LENGEL, C. & TRONICK, S. R. 1983. STRUCTURAL ORGANIZATION AND EXPRESSION OF HUMAN DNA-SEQUENCES RELATED TO THE TRANSFORMING GENE OF AVIAN-MYELOBLASTOSIS VIRUS. *Proceedings of the National Academy of Sciences of the United States of America-Biological Sciences,* 80**,** 7385-7389.

FUNG, S. M., RAMSAY, G. & KATZEN, A. L. 2002. Mutations in Drosophila myb lead to centrosome amplification and genomic instability. *Development,* 129**,** 347-359.

FUSAKI, N., BAN, H., NISHIYAMA, A., SAEKI, K. & HASEGAWA, M. 2009. Efficient induction of transgene-free human pluripotent stem cells using a vector based on Sendai virus, an RNA virus that does not integrate into the host genome. *Proceedings of the Japan Academy Series B-Physical and Biological Sciences,* 85**,** 348-362.

GAO, Y. W., CHEN, J. Y., LI, K., WU, T., HUANG, B., LIU, W. Q., KOU, X. C., ZHANG, Y., HUANG, H., JIANG, Y. H., YAO, C., LIU, X. L., LU, Z. W., XU, Z. J., KANG, L., CHEN, J., WANG, H. L., CAI, T. & GAO, S. R. 2013. Replacement of Oct4 by Tet1 during iPSC Induction Reveals an Important Role of DNA Methylation and Hydroxymethylation in Reprogramming. *Cell Stem Cell,* 12**,** 453-469.

GARCIA, P., BERLANGA, O., WATSON, R. & FRAMPTON, J. 2005. Generation of a conditional allele of the B-myb gene. *Genesis,* 43**,** 189-195.

GARCIA, P. & FRAMPTON, J. 2006. The transcription factor B-Myb is essential for S-phase progression and genomic stability in diploid and polyploid megakaryocytes. *Journal of Cell Science,* 119**,** 1483-1493.

GIACINTI, C. & GIORDANO, A. 2006. RB and cell cycle progression. *Oncogene,* 25**,** 5220-5227.

GIBSON, D. G., YOUNG, L., CHUANG, R. Y., VENTER, J. C., HUTCHISON, C. A. & SMITH, H. O. 2009. Enzymatic assembly of DNA molecules up to several hundred kilobases. *Nature Methods,* 6**,** 343-U41.

GIL, J., BERNARD, D., MARTINEZ, D. & BEACH, D. 2004. Polycomb CBX7 has a unifying role in cellular lifespan. *Nature Cell Biology,* 6**,** 67-U19.

GONDA, T. J. & BISHOP, J. M. 1983. STRUCTURE AND TRANSCRIPTION OF THE CELLULAR HOMOLOG (C-MYB) OF THE AVIAN-MYELOBLASTOSIS VIRUS TRANSFORMING GENE (V-MYB). *Journal of Virology,* 46**,** 212-220.

GONDA, T. J., GOUGH, N. M., DUNN, A. R. & DEBLAQUIERE, J. 1985. NUCLEOTIDE-SEQUENCE OF CDNA CLONES OF THE MURINE MYB PROTOONCOGENE. *Embo Journal,* 4**,** 2003-2008.

GONZÁLEZ, F., GEORGIEVA, D., VANOLI, F., SHI, Z.-D., STADTFELD, M., LUDWIG, T., JASIN, M. & HUANGFU, D. 2013. Homologous Recombination DNA Repair Genes Play a Critical Role in Reprogramming to a Pluripotent State. *Cell Reports*.

GROSSCHEDL, R., GIESE, K. & PAGEL, J. 1994. HMG DOMAIN PROTEINS - ARCHITECTURAL ELEMENTS IN THE ASSEMBLY OF NUCLEOPROTEIN STRUCTURES. *Trends in Genetics,* 10**,** 94-100.

GU, P. L., GOODWIN, B., CHUNG, A. C. K., XU, X. P., WHEELER, D. A., PRICE, R. R., GALARDI, C., PENG, L., LATOUR, A. M., KOLLER, B. H., GOSSEN, J., KLIEWER, S. A. & COONEY, A. J. 2005. Orphan nuclear receptor LRH-1 is required to maintain Oct4 expression at the epiblast stage of embryonic development. *Molecular and Cellular Biology,* 25**,** 3492-3505.

GUALDRINI, F., CORVETTA, D., CANTILENA, S., CHAYKA, O., TANNO, B., RASCHELLA, G. & SALA, A. 2010. Addiction of MYCN Amplified Tumours to B-MYB Underscores a Reciprocal Regulatory Loop. *Oncotarget,* 1**,** 278-288.

GUBBAY, J., COLLIGNON, J., KOOPMAN, P., CAPEL, B., ECONOMOU, A., MUNSTERBERG, A., VIVIAN, N., GOODFELLOW, P. & LOVELLBADGE, R. 1990. A GENE-MAPPING TO THE SEX-DETERMINING REGION OF THE MOUSE Y-CHROMOSOME IS A MEMBER OF A NOVEL FAMILY OF EMBRYONICALLY EXPRESSED GENES. *Nature,* 346**,** 245-250.

GUHA, P., MORGAN, JOHN W., MOSTOSLAVSKY, G., RODRIGUES, NEIL P. & BOYD, ASHLEIGH S. 2013. Lack of Immune Response to Differentiated Cells Derived from Syngeneic Induced Pluripotent Stem Cells. *Cell Stem Cell*.

GUO, G. & SMITH, A. 2010. A genome-wide screen in EpiSCs identifies Nr5a nuclear receptors as potent inducers of ground state pluripotency. *Development,* 137**,** 3185-3192.

GURDON, J. B. 1962. ADULT FROGS DERIVED FROM NUCLEI OF SINGLE SOMATIC CELLS. *Developmental Biology,* 4**,** 256-&.

HANNA, J., SAHA, K., PANDO, B., VAN ZON, J., LENGNER, C. J., CREYGHTON, M. P., VAN OUDENAARDEN, A. & JAENISCH, R. 2009. Direct cell reprogramming is a stochastic process amenable to acceleration. *Nature,* 462**,** 595-U63.

HANNA, J., WERNIG, M., MARKOULAKI, S., SUN, C. W., MEISSNER, A., CASSADY, J. P., BEARD, C., BRAMBRINK, T., WU, L. C., TOWNES, T. M. & JAENISCH, R. 2007. Treatment of sickle cell anemia mouse model with iPS cells generated from autologous skin. *Science,* 318**,** 1920-1923.

HARPER, J. W., ADAMI, G. R., WEI, N., KEYOMARSI, K. & ELLEDGE, S. J. 1993. THE P21 CDK-INTERACTING PROTEIN CIP1 IS A POTENT INHIBITOR OF G1 CYCLIN-DEPENDENT KINASES. *Cell,* 75**,** 805-816.

HARRISON, M. M., CEOL, C. J., LU, X. W. & HORVITZ, H. R. 2006. Some C. elegans class B synthetic multivulva proteins encode a conserved LIN-35 Rb-containing complex distinct from a NuRD-like complex. *Proceedings of the National Academy of Sciences of the United States of America,* 103**,** 16782-16787.

HARTLEY, J. L., TEMPLE, G. F. & BRASCH, M. A. 2000. DNA cloning using in vitro site-specific recombination. *Genome Research,* 10**,** 1788-1795.

HEALD, R., MCLOUGHLIN, M. & MCKEON, F. 1993. HUMAN WEE-1 MAINTAINS MITOTIC TIMING BY PROTECTING THE NUCLEUS FROM CYTOPLASMICALLY ACTIVATED CDC2 KINASE. *Cell,* 74**,** 463-474.

HENG, J. C. D., FENG, B., HAN, J. Y., JIANG, J. M., KRAUS, P., NG, J. H., ORLOV, Y. L., HUSS, M., YANG, L., LUFKIN, T., LIM, B. & NG, H. H. 2010. The Nuclear Receptor Nr5a2 Can Replace Oct4 in the Reprogramming of Murine Somatic Cells to Pluripotent Cells. *Cell Stem Cell,* 6**,** 167-174.

HENGST, L., GOPFERT, U., LASHUEL, H. A. & REED, S. I. 1998. Complete inhibition of Cdk/cyclin by one molecule of p21(Cip1). *Genes & Development,* 12**,** 3882-3888.

HONG, H., TAKAHASHI, K., ICHISAKA, T., AOI, T., KANAGAWA, O., NAKAGAWA, M., OKITA, K. & YAMANAKA, S. 2009. Suppression of induced pluripotent stem cell generation by the p53-p21 pathway. *Nature,* 460**,** 1132-U95.

HONG, S. G., WINKLER, T., WU, C. F., GUO, V., PITTALUGA, S., NICOLAE, A., DONAHUE, R. E., METZGER, M. E., PRICE, S. D., UCHIDA, N., KUZNETSOV, S. A., KILTS, T., LI, L., ROBEY, P. G. & DUNBAR, C. E. 2014. Path to the Clinic: Assessment of iPSC-Based Cell Therapies In Vivo in a Nonhuman Primate Model. *Cell Reports,* 7**,** 1298-1309.

HOPPO, T., FUJII, H., HIROSE, T., YASUCHIKA, K., AZUMA, H., BABA, S., NAITO, M., MACHIMOTO, T. & IKAI, I. 2004. Thy1-positive mesenchymal cells promote the maturation of CD49f-positive hepatic progenitor cells in the mouse fetal liver. *Hepatology,* 39**,** 1362-1370.

HOU, P., LI, Y., ZHANG, X., LIU, C., GUAN, J., LI, H., ZHAO, T., YE, J., YANG, W., LIU, K., GE, J., XU, J., ZHANG, Q., ZHAO, Y. & DENG, H. 2013. Pluripotent Stem Cells Induced from Mouse Somatic Cells by Small-Molecule Compounds. *Science,* 341**,** 651-654.

HSIANG, Y. H., HERTZBERG, R., HECHT, S. & LIU, L. F. 1985. CAMPTOTHECIN INDUCES PROTEIN-LINKED DNA BREAKS VIA MAMMALIAN DNA TOPOISOMERASE-I. *Journal of Biological Chemistry,* 260**,** 4873-4878.

HUANG, Y., WU, J. F., LI, R. Z., WANG, P. C., HAN, L. M., ZHANG, Z. Y. & TONG, T. J. 2011. B-MYB delays cell aging by repressing p16 (INK4 alpha) transcription. *Cellular and Molecular Life Sciences,* 68**,** 893-901.

HUANGFU, D. W., MAEHR, R., GUO, W. J., EIJKELENBOOM, A., SNITOW, M., CHEN, A. E. & MELTON, D. A. 2008a. Induction of pluripotent stem cells by defined factors is greatly improved by small-molecule compounds. *Nature Biotechnology,* 26**,** 795-797.

HUANGFU, D. W., OSAFUNE, K., MAEHR, R., GUO, W., EIJKELENBOOM, A., CHEN, S., MUHLESTEIN, W. & MELTON, D. A. 2008b. Induction of pluripotent stem cells from primary human fibroblasts with only Oct4 and Sox2. *Nature Biotechnology,* 26**,** 1269-1275.

HUSSEIN, S. M., BATADA, N. N., VUORISTO, S., CHING, R. W., AUTIO, R., NARVA, E., NG, S., SOUROUR, M., HAMALAINEN, R., OLSSON, C., LUNDIN, K., MIKKOLA, M., TROKOVIC, R., PEITZ, M., BRUSTLE, O., BAZETT-JONES, D. P., ALITALO, K., LAHESMAA, R., NAGY, A. & OTONKOSKI, T. 2011. Copy number variation and selection during reprogramming to pluripotency. *Nature,* 471**,** 58-U67.

ICHIDA, J. K., BLANCHARD, J., LAM, K., SON, E. Y., CHUNG, J. E., EGLI, D., LOH, K. M., CARTER, A. C., DI GIORGIO, F. P., KOSZKA, K., HUANGFU, D. W., AKUTSU, H., LIU, D. R., RUBIN, L. L. & EGGAN, K. 2009. A Small-Molecule Inhibitor of Tgf-beta Signaling Replaces Sox2 in Reprogramming by Inducing Nanog. *Cell Stem Cell,* 5**,** 491-503.

JOHNSTON, L. A., PROBER, D. A., EDGAR, B. A., EISENMAN, R. N. & GALLANT, P. 1999. Drosophila myc regulates cellular growth during development. *Cell,* 98**,** 779-790.

JOHUNG, K., GOODWIN, E. C. & DIMAIO, D. 2007. Human papillomavirus E7 repression in cervical carcinoma cells initiates a transcriptional cascade driven by the retinoblastoma family, resulting in senescence. *Journal of Virology,* 81**,** 2102-2116.

JONKERS, J. & BERNS, A. 1996. Retroviral insertional mutagenesis as a strategy to identify cancer genes. *Biochimica Et Biophysica Acta-Reviews on Cancer,* 1287**,** 29-57.

JUDSON, R. L., BABIARZ, J. E., VENERE, M. & BLELLOCH, R. 2009. Embryonic stem cell-specific microRNAs promote induced pluripotency. *Nature Biotechnology,* 27**,** 459-461.

KAMACHI, Y., UCHIKAWA, M. & KONDOH, H. 2000. Pairing SOX off with partners in the regulation of embryonic development. *Trends in Genetics,* 16**,** 182-187.

KAMAO, H., MANDAI, M., OKAMOTO, S., SAKAI, N., SUGA, A., SUGITA, S., KIRYU, J. & TAKAHASHI, M. 2014. Characterization of human induced pluripotent stem cell-derived retinal pigment epithelium cell sheets aiming for clinical application. *Stem cell reports,* 2**,** 205-18.

KARAKAIDOS, P., TARAVIRAS, S., VASSILIOU, L. V., ZACHARATOS, P., KASTRINAKIS, N. G., KOUGIOU, D., KOULOUKOUSSA, M., NISHITANI, H., PAPAVASSILIOU, A. G., LYGEROU, Z. & GORGOULIS, V. G. 2004. Overexpression of the replication licensing regulators hCdt1 and hCdc6 characterizes a subset of non-small-cell lung carcinomas - Synergistic effect with mutant p53 on tumor growth and chromosomal instability - Evidence of E2F-1 transcriptional control over hCdt1. *American Journal of Pathology,* 165**,** 1351-1365.

KARWACKI-NEISIUS, V., GOKE, J., OSORNO, R., HALBRITTER, F., NG, J. H., WEISSE, A. Y., WONG, F. C. K., GAGLIARDI, A., MULLIN, N. P., FESTUCCIA, N., COLBY, D., TOMLINSON, S. R., NG, H. H. & CHAMBERS, I. 2013. Reduced Oct4 Expression Directs a Robust Pluripotent State with Distinct Signaling Activity and Increased Enhancer Occupancy by Oct4 and Nanog. *Cell Stem Cell,* 12**,** 531-545.

KATZEN, A. L., JACKSON, J., HARMON, B. P., FUNG, S. M., RAMSAY, G. & BISHOP, J. M. 1998. Drosophila myb is required for the G(2)/M transition and maintenance of diploidy. *Genes & Development,* 12**,** 831-843.

KATZEN, A. L., KORNBERG, T. B. & BISHOP, J. M. 1985. ISOLATION OF THE PROTO-ONCOGENE C-MYB FROM DROSOPHILA-MELANOGASTER. *Cell,* 41**,** 449-456.

KAWAMURA, T., SUZUKI, J., WANG, Y. V., MENENDEZ, S., MORERA, L. B., RAYA, A., WAHL, G. M. & BELMONTE, J. C. I. 2009. Linking the p53 tumour suppressor pathway to somatic cell reprogramming. *Nature,* 460**,** 1140-U107.

KIDDER, B. L., YANG, J. & PALMER, S. 2008. Stat3 and c-Myc Genome-Wide Promoter Occupancy in Embryonic Stem Cells. *Plos One,* 3**,** 14.

KIM, D., KIM, C.-H., MOON, J.-I., CHUNG, Y.-G., CHANG, M.-Y., HAN, B.-S., KO, S., YANG, E., CHA, K. Y., LANZA, R. & KIM, K.-S. 2009a. Generation of Human Induced Pluripotent Stem Cells by Direct Delivery of Reprogramming Proteins. *Cell Stem Cell,* 4**,** 472-476.

KIM, J. B., SEBASTIANO, V., WU, G. M., ARAUZO-BRAVO, M. J., SASSE, P., GENTILE, L., KO, K., RUAU, D., EHRICH, M., VAN DEN BOOM, D., MEYER, J., HUBNER, K., BERNEMANN, C., ORTMEIER, C., ZENKE, M., FLEISCHMANN, B. K., ZAEHRES, H. & SCHOLER, H. R. 2009b. Oct4-Induced Pluripotency in Adult Neural Stem Cells. *Cell,* 136**,** 411-419.

KIM, J. B., ZAEHRES, H., WU, G. M., GENTILE, L., KO, K., SEBASTIANO, V., ARAUZO-BRAVO, M. J., RUAU, D., HAN, D. W., ZENKE, M. & SCHOLER, H. R. 2008a. Pluripotent stem cells induced from adult neural stem cells by reprogramming with two factors. *Nature,* 454**,** 646-U54.

KIM, J. H., LEE, S.-R., LI, L.-H., PARK, H.-J., PARK, J.-H., LEE, K. Y., KIM, M.-K., SHIN, B. A. & CHOI, S.-Y. 2011. High Cleavage Efficiency of a 2A Peptide Derived from Porcine Teschovirus-1 in Human Cell Lines, Zebrafish and Mice. *Plos One,* 6.

KIM, J. W., CHU, J. L., SHEN, X. H., WANG, J. L. & ORKIN, S. H. 2008b. An extended transcriptional network for pluripotency of embryonic stem cells. *Cell,* 132**,** 1049-1061.

KIM, K., DOI, A., WEN, B., NG, K., ZHAO, R., CAHAN, P., KIM, J., ARYEE, M. J., JI, H., EHRLICH, L. I. R., YABUUCHI, A., TAKEUCHI, A., CUNNIFF, K. C., HONGGUANG, H., MCKINNEY-FREEMAN, S., NAVEIRAS, O., YOON, T. J., IRIZARRY, R. A., JUNG, N., SEITA, J., HANNA, J., MURAKAMI, P., JAENISCH, R., WEISSLEDER, R., ORKIN, S. H., WEISSMAN, I. L., FEINBERG, A. P. & DALEY, G. Q. 2010. Epigenetic memory in induced pluripotent stem cells. *Nature,* 467**,** 285-U60.

KIM, Y. S., LEWANDOSKI, M., PERANTONI, A. O., KUREBAYASHI, S., NAKANISHI, G. & JETTEN, A. M. 2002. Identification of Glis1, a novel Gli-related, Kruppel-like zinc finger protein containing transactivation and repressor functions. *Journal of Biological Chemistry,* 277**,** 30901-30913.

KINOSHITA, T., NAGAMATSU, G., KOSAKA, T., TAKUBO, K., HOTTA, A., ELLIS, J. & SUDA, T. 2011. Ataxia-telangiectasia mutated (ATM) deficiency decreases reprogramming efficiency and leads to gnomic instability in iPS cells. *Biochemical and Biophysical Research Communications,* 407**,** 321-326.

KNIGHT, A. S., NOTARIDOU, M. & WATSON, R. J. 2009. A Lin-9 complex is recruited by B-Myb to activate transcription of G(2)/M genes in undifferentiated embryonal carcinoma cells. *Oncogene,* 28**,** 1737-1747.

KOCHE, R. P., SMITH, Z. D., ADLI, M., GU, H. C., KU, M. C., GNIRKE, A., BERNSTEIN, B. E. & MEISSNER, A. 2011. Reprogramming Factor Expression Initiates Widespread Targeted Chromatin Remodeling. *Cell Stem Cell,* 8**,** 96-105.

KORENJAK, M., TAYLOR-HARDING, B., BINNE, U. K., SATTERLEE, J. S., STEVAUX, O., AASLAND, R., WHITE-COOPER, H., DYSON, N. & BREHM, A. 2004. Native E2F/RBF complexes contain Myb-interacting proteins and repress transcription of developmentally controlled E2F target genes. *Cell,* 119**,** 181-193.

KRAKOFF, I. H., BROWN, N. C. & REICHARD, P. 1968. INHIBITION OF RIBONUCLEOSIDE DIPHOSPHATE REDUCTASE BY HYDROXYUREA. *Cancer Research,* 28**,** 1559-&.

LAM, E. W. F., BENNETT, J. D. & WATSON, R. J. 1995. CELL-CYCLE REGULATION OF HUMAN B-MYB TRANSCRIPTION. *Gene,* 160**,** 277-281.

LAM, E. W. F., ROBINSON, C. & WATSON, R. J. 1992. CHARACTERIZATION AND CELL CYCLE-REGULATED EXPRESSION OF MOUSE B-MYB. *Oncogene,* 7**,** 1885-1890.

LAM, E. W. F. & WATSON, R. J. 1993. AN E2F-BINDING SITE MEDIATES CELL-CYCLE-REGULATED REPRESSION OF MOUSE B-MYB TRANSCRIPTION. *Embo Journal,* 12**,** 2705-2713.

LAMMERS, M. & FOLLMANN, H. 1983. THE RIBONUCLEOTIDE REDUCTASES - A UNIQUE GROUP OF METALLOENZYMES ESSENTIAL FOR CELL-PROLIFERATION. *Structure and Bonding,* 54**,** 27-91.

LARUE, L., ANTOS, C., BUTZ, S., HUBER, O., DELMAS, V., DOMINIS, M. & KEMLER, R. 1996. A role for cadherins in tissue formation. *Development,* 122**,** 3185-3194.

LARUE, L., OHSUGI, M., HIRCHENHAIN, J. & KEMLER, R. 1994. E-CADHERIN NULL MUTANT EMBRYOS FAIL TO FORM A TROPHECTODERM EPITHELIUM. *Proceedings of the National Academy of Sciences of the United States of America,* 91**,** 8263-8267.

LAURENT, L. C., ULITSKY, I., SLAVIN, I., TRAN, H., SCHORK, A., MOREY, R., LYNCH, C., HARNESS, J. V., LEE, S., BARRERO, M. J., KU, S., MARTYNOVA, M., SEMECHKIN, R., GALAT, V., GOTTESFELD, J., BELMONTE, J. C. I., MURRY, C., KEIRSTEAD, H. S., PARK, H. S., SCHMIDT, U., LASLETT, A. L., MULLER, F. J., NIEVERGELT, C. M., SHAMIR, R. & LORING, J. F. 2011. Dynamic Changes in the Copy Number of Pluripotency and Cell Proliferation Genes in Human ESCs and iPSCs during Reprogramming and Time in Culture. *Cell Stem Cell,* 8**,** 106-118.

LEE, B. Y., HAN, J. A., IM, J. S., MORRONE, A., JOHUNG, K., GOODWIN, E. C., KLEIJER, W. J., DIMAIO, D. & HWANG, E. S. 2006. Senescence-associated beta-galactosidase is lysosomal beta-galactosidase. *Aging Cell,* 5**,** 187-195.

LEWIS, P. W., BEALL, E. L., FLEISCHER, T. C., GEORLETTE, D., LINK, A. J. & BOTCHAN, M. R. 2004. Identification of a Drosophila Myb-E2F2/RBF transcriptional repressor complex. *Genes & Development,* 18**,** 2929-2940.

LI, F., HE, Z. M., SHEN, J. P., HUANG, Q. A., LI, W. R., LIU, X. J., HE, Y. J., WOLF, F. & LI, C. Y. 2010a. Apoptotic Caspases Regulate Induction of iPSCs from Human Fibroblasts. *Cell Stem Cell,* 7**,** 508-520.

LI, R. H., LIANG, J. L., NI, S., ZHOU, T., QING, X. B., LI, H. P., HE, W. Z., CHEN, J. K., LI, F., ZHUANG, Q. A., QIN, B. M., XU, J. Y., LI, W., YANG, J. Y., GAN, Y., QIN, D. J., FENG, S. P., SONG, H., YANG, D. S., ZHANG, B. L., ZENG, L. W., LAI, L. X., ESTEBAN, M. A. & PEI, D. Q. 2010b. A Mesenchymal-to-Epithelial Transition Initiates and Is Required for the Nuclear Reprogramming of Mouse Fibroblasts. *Cell Stem Cell,* 7**,** 51-63.

LI, X. L. & MCDONNELL, D. P. 2002. The transcription factor B-Myb is maintained in an inhibited state in target cells through its interaction with the nuclear corepressors N-CoR and SMRT. *Molecular and Cellular Biology,* 22**,** 3663-3673.

LI, Y. X., FENG, H. Z., GU, H. H., LEWIS, D. W., YUAN, Y. Z., ZHANG, L., YU, H., ZHANG, P., CHENG, H. Z., MIAO, W. M., YUAN, W. P., CHENG, S. Y., GOLLIN, S. M. & CHENG, T. 2013. The p53-PUMA axis suppresses iPSC generation. *Nature Communications,* 4**,** 9.

LIN, C. Y., LOVEN, J., RAHL, P. B., PARANAL, R. M., BURGE, C. B., BRADNER, J. E., LEE, T. I. & YOUNG, R. A. 2012. Transcriptional Amplification in Tumor Cells with Elevated c-Myc. *Cell,* 151**,** 56-67.

LISTER, R., PELIZZOLA, M., KIDA, Y. S., HAWKINS, R. D., NERY, J. R., HON, G., ANTOSIEWICZ-BOURGET, J., O'MALLEY, R., CASTANON, R., KLUGMAN, S., DOWNES, M., YU, R., STEWART, R., REN, B., THOMSON, J. A., EVANS, R. M. & ECKER, J. R. 2011. Hotspots of aberrant epigenomic reprogramming in human induced pluripotent stem cells. *Nature,* 471**,** 68-U84.

LITOVCHICK, L., SADASIVAM, S., FLORENS, L., ZHU, X., SWANSON, S. K., VELMURUGAN, S., CHEN, R., WASHBURN, M. P., LIU, X. S. & DECAPRIO, J. A. 2007. Evolutionarily conserved multisubunit RBL2/p130 and E2F4 protein complex represses human cell cycle-dependent genes in quiescence. *Molecular Cell,* 26**,** 539-551.

LIVAK, K. J. & SCHMITTGEN, T. D. 2001. Analysis of relative gene expression data using real-time quantitative PCR and the 2(T)(-Delta Delta C) method. *Methods,* 25**,** 402-408.

LOBRICH, M., SHIBATA, A., BEUCHER, A., FISHER, A., ENSMINGER, M., GOODARZI, A. A., BARTON, O. & JEGGO, P. A. 2010. gamma H2AX foci analysis for monitoring DNA double-strand break repair Strengths, limitations and optimization. *Cell Cycle,* 9**,** 662-669.

LOH, Y. H., WU, Q., CHEW, J. L., VEGA, V. B., ZHANG, W. W., CHEN, X., BOURQUE, G., GEORGE, J., LEONG, B., LIU, J., WONG, K. Y., SUNG, K. W., LEE, C. W. H., ZHAO, X. D., CHIU, K. P., LIPOVICH, L., KUZNETSOV, V. A., ROBSON, P., STANTON, L. W., WEI, C. L., RUAN, Y. J., LIM, B. & NG, H. H. 2006. The Oct4 and Nanog transcription network regulates pluripotency in mouse embryonic stem cells. *Nature Genetics,* 38**,** 431-440.

LORVELLEC, M., DUMON, S., MAYA-MENDOZA, A., JACKSON, D., FRAMPTON, J. & GARCIA, P. 2010. B-Myb is Critical for Proper DNA Duplication During an Unperturbed S Phase in Mouse Embryonic Stem Cells. *Stem Cells,* 28**,** 1751-1759.

LUNDBERG, A. S. & WEINBERG, R. A. 1998. Functional inactivation of the retinoblastoma protein requires sequential modification by at least two distinct cyclin-cdk complexes. *Molecular and Cellular Biology,* 18**,** 753-761.

LUNDBERG, A. S. & WEINBERG, R. A. 1999. Control of the cell cycle and apoptosis. *European Journal of Cancer,* 35**,** 531-539.

LUO, M., LING, T., XIE, W. B., SUN, H., ZHOU, Y. G., ZHU, Q. Y., SHEN, M. L., ZONG, L., LYU, G. L., ZHAO, Y., YE, T., GU, J., TAO, W., LU, Z. G. & GRUMMT, I. 2013. NuRD Blocks Reprogramming of Mouse Somatic Cells into Pluripotent Stem Cells. *Stem Cells,* 31**,** 1278-1286.

LYSSIOTIS, C. A., FOREMAN, R. K., STAERK, J., GARCIA, M., MATHUR, D., MARKOULAKI, S., HANNA, J., LAIRSON, L. L., CHARETTE, B. D., BOUCHEZ, L. C., BOLLONG, M., KUNICK, C., BRINKER, A., CHO, C. Y., SCHULTZ, P. G. & JAENISCH, R. 2009. Reprogramming of murine fibroblasts to induced pluripotent stem cells with chemical complementation of Klf4. *Proceedings of the National Academy of Sciences of the United States of America,* 106**,** 8912-8917.

MAEKAWA, M., YAMAGUCHI, K., NAKAMURA, T., SHIBUKAWA, R., KODANAKA, I., ICHISAKA, T., KAWAMURA, Y., MOCHIZUKI, H., GOSHIMA, N. & YAMANAKA, S. 2011. Direct reprogramming of somatic cells is promoted by maternal transcription factor Glis1. *Nature,* 474**,** 225-U268.

MAHERALI, N. & HOCHEDLINGER, K. 2009. Tgf beta Signal Inhibition Cooperates in the Induction of iPSCs and Replaces Sox2 and cMyc. *Current Biology,* 19**,** 1718-1723.

MAHERALI, N., SRIDHARAN, R., XIE, W., UTIKAL, J., EMINLI, S., ARNOLD, K., STADTFELD, M., YACHECHKO, R., TCHIEU, J., JAENISCH, R., PLATH, K. & HOCHEDLINGER, K. 2007. Directly reprogrammed fibroblasts show global epigenetic remodeling and widespread tissue contribution. *Cell Stem Cell,* 1**,** 55-70.

MALATERRE, J., MANTAMADIOTIS, T., DWORKIN, S., LIGHTOWLER, S., YANG, Q., RANSOME, M. I., TURNLEY, A. M., NICHOLS, N. R., EMAMBOKUS, N. R., FRAMPTON, J. & RAMSAY, R. G. 2008. c-Myb is required for neural progenitor cell proliferation and maintenance of the neural stem cell niche in adult brain. *Stem Cells,* 26**,** 173-181.

MANAK, J. R., MITIKU, N. & LIPSICK, J. S. 2002. Mutation of the Drosophila homologue of the Myb protooncogene causes genomic instability. *Proceedings of the National Academy of Sciences of the United States of America,* 99**,** 7438-7443.

MANI, S. A., GUO, W., LIAO, M. J., EATON, E. N., AYYANAN, A., ZHOU, A. Y., BROOKS, M., REINHARD, F., ZHANG, C. C., SHIPITSIN, M., CAMPBELL, L. L., POLYAK, K., BRISKEN, C., YANG, J. & WEINBERG, R. A. 2008. The epithelial-mesenchymal transition generates cells with properties of stem cells. *Cell,* 133**,** 704-715.

MANSOUR, A. A., GAFNI, O., WEINBERGER, L., ZVIRAN, A., AYYASH, M., RAIS, Y., KRUPALNIK, V., ZERBIB, M., AMANN-ZALCENSTEIN, D., MAZA, I., GEULA, S., VIUKOV, S., HOLTZMAN, L., PRIBLUDA, A., CANAANI, E., HORN-SABAN, S., AMIT, I., NOVERSHTERN, N. & HANNA, J. H. 2012. The H3K27 demethylase Utx regulates somatic and germ cell epigenetic reprogramming. *Nature,* 488**,** 409-+.

MARION, R. M., STRATI, K., LI, H., MURGA, M., BLANCO, R., ORTEGA, S., FERNANDEZ-CAPETILLO, O., SERRANO, M. & BLASCO, M. A. 2009. A p53-mediated DNA damage response limits reprogramming to ensure iPS cell genomic integrity. *Nature,* 460**,** 1149-U119.

MARTINEZA, I., CAZALLA, D., ALMSTEAD, L. L., STEITZ, J. A. & DIMAIO, D. 2011. miR-29 and miR-30 regulate B-Myb expression during cellular senescence. *Proceedings of the National Academy of Sciences of the United States of America,* 108**,** 522-527.

MARTINS-TAYLOR, K., NISLER, B. S., TAAPKEN, S. M., COMPTON, T., CRANDALL, L., MONTGOMERY, K. D., LALANDE, M. & XU, R. H. 2011. Recurrent copy number variations in human induced pluripotent stem cells. *Nature Biotechnology,* 29**,** 488-491.

MASSELINK, H., VASTENHOUW, N. & BERNARDS, R. 2001. B-myb rescues ras-induced premature senescence, which requires its transactivation domain. *Cancer Letters,* 171**,** 87-101.

MCINTOSH, P. B., FRENKIEL, T. A., WELLBORN, U., MCCORMICK, J. E., KLEMPNAUER, K. H., FEENEY, J. & CARR, M. D. 1998. Solution structure of the B-Myb DNA-binding domain: A possible role for conformational instability of the protein in DNA binding and control of gene expression. *Biochemistry,* 37**,** 9619-9629.

METTUS, R. V., LITVIN, J., WALI, A., TOSCANI, A., LATHAM, K., HATTON, K. & REDDY, E. P. 1994. MURINE A-MYB - EVIDENCE FOR DIFFERENTIAL SPLICING AND TISSUE-SPECIFIC EXPRESSION. *Oncogene,* 9**,** 3077-3086.

MIKKELSEN, T. S., HANNA, J., ZHANG, X., KU, M., WERNIG, M., SCHORDERET, P., BERNSTEIN, B. E., JAENISCH, R., LANDER, E. S. & MEISSNER, A. 2008. Dissecting direct reprogramming through integrative genomic analysis. *Nature,* 454**,** 49-U1.

MILLER, R. A. & RUDDLE, F. H. 1976. PLURIPOTENT TERATOCARCINOMA-THYMUS SOMATIC-CELL HYBRIDS. *Cell,* 9**,** 45-55.

MIYOSHI, N., ISHII, H., NAGANO, H., HARAGUCHI, N., DEWI, D. L., KANO, Y., NISHIKAWA, S., TANEMURA, M., MIMORI, K., TANAKA, F., SAITO, T., NISHIMURA, J., TAKEMASA, I., MIZUSHIMA, T., IKEDA, M., YAMAMOTO, H., SEKIMOTO, M., DOKI, Y. & MORI, M. 2011. Reprogramming of Mouse and Human Cells to Pluripotency Using Mature MicroRNAs. *Cell Stem Cell,* 8**,** 633-638.

MIZUGUCHI, H., XU, Z. L., ISHII-WATABE, A., UCHIDA, E. & HAYAKAWA, T. 2000. IRES-dependent second gene expression is significantly lower than cap-dependent first gene expression in a bicistronic vector. *Molecular Therapy,* 1**,** 376-382.

MONGE, M., COLAS, E., DOLL, A., GONZALEZ, M., GIL-MORENO, A., PLANAGUMA, J., QUILES, M., ARBOS, M. A., GARCIA, A., CASTELLVI, J., LLAURADO, M., RIGAU, M., ALAZZOUZI, H., XERCAVINS, J., ALAMEDA, F., REVENTOS, J. & ABAL, M. 2007. ERM/ETV5 up-regulation plays a role during myometrial infiltration through matrix metalloproteinase-2 in endometrial cancer. *Cancer Research,* 67**,** 6753-6759.

MONTE, D., BAERT, J. L., DEFOSSEZ, P. A., DELAUNOIT, Y. & STEHELIN, D. 1994. MOLECULAR-CLONING AND CHARACTERIZATION OF HUMAN ERM, A NEW MEMBER OF THE ETS FAMILY CLOSELY-RELATED TO MOUSE PEA3 AND ER81 TRANSCRIPTION FACTORS. *Oncogene,* 9**,** 1397-1406.

MOON, S. H., KIM, J. S., PARK, S. J., LIM, J. J., LEE, H. J., LEE, S. M. & CHUNG, H. M. 2011. Effect of chromosome instability on the maintenance and differentiation of human embryonic stem cells in vitro and in vivo. *Stem Cell Research,* 6**,** 50-59.

MOREY, L., ALOIA, L., COZZUTO, L., BENITAH, S. A. & DI CROCE, L. 2013. RYBP and Cbx7 Define Specific Biological Functions of Polycomb Complexes in Mouse Embryonic Stem Cells. *Cell Reports,* 3**,** 60-69.

MORIZANE, A., DOI, D., KIKUCHI, T., OKITA, K., HOTTA, A., KAWASAKI, T., HAYASHI, T., ONOE, H., SHIINA, T., YAMANAKA, S. & TAKAHASHI, J. 2013. Direct Comparison of Autologous and Allogeneic Transplantation of iPSC-Derived Neural Cells in the Brain of a Nonhuman Primate. *Stem cell reports,* 1**,** 283-92.

MOSTOSLAVSKY, G., FABIAN, A. J., ROONEY, S., ALT, F. W. & MULLIGAN, R. C. 2006. Complete correction of murine Artemis immunodeficiency by lentiviral vector-mediated gene transfer. *Proceedings of the National Academy of Sciences of the United States of America,* 103**,** 16406-16411.

MUCENSKI, M. L., MCLAIN, K., KIER, A. B., SWERDLOW, S. H., SCHREINER, C. M., MILLER, T. A., PIETRYGA, D. W., SCOTT, W. J. & POTTER, S. S. 1991. A FUNCTIONAL C-MYB GENE IS REQUIRED FOR NORMAL MURINE FETAL HEPATIC HEMATOPOIESIS. *Cell,* 65**,** 677-689.

NAIR, M., BILANCHONE, V., ORTT, K., SINHA, S. & DAI, X. 2007. Ovol1 represses its own transcription by competing with transcription activator c-Myb and by recruiting histone deacetylase activity. *Nucleic Acids Research,* 35**,** 1687-1697.

NAKAGAWA, M., KOYANAGI, M., TANABE, K., TAKAHASHI, K., ICHISAKA, T., AOI, T., OKITA, K., MOCHIDUKI, Y., TAKIZAWA, N. & YAMANAKA, S. 2008. Generation of induced pluripotent stem cells without Myc from mouse and human fibroblasts. *Nature Biotechnology,* 26**,** 101-106.

NAKAGOSHI, H., KANEI-ISHII, C., SAWAZAKI, T., MIZUGUCHI, G. & ISHII, S. 1992. Transcriptional activation of the c-myc gene by the c-myb and B-myb gene products. *Oncogene,* 7**,** 1233-40.

NER, S. S. 1992. DNA-BINDING PROTEINS HMGS EVERYWHERE. *Current Biology,* 2**,** 208-210.

NICHOLS, J., ZEVNIK, B., ANASTASSIADIS, K., NIWA, H., KLEWE-NEBENIUS, D., CHAMBERS, I., SCHOLER, H. & SMITH, A. 1998. Formation of pluripotent stem cells in the mammalian embryo depends on the POU transcription factor Oct4. *Cell,* 95**,** 379-391.

NIWA, H., MIYAZAKI, J. & SMITH, A. G. 2000. Quantitative expression of Oct-3/4 defines differentiation, dedifferentiation or self-renewal of ES cells. *Nature Genetics,* 24**,** 372-376.

NODA, A., NING, Y., VENABLE, S. F., PEREIRASMITH, O. M. & SMITH, J. R. 1994. CLONING OF SENESCENT CELL-DERIVED INHIBITORS OF DNA-SYNTHESIS USING AN EXPRESSION SCREEN. *Experimental Cell Research,* 211**,** 90-98.

NOMURA, N., TAKAHASHI, M., MATSUI, M., ISHII, S., DATE, T., SASAMOTO, S. & ISHIZAKI, R. 1988. ISOLATION OF HUMAN CDNA CLONES OF MYB-RELATED GENES, A-MYB AND B-MYB. *Nucleic Acids Research,* 16**,** 11075-11089.

O'CONNOR, M. D., KARDEL, M. D., IOSFINA, I., YOUSSEF, D., LU, M., LI, M. M., VERCAUTEREN, S., NAGY, A. & EAVES, C. J. 2008. Alkaline phosphatase-positive colony formation is a sensitive, specific, and quantitative indicator of undifferentiated human embryonic stem cells. *Stem Cells,* 26**,** 1109-1116.

O'MALLEY, J., SKYLAKI, S., IWABUCHI, K. A., CHANTZOURA, E., RUETZ, T., JOHNSSON, A., TOMLINSON, S. R., LINNARSSON, S. & KAJI, K. 2013. High-resolution analysis with novel cell-surface markers identifies routes to iPS cells. *Nature,* 499**,** 88-+.

OH, I. H. & REDDY, E. P. 1999. The myb gene family in cell growth, differentiation and apoptosis. *Oncogene,* 18**,** 3017-3033.

OHI, Y., QIN, H., HONG, C. B., BLOUIN, L., POLO, J. M., GUO, T. X., QI, Z. X., DOWNEY, S. L., MANOS, P. D., ROSSI, D. J., YU, J. W., HEBROK, M., HOCHEDLINGER, K., COSTELLO, J. F., SONG, J. S. & RAMALHO-SANTOS, M. 2011. Incomplete DNA methylation underlies a transcriptional memory of somatic cells in human iPS cells. *Nature Cell Biology,* 13**,** 541-U328.

OKADA, M., AKIMARU, H., HOU, D. X., TAKAHASHI, T. & ISHII, S. 2002. Myb controls G(2)/M progression by inducing cyclin B expression in the Drosophila eye imaginal disc. *Embo Journal,* 21**,** 675-684.

OKITA, K., ICHISAKA, T. & YAMANAKA, S. 2007. Generation of germline-competent induced pluripotent stem cells. *Nature,* 448**,** 313-U1.

ONDER, T. T., KARA, N., CHERRY, A., SINHA, A. U., ZHU, N., BERNT, K. M., CAHAN, P., MANCARCI, B. O., UNTERNAEHRER, J., GUPTA, P. B., LANDER, E. S., ARMSTRONG, S. A. & DALEY, G. Q. 2012. Chromatin-modifying enzymes as modulators of reprogramming. *Nature,* 483**,** 598-U119.

PAPAPETROU, E. P., TOMISHIMA, M. J., CHAMBERS, S. M., MICA, Y., REED, E., MENON, J., TABAR, V., MO, Q., STUDER, L. & SADELAIN, M. 2009. Stoichiometric and

temporal requirements of Oct4, Sox2, Klf4, and c-Myc expression for efficient human iPSC induction and differentiation. *Proceedings of the National Academy of Sciences of the United States of America,* 106**,** 12759-12764.

PARIKH, N., HILSENBECK, S., CREIGHTON, C. J., DAYARAM, T., SHUCK, R., SHINBROT, E., XI, L., GIBBS, R. A., WHEELER, D. A. & DONEHOWER, L. A. 2014. Effects of TP53 mutational status on gene expression patterns across 10 human cancer types. *Journal of Pathology,* 232**,** 522-533.

PAULL, T. T., ROGAKOU, E. P., YAMAZAKI, V., KIRCHGESSNER, C. U., GELLERT, M. & BONNER, W. M. 2000. A critical role for histone H2AX in recruitment of repair factors to nuclear foci after DNA damage. *Current Biology,* 10**,** 886-895.

PILKINTON, M., SANDOVAL, R., SONG, J., NESS, S. A. & COLAMONICI, O. R. 2007. Mip/LIN-9 regulates the expression of B-Myb and the induction of cyclin A, cyclin B, and CDK1. *Journal of Biological Chemistry,* 282**,** 168-175.

POLO, J. M., ANDERSSEN, E., WALSH, R. M., SCHWARZ, B. A., NEFZGER, C. M., LIM, S. M., BORKENT, M., APOSTOLOU, E., ALAEI, S., CLOUTIER, J., BAR-NUR, O., CHELOUFI, S., STADTFELD, M., FIGUEROA, M. E., ROBINTON, D., NATESAN, S., MELNICK, A., ZHU, J. F., RAMASWAMY, S. & HOCHEDLINGER, K. 2012. A Molecular Roadmap of Reprogramming Somatic Cells into iPS Cells. *Cell,* 151**,** 1617-1632.

POMEROY, S. L., TAMAYO, P., GAASENBEEK, M., STURLA, L. M., ANGELO, M., MCLAUGHLIN, M. E., KIM, J. Y. H., GOUMNEROVA, L. C., BLACK, P. M., LAU, C., ALLEN, J. C., ZAGZAG, D., OLSON, J. M., CURRAN, T., WETMORE, C., BIEGEL, J. A., POGGIO, T., MUKHERJEE, S., RIFKIN, R., CALIFANO, A., STOLOVITZKY, G., LOUIS, D. N., MESIROV, J. P., LANDER, E. S. & GOLUB, T. R. 2002. Prediction of central nervous system embryonal tumour outcome based on gene expression. *Nature,* 415**,** 436-442.

POMMIER, Y. 2009. DNA Topoisomerase I Inhibitors: Chemistry, Biology, and Interfacial Inhibition. *Chemical Reviews,* 109**,** 2894-2902.

QUINLAN, A. R., BOLAND, M. J., LEIBOWITZ, M. L., SHUMILINA, S., PEHRSON, S. M., BALDWIN, K. K. & HALL, I. M. 2011. Genome Sequencing of Mouse Induced Pluripotent Stem Cells Reveals Retroelement Stability and Infrequent DNA Rearrangement during Reprogramming. *Cell Stem Cell,* 9**,** 366-373.

RAHDEN-STARON, I., SZUMILO, M., GROSICKA, E., KRAAKMAN-VAN DER ZWET, M. & ZDZIENICKA, M. Z. 2003. Defective Brca2 influences topoisomerase I activity in mammalian cells. *Acta Biochimica Polonica,* 50**,** 139-144.

RAHL, P. B., LIN, C. Y., SEILA, A. C., FLYNN, R. A., MCCUINE, S., BURGE, C. B., SHARP, P. A. & YOUNG, R. A. 2010. c-Myc Regulates Transcriptional Pause Release. *Cell,* 141**,** 432-445.

RAIS, Y., ZVIRAN, A., GEULA, S., GAFNI, O., CHOMSKY, E., VIUKOV, S., MANSOUR, A. A., CASPI, I., KRUPALNIK, V., ZERBIB, M., MAZA, I., MOR, N., BARAN, D., WEINBERGER, L., JAITIN, D. A., LARA-ASTIASO, D., BLECHER-GONEN, R., SHIPONY, Z., MUKAMEL, Z., HAGAI, T., GILAD, S., AMANN-ZALCENSTEIN, D., TANAY, A., AMIT, I., NOVERSHTERN, N. & HANNA, J. H. 2013. Deterministic direct reprogramming of somatic cells to pluripotency. *Nature,* 502**,** 65-+.

RAMOS-MEJIA, V., MUNOZ-LOPEZ, M., GARCIA-PEREZ, J. L. & MENENDEZ, P. 2010. iPSC lines that do not silence the expression of the ectopic reprogramming factors may display enhanced propensity to genomic instability. *Cell Research,* 20**,** 1092-1095.

RASCHELLA, G., NEGRONI, A., SALA, A., PUCCI, S., ROMEO, A. & CALABRETTA, B. 1995. REQUIREMENT OF B-MYB FUNCTION FOR SURVIVAL AND DIFFERENTIATIVE POTENTIAL OF HUMAN NEUROBLASTOMA-CELLS. *Journal of Biological Chemistry,* 270**,** 8540-8545.

REDINBO, M. R., STEWART, L., KUHN, P., CHAMPOUX, J. J. & HOL, W. G. J. 1998. Crystal structures of human topoisomerase I in covalent and noncovalent complexes with DNA. *Science,* 279**,** 1504-1513.

REDMER, T., DIECKE, S., GRIGORYAN, T., QUIROGA-NEGREIRA, A., BIRCHMEIER, W. & BESSER, D. 2011. E-cadherin is crucial for embryonic stem cell pluripotency and can replace OCT4 during somatic cell reprogramming. *Embo Reports,* 12**,** 720-726.

REIF, A. E. & ALLEN, J. M. V. 1964. AKR THYMIC ANTIGEN + ITS DISTRIBUTION IN LEUKEMIAS + NERVOUS TISSUES. *Journal of Experimental Medicine,* 120**,** 413-&.

REUBINOFF, B. E., PERA, M. F., FONG, C. Y., TROUNSON, A. & BONGSO, A. 2000. Embryonic stem cell lines from human blastocysts: somatic differentiation in vitro. *Nature Biotechnology,* 18**,** 399-404.

RIBALLO, E., KUHNE, M., RIEF, N., DOHERTY, A., SMITH, G. C. M., RECIO, M. J., REIS, C., DAHM, K., FRICKE, A., KREMPLER, A., PARKER, A. R., JACKSON, S. P., GENNERY, A., JEGGO, P. A. & LOBRICH, M. 2004. A pathway of double-strand break rejoining dependent upon ATM, artemis, and proteins locating to gamma-H2AX foci. *Molecular Cell,* 16**,** 715-724.

ROBERTSON, E. J. 1986. PLURIPOTENTIAL STEM-CELL LINES AS A ROUTE INTO THE MOUSE GERM LINE. *Trends in Genetics,* 2**,** 9-13.

ROBINSON, C., LIGHT, Y., GROVES, R., MANN, D., MARAIS, R. & WATSON, R. 1996. Cell-cycle regulation of B-Myb protein expression: Specific phosphorylation during the S phase of the cell cycle. *Oncogene,* 12**,** 1855-1864.

ROBLES, S. J. & ADAMI, G. R. 1998. Agents that cause DNA double strand breaks lead to p16(INK4a) enrichment and the premature senescence of normal fibrolasts. *Oncogene,* 16**,** 1113-1123.

RODDA, D. J., CHEW, J. L., LIM, L. H., LOH, Y. H., WANG, B., NG, H. H. & ROBSON, P. 2005. Transcriptional regulation of Nanog by Oct4 and Sox2. *Journal of Biological Chemistry,* 280**,** 24731-24737.

ROGAKOU, E. P., PILCH, D. R., ORR, A. H., IVANOVA, V. S. & BONNER, W. M. 1998. DNA double-stranded breaks induce histone H2AX phosphorylation on serine 139. *Journal of Biological Chemistry,* 273**,** 5858-5868.

ROWLAND, B. D., BERNARDS, R. & PEEPER, D. S. 2005. The KLF4 tumour suppressor is a transcriptional repressor of p53 that acts as a context-dependent oncogene. *Nature Cell Biology,* 7**,** 1074-1082.

RYAN, M. D., KING, A. M. Q. & THOMAS, G. P. 1991. CLEAVAGE OF FOOT-AND-MOUTH-DISEASE VIRUS POLYPROTEIN IS MEDIATED BY RESIDUES LOCATED WITHIN A 19 AMINO-ACID-SEQUENCE. *Journal of General Virology,* 72**,** 2727-2732.

SADASIVAM, S. & DECAPRIO, J. A. 2013. The DREAM complex: master coordinator of cell cycle-dependent gene expression. *Nature Reviews Cancer,* 13**,** 585-595.

SALA, A. & CALABRETTA, B. 1992. REGULATION OF BALB/C 3T3 FIBROBLAST PROLIFERATION BY B-MYB IS ACCOMPANIED BY SELECTIVE ACTIVATION OF CDC2 AND CYCLIN-D1 EXPRESSION. *Proceedings of the National Academy of Sciences of the United States of America,* 89**,** 10415-10419.

SAMAVARCHI-TEHRANI, P., GOLIPOUR, A., DAVID, L., SUNG, H. K., BEYER, T. A., DATTI, A., WOLTJEN, K., NAGY, A. & WRANA, J. L. 2010. Functional Genomics Reveals a BMP-Driven Mesenchymal-to-Epithelial Transition in the Initiation of Somatic Cell Reprogramming. *Cell Stem Cell,* 7**,** 64-77.

SANTILLI, G., SCHWAB, R., WATSON, R., EBERT, C., ARONOW, B. J. & SALA, A. 2005. Temperature-dependent modification and activation of B-MYB - Implications for cell survival. *Journal of Biological Chemistry,* 280**,** 15628-15634.

SAVILLE, M. K. & WATSON, R. J. 1998. The cell-cycle regulated transcription factor B-Myb is phosphorylated by cyclin A/Cdk2 at sites that enhance its transactivation properties. *Oncogene,* 17**,** 2679-2689.

SCHOLER, H. R., BALLING, R., HATZOPOULOS, A. K., SUZUKI, N. & GRUSS, P. 1989a. OCTAMER BINDING-PROTEINS CONFER TRANSCRIPTIONAL ACTIVITY IN EARLY MOUSE EMBRYOGENESIS. *Embo Journal,* 8**,** 2551-2557.

SCHOLER, H. R., HATZOPOULOS, A. K., BALLING, R., SUZUKI, N. & GRUSS, P. 1989b. A FAMILY OF OCTAMER-SPECIFIC PROTEINS PRESENT DURING MOUSE EMBRYOGENESIS - EVIDENCE FOR GERMLINE-SPECIFIC EXPRESSION OF AN OCT FACTOR. *Embo Journal,* 8**,** 2543-2550.

SCHOLER, H. R., RUPPERT, S., SUZUKI, N., CHOWDHURY, K. & GRUSS, P. 1990. New Type Of Pou Domain In Germ Line-Specific Protein Oct-4. *Nature,* 344**,** 435-439.

SCHREINER, S., BIRKE, M., GARCIA-CUELLAR, M. P., ZILLES, O., GREIL, J. & SLANY, R. K. 2001. MLL-ENL causes a reversible and myc-dependent block of myelomonocytic cell differentiation. *Cancer Research,* 61**,** 6480-6486.

SCHWARTZ, S. D., HUBSCHMAN, J. P., HEILWELL, G., FRANCO-CARDENAS, V., PAN, C. K., OSTRICK, R. M., MICKUNAS, E., GAY, R., KLIMANSKAYA, I. & LANZA, R. 2012. Embryonic stem cell trials for macular degeneration: a preliminary report. *Lancet,* 379**,** 713-720.

SEGRE, J. A., BAUER, C. & FUCHS, E. 1999. Klf4 is a transcription factor required for establishing the barrier function of the skin. *Nature Genetics,* 22**,** 356-360.

SELVAKUMARAN, M., LIEBERMANN, D. & HOFFMAN, B. 1996. The proto-oncogene c-myc blocks myeloid differentiation independently of its target gene ornithine decarboxylase. *Blood,* 88**,** 1248-1255.

SERRANO, F., CALATAYUD, C. F., BLAZQUEZ, M., TORRES, J., CASTELL, J. V. & BORT, R. 2013. Gata4 Blocks Somatic Cell Reprogramming By Directly Repressing Nanog. *Stem Cells,* 31**,** 71-82.

SERRANO, M., HANNON, G. J. & BEACH, D. 1993. A NEW REGULATORY MOTIF IN CELL-CYCLE CONTROL CAUSING SPECIFIC-INHIBITION OF CYCLIN-D/CDK4. *Nature,* 366**,** 704-707.

SERRANO, M., LEE, H. W., CHIN, L., CORDONCARDO, C., BEACH, D. & DEPINHO, R. A. 1996. Role of the INK4a locus in tumor suppression and cell mortality. *Cell,* 85**,** 27-37.

SHARAN, S. K., MORIMATSU, M., ALBRECHT, U., LIM, D. S., REGEL, E., DINH, C., SANDS, A., EICHELE, G., HASTY, P. & BRADLEY, A. 1997. Embryonic lethality and radiation hypersensitivity mediated by Rad51 in mice lacking Brca2. *Nature,* 386**,** 804-810.

SHEINESS, D. & GARDINIER, M. 1984. Expression of a proto-oncogene (proto-myb) in hemopoietic tissues of mice. *Mol Cell Biol,* 4**,** 1206-12.

SHEPARD, J. L., AMATRUDA, J. F., STERN, H. M., SUBRAMANIAN, A., FINKELSTEIN, D., ZIAI, J., FINLEY, K. R., PFAFF, K. L., HERSEY, C., ZHOU, Y., BARUT, B., FREEDMAN,

M., LEE, C., SPITSBERGEN, J., NEUBERG, D., WEBER, G., GOLUB, T. R., GLICKMAN, J. N., KUTOK, J. L., ASTER, J. C. & ZON, L. I. 2005. Zebrafish bmyb mutation causes genome instability and increased cancer susceptibility. *Proceedings of the National Academy of Sciences of the United States of America,* 102**,** 13194-13199.

SHINAGAWA, T., TAKAGI, T., TSUKAMOTO, D., TOMARU, C., HUYNH, L. M., SIVARAMAN, P., KUMAREVEL, T., INOUE, K., NAKATO, R., KATOU, Y., SADO, T., TAKAHASHI, S., OGURA, A., SHIRAHIGE, K. & ISHII, S. 2014. Histone Variants Enriched in Oocytes Enhance Reprogramming to Induced Pluripotent Stem Cells. *Cell Stem Cell,* 14**,** 217-227.

SHINOHARA, A., OGAWA, H. & OGAWA, T. 1992. RAD51 PROTEIN INVOLVED IN REPAIR AND RECOMBINATION IN SACCHAROMYCES-CEREVISIAE IS A RECA-LIKE PROTEIN. *Cell,* 69**,** 457-470.

SILVA, J., NICHOLS, J., THEUNISSEN, T. W., GUO, G., VAN OOSTEN, A. L., BARRANDON, O., WRAY, J., YAMANAKA, S., CHAMBERS, I. & SMITH, A. 2009. Nanog Is the Gateway to the Pluripotent Ground State. *Cell,* 138**,** 722-737.

SIMON, A. L., STONE, E. A. & SIDOW, A. 2002. Inference of functional regions in proteins by quantification of evolutionary constraints. *Proceedings of the National Academy of Sciences of the United States of America,* 99**,** 2912-2917.

SINCLAIR, A. H., BERTA, P., PALMER, M. S., HAWKINS, J. R., GRIFFITHS, B. L., SMITH, M. J., FOSTER, J. W., FRISCHAUF, A. M., LOVELLBADGE, R. & GOODFELLOW, P. N. 1990. A GENE FROM THE HUMAN SEX-DETERMINING REGION ENCODES A PROTEIN WITH HOMOLOGY TO A CONSERVED DNA-BINDING MOTIF. *Nature,* 346**,** 240-244.

SINCLAIR, W. K. 1965. HYDROXYUREA - DIFFERENTIAL LETHAL EFFECTS ON CULTURED MAMMALIAN CELLS DURING CELL CYCLE. *Science,* 150**,** 1729-&.

SINGH, A. M. & DALTON, S. 2009. The Cell Cycle and Myc Intersect with Mechanisms that Regulate Pluripotency and Reprogramming. *Cell Stem Cell,* 5**,** 141-149.

SINGHAL, N., GRAUMANN, J., WU, G. M., ARAUZO-BRAVO, M. J., HAN, D. W., GREBER, B., GENTILE, L., MANN, M. & SCHOLER, H. R. 2010. Chromatin-Remodeling Components of the BAF Complex Facilitate Reprogramming. *Cell,* 141**,** 943-955.

SITZMANN, J., NOBENTRAUTH, K., KAMANO, H. & KLEMPNAUER, K. H. 1996. Expression of B-Myb during mouse embryogenesis. *Oncogene,* 12**,** 1889-1894.

SITZMANN, J., NOBENTRAUTH, K. & KLEMPNAUER, K. H. 1995. Expression of mouse c-myb during embryonic development. *Oncogene,* 11**,** 2273-2279.

SKOTHEIM, R. I., MONNI, O., MOUSSES, S., FOSSA, S. D., KALLIONIEMI, O. P., LOTHE, R. A. & KALLIONIEMI, A. 2002. New insights into testicular germ cell tumorigenesis from gene expression profiling. *Cancer Research,* 62**,** 2359-2364.

SOLDNER, F., HOCKEMEYER, D., BEARD, C., GAO, Q., BELL, G. W., COOK, E. G., HARGUS, G., BLAK, A., COOPER, O., MITALIPOVA, M., ISACSON, O. & JAENISCH, R. 2009. Parkinson's Disease Patient-Derived Induced Pluripotent Stem Cells Free of Viral Reprogramming Factors. *Cell,* 136**,** 964-977.

SOMMER, C. A., SOMMER, A. G., LONGMIRE, T. A., CHRISTODOULOU, C., THOMAS, D. D., GOSTISSA, M., ALT, F. W., MURPHY, G. J., KOTTON, D. N. & MOSTOSLAVSKY, G. 2010. Excision of Reprogramming Transgenes Improves the Differentiation Potential of iPS Cells Generated with a Single Excisable Vector. *Stem Cells,* 28**,** 64-74.

SOMMER, C. A., STADTFELD, M., MURPHY, G. J., HOCHEDLINGER, K., KOTTON, D. N. & MOSTOSLAVSKY, G. 2009. Induced Pluripotent Stem Cell Generation Using a Single Lentiviral Stem Cell Cassette. *Stem Cells,* 27**,** 543-549.

SONCIN, F., MOHAMET, L., ECKARDT, D., RITSON, S., EASTHAM, A. M., BOBOLA, N., RUSSELL, A., DAVIES, S., KEMLER, R., MERRY, C. L. R. & WARD, C. M. 2009. Abrogation of E-Cadherin-Mediated Cell-Cell Contact in Mouse Embryonic Stem Cells Results in Reversible LIF-Independent Self-Renewal. *Stem Cells,* 27**,** 2069-2080.

SORLIE, T., PEROU, C. M., TIBSHIRANI, R., AAS, T., GEISLER, S., JOHNSEN, H., HASTIE, T., EISEN, M. B., VAN DE RIJN, M., JEFFREY, S. S., THORSEN, T., QUIST, H., MATESE, J. C., BROWN, P. O., BOTSTEIN, D., LONNING, P. E. & BORRESEN-DALE, A. L. 2001. Gene expression patterns of breast carcinomas distinguish tumor subclasses with clinical implications. *Proceedings of the National Academy of Sciences of the United States of America,* 98**,** 10869-10874.

SOTIRIOU, C., NEO, S. Y., MCSHANE, L. M., KORN, E. L., LONG, P. M., JAZAERI, A., MARTIAT, P., FOX, S. B., HARRIS, A. L. & LIU, E. T. 2003. Breast cancer classification and prognosis based on gene expression profiles from a population-based study. *Proceedings of the National Academy of Sciences of the United States of America,* 100**,** 10393-10398.

SOUFI, A., DONAHUE, G. & ZARET, K. S. 2012. Facilitators and Impediments of the Pluripotency Reprogramming Factors' Initial Engagement with the Genome. *Cell,* 151**,** 994-1004.

SRIDHARAN, R., TCHIEU, J., MASON, M. J., YACHECHKO, R., KUOY, E., HORVATH, S., ZHOU, Q. & PLATH, K. 2009. Role of the Murine Reprogramming Factors in the Induction of Pluripotency. *Cell,* 136**,** 364-377.

STADTFELD, M., MAHERALI, N., BORKENT, M. & HOCHEDLINGER, K. 2010. A reprogrammable mouse strain from gene-targeted embryonic stem cells. *Nature Methods,* 7**,** 53-U10.

STADTFELD, M., NAGAYA, M., UTIKAL, J., WEIR, G. & HOCHEDLINGER, K. 2008. Induced Pluripotent Stem Cells Generated Without Viral Integration. *Science,* 322**,** 945-949.

STAERK, J., DAWLATY, M. M., GAO, Q., MAETZEL, D., HANNA, J., SOMMER, C. A., MOSTOSLAVSKY, G. & JAENISCH, R. 2010. Reprogramming of Human Peripheral Blood Cells to Induced Pluripotent Stem Cells. *Cell Stem Cell,* 7**,** 20-24.

STEAD, E., WHITE, J., FAAST, R., CONN, S., GOLDSTONE, S., RATHJEN, J., DHINGRA, U., RATHJEN, P., WALKER, D. & DALTON, S. 2002. Pluripotent cell division cycles are driven by ectopic Cdk2, cyclin A/E and E2F activities. *Oncogene,* 21**,** 8320-8333.

STERN, H. M., MURPHEY, R. D., SHEPARD, J. L., AMATRUDA, J. F., STRAUB, C. T., PFAFF, K. L., WEBER, G., TALLARICO, J. A., KING, R. W. & ZON, L. I. 2005. Small molecules that delay S phase suppress a zebrafish bmyb mutant. *Nature Chemical Biology,* 1**,** 366-370.

STOBERGRASSER, U., BRYDOLF, B., BIN, X., GRASSER, F., FIRTEL, R. A. & LIPSICK, J. S. 1992. THE MYB DNA-BINDING DOMAIN IS HIGHLY CONSERVED IN DICTYOSTELIUM-DISCOIDEUM. *Oncogene,* 7**,** 589-596.

SZYMCZAK, A. L. & VIGNALI, D. A. A. 2005. Development of 2A peptide-based strategies in the design of multicistronic vectors. *Expert Opinion on Biological Therapy,* 5**,** 627-638.

TADA, M., TAKAHAMA, Y., ABE, K., NAKATSUJI, N. & TADA, T. 2001. Nuclear reprogramming of somatic cells by in vitro hybridization with ES cells. *Current Biology,* 11**,** 1553-1558.

TAHMASEBI, S., ALAIN, T., RAJASEKHAR, V. K., ZHANG, J. P., PRAGER-KHOUTORSKY, M., KHOUTORSKY, A., DOGAN, Y., GKOGKAS, C. G., PETROULAKIS, E., SYLVESTRE, A., GHORBANI, M., ASSADIAN, S., YAMANAKA, Y., VINAGOLU-BAUR, J. R., TEODORO, J. G., KIM, K., YANG, X. J. & SONENBERG, N. 2014. Multifaceted Regulation of Somatic Cell Reprogramming by mRNA Translational Control. *Cell Stem Cell,* 14**,** 606-616.

TAKAHASHI, K., TANABE, K., OHNUKI, M., NARITA, M., ICHISAKA, T., TOMODA, K. & YAMANAKA, S. 2007. Induction of pluripotent stem cells from adult human fibroblasts by defined factors. *Cell,* 131**,** 861-872.

TAKAHASHI, K. & YAMANAKA, S. 2006. Induction of pluripotent stem cells from mouse embryonic and adult fibroblast cultures by defined factors. *Cell,* 126**,** 663-676.

TAKEICHI, M. 1991. CADHERIN CELL-ADHESION RECEPTORS AS A MORPHOGENETIC REGULATOR. *Science,* 251**,** 1451-1455.

TAM, P. P. L. & ROSSANT, J. 2003. Mouse embryonic chimeras: tools for studying mammalian development. *Development,* 130**,** 6155-6163.

TANAKA, Y., PATESTOS, N. P., MAEKAWA, T. & ISHII, S. 1999. B-myb is required for inner cell mass formation at an early stage of development. *Journal of Biological Chemistry,* 274**,** 28067-28070.

TARASOV, K. V., TARASOVA, Y. S., TAM, W. L., RIORDON, D. R., ELLIOTT, S. T., KANIA, G., LI, J., YAMANAKA, S., CRIDER, D. G., TESTA, G., LI, R. A., LIM, B., STEWART, C. L., LIU, Y., VAN EYK, J. E., WERSTO, R. P., WOBUS, A. M. & BOHELER, K. R. 2008. B-MYB Is Essential for Normal Cell Cycle Progression and Chromosomal Stability of Embryonic Stem Cells. *Plos One,* 3.

TAYLOR, C. J., PEACOCK, S., CHAUDHRY, A. N., BRADLEY, J. A. & BOLTON, E. M. 2012. Generating an iPSC Bank for HLA-Matched Tissue Transplantation Based on Known Donor and Recipient HLA Types. *Cell Stem Cell,* 11**,** 147-152.

THEUNISSEN, T. W. & JAENISCH, R. 2014. Molecular control of induced pluripotency. *Cell stem cell,* 14**,** 720-34.

THOMSON, J. A., ITSKOVITZ-ELDOR, J., SHAPIRO, S. S., WAKNITZ, M. A., SWIERGIEL, J. J., MARSHALL, V. S. & JONES, J. M. 1998. Embryonic stem cell lines derived from human blastocysts. *Science,* 282**,** 1145-1147.

THOMSON, J. A., KALISHMAN, J., GOLOS, T. G., DURNING, M., HARRIS, C. P., BECKER, R. A. & HEARN, J. P. 1995. ISOLATION OF A PRIMATE EMBRYONIC STEM-CELL LINE. *Proceedings of the National Academy of Sciences of the United States of America,* 92**,** 7844-7848.

TICHY, E. D. & STAMBROOK, P. J. 2008. DNA repair in murine embryonic stem cells and differentiated cells. *Experimental Cell Research,* 314**,** 1929-1936.

TOSCANI, A., METTUS, R. V., COUPLAND, R., SIMPKINS, H., LITVIN, J., ORTH, J., HATTON, K. S. & REDDY, E. P. 1997. Arrest of spermatogenesis and defective breast development in mice lacking A-myb. *Nature,* 386**,** 713-717.

TOWNS, C. R. & JONES, D. G. 2004. Stem cells, embryos, and the environment: a context for both science and ethics. *Journal of Medical Ethics,* 30**,** 410-413.

TRAUTH, K., MUTSCHLER, B., JENKINS, N. A., GILBERT, D. J., COPELAND, N. G. & KLEMPNAUER, K. H. 1994. MOUSE A-MYB ENCODES A TRANSACTIVATOR AND

IS EXPRESSED IN MITOTICALLY ACTIVE-CELLS OF THE DEVELOPING CENTRAL-NERVOUS-SYSTEM, ADULT TESTIS AND B-LYMPHOCYTES. *Embo Journal,* 13**,** 5994-6005.

TSUKITA, S., OISHI, K., SATO, N., SAGARA, J. & KAWAI, A. 1994. ERM FAMILY MEMBERS AS MOLECULAR LINKERS BETWEEN THE CELL-SURFACE GLYCOPROTEIN CD44 AND ACTIN-BASED CYTOSKELETONS. *Journal of Cell Biology,* 126**,** 391-401.

TURNER, M., LESLIE, S., MARTIN, N. G., PESCHANSKI, M., RAO, M., TAYLOR, C. J., TROUNSON, A., TURNER, D., YAMANAKA, S. & WILMUT, I. 2013. Toward the Development of a Global Induced Pluripotent Stem Cell Library. *Cell Stem Cell,* 13**,** 382-384.

UTIKAL, J., POLO, J. M., STADTFELD, M., MAHERALI, N., KULALERT, W., WALSH, R. M., KHALIL, A., RHEINWALD, J. G. & HOCHEDLINGER, K. 2009. Immortalization eliminates a roadblock during cellular reprogramming into iPS cells. *Nature,* 460**,** 1145-U112.

VOUSDEN, K. H. & PRIVES, C. 2009. Blinded by the Light: The Growing Complexity of p53. *Cell,* 137**,** 413-431.

WALKER, E., OHISHI, M., DAVEY, R. E., ZHANG, W., CASSAR, P. A., TANAKA, T. S., DER, S. D., MORRIS, Q., HUGHES, T. R., ZANDSTRA, P. W. & STANFORD, W. L. 2007. Prediction and Testing of Novel Transcriptional Networks Regulating Embryonic Stem Cell Self-Renewal and Commitment. *Cell Stem Cell,* 1**,** 71-86.

WALKER, P. S., HENGGE, U. R., UDEY, M. C., AKSENTIJEVICH, I. & VOGEL, J. C. 1996. Viral interference during simultaneous transduction with two independent helper-free retroviral vectors. *Human Gene Therapy,* 7**,** 1131-1138.

WANG, J. C. 1996. DNA topoisomerases. *Annual Review of Biochemistry,* 65**,** 635-692.

WANG, T., CHEN, K. S., ZENG, X. M., YANG, J. G., WU, Y., SHI, X., QIN, B. M., ZENG, L. W., ESTEBAN, M. A., PAN, G. J. & PEI, D. Q. 2011. The Histone Demethylases Jhdm1a/1b Enhance Somatic Cell Reprogramming in a Vitamin-C-Dependent Manner. *Cell Stem Cell,* 9**,** 575-587.

WARREN, L., MANOS, P. D., AHFELDT, T., LOH, Y.-H., LI, H., LAU, F., EBINA, W., MANDAL, P. K., SMITH, Z. D., MEISSNER, A., DALEY, G. Q., BRACK, A. S., COLLINS, J. J., COWAN, C., SCHLAEGER, T. M. & ROSSI, D. J. 2010. Highly Efficient Reprogramming to Pluripotency and Directed Differentiation of Human Cells with Synthetic Modified mRNA. *Cell Stem Cell,* 7**,** 618-630.

WERNIG, M., LENGNER, C. J., HANNA, J., LODATO, M. A., STEINE, E., FOREMAN, R., STAERK, J., MARKOULAKI, S. & JAENISCH, R. 2008. A drug-inducible transgenic system for direct reprogramming of multiple somatic cell types. *Nature Biotechnology,* 26**,** 916-924.

WERWEIN, E., SCHMEDT, T., HOFFMANN, H., USADEL, C., OBERMANN, N., SINGER, J. D. & KLEMPNAUER, K. H. 2012. B-Myb promotes S-phase independently of its sequence-specific DNA binding activity and interacts with polymerase delta-interacting protein 1 (Pdip1). *Cell Cycle,* 11**,** 4047-4058.

WHYTE, W. A., ORLANDO, D. A., HNISZ, D., ABRAHAM, B. J., LIN, C. Y., KAGEY, M. H., RAHL, P. B., LEE, T. I. & YOUNG, R. A. 2013. Master Transcription Factors and Mediator Establish Super-Enhancers at Key Cell Identity Genes. *Cell,* 153**,** 307-319.

WILMUT, I., SCHNIEKE, A. E., MCWHIR, J., KIND, A. J. & CAMPBELL, K. H. S. 1997. Viable offspring derived from fetal and adult mammalian cells. *Nature,* 385**,** 810-813.

WOLTJEN, K., MICHAEL, I. P., MOHSENI, P., DESAI, R., MILEIKOVSKY, M., HAEMAELAEINEN, R., COWLING, R., WANG, W., LIU, P., GERTSENSTEIN, M., KAJI, K., SUNG, H.-K. & NAGY, A. 2009. piggyBac transposition reprograms fibroblasts to induced pluripotent stem cells. *Nature,* 458**,** 766-U106.

WORRINGER, K. A., RAND, T. A., HAYASHI, Y., SAMI, S., TAKAHASHI, K., TANABE, K., NARITA, M., SRIVASTAVA, D. & YAMANAKA, S. 2014. The let-7/LIN-41 Pathway Regulates Reprogramming to Human Induced Pluripotent Stem Cells by Controlling Expression of Prodifferentiation Genes. *Cell Stem Cell,* 14**,** 40-52.

XU, D., ALIPIO, Z., FINK, L. M., ADCOCK, D. M., YANG, J. C., WARD, D. C. & MA, Y. P. 2009. Phenotypic correction of murine hemophilia A using an iPS cell-based therapy. *Proceedings of the National Academy of Sciences of the United States of America,* 106**,** 808-813.

YAMAGUCHI, S., HIRANO, K., NAGATA, S. & TADA, T. 2011. Sox2 expression effects on direct reprogramming efficiency as determined by alternative somatic cell fate. *Stem Cell Research,* 6**,** 177-186.

YAMAUCHI, T., ISHIDAO, T., NOMURA, T., SHINAGAWA, T., TANAKA, Y., YONEMURA, S. & ISHII, S. 2008. A B-Myb complex containing clathrin and filamin is required for mitotic spindle function. *Embo Journal,* 27**,** 1852-1862.

YANG, D. H. & MOSS, E. G. 2003. Temporally regulated expression of Lin-28 in diverse tissues. *Gene Expression Patterns,* 3**,** 719-726.

YANG, P., WANG, Y. X., CHEN, J. Y., LI, H., KANG, L., ZHANG, Y., CHEN, S., ZHU, B. & GAO, S. R. 2011. RCOR2 Is a Subunit of the LSD1 Complex That Regulates ESC Property and Substitutes for SOX2 in Reprogramming Somatic Cells to Pluripotency. *Stem Cells,* 29**,** 791-801.

YANG, S., LIN, G., TAN, Y. Q., ZHOU, D., DENG, L. Y., CHENG, D. H., LUO, S. W., LIU, T. C., ZHOU, X. Y., SUN, Z., XIANG, Y., CHEN, T. J., WEN, J. F. & LU, G. X. 2008. Tumor progression of culture-adapted human embryonic stem cells during long-term culture. *Genes Chromosomes & Cancer,* 47**,** 665-679.

YARBRO, J. W. 1992. MECHANISM OF ACTION OF HYDROXYUREA. *Seminars in Oncology,* 19**,** 1-10.

YOUNG, C. W. & HODAS, S. 1964. HYDROXYUREA - INHIBITORY EFFECT ON DNA METABOLISM. *Science,* 146**,** 1172-&.

YU, J. & ZHANG, L. 2008. PUMA, a potent killer with or without p53. *Oncogene,* 27**,** S71-S83.

YU, J. Y., VODYANIK, M. A., SMUGA-OTTO, K., ANTOSIEWICZ-BOURGET, J., FRANE, J. L., TIAN, S., NIE, J., JONSDOTTIR, G. A., RUOTTI, V., STEWART, R., SLUKVIN, II & THOMSON, J. A. 2007. Induced pluripotent stem cell lines derived from human somatic cells. *Science,* 318**,** 1917-1920.

YUAN, H. B., CORBI, N., BASILICO, C. & DAILEY, L. 1995. DEVELOPMENTAL-SPECIFIC ACTIVITY OF THE FGF-4 ENHANCER REQUIRES THE SYNERGISTIC ACTION OF SOX2 AND OCT-3. *Genes & Development,* 9**,** 2635-2645.

ZELLER, K. I., ZHAO, X., LEE, C. W. H., CHIU, K. P., YAO, F., YUSTEIN, J. T., OOI, H. S., ORLOV, Y. L., SHAHAB, A., YONG, H. C., FU, Y., WENG, Z., KUZNETSOV, V. A., SUNG, W.-K., RUAN, Y., DANG, C. V. & WEI, C.-L. 2006. Global mapping of c-Myc binding sites and target gene networks in human B cells. *Proceedings of the National Academy of Sciences of the United States of America,* 103**,** 17834-17839.

ZHANG, H., HANNON, G. J. & BEACH, D. 1994. P21-CONTAINING CYCLIN KINASES EXIST IN BOTH ACTIVE AND INACTIVE STATES. *Genes & Development,* 8**,** 1750-1758.

ZHANG, J. Q., TAM, W. L., TONG, G. Q., WU, Q., CHAN, H. Y., SOH, B. S., LOU, Y. F., YANG, J. C., MA, Y. P., CHAI, L., NG, H. H., LUFKIN, T., ROBSON, P. & LIM, B. 2006. Sall4 modulates embryonic stem cell pluripotency and early embryonic development by the transcriptional regulation of Pou5f1. *Nature Cell Biology,* 8**,** 1114-U125.

ZHANG, M., YANG, C., LIU, H. & SUN, Y. 2013. Induced pluripotent stem cells are sensitive to DNA damage. *Genomics, proteomics & bioinformatics,* 11**,** 320-6.

ZHAO, W., LI, Q. T., AYERS, S., GU, Y. F., SHI, Z., ZHU, Q. Y., CHEN, Y. D., WANG, H. Y. & WANG, R. F. 2013. Jmjd3 Inhibits Reprogramming by Upregulating Expression of INK4a/Arf and Targeting PHF20 for Ubiquitination. *Cell,* 152**,** 1037-1050.

ZHAO, Y., YIN, X. L., QIN, H., ZHU, F. F., LIU, H. S., YANG, W. F., ZHANG, Q., XIANG, C. A., HOU, P. P., SONG, Z. H., LIU, Y. X., YONG, J., ZHANG, P. B., CAI, J., LIU, M., LI, H. G., LI, Y. Q., QU, X. X., CUI, K., ZHANG, W. Q., XIANG, T. T., WU, Y. T., ZHAO, Y. D., LIU, C., YU, C., YUAN, K. H., LOU, J. N., DING, M. X. & DENG, H. K. 2008. Two Supporting Factors Greatly Improve the Efficiency of Human iPSC Generation. *Cell Stem Cell,* 3**,** 475-479.

ZHOU, H., WU, S., JOO, J. Y., ZHU, S., HAN, D. W., LIN, T., TRAUGER, S., BIEN, G., YAO, S., ZHU, Y., SIUZDAK, G., SCHOELER, H. R., DUAN, L. & DING, S. 2009. Generation of Induced Pluripotent Stem Cells Using Recombinant Proteins. *Cell Stem Cell,* 4**,** 381-384.

ZHOU, T., BENDA, C., DUZINGER, S., HUANG, Y. H., LI, X. Y., LI, Y. H., GUO, X. P., CAO, G. K., CHEN, S., HAO, L. L., CHAN, Y. C., NG, K. M., HO, J. C., WIESER, M., WU, J. Y., REDL, H., TSE, H. F., GRILLARI, J., GRILLARI-VOGLAUER, R., PEI, D. Q. & ESTEBAN, M. A. 2011. Generation of Induced Pluripotent Stem Cells from Urine. *Journal of the American Society of Nephrology,* 22**,** 1221-1228.

ZHU, S., LI, W., ZHOU, H., WEI, W., AMBASUDHAN, R., LIN, T., KIM, J., ZHANG, K. & DING, S. 2010. Reprogramming of Human Primary Somatic Cells by OCT4 and Chemical Compounds. *Cell Stem Cell,* 7**,** 651-655.

ZHU, W. C., GIANGRANDE, P. H. & NEVINS, J. R. 2004. E2Fs link the control of G1/S and G2/M transcription. *Embo Journal,* 23**,** 4615-4626.

ZINDY, F., QUELLE, D. E., ROUSSEL, M. F. & SHERR, C. J. 1997. Expression of the p16(INK4a) tumor suppressor versus other INK4 family members during mouse development and aging. *Oncogene,* 15**,** 203-211.